Provenance of Late Quaternary Continental Sediments in Western India: Insights from Trace Element and Isotope Geochemistry

Thesis submitted to

The Maharaja Sayajirao University of Baroda

Vadodara, India

For the degree of

Doctor of Philosophy in Geology

by

Anirban Chatterjee

September, 2017

Geosciences Division

Physical Research Laboratory

Ahmedabad – 380009, India

CERTIFICATE

I certify that the thesis entitled *"Provenance of Late Quaternary Continental Sediments in Western India: Insights from Trace Element and Isotope Geochemistry"* by Mr. Anirban Chatterjee was prepared under my guidance. He has completed all requirements as per Ph. D. regulations of the University. I am satisfied with the analysis of data, interpretation of results and conclusions drawn. I recommend the submission of the thesis.

Date:

Certified by

Prof. Jyotiranjan S. Ray (Guide)
Physical Research Laboratory
Ahmedabad-380009, India

Prof. L. S. Chamyal (Co-guide)
Head of the Department
Department of Geology
The Maharaja Sayajirao University of Baroda
Vadodara – 390002, India

DECLARATION

I Anirban Chatterjee, hereby declare that the research work incorporated in the present thesis entitled *"Provenance of Late Quaternary Continental Sediments in Western India: Insights from Trace Element and Isotope Geochemistry"* is my own work and is original. This work (in part or in full) has not been submitted to any university or institute for the award of a Degree or a Diploma. I have properly acknowledged the material collected from secondary sources wherever required. I solely own the responsibility for the originality of the entire content.

Date:

Anirban Chatterjee

(Author)

Dedicated to

my teachers

Acknowledgements

Six years back when I left the city of joy for pursuing my dream, I had least expected to fall in love with any other place. Then, during the journey of my Ph.D., I fell in love with the city of Ahmedabad. Once, one of my best friends told me that we start loving a place because of the beautiful human beings who surround us in that place. True to her words, I have found many amazing people around me who have helped me to survive the ups and downs of Ph.D. life. I personally have evolved into a new and more experienced person. Finally, when I am compiling my research works in this thesis, I have an opportunity to thank all of those remarkable persons who have assisted me to reach my goal.

I am privileged to be guided by Prof. Jyotiranjan S. Ray, one of the brightest Indian geologists. I was introduced to the fascinating world of geochemistry by him. His innovative suggestions, critical comments and discussions helped me to materialize my PhD project to its present form and prepare the thesis. He has motivated me throughout the journey with his enthusiasms and introduced me to the path of scientific pursuit. We used to have long discussions regarding a variety of topics which intrigued me to discover more of my academic interests. He has tolerated me through my sluggishness, emotional breakdowns and mistakes. I express my sincere gratitude to my teacher, my mentor, Prof. J. S. Ray. I also thank my co-guide Prof. L. S. Chamyal of the M.S. University, Baroda for his advice on academic and technical matters.

I thank Dr. Navin Juyal for his constant encouragement and motivational conversations. He has introduced me to the world of Quaternary geology. His critical comments and suggestions have facilitated my research work. I have never seen an energetic person like him. I am grateful to Dr. A. D. Shukla for his scientific guidance in various laboratory activities and constant encouragement. I express my deep gratitude to Prof. R. Ramesh, Dr. Vinai Rai, Dr. M. G. Yadava, Dr. R. D. Deshpande, Dr. Sanjeev Kumar, Dr. Arvind Singh, Prof. S. K. Singh, Prof. A. K. Singhvi and Late Prof. S. Krishnaswamy for their constant encouragements and constructive suggestions. I am grateful to Prof. Kanchan Pande, IIT Bombay, for providing me the Ar-Ar dates. I am thankful to N. B. Vaghela Bhai for his helps in the radiocarbon laboratory and constant supports. I am thankful to Manan and Lakhan Bhai for their technical supports whenever I ran into any trouble regarding the machines. I express my gratitude to Jaldhi and Ramsha for making the official works smooth.

I would also like to acknowledge the academic committee, PRL for suggestions during every step of my PhD. I thank the Director, PRL for providing me all the facilities during my PhD work. I also acknowledge the support of all the staff-members of library, workshop, purchase, computer centre, accounts, administration, medical, canteen and maintenance section for their assistance and cooperation.

During my years in PRL, the life was eventful due to the presence of a wide spectrum of friends. I express my gratitude to my lab mates Alok, Neeraj, Gaurav, Shrema, Souvik, Ikshu, Bivin and Jitender for their constant support at the lab. My office memories will shine forever with the memories made with Bivin and Ikshu. My batch mates became my family away from my home. I am fortunate to have these wonderful people in my life and I thank Shraddha, Saweeta, Ikshu, Manu, Abhaya, Gaurava, Tanmoy, Girish, Arun, Guru, Kuldeep, Sanjay, Alok, Chithrabhanu and Swapna for being there throughout the ups and downs. I will cherish all our adventures and late night endeavours for the rest of my life. I have rediscovered myself and explored deep philosophical thoughts during the long and enlightening discussions with Abhishek, Raza, Ananta, Lalit, Gaurava, Chithrabhanu, Shrema and Harsh during several occasions. Life at PRL would not have been same without the wonderful friendship of Avdesh, Naveen, Sudip, Vineet, Dimple, Manojit, Bhavya, Midhun, Lekshmi, Gaurav, Balaji, Damu, Venki, Chandana, Upasana, Navpreet, Deepjyoti, Aslam, Sneha, Srinivas, Subhanand, Chinmay, Anil, Nitesh, Nijil, Vishnu, Niharika, Rupa, Kiran, Bhavesh, Bharti, Apurv, Ashim, Jinia, Newton, Deepak, Dipti, Priyabrata, Amitava, Pradeep, Rukmani, Soumik, Aman, Balbeer, Arvind, Asish, Kaustav, Prahlad, Arthy, Jabir, Subhra, Manab, Deepika, Sangeeta, Satish, Ali, Naman, Debrup, Kuldeep, Harsh and a whole host of others too numerous to mention. I am thankful to Shrema for being the encouragement during my lowest times and helped me to overcome the situations whenever I was about to quit. I am thankful to Kaku and Kakima for their constant supports and encouragements and being my extended family.

I express my deep gratitude to Maa and Baba, who have kept faith in my dream during this period and provided the required strength to pursue it. I am thankful to Jethu, Boroma, Jhilik and all of my family members for being constant source of support.

Anirban Chatterjee

Abstract

Quaternary is the youngest period in Earth's history, spanning from 2.6 Ma to the present. The extreme climatic conditions during this period carved the earth-surface to its present form. The human civilization came into existence during the late phase of this period. Studying past environmental records is the best way to understand the geomorphic evolution during the Quaternary. The most faithful record keepers of the surficial processes are the sedimentary deposits. The western part of the Indian sub-continent is home to a huge repository of Quaternary sediments representing different climatic and geomorphic regimes. The well-watered floodplains of the Indus and its tributaries border the vast expanse of arid Thar Desert, devoid of any major rivers. Just south of the great sand sea lies the salt encrusted low lands of the Great Rann of Kachchh, unique of its kind, which was probably a shallow marine gulf during the early Holocene. Eastern boundary of the desert is demarcated by the alluvial deposits of seasonal rivers originating from the ancient mountain ranges of the Aravallis. In this enigmatic backdrop of extreme climatic conditions and contrasting landscapes, appeared the Bronze Age Harappan Civilization. In an attempt to understand the geomorphological evolution of these terrains and its role in the evolution of the Harappan Civilization, I have studied the sedimentary archives of this region in my Ph.D. The present work involves establishment of stratigraphy using field relationships and geochronology. Using trace element and isotope geochemistry, I have determined the sources of sediments in these vast sediment sinks and their depositional pathways, which are critical to our understanding of the evolution of the fluvial landscape during the Harappan period. My work involving the alluvium of the river Ghaggar, an ephemeral river located at the northern most boundary of the Thar, suggests that the river had a glacial past during the late Pleistocene. Sedimentary records indicate that the discharge in the river decreased during the last glacial maxima with deposition of locally reworked sediments by the channel. During the beginning of the Holocene, sediments originating from the glaciated Higher and Lesser Himalaya again started depositing in the Ghaggar alluvium. The pathways for the sediments were probably the distributaries of the Sutlej. This rejuvenated phase of the river sustained until the mid-Holocene (~5 ka), after which the river became a rain-fed ephemeral system. The beginning of the agro-pastoral farming settlements of the pre-Harappan people coincides with the

rejuvenated phase of the Gahggar during the early Holocene. Therefore, we believe that the reactivation of the river system triggered the nucleation of early settlements along the banks of the Ghaggar. However, before beginning of the mature Harappan phase, the river began having dwindling water supply. This led us to conclude that the demise of the river may not be a triggering factor for the decline of the mature Harappan phase. Our geochemical provenance study of the sedimentary deposits of western Great Rann of Kachchh indicates that a continuous Ghaggar-Hakra-Nara channel used to deliver sediments into the GRK until about 1 ka. The deposition, however, was not continuous and was related to occasional monsoonal floods only. Therefore, the ephemeral channel of the Ghaggar river continued to exist up to ~1 ka even though the river system started declining dring the mid-Holocene. The geochemical provenance study of the sediments deposited along the margins of the rocky islands of the eastern GRK indicates that the sediments in this part of the basin were derived locally. We also found that the depositional environment of these sediments was mainly estuarine. The study involving the source identification and quantification of the Thar desert sand reveals that the desert sand was mainly derived from local sources, contrary to that previously proposed: a distant Indus delta. The influence of the Indus river derived sediments are maximum in the western margin of the desert (up to 60%), which decreases significantly towards the eastern and central part of the desert. We determined that the sedimentary rocks of the Proterozoic Marwar Supergroup in Rajasthan were the major sediment contributors to the desert sand. Towards the south eastern part of the desert, the Luni river alluvium becomes the main source of the aeolian sand. The Luni river alluvium on the other hand received its sediments from the Aravalli ranges in the east. The main sources for the Luni sediments were the pockets of mafic/ultrafic rocks exposed along the western flank of the Aravalli ranges. Other major lithologies of this region (e.g. granitoids and felsic volcanics) contributed comparatively fewer amounts to the sedimentary budget. Rare Earth Element (REE) composition of the Luni river sediments suggests that their abundances are primarily controlled by the weathering intensity and sediment sorting. The incipient chemical weathering and dominant physical weathering in the catchment region might have been the main reason for this.

Contents

Chapter – 7

Chapter – 1

Introduction

1.1 The youngest period of the Earth

Quaternary is the youngest period in Earth's history, spanning from 2.6 Ma to the present (Walker et al., 2013). During this interval the global climate had changed frequently and dramatically, with alternating cold ice ages and warm interglacial periods (Richards and Andersen, 2013). The extreme climatic conditions carved the surface of the earth to create fascinating landscapes. Towards the end of the Quaternary (~ 0.2 Ma), anatomically modern humans appeared on this planet and finally the earth witnessed the dawn of human civilizations. Therefore, Quaternary is not only a period of mesmerizing geological changes but also a period of human-nature interactions. People of twenty-first century are witnessing the latest phase of the Quaternary, known as Holocene when Earth is experiencing an unusually warm climate. The geological consequences of the rapid climatic change have its own potential dangers to the human habitability on this planet. Therefore, scientists from multiple fields of research are involved in studying dynamic changes of this youngest phase of the earth. One of the best ways to understand the future course of the changing earth is to study the ancient environmental archives which preserve the effects of past changes. The most faithful record keepers of the surficial process are the sediments. They preserve records of various geo-tectonic and climate induced surface processes as well as biological activities. In addition, they also preserve traces of mankind's evolution. The effects of climate induced surficial processes (e.g, glacio-fluvial, aeolian activities etc.) which mould earth's crust are more prominent and well preserved during the Quaternary than any other geological periods (Richard and Anderson, 2013) because, tectonics plays a minor role in continental re-distributions during short timescales. Although, the Quaternary period is geologically well studied, a lot of questions pertaining to how the coupling of climate and tectonics shapes the landscapes that ultimately influences the course of human civilizations have remained unanswered. Therefore I undertook this study of geochemical and isotopic investigation of late Quaternary sedimentary archives of western India to answer some of these questions particularly those related to the interplay of climate, geomorphology and human civilization.

1.2 Sediment provenance and Landscape evolution

One of the important steps to understand the landform evolutionary processes is to decipher the sources and transport pathways of the sediments that form the integral part of the

landscapes. The study of sediment provenance basically deals with the identification of possible sources and reconstruction of the past climatic and physiographic conditions under which the sediments got generated and transported to the sink. In general, deciphering the provenance of sediments in a given basin which might have been derived from multiple sources is a complex affair. The study becomes further complicated due to various sedimentary processes and post-depositional alteration those after the original source signatures. The initial studies on sediment provenance began in the 19th century, however, most of these were qualitative and primarily depended on mainly heavy mineral assemblages and petrography (Judd, 1886; Mackie, 1899a, 1899b; Thurach, 1884). The next century witnessed the advancement in provenance investigations when attempts were made to quantify the source contributions and identify source tectonic settings from mineralogical assemblages (Pettijohn et al., 1972). Geochemistry as a tool for studying sedimentary archives became important in the late 20th century. Several workers used sedimentary geochemistry to calculate the composition of continental crust as well as quantifying provenance (Bhatia, 1983; Bhatia and Crook, 1986; Roser and Korsch, 1986; Taylor and McLennan, 1985). It is now a common practice to use chemical composition of sediments for identifying provenance, interpreting tectonic settings at the source region and reconstructing the prevailing climatic conditions during sediment generation and deposition. Trace elements, especially the Rare Earth Elements (REEs) are known to behave as a chemically coherent group and are useful in deciphering the sediment provenance due to their non-fractionating behaviour during weathering or diagenesis (Taylor and McLennan, 1985). Similarly, Sr-Nd isotopic compositions of the sediments have been used to fingerprint the source signature of sediments. Although, Sr isotopes are reported to get altered during extensive chemical weathering, abundances of Nd isotopes do not undergo any change during weathering, transportation and diagenetic processes (Basu et al., 1990; DePaolo, 1988; Gleason et al., 1994; Miller and O'Nions, 1984; Nelson and DePaolo, 1988). The combined Sr-Nd isotopic systematics is one of the most robust and popular tool for determining sedimentary provenance. In the recent decade Pb-Pb geochronology of the detrital zircons has also become a popular tool for such studies. In the present work, attempts have been made to understand the sediment sources and their depositional pathways using trace element geochemistry and Sr-Nd isotopic ratios of bulk sediment as tools.

Figure 1.1: Google Earth image of the western Indian subcontinent, showing the major Quaternary geomorphic terrains.

1.3 Quaternary of Western India

The Quaternary sedimentary deposits can be found almost all over the globe. However, the interest of this work is to study a region where multiple Quaternary geomorphological provinces representing various environmental conditions have coexisted together and have played a major role in building up the history of humanity. Such a unique combination can be found in the Indian sub-continent. The western part of the Indian sub-continent is home to a unique repository for Quaternary sediments representing different climatic and geomorphic regimes (Fig. 1.1). Originating from the Higher Himalayas, five perennial rivers of Punjab flow towards south-west, and meet the river Indus at Mithankot in Pakistan creating one of the most fertile and well-watered interfluves of the world. Surrounded in the north and west by the floodplains of the mighty glacial-fed rivers, lies the vast expanse of arid Thar Desert, covered with aeolian sands and is devoid of any major rivers. Just south of the great sand sea lies the salt encrusted low lands of the Great Rann of Kachchh, unique of its kind, which was probably a shallow marine gulf during the early Holocene. The eastern boundary of the desert is demarcated by the Proterozoic Delhi-Aravalli fold belt. The semi-arid zone ephemeral rivers (e.g., Luni) originating from this mountain ranges create their alluvial deposits along the eastern fringes of the desert. In this enigmatic backdrop of extreme climatic conditions and contrasting landscapes, the seed of the first Indian civilization was sowed. On this very land, appeared the Bronze Age Harappan Civilization. The Harappan Civilization thrived along the floodplains of the Indus and associated rivers, now arid region of the Thar Desert and the Great Rann of Kachchh (Fig 1.2). The growth and decline of this pre-historic civilization was directly linked with the late Quaternary environmental changes and landscape evolutions in the western Indian sub-continent. However, there are debates over the exact factor(s) for the decline. Some believe that this civilization flourished along a mighty paleo-river called the Saraswati, originating in the Higher Himalayas, flowing through the now arid land of the Thar Desert and draining through the Great Rann of Kachchh into the Arabian Sea as an independent river parallel to the Indus, during ~5000-3500 years ago (Ghose et al., 1979; Valdiya, 2013). Many, however, postulate that the river had stopped flowing much before 5000 years ago and that the human settlements of the Harappan age occupied paleo-channels of this river (Clift et al., 2012; Giosan et al., 2012; Tripathi et al., 2004). Many workers consider the climatic changes and associated adversities caused the demise of the Harappans (Giosan et al., 2012; Sarkar et al.,

2016). The existence of the lost river and its association with the Harappans is still a matter of debate.

The present work makes an attempt to unravel some of the mysteries by trying to understand the overall landscape evolution in the western Indian sub-continent during late Quaternary using the sedimentary proxies from different environmental conditions as a window to the past of this land and its people.

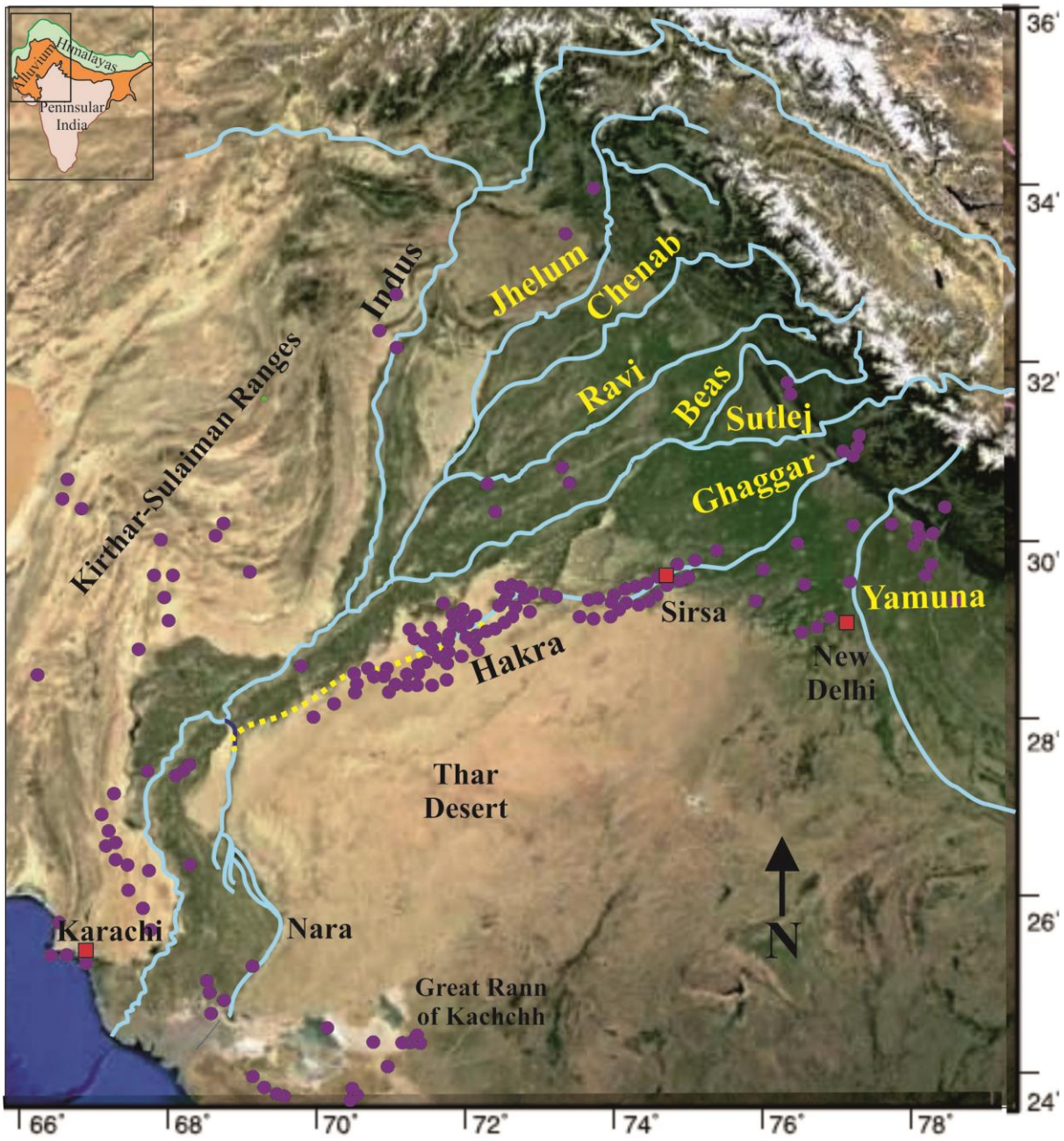

Figure 1.2: Settlement distribution of Harappan Civilization in the Western Indian sub-continent.

1.4 Quaternary sedimentary deposits of Western India

As discussed in previous sections, the western part of the Indian subcontinent hosts a unique combination of extreme geomorphological terrains which got developed primarily during the course of the Quaternary period. Brief introductions to each of the western Indian Quaternary landscapes are provided below. The geology, previous work and evolution of these terrains will be discussed in detail in the subsequent chapters.

- ***The Ghaggar Floodplain***: Just below the foothills of the Himalayas lie the vast Indus-Ganga-Brahmaputra floodplains. Numerous glacier-fed and rain-fed rivers flow within these plains. If we look only at the western part of the plain, we can see a clear drainage division (Fig 1.3A). The five rivers of Punjab (Sutlej, Beas, Ravi, Chenab and Jhelum) flow towards the west and meet the river Indus, which flows into the Arabian sea. On the other hand, Yamuna and its tributaries meet the Ganga and flow towards east into the Bay of Bengal. In between the Sutlej and Yamuna interfluve lays the floodplain of a small ephemeral river called the Ghaggar. Apparently insignificant, this river channel has a fascinating yet debated past. This river has often been associated with the previously discussed paleo-mega river (Saraswati) which has been hypothesised to water the Harappan heartland. The decline of the river system was probably due to river piracy and increased aridity or some other reason that is yet to be discovered. The present day small river channel of Ghaggar is therefore archaeologically significant. More than a century of scholarly works have been done on this area. However, due to lack of robust chronological and geochemical data, the antiquity and past nature of the river are still being debated. In the present study an attempt has been made to resolve these issues.
- ***The Great Rann of Kachchh***: The Quaternary terrain of the Great Rann of Kachchh is situated at the western most end of India (Fig. 1.3B). It is a monotonously flat, salt encrusted and desolate landscape. The sediment deposition in the GRK began in an extensional setup during the Mesozoic and continued through the Quaternary (Biswas, 1987). However, during the course of this deposition subsequent to India-Eurasia collision, the basin changed from an extensional regime to a compressional. The GRK basin was part of a shallow marine gulf even during the pre-historic times and played a major role in the maritime activities when the Harappans settled in this area (Merh, 2005). The GRK is also

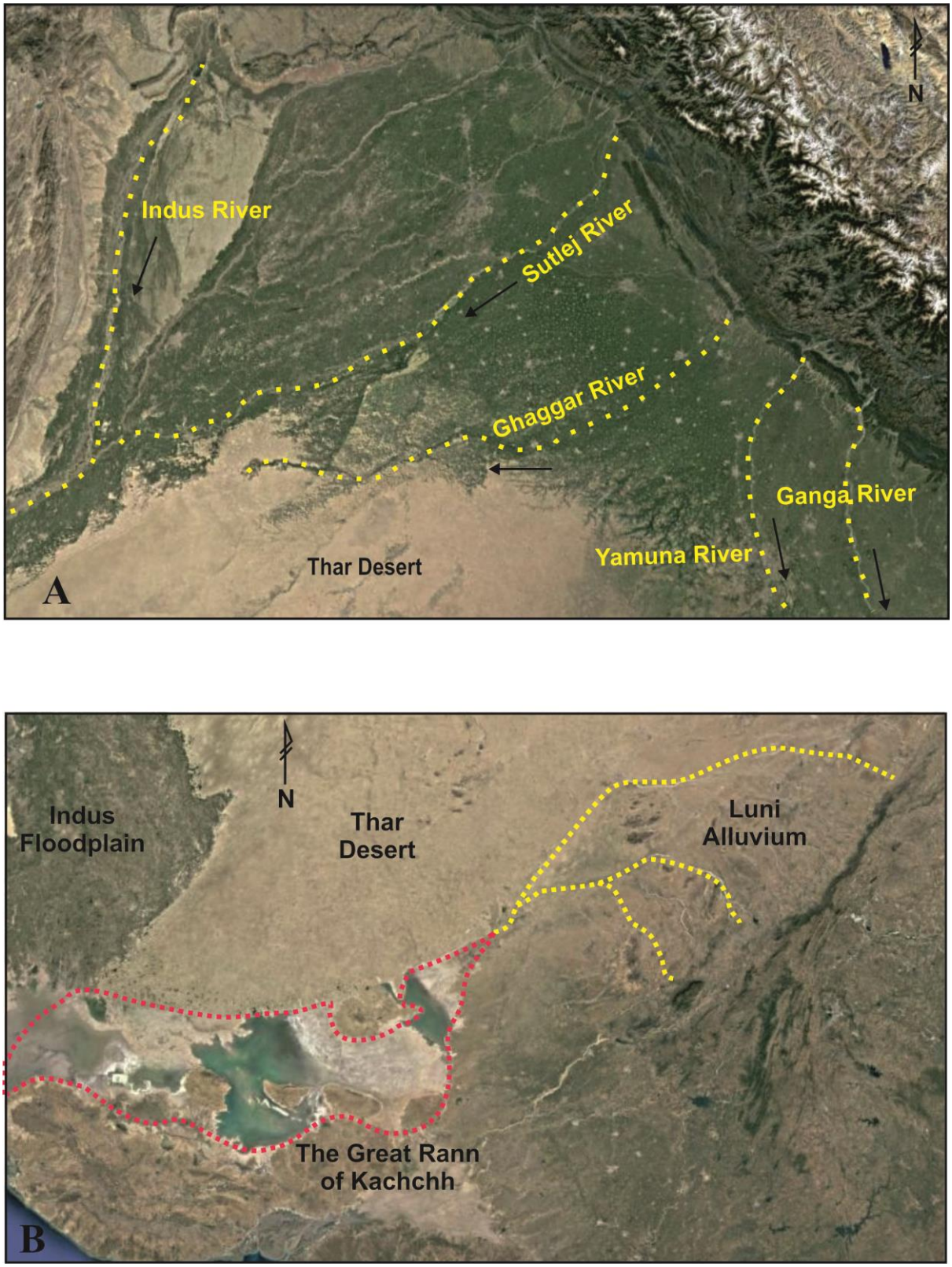

Figure 1.3: (A) River network in the Indus-Ganga floodplains. The Ghaggar river can be seen as a small discontinuous channel flowing in the drainage divide between the Sutlej and Yamuna interfluves.
(B) Google Earth image of the Luni river alluvium and the Great Rann of Kachchh.

hypothesised to host the purported delta of the mega glacial fed river (Saraswati) which used to flow through the now arid western parts of the Thar Desert (Malik et al., 1999). In spite of its geological and archaeological importance, very little is known about the source and depositional pathways of the sediments in the GRK basin. Therefore, in the current study emphasis is given on understanding the provenance of sediments in the GRK.

- ***The Luni River Alluvium****:* The only major drainage of the Great Indian Desert is the Luni river (Fig. 1.3B). The Luni is an ephemeral river which originates at the foothills of the Aravalli ranges and flows westward into the Great Rann of Kachchh. The Luni is an arid zone river system thus, responds rapidly to minor changes in climatic conditions. Many earlier workers have studied the climate controlled alluvium development of this river. However, very little is known about the geochemical composition and provenance of the Luni sediments. The sediments of the Luni floodplain are derived primarily through physical weathering. Besides the source rock geochemistry, different sedimentological processes and weathering intensity also control the chemical composition of sediments deposited in the basin. Therefore, in the current study attempts have been made to geochemically characterize the Luni alluvium and understand the control of climate, weathering and source lithologies, on the chemical compositions of the sediments.
- ***The Thar Desert***: The most enigmatic landscape of the western India is probably the Thar Desert which is the easternmost extension of the great Sahara-Arabian sand sea. Bounded in the north and west by the floodplains of major river systems, in the west by the Aravallis and in the south by the Great Rann of Kachchh, the Thar Desert stands as unique landscape (Fig. 1.1). Due to the arid climate, wind activity has been dominating this region and sand dunes have been forming over the past 200 kyrs (Dhir and Singhvi, 2012). During the last glacial maxima (LGM), expansion of the desert was the largest during entire existence. Towards south it had extended up to the Orsang valley, Gujarat (Juyal et al., 2006). Following the LGM the desert shrunk westward. At present, the most active part of the desert lies in its north and north-western sectors. A lot of efforts have been made on the understanding of the antiquity of the Thar Desert, dune dynamics and climatic control over the desert activities. However, knowledge on the sources of Thar sand is very poor. For understanding the development of the Thar, one major step would be to identify and quantify the provenance of the sand. Therefore, during the course of the present investigation, a reconnaissance geochemical study was carried out on the sub-surface sands from strategically selected locations that spread all across the desert.

1.5 Objectives and Approach

The present study aims to understand the origin and evolution of the thick sequence of Late Quaternary sediments in the western India. The specific objectives of my work to achieve the above were to:

- study the sediment provenance of the Ghaggar and the Luni river alluviums, the Great Rann of Kachchh and the Thar Desert
- recognise paleo-drainage patterns to decipher the fluvial conditions during the Harappan period
- understand the Paleo-environmental conditions and the response of fluvial systems to the changes in climatic conditions
- construct the late Quaternary landscape evolution of the western Indian sub-continent.

Approach: To achieve the objectives of this study several field and laboratory methods were employed. Field works were integral part of this study for establishing field relationship of different sedimentary facies based on stratigraphic principles and for collecting appropriate samples. Ages of the collected samples were constrained using several geochronological techniques (eg. C-14 and Optically Stimulated Luminescence dating). Further chemical analyses were performed after establishing the stratigraphy. For identifying and quantifying different sediment sources we have analysed the trace element geochemistry and Sr-Nd isotope geochemistry of the collected sediment samples. Also in the Ar-Ar age of detrital mica grains were analysed for the source identification purpose.

1.6 Thesis outline

The present thesis is divided into seven chapters.

- The ***First Chapter (Introduction)***, as already described above, provides an introduction to the Quaternary continental sediments deposited in the western Indian sub-continent and introduces the scope of the work and its importance in understanding of the landscape evolution of the region. It also lists the major objectives of this work.

- The ***Second Chapter (Methodologies),*** deals with sampling procedures and details of various analytical techniques used in this study.
- The ***Third Chapter (Evolution of the Ghaggar River System in NW India and its archaeological connection),*** presents the results of my geochemical and chronological studies on the sediments, shells and archaeological artefacts from the Ghaggar alluvium of NW India. Here, I discuss the evolution of the Ghaggar river system during the Late Quaternary and its connection to the development of the Bronze Age Harappan Civiliztion.
- In the ***Fourth Chapter (Provenance of Mid-Holocene Sediments in the Great Rann of Kachchh),*** an attempt has been made to delineate the provenances of the sediments deposited in the GRK basin since mid-Holocene using geochemical and isotopic tracers and to reconstruct the palaeo-drainage condition around this area.
- The ***Fifth Chapter (Geochemistry of Quaternary Alluvium in the Luni River Basin),*** focuses on the geochemical properties of the sediments deposited in the Luni river alluvium and the control of weathering on sediment composition. It also deals with the isotopic provenance identification of the Luni river sediments.
- In the ***Sixth Chapter (Geochemical Provenance of the Thar Desert Sand),*** an attempt has been made to identify and quantify the sources which contributed sands into the Thar Desert, using geochemical and isotopic tracers on aeolian sediments collected from all across the desert.
- The ***Seventh Chapter (Summary and Conclusions)***, summarizes important findings of the study and describes future research directions to further resolve the outstanding issues in the Quaternary evolution of the Western India.

Chapter - 2

Methodologies

To achieve the goals of this study several field and laboratory methods were employed. Field studies and collection of appropriate samples for various experimental studies were a key component of this work. Field studies were also aimed at establishing accurate stratigraphy of the sampled horizons. Experimental studies included geochronology, trace element geochemistry and isotope geochemistry. Since each chapter hereafter contains some details of the experimental data and these analytical methods are established techniques, only brief descriptions of each of the methods are given here with appropriate referencing.

2.1 Field studies

Strategic sampling was integral part of this work. The collection of the Quaternary sediment samples is tricky as the older sediment horizons are buried below the present day alluvium in most of the cases. For the current study, we have made our sampling strategy at the initial stages, based on the existing reports and satellite imageries which delineate the palaeo-drainages. During the course of the work we further explored the terrains with several field works and sampled new sediment horizons. The sampling was done during the period of 2013-2016 in several field works. The field areas included the Ghaggar floodplain, the Luni alluvium, the Thar desert, the Great Rann of Kachchh and the Aravalli mountain ranges. Sampling was mainly done from exposed cliff sections/terraces, pits, trenches made at field, bore holes, wells and dune fields. The detailed sampling locations and lithologs are presented in the subsequent chapters.

Before venturing into the provenance studies establishment of a proper stratigraphy is of utmost importance. The problem with the Late Quaternary sediment deposits especially those associated with fluvial systems is that they are spatially not continuous. Due to the highly dynamic character of the fluvial and aeolian environments and discontinuities in depositions, the events happening in a particular time period are not preserved in every location of these terrains. The events are preserved in pieces, all along the alluvium. Things become more complex in cases of buried paleo-fluvial systems (eg. the Ghaggar alluvium) where the present day surficial deposits cover the older horizons. Therefore, during the present work we have covered larger areas and several locations in particular alluviums for sampling. While doing so, we have emphasised on establishing the field relation between

various sedimentary facies based on stratigraphic principles. The depths of occurrence of different sedimentary facies are noted properly for preparing the lithologs. The details of the field co-relations and lithologs are discussed in subsequent chapters. The stratigraphy was further established with the help of C-14 and Optically Stimulated Luminescence (OSL) dating of different sediment horizons. For sampling the Thar desert sand we have taken several traverses across the desert.

2.2 Pre-treatment of samples before analysis

Various methodologies were used to generate analytical data for chronology and geochemistry, for achieving the objectives of the current work. Care was taken to avoid any type of contamination during the analyses. Prior to analysis all the collected samples have gone through several cleaning/pre-treatment procedures as follows:

- First the samples were grinded to very fine powder for homogenization and further processing.
- Samples were then washed with MILLI-Q water multiple times to remove salt and then dried at 110^{o}C. The samples were then re-homogenized using agate mortar.
- Powdered samples were then heated at 650^{o}C for 2 h to remove organic matter and leached in dilute HCl to remove carbonates.
- For all the geochemical and isotopic analyses we have used the silicate fractions only.
- For separation of various grains sizes we have passed the non-powdered samples through different sieves of required diameters. To separate the clay and silt sized fractions from the rest we used gravity separation technique. Once the desired grain size fraction is separated, it is treated following the above mentioned procedure before further chemical analysis.
- The decarbonated, homogenized powdered samples were then dissolved using standard HF-HNO_3 silicate dissolution procedure. The details are discussed in the subsequent sections of this chapter.

2.3 Geochronology

2.3.1 C-14 dating

In the arid to semi-arid climate of the western India, preservation of organic carbon within the sandy sediments is rare. We have focussed on collecting mollusc shells (bivalves and gastropods) buried along with the sediments for C-14 dating which can give a constrain to the sediment depositional ages. The mollusc samples collected for the C-14 dating were pre-cleaned with Milli-Q. Then the shells were soaked in H_2O_2 to remove any organic matter. Followed by it the shells were soaked in 0.1N HCl for a very short period to remove the outermost altered layer. For the AMS dating samples were drilled from the umbo region of the shells (generally least altered) using a micro-drill. Also, bulk sediments containing abundant foraminifera shells from the Great Ran of Kachchh, have been analysed for dating using conventional C-14 dating.

Radiocarbon dating was carried out on bivalve samples from Anupgarh region and inorganic carbonates of bulk sediments from Khadir island, to determine their ages by the conventional β-counting method at the PRL, Ahmedabad. 10 gm of powdered fresh bivalve sample was taken in an evacuated flask and reacted with Orthophosphoric acid. For the bulk sediments larger amount of sample was taken and then reacted with Orthophosphoric acid. The emitting carbon dioxide generated by the reaction was then converted to benzene. Then, its C-14 activity was measured using a liquid scintillation counter (Quantulus 1220). Radiocarbon dating was carried out by liquid scintillation spectrometry method at the PRL following procedures described in Yadava and Ramesh (1999). The half-life used for the conventional C-14 dating is 5730 years. Average $\delta^{13}C$ value used for fractionation correction for the foram bearing bulk sediments was 1.0 $^{0}/_{00}$ with respect to V-PDB. For the bivalve samples collected from the fluvial sands of the Ghaggar alluvium $\delta^{13}C_{PDB}$ was considered to be -10 $^{0}/_{00.}$

Further, for more precise dating of the bivalve samples, AMS C-14 dating was carried out at Centro Nacional de Aceleradores (CNA), Spain. The C-14 dates have been calibrated using INTCAL 13 curve of Reimer et al., (2013).

2.3.2 Optically Stimulated Luminescence (OSL) dating

Optically stimulated luminescence dating is a method to determine the depositional age of buried sediment horizons. It is considered that the geological luminescence reduces to a zero or near zero value due to sunlight exposure during the sediment transport (Aitken, 1998; Singhvi et al., 2001). Post burial the luminescence signal starts accumulating due to the ambient radioactivity and continues until the sediment is excavated. The luminescence level in a sample is proportional to the burial time and the concentration of the radioactivity in the sample environment, with a presumption that the rate of irradiation is generally constant. The sediment samples were collected from freshly cleaned up sections using specially designed aluminium pipes (Chandel et al., 2006). At the laboratory, all samples were processed in subdued red light conditions. The 90 – 125μm grain-size fraction was used for dating, after treatment with hydrochloric acid and hydrogen peroxide to remove carbonates and organic matter, respectively. Magnetic separation was carried out to isolate the quartz grains, and the resulting material was etched using hydrofluoric acid to remove the alpha-irradiated outer surface of the quartz grains and remove any non-quartz minerals still present. Using the Single Aliquot Regeneration (SAR) protocol proposed by Murray and Wintle (2000) the OSL dating of the separated quartz grains was done. The paleodose (De) measurements for age calculations were based on a weighted mean of values in the region defined by the minimum value and the minimum value + (2σ) (Juyal et al., 2006).

2.3.3 Ar-Ar dating of Detrital Muscovite

About 200 mg of muscovites are separated by handpicking from pre-cleaned sediments (grain size > 250 mm) was packed in aluminium capsules and irradiated in the DHRUVA reactor at BARC, Mumbai, for ~120 h. The Minnesota hornblende reference material (MMhb-1) of age 523.1 ± 2.6 Ma (Renne et al., 1998) was used as the flux monitor and high-purity CaF_2 and K_2SO_4 salts for interference corrections arising from the production of Ar from Ca and K isotopes (Pande et al., 2017). Argon was extracted by incremental heating between 750°C and 1400°C at steps of 50°C and isotopic ratios were measured in a Thermo Fisher ARGUS-VI multi-collector mass spectrometer at the National Facility in the Department of Earth Sciences, IIT Bombay, India (Ray et al., 2005). Plateau and isochron ages were calculated and plotted using the software ISOPLOT 2.49 (Ludwig, 2000). The Fisc

Canyan Sanidine (26.27-28.29 Ma) standard was used as an unknown sample and it gave an age of 28.24 Ma.

2.4 Trace element analysis

All the trace element concentrations including Rare Earth Elements (REEs) were measured on silicate fractions of bulk sediments using Thermo X-Series 2 Q-ICPMS facility, at Geosciences Division, of Physical Research Laboratory (PRL), India. The set-up, installation and calibration for routine measurement of rock samples were carried out during research activity (Ray et al., 2008). 50-60 mg of decarbonated samples were then dissolved using a combination of ultrapure HF and HNO_3 (2:1) acid mixture (Acids were from Seastar Chemicals®) in a Savillex Teflon vial. The sample was further treated with 8N HNO_3. Finally, a stock sample solution (~50 ml) was prepared using 2% HNO_3 with ~1000 dilution factor. An international rock standard from USGS, BHVO-2 was used to check the accuracy and precision of analyses. Several aliquots of BHVO-2 were digested and analysed as unknowns. Blank solutions and various dilutions of BHVO-2 were used to generate Calibration curves. Reproducibility of trace element contents, based on repeated analyses of the standard, was ≤3% for REEs and ≤6% for all other trace elements at 2σ level. Table 2.1 represents the BHVO-2 values from this study and the recommended values.

Table 2.1 Trace element data for BHVO-2 Standard. Concentrations are in ppm. Reproducibility (2σ): REE ≤ 3%; others ≤ 6%. Reported values for BHVO-2 are from Jochum et al. (2005).

Sample	BHVO-2 (Reported)	2σ	BHVO-2 (Measured)
Cs	0.1	0.1	0.12
Rb	9.11	0.04	10.3
Ba	131	1	130
Th	1.22	0.06	1.1
U	0.403	0.001	0.42
Nb	18.1	1	17
Ta	1.14	0.006	0.95
La	15.2	0.1	15
Ce	37.5	0.2	39
Pb	1.6	0.3	1.2
Pr	5.35	0.17	5.2

Sr	396	1	388
Nd	24.5	0.1	24
Zr	172	11	163
Hf	4.36	0.14	3.9
Sm	6.07	0.01	5.9
Eu	2.07	0.02	2
Gd	6.24	0.03	6.1
Tb	0.92	0.03	0.84
Dy	5.31	0.02	5.2
Y	26	2	23.4
Ho	0.98	0.04	0.89
Er	2.54	0.01	2.5
Tm	0.33	0.01	0.3
Yb	2	0.01	1.9
Lu	0.274	0.005	0.26

2.5 Analysis of Radiogenic Isotopes

The chemical procedures for the separation of Sr and Nd from samples and associated mass spectrometric analyses on Thermal Ionisation Mass Spectrometer (TIMS) and Multi Collector Inductively Coupled Plasma Mass Spectrometer (MC-ICP-MS) are mentioned only briefly in this section as they were based on already established routine procedures of our laboratory.

In Sr-Nd isotope analyses, decarbonated sediment samples were dissolved using the standard HF-HNO_3-HCl dissolution procedure for silicate rocks, as discussed in the earlier section. Separation of Sr was done by conventional cation exchange column chemistry (Resin AG® 50W-X8, 200-400 mesh size) and Nd was separated from other REEs using Ln-specific resin from Eichrom® with dilute HCl (0.18N) as elutant (Awasthi et al., 2014; Dickin, 2000). In case of Sr isotopic measurements of the mollusc shells, ~50mg of sample was dissolved using HCl and then was passed through Eichrom Sr-specific resin. The Sr was collected with Milli-Q elutant. $^{87}Sr/^{86}Sr$ and $^{143}Nd/^{144}Nd$ were measured in static multicollection mode on an Isoprobe-T thermal ionization mass spectrometer (TIMS) and Thermo Neptune Multicollector-Inductively Coupled Plasma Mass Spectrometer (MC-ICPMS) respectively, at the PRL, Ahmedabad (Awasthi et al., 2014). Sr samples were loaded with 0.1 M phosphoric acid on pre-degassed, oxidized single Ta filaments while Nd samples were loaded on the outer Ta filaments of triple (Ta-Re-Ta) filament arrangements for the TIMS measurements.

The measured isotopic ratios were corrected for fractionation using $^{86}Sr/^{88}Sr = 0.1194$ and $^{146}Nd/^{144}Nd = 0.7219$, respectively. The average values for NBS987 and JNdi measured on TIMS over a period of 5 years are $^{87}Sr/^{86}Sr = 0.71023 \pm 0.00001$ (n = 70) and $^{143}Nd/^{144}Nd = 0.512104 \pm 0.000004$ (n = 60; ±0.1 in εNd units) at 2σ level of uncertainty. The value of $^{143}Nd/^{144}Nd = 0.512104$ for JNdi corresponds to a value of 0.511847 for the widely used La Jolla Nd standard (Tanaka et al., 2000). USGS standard BHVO-2 was analysed for $^{87}Sr/^{86}Sr$ and $^{143}Nd/^{144}Nd$ during the course of the analyses regularly with each set of samples. $^{87}Sr/^{86}Sr$ and $^{143}Nd/^{144}Nd$ for BHVO-2 measured gave values of 0.70346 ± 0.00004 and 0.512967 ± 0.000008 (n = 10; ±0.2 in εNd units at 2σ) respectively, which are same as the reported values of 0.70344 ± 0.00003 and 0.51296 ± 0.00004 within 2σ (Raczek et al., 2001). To compare our data with that from literature, all the $^{87}Sr/^{86}Sr$ and $^{143}Nd/^{144}Nd$ ratios were normalized to 0.71025 for NBS987 and 0.511858 for La Jolla, respectively. The average $^{143}Nd/^{144}Nd$ of the in-house lab standard, Merck Nd solution, was 0.511705±27 (2σ, n=56) for the MC-ICPMS measurements. The sample data were normalized using its reported $^{143}Nd/^{144}Nd$ ratio of 0.511734, which is equivalent to La Jolla $^{143}Nd/^{144}Nd$ ratio of 0.511858 (Yang et al., 2011). BHVO-2 yielded $^{143}Nd/^{144}Nd$ ratio of 0.512971±18 (2σ, n=19), which is within the reported $^{143}Nd/^{144}Nd$ ratio of 0.512979±28 (2σ), (Jochum et al., 2005). All plots and discussion in this work are based on the normalized ratios. $^{143}Nd/^{144}Nd$ ratios in this work are presented as ε_{Nd}. It is defined as, $\varepsilon_{Nd} = [(^{143}Nd/^{144}Nd)_{sample}/ (^{143}Nd/^{144}Nd)_{Chondrite}-1] \times 10^4$. The present day $(^{143}Nd/^{144}Nd)_{Chondrite}$ value is considered to be 0.512638.

Chapter – 3

Evolution of the Ghaggar river system in NW India and its archaeological connection

3.1 Introduction

The Ghaggar River of north-west India is a mostly defunct small ephemeral river system, originating in the Siwalik Himalayas near the Indian city of Chandigarh (Fig. 3.1). At present it gets flooded occasionally during the high monsoonal rains and mainly carries suspended sediments, reworked from older deposits of the interfluve (Singh et al., 2016a). Soon after crossing the state of Rajasthan, the dry river-bed (known as Hakra at downstream) vanishes in the Cholistan desert of Pakistan. It is one of the numerous foothill-fed rivers which flow in the interfluves between the mighty glacier-fed rivers of the vast Indo-Gangetic-Brahmaputra plains (Sinha and Friend, 1994). In spite of being small and mostly dry, the river valley has attracted a lot of attention because of its unique geological past and archaeological connection. More than a century of scholarly works have confirmed the existence of a network of buried paleo-channels along the Ghaggar-Hakra valley (Valdiya, 2017 and the references therein) indicating a strong fluvial past unlike the present scenario. These ancient water courses remain the centre of debate as they are speculated to be the relicts of an ancient glacier fed river and often been correlated with the mythical lost river Saraswati, first described in the three millennia old scriptures of Rig-Veda (Ghose et al., 1979; Kochar, 2000; Oldham, 1893; Pal et al., 1980; Radhakrishan and Merh, 1999; Valdiya, 2013). It is considered by many that this dramatic transformation of the river has occurred very recently, during the mid-Holocene, due to regional reorganisations of major Himalayan Rivers induced by neo-tectonics (Valdiya, 2013 and the references therein).

With the discovery of the Bronze Age Harappan/Indus Valley tradition the problem became more intriguing. Years of archaeological excavations indicated that, apart from the Indus River valley, a great majority of the Harappan settlements were concentrated along the dry beds of Ghaggar-Hakra river system (Misra, 2001; Stein, 1942). Considering the fact that availability of water is one of the key requirements for the development of civilizations, it can be considered that the ephemeral Ghaggar-Hakra stream must have had a strong fluvial history during the Indus Valley tradition. One of the two main hypotheses suggests that the drying up of Ghaggar-Hakra River owing to drainage reorganisation, could be a triggering factor for the sudden and puzzling decline of the Harappans four millennia ago (Kenoyer, 2008; Misra, 1984; Mughal, 1997; Possehl, 2002; Wright et al., 2008). But controversies do not cease to surround this lost river and its pre-historic civilization. Non-availability of relevant geochemical and geochronological data makes it difficult to constrain the antiquity

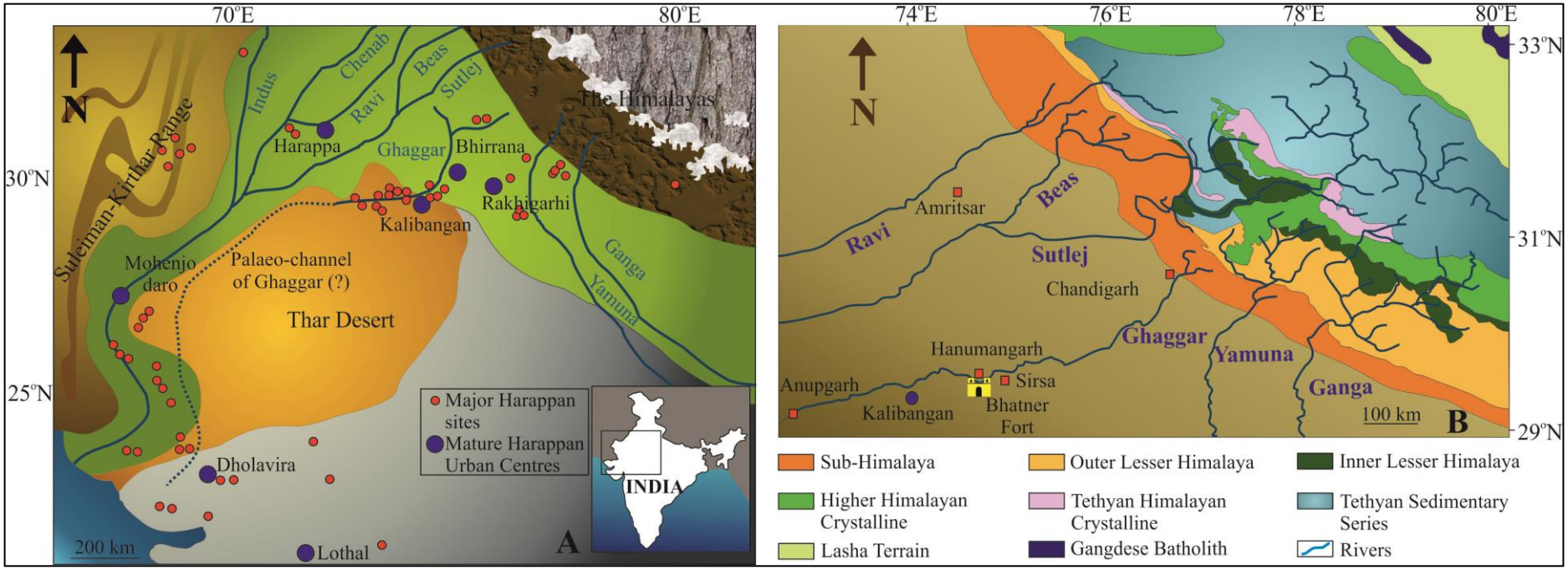

Figure 3.1: (A) Regional geomorphological map of north-western India showing the major landscapes. The putative course of paleo-Ghaggar is shown as dotted line and the pre-historic Harappan settlements are shown. Map is modified after Sarkar et al., 2016.
(B) Different litho-tectonic units of the Himalayas from where different western Indian rivers have originated. Also shown are the positions of Kalibangan and Bhatner Fort on the bank of the Ghaggar. Map is modified after Singh et al., (2016a).

of the fluvial past.

The other competing hypothesis argues that the geomorphic changes in the Ghaggar river valley had occurred much earlier during the Pleistocene (prior 10 ka) and the channels were abandoned at about 4-5ka (Clift et al., 2012). These studies also suggest that the river had already become foothill-fed monsoonal river and lost its glacial sources by the time Harappans settled on its banks (Clift et al., 2012; Giosan et al., 2012; Tripathi et al., 2004). Finally, the declining monsoon during mid-Holocene was detrimental for both the river and the civilization. This hypothesis however, cannot explain the younger fluvial activities (2.9-0.7 ka) which have been reported both from upper and lower Ghaggar-Hakra floodplains (Giosan et al., 2012; Saini and Mujtaba, 2012). Because a meandering river system frequently changes its course and creates numerous abandoned channels and therefore, depositional ages of sand from only a few sections may not reveal the true temporal extent of the river (Valdiya, 2013), and therefore, the issue of the paleo-fluvial condition of Ghaggar river and its archaeological connection remains far from settled.

For the present study, we sampled sub-surface sand bodies present beneath the modern Ghaggar-alluvium between Hanumangarh and Anupgarh along a stretch of ~120 km (Fig. 3.1). Using OSL and radiocarbon dating methods we constrained the ages of deposition of these sand bodies. We also studied trace element and Sr-Nd isotopic characteristics to constrain their provenance. Further, Ar-Ar ages of samples of detrital muscovite grains from these sand bodies were determined and used as source indicators, because white micas of different litho-tectonic units of Himalaya represent distinct chronological events. In addition to sediments, we also studied isotopic composition of archaeological artefacts to shed light on the living environments of the pre-historic people in the region. Ancient potters generally used materials available in their near geographical vicinity to create potteries (Krishnan, 2002). In case of the Indus valley tradition, source material for the potteries would have been the abundant flood-plain sediments deposited by the rivers on whose bank the Indus valley cities were built. Therefore, one would expect that the geochemical composition of potteries retrieved from the Ghaggar valley would provide insight into the sediment composition of the river during that period.

3.2 Background and earlier work

3.2.1 Palaeo-hydrological condition of the Ghaggar

The search for a lost river in the Indian desert goes back to at least two centuries, when British geographers were surveying their newly occupied colony. C. F. Oldham first traced the dry beds of the Ghaggar-Hakra and its tributaries. It was he who first proposed that the Sutlej used to flow through the Ghaggar channel during historic times (Oldham, 1893). It was hypothesised that the Ghaggar-Hakra used to be a parallel river system to the Indus, flowing separately all the way down to the Arabian Sea. The following centuries saw a plethora of scientific investigations in the Ghaggar valley that led to the discovery of chalcolithic Harappan civilization along the dry beds of this river. Based on geomorphological and archaeological evidence earlier workers had proposed a perennial glacieal-fed, through the Sutlej and Yamuna, Ghaggar river system (mythological Saraswati?) which ultimately got defunct due to river piracy. With the advance of satellite-radar imagery the search for the dry channels of the lost river became more intense during the last few decades. Ghose et al., (1979) and Gupta et al., (2011) based on such imageries proposed the existence of several buried palaeo-channels along the Ghaggar-Hakra flood-plains extending upto the Graet Rann of Kachchh. Several scholars have also attempted to reconstruct the buried paleo channels of the Upper Ghaggar alluvium based on geophysical and field surveys (Saini et al., 2009; Sinha et al., 2013) and they found evidence for existence of a multi-channelled mega-fluvial system during the Pleistocene and a smaller fluvial system during the mid-Holocene near Sirsa, Haryana. However, based on radar topographic studies and the existing knowledge on the dynamics of the Harappan settlements, Giosan et al., (2012) first proposed that the Ghaggar-Hakra river never had any glacier source during the Holocene and by the time early Harappans settled there, it was only a foothill fed monsoonal river. Studies based on U-Pb dating of detrital zircons in the middle reaches of the Hakra suggested that the Sutlej, Yamuna and Beas rivers were once tributaries of the Ghaggar-Hakra river making it a perennial one (Clift et al., 2012). However, these studies also suggested that the perennial glacier fed tributaries of the Ghaggar reorganised themselves to their present position abandoning the Ghaggar channel prior to 10 ka, and during the mid-Holocene (~4-5 ka) the Ghaggar River ceased to flow, eventually getting buried by progressive Thar Desert dunes by 1.5 ka. On the other hand, geochronological studies in the upper reaches of the Ghaggar

suggested that the river was active until 2.9 ka (Saini et al., 2009; Saini and Mujtaba, 2010). In the absence of geochemical data these studies couldn't conclude on the provenance of these younger sediments. Other workers have also reported fluvial activities in the lower Ghaggar-Hakra floodplains (kown as Nara River) until about 700 years ago conforming to the earlier idea of C. F. Oldham (Giosan et al., 2012; Ngangom et al., 2012). However, these later studies described these younger fluvial activities to have been driven by increased Monsoon. Recent work of Singh et al., (2016a), proposed that the sediments of the Ghaggar-Hakra river were sourced from the glaciated higher and lesser Himalayas with the higher-Himalayan inputs in younger sediments. Thus, at present the fluvial history of the Ghaggar-Hakra remains inconclusive.

3.2.2 The Harappan settlements along the Ghaggar

The Indus Valley/Harappan cultural tradition developed along the North-Western Indian sub-continent during the mid-Holocene (Fig. 3.1). People of this culture settled over an area larger than the contemporaneous Mesopotamian and Egyptian civilizations. The duration of existence of this culture, based on radiometric dates from Harappa and nearby localities, have been divided into four phases/periods (Kenoyer, 1998; Wright et al., 2008; Dikshit, 2013). Around 5.7 ka agro-pastoral Ravi culture flourished, followed by the transitional Kot Diji Phase (~4.8 ka). The sophisticated urban civilization of the Mature Harappan phase started around 4.6 ka and disintegrated at ~3.9 ka, followed by a de-urbanisation era of Late Harappan phase that lasted until ~3.3 ka. Possehl, (2002) on the other hand, had proposed a much older age for the Harappan culture based on spatio-temporal distribution of archaeological remains that spread across the Indian sub-continent. Earlier, Mughal, (1997) had reported such older pre-Harappan settlements along the Hakra river of Cholistan desert and named it as the Hakra Phase. Later, numerous other sites of the Hakra phase were discovered along the dry beds of the Ghaggar (the upstream continuation of the Hakra) including Kalibangan (the present study site), Farmana, Bhirrana and Rakhigarhi. Based on available chronological information the antiquity of the Hakra Phase can be pushed back to ~ 9.5 ka (Sarkar et al. 2016 and the references therein). It is also believed that the Early mature Hrappan phase has started a few millennia earlier (~6.5 ka) in the Ghaggar-Hakra valley compared to that in the Indus valley (Possehl, 2002). Indeed in a study on spatio-temporal evolution of the Hrappan settlements Gangal et al., (2010) has demonstrated that 7 ka onwards settlements had started flourishing in three distinct geographical locations

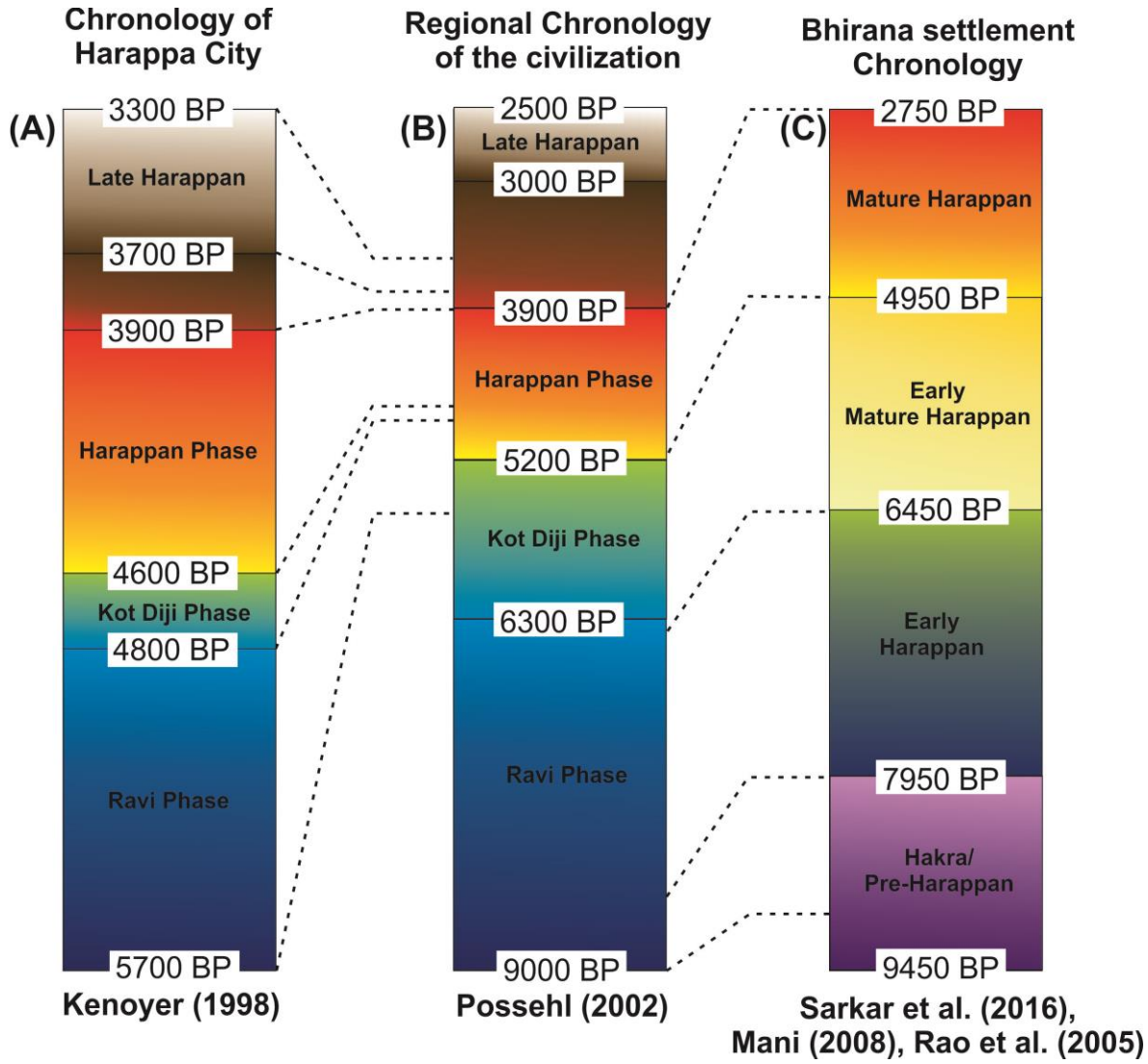

Figure 3.2: A comparison of chronologies of various phases in the Harappan cultural centres.
(A) Hrappan cultural chronology based on the cultural layers and dating from the acropolis of Harappa (Kenoyer, 1998).
(B) Hrappan cultural chronology inclusive of all regional settlements (Possehl, 2002).
(C) Hrappan cultural chronology based on the cultural layers and dating from the acropolis of Bhirana (Mani, 2008; Rao et al., 2005; Sarkar et al., 2016).

separated from each other in the Baluchistan region, the Ghaggar plain and the Gujarat region. Subsequent to this period saw a steady increase in the density of settlement, in these three localities. Surprisingly, the first settlements along the Indus river system started developing only during 5.2 ka, prompting the experts to suggest that the urban settlements of lower Indus-valley were the extensions of the Baluchisthan and Ghaggar settlements (Gangal et al., 2010). Finally, the civilization reached its zenith during 4.5 ka. From 3.9 ka onwards the de-urbanisation started and the density of settlement started decreasing in the main centres. It is observed that the Harappan settlements gradually shifted north-eastward to the upper Haryana plains during this period (Gangal et al., 2010; Giosan et al., 2012). A comparison of chronologies of various phases in the Harappan cultural centers is shown in figure 3.2.

During the course of the present study, we have visited Kalibangan which is one of the important Harappan cities situated on the southern bank of the river Ghaggar (Fig. 3.1B) and has a continuous history since the Hakra Phase, up to the Late Harappan (Thapar, 1975). The oldest dated sequence of Kalibangan is 7.6 ka (Sarkar et al., 2016). The settlement has two fortified sections, the Citadel (KLB-I) and the lower city (KLB-II) located to the east of the citadel (Fig. 3.3A). The Mature Harappan settlements are found over the ruins of the Hakra Phase in KLB-I mound, whereas, the mound of KLB-II is represented by only the former. Figure 3.3B shows the mound of KLB-II as photographed during our field work in 2014. The remains of brick walls and terracotta pipelines can be seen in Fig. 3.3C. To understand the source of the clay used in making the potteries and bricks by the Mature Harappans we restricted our sampling to the KLB-II mound. Photographs of some of these samples are shown in Fig. 3.3D.

The Ghaggar-Hakra valley was later re-occupied by the Painted Grey Ware sites during 3.0-2.6 ka. Also during the Medieval period fortifications were made along these floodplains (Mughal, 1997). The Bhatner Fort (12^{th} century AD) of Hanumangarh is one of them (Fig. 3.1B). For the present study we also sampled bricks from this fort.

Figure 3.3: (A) The settlement map of the Harappan acropolis of Kalibangan. Map is modified after Thapar (1975).
(B) The KLB-II mound of Kalibangan as photographed during field work in 2014.
(C) The remains of brick walls can be seen through the gaps in the mound. In the inset image terracotta drainage pipes can be seen.
(D) Samples of Mature Harappan potteries collected from the KLB-II mound.
Figures are modified from Chatterjee and Ray, (2017a).

3.3 Results and Discussion

3.3.1 Facies architecture of the Ghaggar alluvium

At present the course of the Ghaggar River is very difficult to trace downstream because of heavy irrigation and shallow channel chocked with heavy suspended load. The flood plain topography is monotonously flat land with aeolian dunes. The dry bed of the river can only be discretely recognised by ridges of discontinuous sand dunes bordering the floodplain. Interestingly, the subsurface sedimentary facies is quite different from what appears on the surface of the dry river bed. Figure 3.4 presents a comparison of the subsurface stratigraphy from different localities along the flood plain, constructed using field data from the present and earlier works. Samples for this study were collected mainly from shallow dug pits and wells along the 250km stretch of the Ghaggar alluvium (Fig.3.4).

Sampling locations are also shown in the figure. Following inferences can be drawn from the field observations in the Ghaggar alluvium.

- Layer of brown silty-clay occurs as the topmost alluvium cover. Its thickness varies from 10 – 20 m at different locations along the alluvium. The brown silty-clay directly overlies either a yellowish-brown fine fluvial sand deposit or a grey micaceous sand deposit.
- A detailed clay mineralogical study has been conducted by Alizai et al., (2012) which characterises the clay depositions of the Ghaggar alluvium, further downstream at Fort Abbas, Marot and Tilwala in Pakistan (Fig. 3.5). Considering that no tributaries join the Ghaggar downstream beyond Shatrana, it can be inferred that the clay mineralogical composition should have remained similar all along the floodplain. As suggested by Alizai et al., (2012) the most abundant clay mineral in the Ghaggar alluvium is smectite (51-59%), followed by illite (30-37%). The minor constituents are chlorite (5-7 %) and kaolinite (2-5%). It can be observed in figure 3.5 that the abundances of these four clay minerals had remained spatially and temporally invariant during the Holocene. The presence of illite as a major clay indicates that the sediments were sourced from the Himalaya where physical weathering dominates. On the other hand dominance of smectite, which is primarily a product of chemical weathering, is not in accordance with a Himalayan source where chemical weathering is very less. Such a scenario can be explained by two-cycle weathering (Singh et al., 2005), one at the source and the other within the floodplains with smectite being generated in the latter as a result of chemical weathering.
- During the course of present work, we encountered layers of sub-surface grey micaceous sand body all along the Ghaggar flood-plain. Raikes, (1968) first reported the occurrence of a thick body of coarse micaceous grey sand, resembling to the sediment carried by modern glacier-fed rivers like Ganga or Yamuna, buried below layers of silty-clay floodplain deposits of the Ghaggar near Kalibangan. Similar facies has also been reported from several other locations of the floodplain (Saini et al., 2009, Saini and Mujtaba, 2010, Singh et al., 2016a). The coarse and immature character of these sand layers probably represents their bed load and bears the testimony of being part of an extinct active fluvial system. The contact between the grey sand and overlying brown silty-mud is very sharp. In places root-casts can be observed along the contact. All observations suggest a depositional hiatus after the deposition of the grey sand. Quartz is the most dominant mineral in the grey sandy facies, followed by feldspar and muscovite. Accessory phases include biotite,

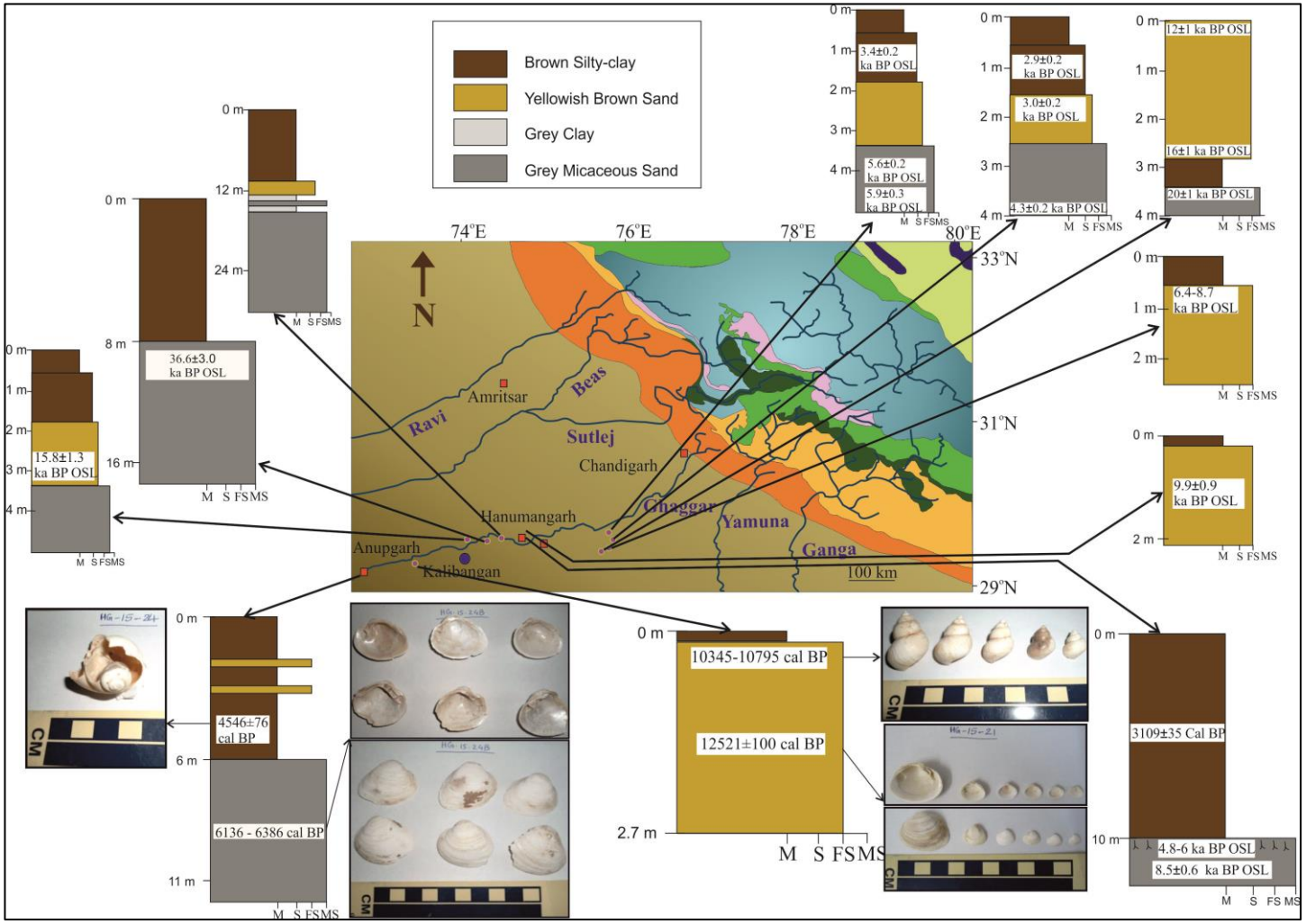

Figure 3.4: A comparison of the subsurface stratigraphy from different localities along the Ghaggar floodplain, constructed using field data from the present and earlier works. The sampling locations associated with each litho-section are marked with arrows in the map. The chronologies of different sedimentary horizons are mentioned alongside the stratigraphic columns. Also images of different bivalve and gastropod shells used for AMS C-14 dating are shown and the horizons from where the shells were collected are marked.

amphibole, kyanite, sillimanite, garnet and pyroxene (Saini et al., 2009). The clay content of the grey micaceous sand is almost negligible implying that these were high energy depositions.A typical facies association of grey micaceous sand and overlying floodplain deposits in trench sections across the Ghaggar alluvium is shown in figure 3.6A. Figure 3.6B represents the typical appearance of the Grey micaceous sand and the Brown clay observed in the Ghaggar alluvium.

- In three of the sections, the grey micaceous sand is found to be overlain /intercalated by a layer of grey clay. The thickness of this grey clay is much less than that of the brown silty-clay deposits.
- At other places these grey fluvial sand horizons are overlain by yellowish-brown fine fluvial sands. These fine fluvial sands appear to have been deposited by a weaker phase of fluvial activity and sediment reworking from local dunes and generally occur in fining upward sequences, overlain by silt and followed by clay horizons. Mineralogically, these sand deposits are predominantly composed of quartz and feldspar. Unlike the grey sandy facies, mica is less abundant and occurs as fine round-edged grains (recycled).
- In three of the sections, the grey micaceous sand is found to be overlain /intercalated by a layer of grey clay. The thickness of this grey clay is much less than that of the brown silty-clay deposits.
- At other places these grey fluvial sand horizons are overlain by yellowish-brown fine fluvial sands. These fine fluvial sands appear to have been deposited by a weaker phase of fluvial activity and sediment reworking from local dunes and generally occur in fining upward sequences, overlain by silt and followed by clay horizons. Mineralogically, these sand deposits are predominantly composed of quartz and feldspar. Unlike the grey sandy facies, mica is less abundant and occurs as fine round-edged grains (recycled).

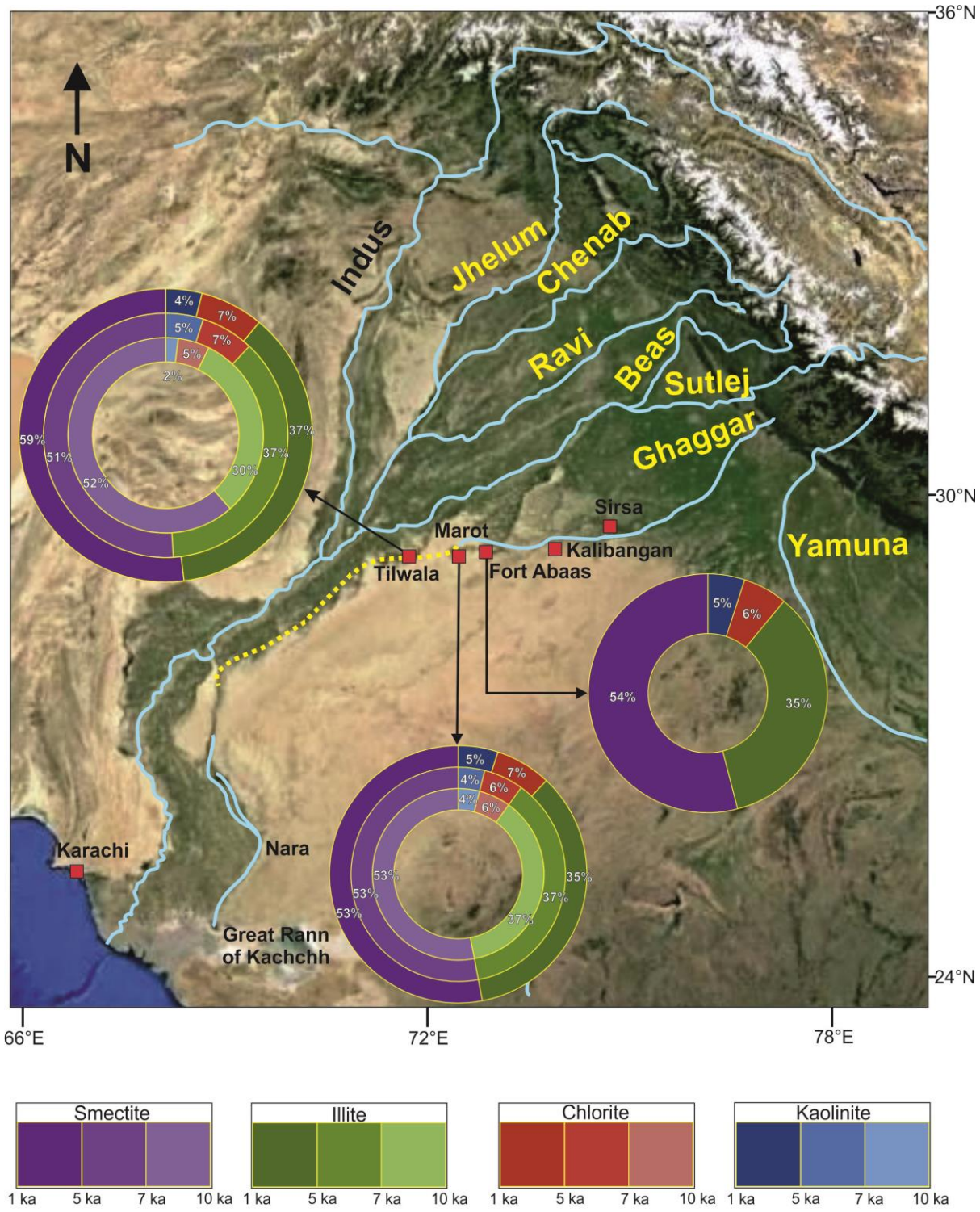

Figure 3.5: Pie chart showing the compositional variations of clay minerals across the Ghaggar alluvium during the Holocene. Figures is modified from Chatterjee and Ray, (2017a).

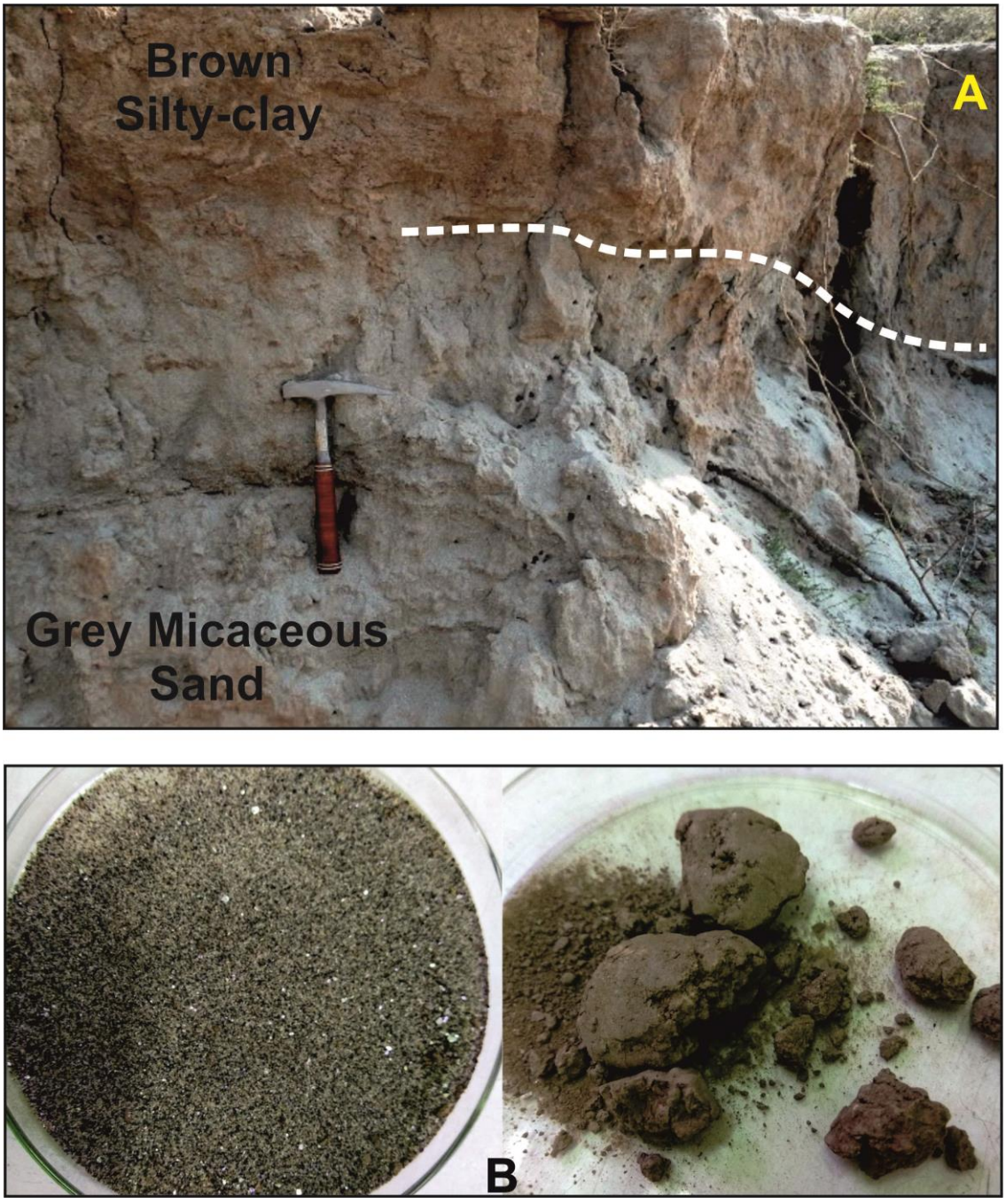

Figure 3.6: (A) A typical association of brown silty-clay and underlying grey micaceous sand in the Ghaggar alluvium. The sharp contact between the two facieses can be observed in this trench section.
(B) Appearance of grey micaceous sand (left hand side) and brown silty-clay (right hand side) in mesoscopic scale. The coarse muscovite grains can be observed within the grey sand.

3.3.2 Antiquity of the Ghaggar alluvium

Between Hanumangarh and Anupgarh a number of fluvial deposits have been dated during this work. Depositional ages of various samples analysed during the present work generally vary from the late Pleistocene to mid-Holocene. The details of OSL ages and C-14 ages are presented in Table 3.1. The age constrains and sedimentation history of the Ghaggar alluvium is discussed below.

3.3.2.1 Brown floodplain silt/mud :

- The AMS C-14 dating of the gastropod shells from the brown clay horizon near Hanumangarh yielded an age of 3109 ± 35 cal BP, which can be considered as the age of deposition of the layer (Fig. 3.4).
- Near Anupgarh gastropod shells from similar brown floodplain mud gave AMS C-14 age of 4564 ± 76 cal BP.
- Earlier Saini et al., (2009) had reported OSL depositional ages of 2.9 ± 0.2 ka BP and 3.4 ± 0.2 ka BP for the similar stratigraphic horizons from the Ghaggar floodplain, at Sirsa-Fatehbad region – upstream to our sampling sites.
- These results suggest that the sediment load of the river has been dominated by the suspended material at least since 4.5 ka. This in turn suggests that by 4.5 ka the river was already a foothill fed river similar to its present condition.

3.3.2.2 Grey micaceous fluvial sand:

- The depositional age of the underlying grey micaceous fluvial sand, on the other hand can be traced back to the Pleistocene.
- OSL dating of this sand horizon between Hanumangarh and Kalibangan gave an age of 36.6 ± 3.0 ka. Singh et al., (2016a) had reported depositional age of these grey micaceous sands from Kalibangan region to be from ~70 to ~20ka.
- In Pilibangan region, just north of Kalibangan, the yellowish brown fine sand overlying the grey sand horizon gave a depositional age of 15.8 ± 1.1 ka suggesting that the underlying grey sand might have been deposited during the last glacial maxima (LGM) period, i.e. during 22-16 ka (Clark et al., 2009).

- In contrast to the above, in several other places the grey micaceous sand yielded much younger depositional ages. For example, at Hanumangarh where it is in contact with the overlying floodplain mud, it gave OSL depositional ages of 6.0 ± 0.5 and 5.4 ± 0.6 ka. The deposition was probably continuous in this region for a few millennia, which is reflected in the depositional age of 8.5 ± 0.6 ka for the sand, a few centimetres below the contact.
- Evidence of the younger fluvial activity depositing similar grey sand also comes from downstream at Anupgarh region. At Anupgarh a colony of fresh-water bivalve shells was encountered embedded *in situ* within this micaceous grey sand layer (Fig. 3.4). The AMS C-14 dating of a few bivalve shells yielded ages of 6386 ± 62, 6307 ± 14, 6136 ± 98 cal yr BP respectively. The conventional C-14 date also gave similar age of 4652±198 cal yr BP. The fact that the shells were unaltered and embedded in their *in situ* position, the dates can be considered as the depositional age of the fluvial sand horizon.
- The youngest age for similar grey sand from upstream in the Sirsa-Fatehbad region is reported to be 4.3± 0.2 ka by Saini et al., (2009).

3.3.2.3 Yellowish brown fluvial sand:

- As discussed earlier, the yellowish brown fine sand lying on top of the grey sand yielded an OSL depositional age of 15.8 ± 1.1 ka at Pilibangan.
- Bivalve and gastropod shells recovered from similar sand horizon exposed in a freshly dug pit, downstream near Suratgarh gave AMS C-14 ages of 12521 ± 100, 10695 ± 100 and 10484 ± 139 cal yr BP.
- Although this particular type of sand was not encountered in the pit at Hanumangarh, it was found towards the north of Hanumangarh town. The OSL depositional age of this sand layer is 9.9 ± 0.9 ka.
- Another much younger phase of occurrences of this facies have been reported by Saini et al., (2009). In the upstream Sirsa region the depositional age is ~3ka.

The sedimentary facieses and their depositional ages suggest that there were multiple changes in fluvial activity in the Ghaggar floodplain. It appears that a much stronger fluvial system of past has gradually reduced into a dwindling meandering system during the Holocene. During the latter phase other plain-fed tributaries of the river started dominating

the floodplain depositions (weaker system, thus finer sediments). For proper characterization of the sources of the sediments and to understand the depositional pathways, we studied the geochemical properties of these sediments along the Ghaggar floodplain.

3.3.3 Ar-Ar geochronology of detrital muscovite

The Ar-Ar ages of muscovite micas represent the time period when the rocks containing these grains get cooled below 350˚C (Hodges, 2003). Given the fact that different litho-tectonic units of the Himalaya had exhumed diachronously, they are likely to contain various age populations of muscovite representing each exhumation event. Therefore, the Ar-Ar ages of detrital muscovite, which represents their formation or Ar closure ages, can be used as powerful provenance indicators for the Himalaya derived sediments (Clift et al., 2010). The ranges of Ar-Ar ages of muscovite found in different Himalayan litho-tectonic units as documented by earlier workers are presented in the figure 3.7.

Muscovite grains are one of the abundant minerals in the sandy facies of the Ghaggar alluvium. The subsurface fluvial grey sands have a lot of coarse grained white mica flakes. Their coarse grained nature and angular character indicate low degree of reworking and/or chemical weathering of the host sediments. Therefore, it is safe to assume that these mica grains have been derived directly from the source rocks (not reworked from the older floodplain deposits) and can serve as a good provenance indicator.

In the present work, we have separated coarse (>150 μ) muscovite grains (concentrates) from three of the grey sand bodies from the Ghaggar floodplain and determined their Ar-Ar ages using the standard step heating protocol (Awasthi et al., 2015; Ray et al., 2015). The reason behind Ar-Ar analysis of multigrain mica concentrates as against single aliquot was to capture the predominant age group in order to zero in on the major sediment contributor to the ancient Ghaggar floodplain. Three, mica concentrates with depositional ages of ~37 ka, >16 ka and ~6.3 ka were chosen for the purpose. The oldest sample represented the strongest phase of the fluvial activity. It came from a layer that is present below a 15.8 ka yellowish-brown sandy layer possibly representing the dwindling phase of the river during the last glacial maxima. The youngest sample came from a layer that represented the youngest phase of fluvial activity, as discussed in Section 3.2. Figure 3.8

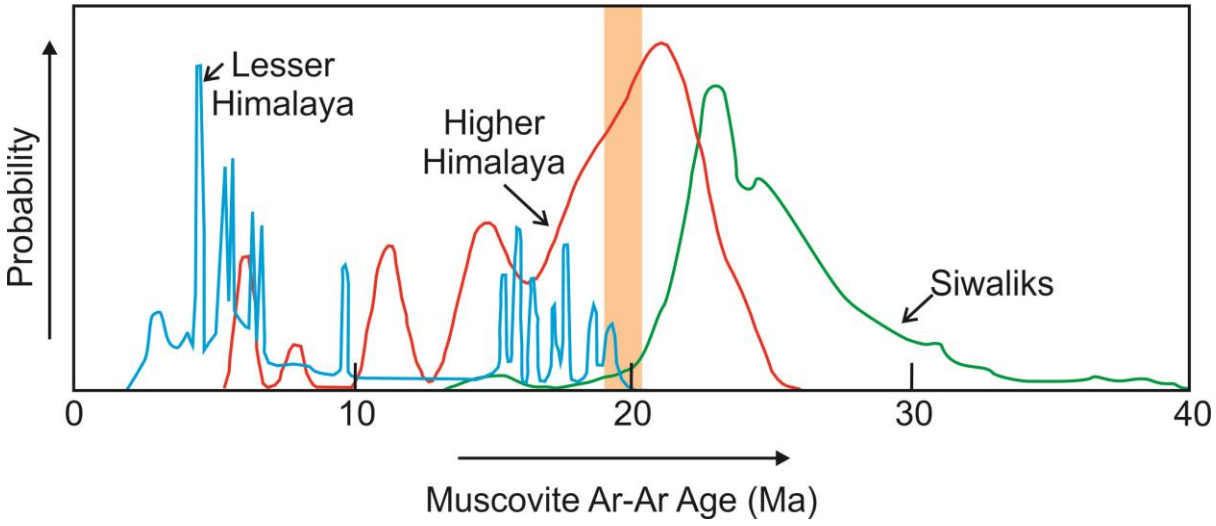

Figure 3.7: Probability density plots showing the range of Ar-Ar mica ages of possible source regions in different Himalayan litho-tectonic units as documented by earlier workers (Bollinger et al., 2004; Catlos et al., 2001; Inger, 1998; Metcalfe, 1993; Searle et al., 1992; Stephenson et al., 2001; Szulc et al., 2006; Vannay et al., 2004; Walker et al., 1999; White et al., 2002).The age range (18.6-20.1 Ma) of mica concentrates from the grey micaceous sand of the Ghaggar alluvium, measured during the present study is marked as an orange column in the figure.

shows the Ar-Ar plateau and isochron plots for the concentrates of white mica from these three samples. Based on the indistinguishable plateau and isochron ages and intercepts showing atmospheric $^{36}Ar/^{40}Ar$ compositions, we make the following observations.

- The plateau age of the micas can be considered as their formation or Ar-closure ages, suggesting that they belonged to magmatic or metamorphic rocks that had cooled down to ~350˚C during 20.1 and 18.6 Ma.
- With overlapping ages, it is clear that the sources of these micas had remained same or similar during the entire period of their deposition, i.e. ~37 ka to 6.3 ka.
- A comparison of these ages (20.1-18.6 Ma) with the distribution of available mica ages in literature from various litho-units (Fig. 3.7) reveals that the mica ages of our samples overlap with those observed in all the three units, i.e. the Higher Himalaya, Lesser Himalaya and Siwaliks.
- The Siwaliks could not have been the source of micas in Ghaggar because the Siwalik sediments themselves have been derived from the other two units and further recycling would only have produced clays as a result of weathering.

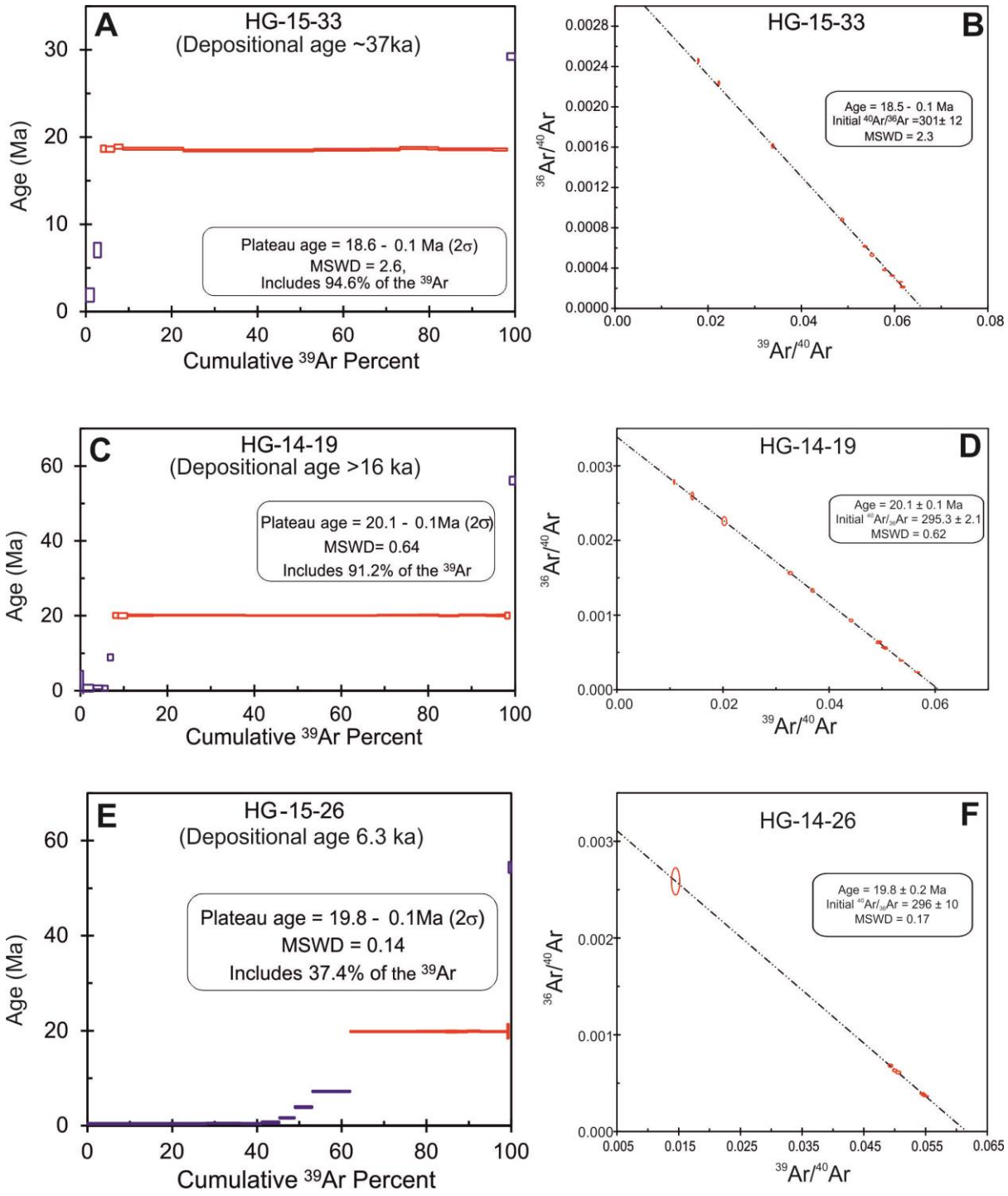

Figure 3.8: Ar-Ar plateau and isochron plots for the concentrates of white mica collected from three samples of grey micaceous sands. (A) & (B) are for the sample HG-15-33 (depositional age ~ 37 ka); (B) & (C) are for the sample HG-14-19 (depositional age > 16 ka); (D) & (E) are for the sample HG-15-26 (depositional age 6.3 ka).

- Sourcing from the Lesser Himalaya can also be ruled out because if that were the case then the mica concentrates should have shown an age of ~12 Ma, the average of the two modes in the age distribution of white micas.
- In view of the above two points, it is apparent that the white micas of the Ghaggar alluvium were derived from the Higher Himalaya. The dominant lithology which could have contributed the micas is the leucogranites, which were emplaced during 17-24 Ma and contain abundant muscovite (Sachan et al., 2010). These rocks were believed to have been exposed during the formation of the Himalayan Central Thrust (HCT) at ~21 Ma (Valdiya, 2010).
- It is therefore logical to conclude that like the micas their host grey sands have also been derived from the glaciated Higher Hiamalaya.

To further constrain the provenance of the Ghaggar alluvium we took help of geochemical proxies, which are discussed below.

3.3.4 Geochemistry of the Ghaggar alluvium

3.3.4.1 Trace element geochemistry

The trace element data of sediment samples are presented in Table 3.2 and plotted in Post Archean Australian Shale (PAAS) normalized diagram in figure 3.9. Following observations can be made from the figure.

- All different types of sediments show similar trace element patterns. Even the modern surface mud deposited during the latest flooding event shows a similar pattern.
- The only difference between different sediments is the elemental concentrations. The modern mud in the river has the highest trace element contents, whereas the oldest alluvium, the coarse grey sand, has the lowest content. This can be attributed to effect of dilution because of presence of abundant quartz in the latter.
- Notwithstanding the differences in the contents, comparable patterns of trace elements in different sediments, point to their derivation from analogous sources.
- The observed patterns are similar to that of sediments in rivers of Punjab. This suggests that the likely provenance of Ghaggar alluvium is the Himalayas.

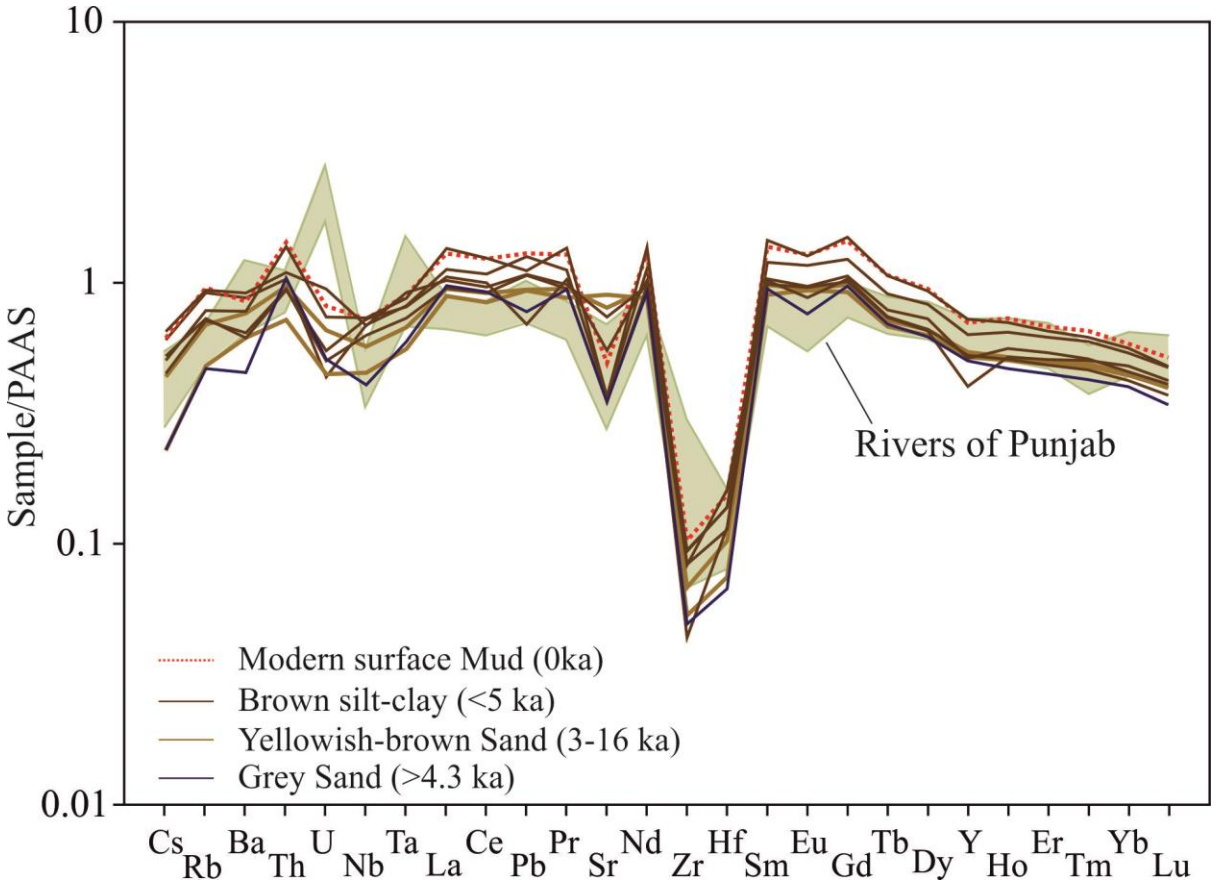

Figure 3.9: PAAS normalised trace element distribution of various sedimentary facies from the Ghaggar alluvium. The green coloured field in the background shows the range of composition observed in the rivers of Punjab. Data source: Alizai et al.(2011a).

The trace element characteristics of Ghaggar alluvium, however, do not make it clear whether the sediments were derived from the glaciated Higher and Lesser Himalayas or the Siwaliks.

3.3.4.2 Sr-Nd isotopic fingerprinting of the Ghaggar sediments

To resolve the above issue we took the help of Sr-Nd isotopic composition of bulk sediments. The isotopic data of the Ghaggar alluvium are presented in the Table 3.3. Different litho-tectonic units of the Himalayas are well characterised with respect to Sr-Nd isotopic compositions and can be used for tracing the provenance of the sediments in frontal alluvial plain. The Sr-Nd isotopic compositions of different Himalayan litho-tectonic units, based on the available data, are shown in figure 3.10.

The glaciated region of the Himalayas is made up of rocks of the Higher Himalayan Crystalline Series (HHCS) and Lesser Himalayan Series (LHS). Rivers originating from the glaciers carry sediments derived from these two sources and hence, they possess a mixed signal. In figure 3.11A we compare the Sr-Nd isotopic data for the Ghaggar alluvium with that of the sub-Himalayan lithologies and of sediments in the rivers originating from the Higher-Himalaya. From the figure the following observations can be made.

- All the grey micaceous sand bodies encountered in the Ghaggar alluvium during the present course of the study have high $^{87}Sr/^{86}Sr$ (>0.75) and low ε_{Nd} (<-17).
- The $^{87}Sr/^{86}Sr$ and ε_{Nd} values of the Holocene grey sand deposits (present study) overlap with the range of values shown by sediments in most glacier fed rivers thus suggesting a provenance in the glaciated Himalayas.

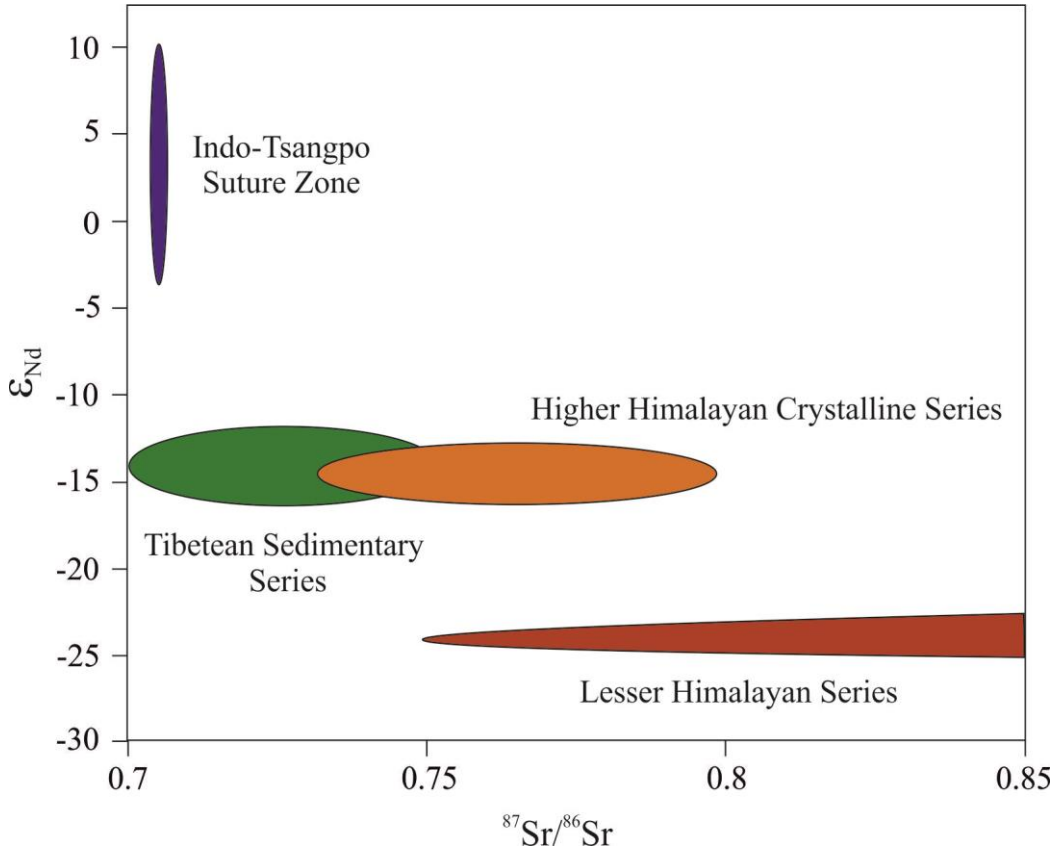

Figure 3.10: εNd vs. $^{87}Sr/^{86}Sr$ plot of major Himalayan litho-tectonic units showing their range of values. Data: Najman et al. (2000).

- The Sr-Nd isotopic ratios of older (>20 ka) grey micaceous sand bodies near Kalibangan also show similar (Singh et al., 2016a) compositions implying dominance of the higher Himalayan provenance.
- Binary mixing curves suggest that these grey sands were derived from a mixed HHCS and LHS sources (Fig. 3.11B).
- The thin layers of Grey clay encountered in a few of the sections (Section 3.1, Fig. 3.4) also show a higher Himalayan provenance. However, their Sr isotopic values are less radiogenic than that of the micaceous grey sands. This may be attributed to the dominance of physical weathering over chemical weathering in the Himalayas (Singh et al., 2008). Generally, higher chemical weathering leads to more radiogenic detritus which is largely controlled by higher $^{87}Sr/^{86}Sr$ bearing fine-grained (clay) fraction, primarily derived from high-Rb bearing micas in the source rocks (Garçon et al., 2014; Meyer et al., 2011). Therefore, in case of less chemical weathering the produced clay will be less radiogenic as the mica grains will be retained in the sand fractions.
- The brown coloured silty-clay possesses distinctly different isotopic ratios than that of the grey sand (Fig. 3.11 A and 3.11B); implying that the provenances of the formers are different from that of the Higher-Himalaya originated grey sands. These sediments are less radiogenic in Sr and more radiogenic in Nd isotopic composition with respect to the grey micaceous sand. They are also different in composition from the surrounding sand dunes, indicating very little, if any, input from the dunes via reworking.
- Figure 3.1B shows that the modern Ghaggar river has its catchment in the sub-Himalayas which includes the Siwalik Group, and formations of the Kasauli, Dagsahi and Subathu. Consequently, the river is expected to carry sediments derived from these lithologies. Sr-Nd isotopic compositions of these lithologies are shown in Fig. 3.11A. Tripathi et al., (2013) have argued for a significant contribution of the Subathu Formation in the Ghaggar Alluvium. However, our observations suggest that the Subathu Formation having very different isotopic compositions might have had very little influence on the Ghaggar sediments (Fig. 3.11A). It appears that the rocks of the Siwalik Group, Kasauli and Dagsahi Formations are the major sources for the brown mud and yellowish-brown sand of the Ghaggar flood-plain (Fig. 3.11A).
- The more radiogenic Nd of the marginal desert dunes can very well be the results of sediment mixing from the river Indus.

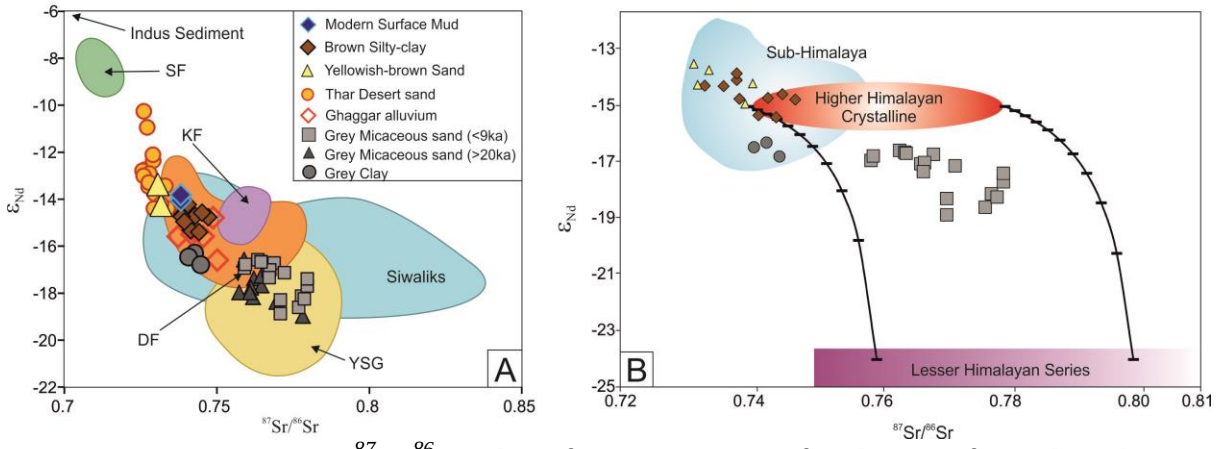

Figure 3.11: (A) ε_{Nd} vs. $^{87}Sr/^{86}Sr$ plot of various types of sediments from the Ghaggar alluvium compared with the sub-Himalayan provenances. Data for Ghaggar alluvium (red open diamonds) and grey micaceous sand (grey triangles) are from Tripathi et al. (2013) and Singh et al., (2016a) respectively. SF: Subathu Formation; KF: Kasauli Formation; DF: Dagsahi Formation; YSG: Yamuna-Sutlej-Ganga sediments.
(B) Binary mixing diagram involving the grey micaceous sands (<9 ka), grey clay and brown silty-clay. The two end-members are the glaciated Higher and the Lesser Himalayas.

Temporal variations of Sr-Nd isotopic compositions in the Ghaggar alluvium since the Pleistocene are presented in the figure 3.12. As can be seen the isotopic compositions changes with the lithology, in the composite stratigraphy which suggest change in sedimentary provenance over time. From the figure it can be observed that:

- The oldest micaceous grey sand has high $^{87}Sr/^{86}Sr$ (~0.76) and low ε_{Nd} (~ -16) values hinting at a mixed Higher and Lesser Himalayan origin for the source.
- A sharp change in provenance can be observed in the period following the last glacial maxima at ~20 ka.
- For a long period sediments showed a low $^{87}Sr/^{86}Sr$ and high ε_{Nd} values corresponding to sub-Himalayan sources.
- ~9 ka onwards a shift towards Higher and Lesser Himalayan provenance can be observed.

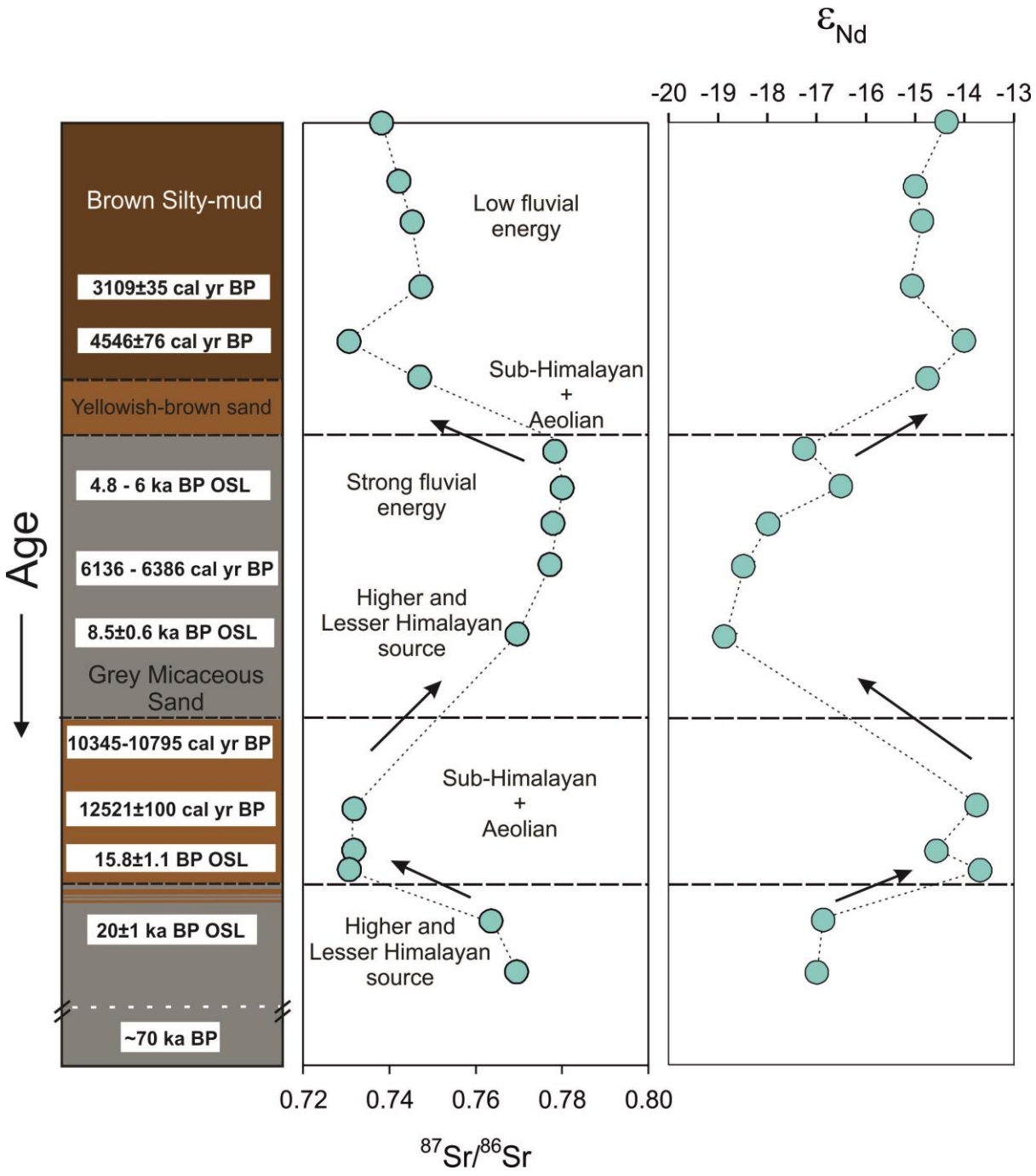

Figure 3.12: The temporal variation of $^{87}Sr/^{86}Sr$ and ε_{Nd} values in a composite stratigraphy of the Ghaggar alluvium.

- ~5 ka onwards the sediment provenance again shifted to the sub-Himalays, suggesting less importance of the Higher and Lesser Himalayan sediment sources in the Ghaggar river system.

The above observations appear to suggest that the Himalayan glacier-fed paleo-river(s) delivered sediments into the present day dry ephemeral river channel of Ghaggar during various periods in the past. However, Ghaggar river basin itself has no evidence of any direct connection with the glaciated Higher Himalayas. Therefore, the only possible pathways for the Higher Himalayan sediments to reach the Ghaggar alluvium could have been via the neighbouring rivers the Sutlej and the Yamuna. However, Clift et al. (2012) had suggested based on detrital zircon age data that the Yamuna had shifted from the Ghaggar channel probably at 45 ka. This leaves us with only one option for the choice of pathway for the glacial water and that is Sutlej. During the present work it was observed that the $^{87}Sr/^{86}Sr$ ratios of the *in-situ* mollusc shells from these sand bodies are 0.7187±0.0003 (Fig. 3.13) and resemble that of the water of the Sutlej rather than that of the Yamuna, which is generally more radiogenic ($^{87}Sr/^{86}Sr$: 0.7166 – 0.7218 , Karim and Veizer, 2000; Pande et al., 1994). This observation further confirms the inference that the Sutlej was the main pathway for the Higher Himalayan sediments into the Ghaggar valley (Danino, 2010).

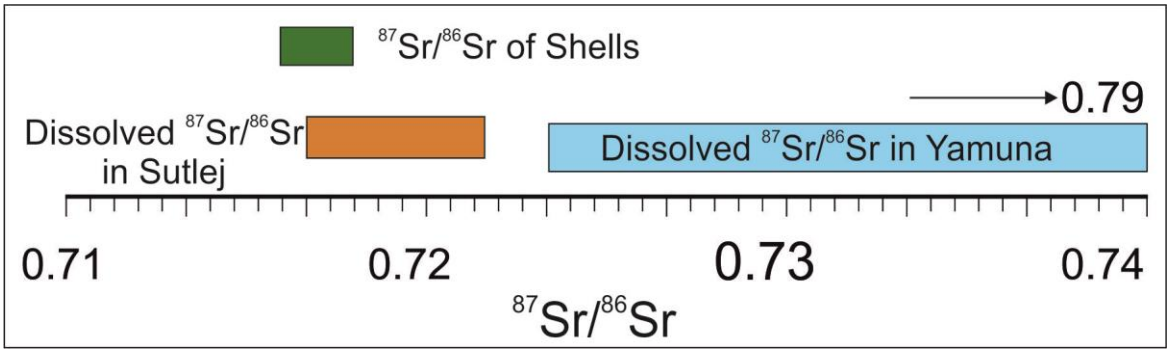

Figure 3.13: Range of $^{87}Sr/^{86}Sr$ values observed in the bivalve shells from the Ghaggar alluvium with respect to the dissolved $^{87}Sr/^{86}Sr$ values of the Sutlej and the Yamuna river.

In a recent work, (Mehdi et al., 2016) has found several paleo-channels connecting the present day Sutlej with the Ghaggar channel. This satellite based work further confirms our

inference. However, Giosan et al. (2012) had proposed that no mega-fluvial system was active along the Ghaggar valley during the Holocene period. We therefore hypothesise that some distributaries of the Sutlej could have been flowing into the paleo-Ghaggar during the mid-Holocene (≥6 ka), which later migrated away making the Ghaggar an ephemeral river.

3.3.5 Isotopic Fingerprinting of Kalibangan Potteries

Potters of Bhirana, a Harappan acropolis on the bank of the Ghaggar, used to make earthenware using clay from nearby localities (Krishnan et al., 2012). Extending this finding to Kalibangan it could be argued that potters here too had utilized the silty-clay which was available aplenty in the nearby Ghaggar floodplain. The very fact that common clay (illite/smectite, kaolinite and micas) can be utilized for general ceramics (Valášková, 2015) it is highly likely that the Harappans at Kalibangan made use of locally available clays, the mineralogical details of which are shown in figure 3.5 and discussed in section 3.1. The usability of these silty-clay horizons is very much evident even today in the numerous active brick kilns all along the Ghaggar floodplain.

Another important understanding of ancient pottery making is that pure clay was never used for the purpose (Krishnan, 2002; Krishnan and Rao, 1994). For strengthening and creating different textures, various amounts of coarser material, generally sand, were mixed with pure clay to prepare the raw material. Therefore, one expects to find mixed geochemical signatures of sand and clay of the Ghaggar flood plain in the Kalibangan potteries. The Sr-Nd isotopic compositions of the potteries are presented in the table 3.4.

Figure 3.14 presents ε_{Nd} versus $^{87}Sr/^{86}Sr$ plot comparing the compositions of Harappan potteries with that of the different types of Ghaggar flood plain sediments. It can be observed that the isotopic compositions of pottery samples lie within the range of brown silty-clay/ surface mud and yellowish-brown sand. Possible contribution from surrounding aeolian sand cannot be ruled out. However, there appears to be a clear absence of any grey micaceous sand component within the pottery, which suggests non-availability of such sediment during pottery making. This, on the other hand, implies that by the time the Mature Harappans settled in Kalibangan, the glacial connection to the Ghaggar was significantly reduced and little sediment originating from glaciated terrains was depositing in the channels.

Validation of this hypothesis comes from isotopic compositions of the brick sampled from the Bhatner Fort. It is a well-known historical fact that the Fort was established on the banks of an ephemeral Ghaggar during 12th century AD. The bricks of the fort, made using Ghaggar sediments, show similar compositions as that of the pre-historic potteries. This clearly suggests use of identical raw materials even after two millennia which in turn supports the theory that the river was already ephemeral (not glacier fed) during the Mature Harappan Period.

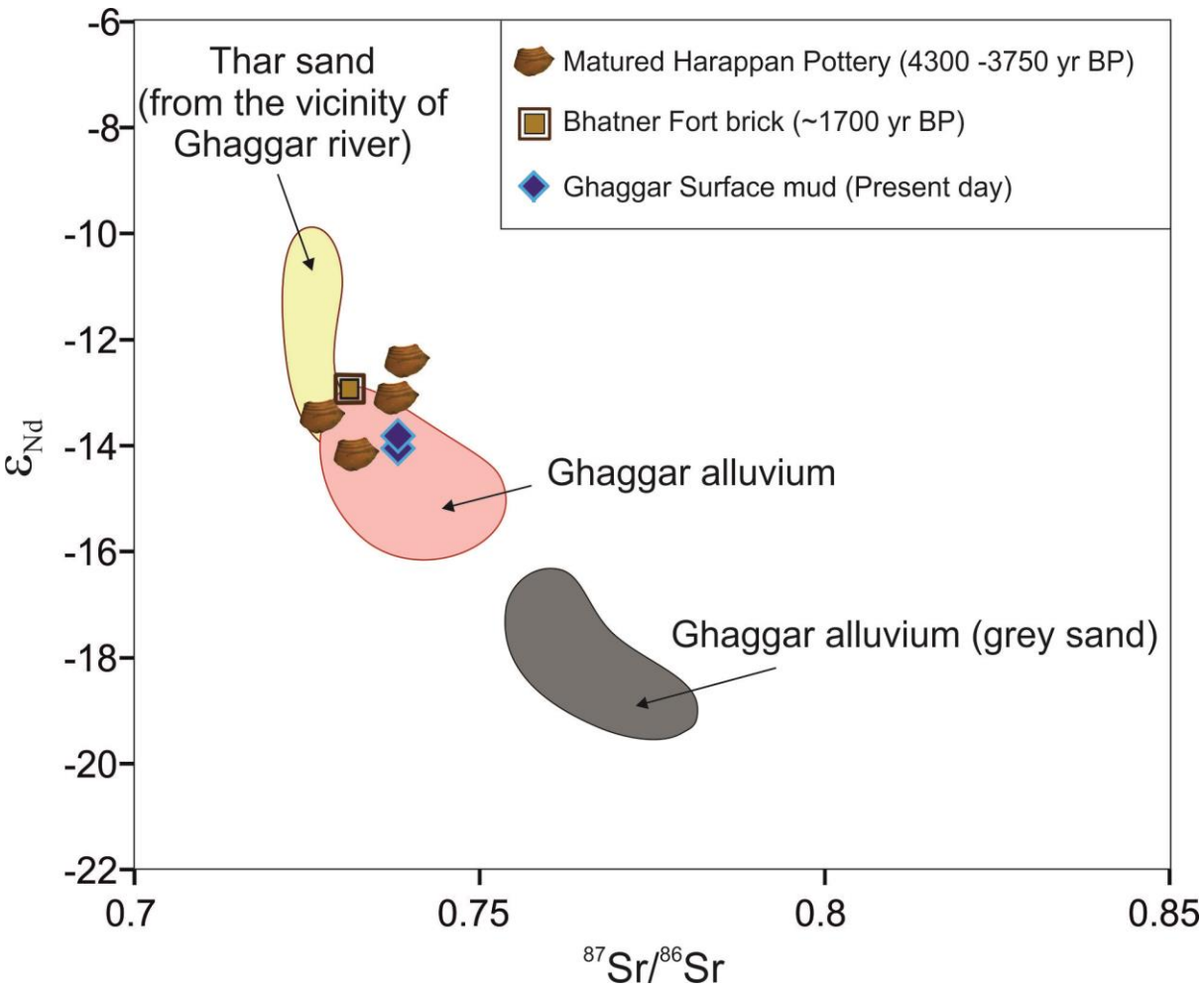

Figure 3.14: ε_{Nd} vs. $^{87}Sr/^{86}Sr$ plot of different archaeological artefacts compared with the probable raw material sources in the Ghaggar flood plain. Figure is modified from Chatterjee and Ray, (2017a).

3.3.6 The River – Culture – Climate connection

A graphical representation showing temporal dominance of different sedimentary facies within the Ghaggar flood plain during the last 70 kyrs and their relationship with the

major climatic events and development of the Indus valley cultural tradition is shown in figure 3.15. The following observations and interpretations can be made from the figure.

- The earliest phases of grey micaceous sand deposition (~70-20 ka) occurred during the MIS-3 and MIS-4. During this period the sediments deposited in the Ghaggar valley had its origin mainly from the glaciated Higher Himalayan sources. The thick and continuous deposition of fluvial sand during this period (Singh et al., 2016a) is indicative of a strong fluvial system during this time.
- Towards the end of MIS-3 aridity started increasing (Petit et al., 1999). During the last glacial maxima (25 – 18 ka) and during the MIS-2 aridity and glaciation was at its peak. The discharge in the Himalayan rivers was at their lowest as evident from the incised river valleys, especially in the western India (Giosan et al., 2012). During this period the fluvial grey sand beds in the Ghaggar alluvium had become thinner with the appearance of alternate yellowish-brown sand layers. This observation suggests that during the glacial maxima, the river had started dwindling with limited discharge from the glacial sources. The yellowish brown sand deposited during this time appears to have been sourced from the provenance of the sub-Himalaya (Siwaliks) and reworking of local dunes.

During most of the period of the MIS-2 and the beginning of the MIS-1, Ghaggar valley witnessed deposition of yellowish-brown silty sand facies mainly. No record of grey sand facies was observed during this study or reported by earlier works. As discussed earlier, sediments were originating from the Sub-Himalayas and local reworking during this period which was probably a result of a weak monsoon. The fluvial activity was at its lowest.

- Indian Summer Monsoon is known to have been re-intensified in the MIS-1, subsequent to the LGM (Sarkar et al., 2016). This along with the melting of the glaciers should have increased discharge in the Himalayan rivers. During this period (~9 ka onwards), we observe appearance of grey micaceous sand again. Its deposition continued up to ~4.5 ka, albeit as limited channel fills.
- This second phase indicates renewed phase of fluvial activity originating from the Higher Himalayas. Bookhagen et al., (2005) had shown that during the intensified Holocene monsoon, sediment flux increased manifold from the higher parts of Sutlej valley in the NW Himalaya. This caused enhanced sediment evacuation in the Himalayan foreland basins. Probably during these phase of monsoon intensification and deglaciation, the Ghaggar received sediment and water originating from the Higher Himalayas via rejuvenated distributaries of the Sutlej.

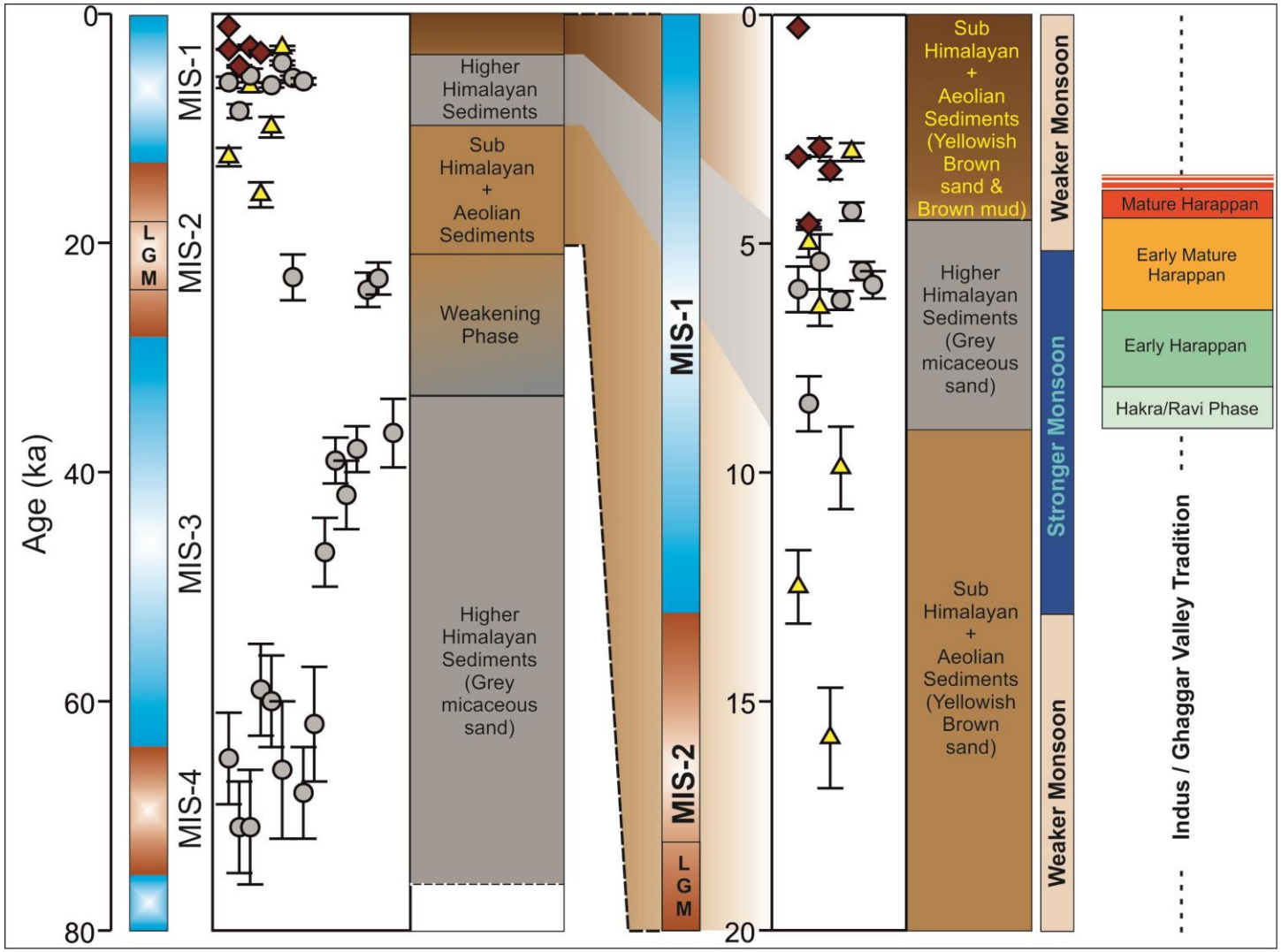

Figure 3.15: Graphical representation of the temporal dominance of different sedimentary facies within the Ghaggar flood plain during the last 70 kyrs and their relationship with the major climatic events and development of the Indus valley cultural tradition. The last 20 kyrs window has been zoomed in for better visualisation of the events happening during that period.

- One noticeable development during the renewed phase of the fluvial activity is the beginning of the earliest Indus valley (Harappan) tradition. The seed of the future Harappan civilization was being sown in the early Holocene. The earliest known settlement of Bhirrana in the Ghaggar valley dates back to ~9 ka (Sarkar et al., 2016). By 6 ka the Ghaggar valley was crowded with early Harappan (Hakra phase) settlements. This development during the renewed phase of the river indicates that the early settlers witnessed perenniality in the river system. Soon after they developed into the Early Mature Harappan tradition.
- The river had started to lose its glacial sources making it dependent on rainfall only when the Harappan civilization had entered into its mature phase, 4.6-3.9 ka. This is evident from the sedimentological and geochemical properties of alluvium and archaeological artefacts from the Ghaggar valley. By the time the Indus Valley/ Harappan Civilization had reached its peak (~4.6 ka), the Ghagagr river had lost its glacial sources completely. From ~5ka onwards sediments deposited in the Ghaggar valley had become silty clay dominated and were derived mainly from the sub-Himalayas.
- The zeneith of the civilization overlaps with the terminal phase of the river, which suggests that the rainfall was adequate for the Ghaggar valley dwellers to sustain their civilization.
- Gradually the climate became more arid and the river Ghaggar became an ephemeral rain-fed river much more like its present day condition. The Mature Harappans, who were dependent mainly on the monsoonal rain, also got affected by the rapid change in the climate and its negative effect on the flow of the Ghaggar. This caused a domino effect and within a few centuries the developed urban societies of the Harappans disintegrated of various reasons like crop cycling (Sarkar et al., 2016), diseases, abandonment of urban centres etc. Inadequate water supply was a major reason for the demise of the civilization. By 3.9 ka the people migrated from their localities towards the northern Himalayan foothills, where rainfall was much higher (Giosan et al., 2012).

3.4 Summary and Conclusions

Our study of chronology, geochemistry and isotopic compositions of various proxies from the present-day Ghaggar valley revealed the following information about the evolution of the river and its connection with the Harappan Civilization in the NW India.

- The Ghaggar alluvium is a repository of sediments originated from two distinct provenances: 1) the glaciated Higher and Lesser Himalayas, 2) the sub-Himalayas.
- The grey micaceous sand deposits had their source in the glaciated Higher and Lesser Himalayas. This sand appears twice in two distinct time period: 1) 70-20 ka, 2) 9-5 ka.
- The oldest phase of grey micaceous sand (~70-20 ka) got deposited during the MIS-3 and MIS-4 and suggests a strong fluvial past of the river.
- The geomorphology of the Ghaggar floodplain was very different at that time with the Yamuna and the Sutlej flowing into its channel making it a perennial river system (Fig 3.16A).
- Yamuna abandoned its course ~45 ka (Fig 3.16B).
- During the last glacial maxima (25-18 ka) the river started dwindling and the sediment influx from the glaciated higher Himalaya gradually decreased.
- During the drier periods of the MIS-2, sediments (yellowish-brown sand) originating mostly from the sub-Himalayas and reworked from the dune fields were deposited in the Ghaggar valley.
- At the beginning of the Holocene Indian Summer Monsoon intensified and the appearance of micaceous grey sand derived from glaciated Higher Himalayas reappeared in the Ghaggar stream (~9 ka onwards). This period roughly coincided with the MIS-1 period.
- During this period the Ghaggar received its share of Higher Himalaya originated glacier water probably via distributaries of the river Sutlej (Fig 3.16C).
- Also during this rejuvenated phase of the river the earliest people of the Indus valley tradition (pre-Harappans) settled down in the Ghaggar valley.
- By mid-Holocene the river had lost its glacial sources (Fig 3.16D). However, this did not affect the settlers along the river bank. Rather the civilization reached its peak during this period sustained by water from monsoonal rain. Therefore, the dramatic loss of the perennial glacier source from the Ghaggar river may not be a reason for the decline of the Harappan Civilization.
- Subsequently, the decrease in rainfall caused the river to be seasonal and unpredictable. This situation became detrimental for the survival of the settlements along the Ghaggar river valley.

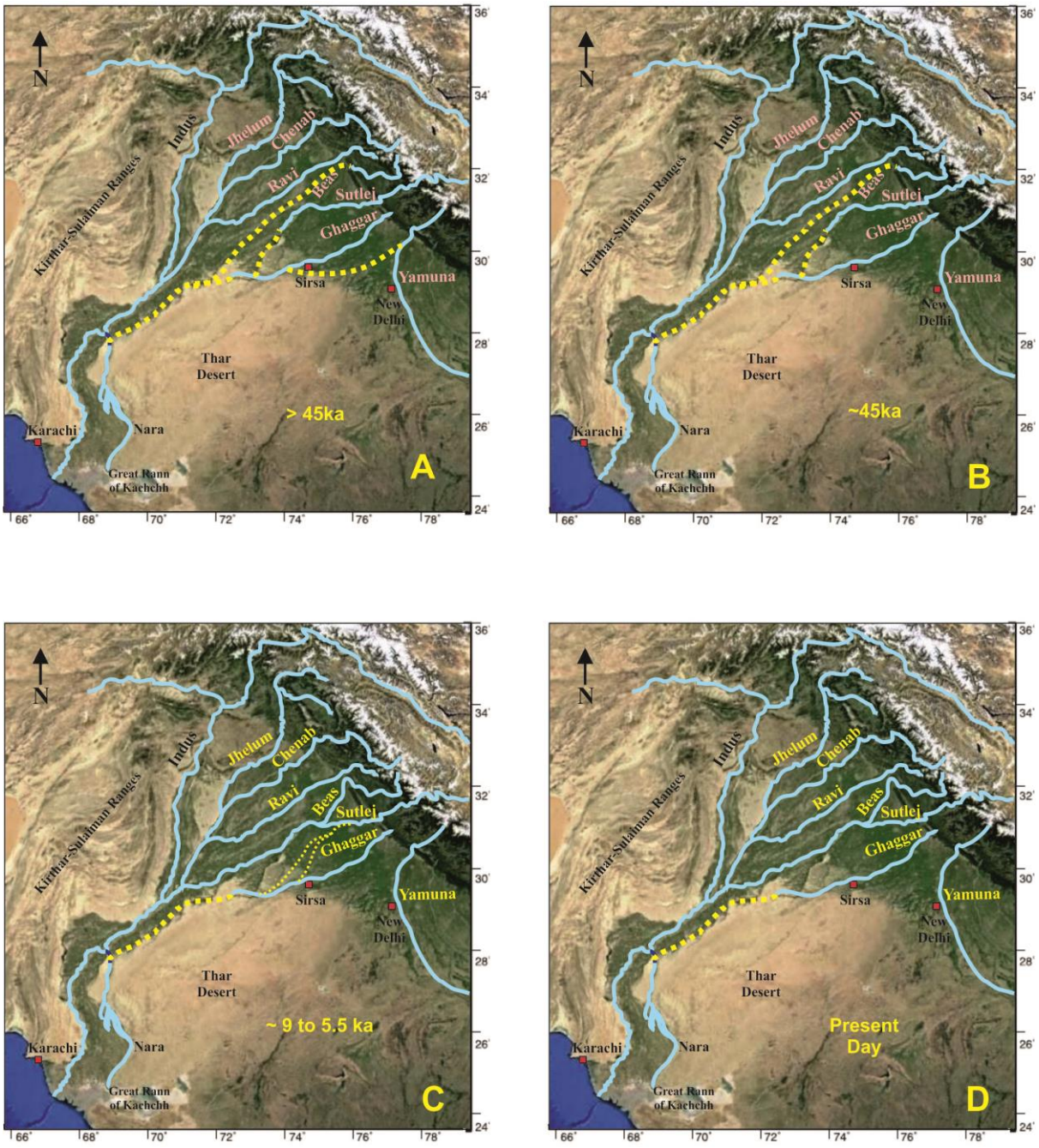

Figure 3.16: Reconstruction of the palaeo-drainage patterns in the western part of the Indian sub-continent. The blue lines represent the present-day drainage and the yellow dotted lines represent the proposed palaeo-drainages.
(A) Ravi, Sutlej and Yamuna used to flow into the Ghaggar river channel before 45 ka (figure modified from Clift et al., 2012).
(B) During 45 ka the Yamuna shifted away from the Ghaggar channel (figure modified from Clift et al., 2012).
(C) During 9-5.5 ka only some distributaries of the Sutlej river used to flow into the Ghaggar channel (reconstructed from the present study).
(D) The present day drainage pattern. It remained similar since the mid-Holocene.

- Although the decline of the Harappan Civilization along the Ghaggar valley postdates the dramatic changes in the fluvial activity, a stronger perennial fluvial system helped the early societies to sow the seeds of the earliest known civilization in India.

Table 3.1(A) Equivalent dose (De),Dose Rate and ages obtained on the Ghaggar sediments

Sample	OD	U(ppm)	Th(ppm)	K(wt%)	De	Dose rate (μGy/a)	Age (ka)
HG-OSL-7	27.5	4.43±0.07	20.0±0.4	1.43±0.02	20.6±0.7	3.46±0.23	**6.0±0.5**
HG-OSL-6	13.4	2.65±0.07	12.1±0.3	2.0±0.03	26.4±0.5	3.1±0.2	**8.5±0.6**
HG-OSL-4	23	3.25±0.09	14.4±0.4	1.73±0.03	49.5±1.3	3.1±0.2	**15.8±1.1**
HG-OSL-15-A(15/5)	29.7	2.20±0.07	10.2±0.4	1.47±0.03	24.3±1.5	2.5±0.2	**9.9±0.9**
HG-OSL-15-C(15/13)	34.6	3.83±0.09	17.5±0.5	1.39±0.03	106±14	3.2±0.2	**36.6±3.0**
HG-OSL-15-D/OSL-6	27	2.65±0.07	12.1±0.3	2.0±0.03	16.8±1.5	3.1±0.2	**5.4±0.6**

Table 3.1 (B) Details of the AMS C-14 dates of the mollusc shells

Sample	Sample type	age (y)	±(y)	$\delta^{13}C$ (‰)	Cal BC	±(y)	Cal BP
JSR-1	Gastropod	4,021	34	-1.3	2,546	76	**4,546**
JSR-2	Bivalve	5,506	36	-5.1	4,386	62	**6,386**
JSR-3	Bivalve	5,347	36	-5.7	4,307	14	**6,307**
JSR-4	Bivalve	5,285	35	-5.1	4,136	98	**6,136**
JSR-5	Bivalve	10,480	46	-8.2	10,521	100	**12,521**
JSR-6	Bivalve	9,410	44	-8.6	8,695	100	**10,695**
JSR-7	Gastropod	9,272	43	-5.6	8,484	139	**10,484**

Table 3.2 Trace element concentrations of the Ghaggar river sediments. Concentrations are in ppm.

Samples	HG-14-4 (Brown silty-mud)	HG-14-8 (Brown silty-mud)	HG-14-16 (Brown silty-mud)	HG-14-20 (Brown silty-mud)	HG-14-21 (Brown silty-mud)	HG-14-39 (Brown silty-mud)	HG-14-18 (Brown silty-mud)
Cs	7.49	8.98	6.67	9.67	6.48	7.78	9.14
Rb	124.1	145.2	113.7	148.7	109.7	115.6	151.9
Ba	501	565	414	589	493	396	546
Th	20.0	15.0	13.7	15.9	14.0	13.6	20.7
U	2.27	1.34	1.54	2.91	2.02	1.69	2.50
Nb	14	13	12	13	11	14	14
Ta	1.11	1.04	0.93	1.16	0.86	1.03	1.14
La	51	42	36	38	36	40	49
Ce	99	86	73	76	72	79	98
Pb	22.1	25.0	21.2	21.3	18.7	13.8	25.7
Pr	11.9	9.8	8.3	8.6	8.3	9.0	11.2
Sr	72	72	69	147	159	109	98
Nd	43	36	31	31	30	32	41
Zr	17	19	9	17	14	20	21
Hf	0.6	0.7	0.6	0.8	0.5	0.7	0.8
Sm	8.1	6.7	5.7	5.5	5.5	5.7	7.6
Eu	1.4	1.3	1.1	1.0	1.0	1.0	1.4
Gd	7.0	5.7	4.9	4.7	4.6	4.8	6.7
Tb	0.81	0.69	0.60	0.56	0.55	0.57	0.82
Dy	4.1	3.6	3.2	2.9	2.9	2.9	4.1
Y	19.4	16.9	13.7	10.7	14.5	14.1	18.8
Ho	0.70	0.64	0.55	0.51	0.51	0.50	0.72
Er	1.9	1.8	1.6	1.5	1.4	1.4	2.0
Tm	0.2	0.2	0.2	0.2	0.2	0.2	0.3
Yb	1.6	1.5	1.3	1.3	1.2	1.2	1.6
Lu	0.20	0.20	0.17	0.18	0.17	0.16	0.22
Samples	HG-14-17 (Grey sand)	HG-14-19 (Grey sand)	HG-14-29 (Grey sand)	HG-14-30 (Grey sand)	HG-14-31 (Grey sand)	HG-14-40 (Grey sand)	HG-14-22 (Yellow-brown sand)
Cs	3.40	6.01	3.68	3.80	4.70	3.88	3.38
Rb	74.2	112.9	86.5	86.7	102.5	84.2	76.0
Ba	292	407	332	325	370	332	396
Th	15.1	10.1	11.1	13.1	6.8	15.3	10.4
U	1.57	1.24	1.32	1.77	0.87	1.97	1.37
Nb	8	8	6	8	6	10	9
Ta	0.75	0.74	0.55	0.73	0.63	0.90	0.71
La	37	24	29	34	19	45	33

Ce	73	48	57	66	38	91	67
Pb	15.4	20.8	18.0	17.9	20.1	17.7	18.5
Pr	8.2	5.5	6.3	7.5	4.4	10.3	7.6
Sr	69	91	75	74	79	112	179
Nd	29	20	23	27	16	37	28
Zr	10	7	6	8	1	8	11
Hf	0.3	0.2	0.3	0.3	0.2	0.3	0.4
Sm	5.3	3.5	4.0	4.7	2.8	6.7	5.0
Eu	0.8	0.7	0.7	0.8	0.6	1.1	1.0
Gd	4.5	3.0	3.4	4.0	2.3	5.8	4.3
Tb	0.53	0.35	0.40	0.46	0.28	0.70	0.52
Dy	2.7	1.9	2.0	2.3	1.4	3.8	2.7
Y	13.4	9.5	9.8	11.6	7.1	17.0	13.9
Ho	0.46	0.34	0.34	0.40	0.25	0.68	0.50
Er	1.3	0.9	1.0	1.1	0.7	1.9	1.4
Tm	0.2	0.1	0.1	0.2	0.1	0.3	0.2
Yb	1.1	0.8	0.8	1.0	0.6	1.7	1.2
Lu	0.14	0.11	0.11	0.14	0.08	0.23	0.17

Table 3.3 Sr-Nd isotopic compositions of the Ghaggar river sediments.

Samples	**Brown Silty-clay (<4.5 ka)**							
	HG-14-4	HG-14-8	HG-14-16	HG-14-34	HG-14-35	HG-14-38	HG-14-39	HG-14-20
$^{87}Sr/^{86}Sr$	0.743022	0.745287	0.747306	0.744301	0.741571	0.738601	0.736119	0.733185
ε_{Nd}	-14.7	-14.6	-14.8	-15.4	-15.3	-14.7	-14.3	-14.3
Samples	**Modern surface mud**			**Yellowish brown sand**				
	HG-14-18	HG-14-18R		HG-14-21	HG-14-22	HG-14-36	HG-15-3	HG-15-19
$^{87}Sr/^{86}Sr$	0.738182	0.738182		0.731733		0.740603	0.739478	0.733869
ε_{Nd}	-14.1	-13.8		-14.3	-13.4	-14.2	-14.9	-13.7
Samples	**Grey Micaceous sand (>5 ka)**							
	HG-14-17	HG-14-19	HG-14-19R	HG-14-29	HG-14-30	HG-14-31	HG-14-31R	HG-14-33
$^{87}Sr/^{86}Sr$	0.768847	0.770905	0.770905	0.777894	0.776909	0.779743	0.779743	0.763566
ε_{Nd}	-16.7	-18.9	-18.3	-18.1	-18.6	-17.7	-17.4	-16.6
Samples	**Grey Micaceous sand (>5 ka)**							
	HG-14-41	HG-15-10	HG-15-10R	HG-15-12	HG-15-13	HG-15-24	HG-15-26	HG-15-28
$^{87}Sr/^{86}Sr$	0.772213	0.764594	0.764594	0.766860	0.767445	0.759107	0.759457	0.767271
ε_{Nd}	-17.1	-16.6	-16.7	-17.0	-17.0	-16.9	-16.8	-17.3
Samples	**Grey Micaceous sand (>5 ka)**			**Grey Clay**				
	HG-15-33			HG-15-34	HG-15-11	HG-15-17		
$^{87}Sr/^{86}Sr$	0.778758			0.742829417	0.740871862	0.744841974		
ε_{Nd}	-18.2			-16.3	-16.5	-16.8		

Table 3.4 Sr-Nd isotopic compositions of the potteries from Kalibangan and Hanumangarh Fort

Samples	Kalibangan Pottery and brick (4.6 – 3.9 ka)				Bhatner Fort Brick (~0.9 ka)
	KBP-1	KBP-2	KBP-3	KBP-4	HGP-1
$^{87}Sr/^{86}Sr$	0.739043	0.731819	0.737543	0.726857	0.730976
ε_{Nd}	-12.4	-14.2	-13.1	-13.5	-12.9

.

Chapter- 4

Provenance of Mid-Holocene Sediments in the Great Rann of Kachchh

4.1 Introduction

At the western margin of the Indian subcontinent lies a unique Quaternary terrain known as the Great Rann of Kachchh (GRK). The GRK can be described as a vast expanse of monotonously flat, salt encrusted land which lies marginally above the mean sea level (~4 m). Whereas the eastern GRK primarily receives seasonal fluvial contribution from the Luni river, the western GRK is inundated by storm tides during the southwest Indian monsoon (Glennie and Evans, 1976), and receives water from the ephemeral Nara river during flooding in the Indus (Fig. 4.1), channelized through man-made canals (Syvitski et al., 2013). The desolate landscape of the GRK was not always like this. It is hypothesised that the GRK was a former gulf of the Arabian sea and recurrent seismic activities caused the Rann surface to uplift and finally dry up (Merh, 2005). The archaeological evidence of several Harappan settlements around the GRK points to its eventful past. It is believed that the urban Harappan people had settled down in the semi-arid GRK during 4600-3900 yrs BP (Lindstrom, 2013; Rajesh, 2011) and were using the shallow navigable sea of the Rann, for their maritime activities (Gaur et al., 2013). The remains of one of the largest Harappan acropolises at Dholavira, located in the island of Khadir in the very heart of GRK, bear the testimony of highly active past of the GRK. For the sustenance of human settlements, availability of fresh water as well as connectivity to outer world is very important, however, the present conditions of GRK do not satisfy these conditions.

Moreover, in the previous chapter we have discussed about the fluvial past of the Ghaggar-Hakra river and its connection to the development and decline of the Harappan civilization. The remains of Harappan settlements around the GRK and along the Nara river channel (Fig 4.1), led to the suggestion that the Ghaggar-Hakra and Nara perhaps were a continuous and perennial fluvial system during the mature Harappan period and that the decline of the civilization was triggered by drying up of the river (Misra, 1984; Mughal, 1997; Wright et al., 2008). Indeed some workers, with the help of satellite based studies and historical documents, have identified paleo-river channels that flowed through the present-day arid western margin of the Thar Desert into the Arabian Sea (Ghose et al., 1979; Gupta et al., 2011; Syvitski et al., 2013) and created a delta system in the western Great Rann of Kachchh (Malik et al., 1999). Moreover, a continuous Ghaggar-Hakra-Nara river system has often been equated with the Saraswati, a mythical glacier-fed perennial river (Ghose et al.,

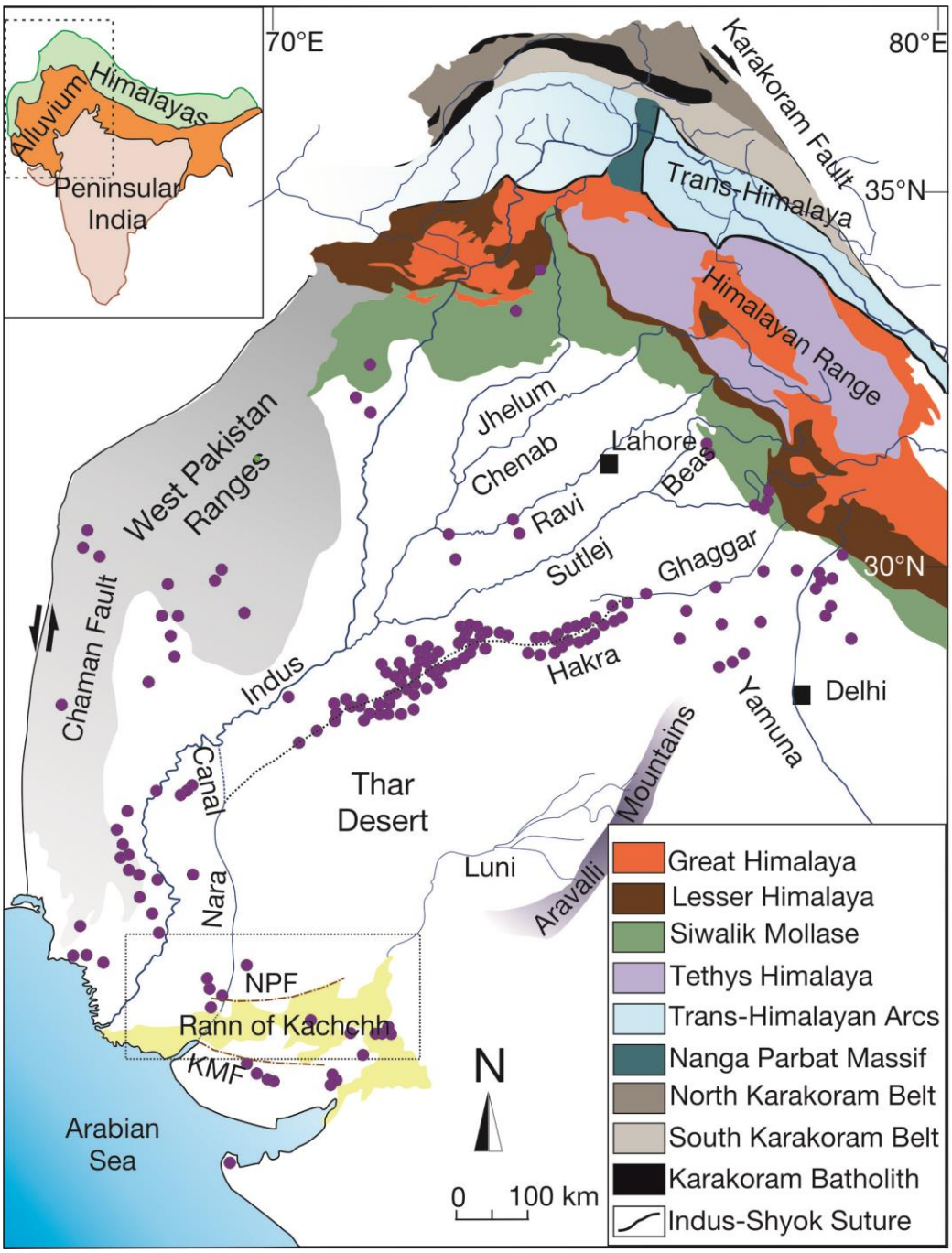

Figure 4.1: Schematic geological sketch map (modified from_Garzanti et al., 2005) showing the major river systems of north-western India and eastern Pakistan (highlighted portion of the map shown in the inset) and lithology of their catchments. Also shown are different geomorphic features/divisions of the region. The dotted line is the speculated major paleochannel (Vedic Saraswati) that connected the Ghaggar with Hakra and Nara during the Harappan period. NPF = Nagar Parker Fault; KMF = Kachchh Mainland Fault. Harappan sites are marked as purple circles.

1979; Kochar, 2000; Oldham, 1893; Pal et al., 1980; Radhakrishan and Merh, 1999; Valdiya, 2013). The sediments exposed in structurally raised sandy mounds ('bet' in local language, Fig. 4.2) and layered sand-silt sediments in the terraces around the margins of the islands (Patcham, Khadir and Bhanjada; Fig. 4.3) bear the testimony of an active fluvial past of the GRK. However, in the absence of robust sedimentological and chronological constrains, the existence of a continuous Ghaggar-Halra-Nara fluvial system flowing into the GRK during the Harappan civilization remains a conjecture. In addition to this, several other workers have suggested that the Nara was only a distributary of the Indus and had no connection to the Ghaggar-Hakra (Alizai et al., 2016, 2011b).

In the above scenario, the Great Rann of Kachchh (GRK) of western India (Fig. 4.2), which is located in the confluence zone between the lost river (vedic Saraswati?) and the Arabian Sea (Valdiya, 2013), becomes an important piece of the puzzle. Therefore, unravelling of the sedimentation history of the GRK since the mid-Holocene, besides being geologically important, has profound geo-archaeological implications towards deciphering the existence of any notable fluvial system (other than Indus) during the proliferation of Harappan civilization. To investigate this aspect of the GRK, we have studied trace element and Sr -Nd isotope geochemistry of sediments deposited in the basin during the last 5.5 kyr, and quantified, for the first time, sediment contributions from various terrigenous sources. We have also made an attempt to decipher sediment transport pathways in order to throw some light on the fluvial scenario of the Harappan period and in the process explored possible existence of a glacial fed river, originating from the higher Himalaya, draining into the Kachchh basin. Our samples came from the relict delta of the river Nara – the purported delta of the Saraswati, central and eastern GRK, mouth of the river Luni, and dunes of the southern-eastern Thar Desert (Fig. 4.2 and 4.3).

4.2 Geology of the Great Rann of Kachchh

The GRK is an enigmatic geomorphic terrain that encompasses a vast stretch of low-lying salty desert (~16,000 sq. km) at the western margin of India, and is devoid of any major drainage; except for the ephemeral river Luni and river Nara – a distributary of the Indus (Fig. 4.1). It is flanked by parabolic dunes in the north and northwest, the Banni Plain and the Wagad Upland in the south (Fig. 4.2). Structurally, the GRK is part of an east-west trending

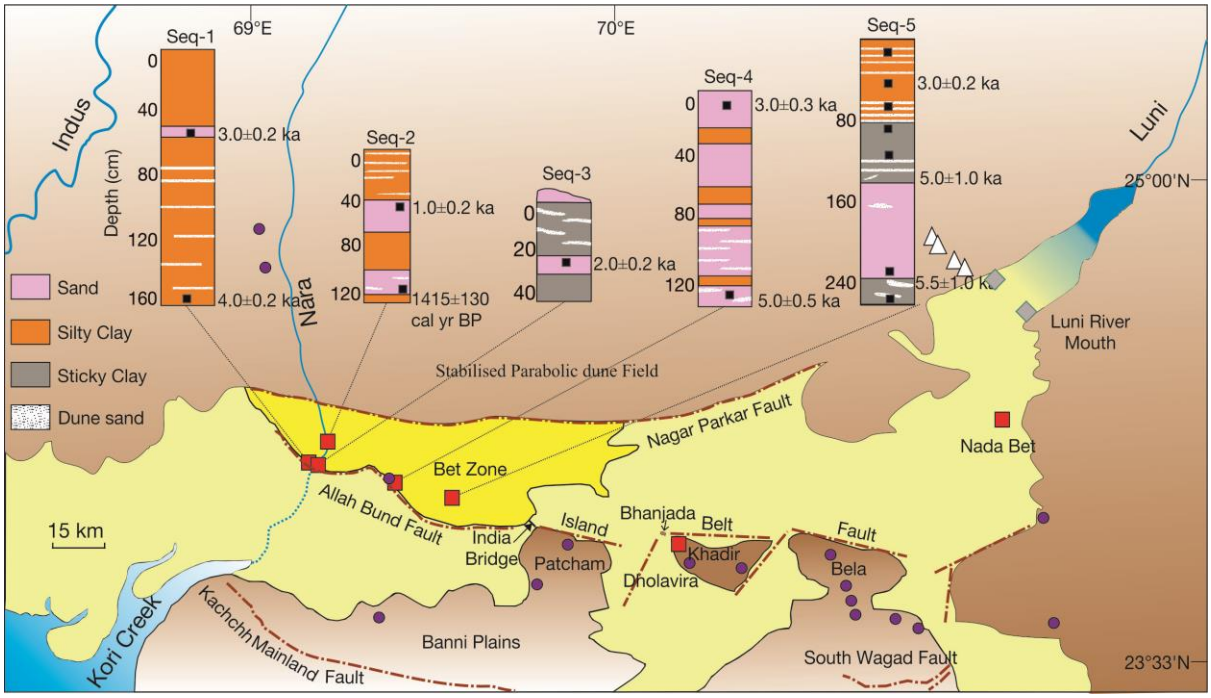

Figure 4. 2: Schematic sketch map (modified from Tyagi et al., 2012) of the blow up of the area marked in (A) showing the major geological/morphological features of the Great Rann of Kachchh (light/dark yellow) and adjoining region. Sampling locations are marked: red squares for Rann (low lands) and bet (uplifted surfaces), grey diamonds for the Luni river mouth, and white triangles for the Thar dune field. Also shown is the stratigraphy of the sedimentary sequences of the sampled horizons (Seq-1 through Seq-5) in the western Great Rann of Kachchh with OSL/radiocarbon ages marked (in ka/cal yr BP). Positions of the samples on the stratigraphic columns are marked as black squares.

paleo-rift graben believed to have formed in the Early Mesozoic (Biswas, 1987) and is bounded in the north by the Nagar Parkar Fault and in the south by the Kachchh Mainland and the South Wagad faults (Fig. 4.2). In between, there exist two other east-west trending faults; namely the Allah Bund and Island Belt (Fig. 4.2), which are known to have influenced the Quaternary morphology of the GRK (Mathew et al., 2006; Maurya et al., 2008; Rajendran and Ranjendran, 2001). It has been suggested that the present day Rann surface is an uplifted floor of a former shallow marine gulf of the Arabian Sea that had formed during sea level rise at the immediate aftermath of the last glacial period (Maurya et al., 2008; Merh, 2005; Oldham, 1926).The latest uplift is believed to have occurred at ~2 kyr ago (Tyagi et al., 2012).

Monotonously flat topography, except for small bets, makes it difficult to determine the history of sedimentation in the western part of the GRK. It is believed that much of the

Holocene sediments in the western part of the basin were derived from the Indus and Nara rivers that once flowed into the basin (Glennie and Evans, 1976). Modern silty-clay deposits are attributed to storm tides, which bring in material from the Indus Delta aided by long-shore current, during the southwest monsoon (Glennie and Evans, 1976; Tyagi et al., 2012). The Banni Plain, which receives sediments from the Mesozoic sedimentary rocks of the northern Kachchh Mainland (Glennie and Evans, 1976; Maurya et al., 2013; Fig. 4.2), acts as a buffer between the Mainland and the western GRK. Considering that the dry highlands and deserts surround the entire GRK, it is reasonable to expect aeolian contribution in the Rann sedimentation during periods of intense wind activity.

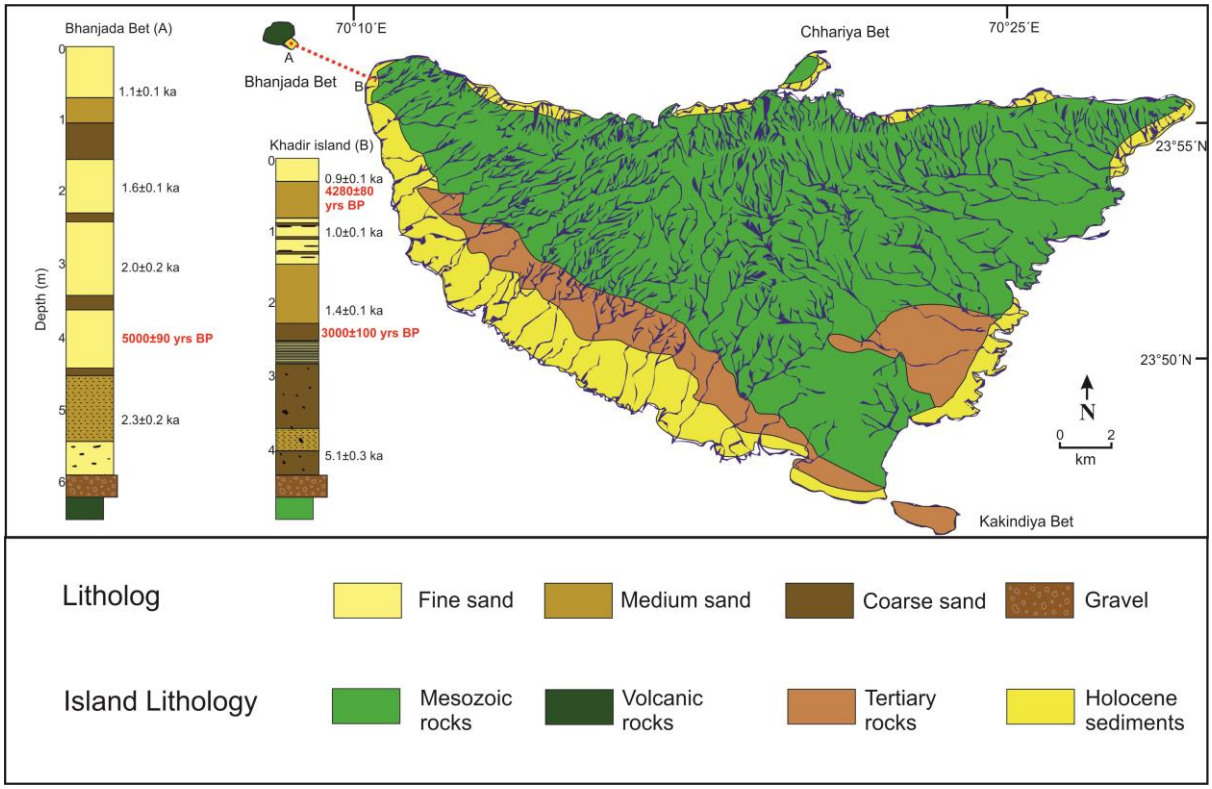

Figure 4. 3: A geological map of Khadir island showing the different lithologies exposed and the drainages present on the island (modified after Ngangom et al., 2017). Also presented is the lithologs of alluvium, exposed around the western margin of the island and eastern margin of the Bhanjada island (modified after Ngangom et al., 2016). The OSL depositional ages reported by Ngangom et al., 2017 are mentioned beside the lithologs. C-14 ages of inorganic (carbonate) carbon from bulk sediment samples measured in the present study are also presented along the lithologs, in red colour.

Unlike western GRK the eastern part has rocky islands made up of Mesozoic and Tertiary rocks (Biswas, 1987). Bela, Khadir and Patcham islands are the major ones. At present, the central and eastern GRK remains detached from the western GRK, along a

median high that passes through north-west of the Patcham Island along the India Bridge (Fig. 4.2). Alluvial successions can be observed along the margins of these rocky islands, especially the Khadir and Bhanjada islands. Both north and south flowing rivers drain the Khadir island from its northern escarpment (Fig. 4.3). The alluvial successions are preserved along the western margin of the Khadir and along the eastern margin of the Bhanjada, which is a sub-volcanic plug (Fig. 4.3). However, the origins of these alluvial successions are debated. Whereas Khonde et al., (2011) suggest that these horizons are tectonically raised Rann sediments, Ngangom et al., (2016) classify them as fluvial deposits.

Tectonically, the GRK is an active landform (Rajendran and Rajendran, 2003; Rajendran and Ranjendran, 2001) . The western GRK had seen one of the largest earthquakes of this region (M_W 7.9) in 1819 that created the Allah Band Fault Scarp. In comparison, the eastern part of the GRK is tectonically less active and there are no historical records of major earthquakes in this region especially during the Harappan times (Rajendran et al., 2008).

4.3 Stratigraphy and Sample Details

4.3.1 Sampling in the Kachchh Basin

- *Western Great Rann of Kachchh*: Sediment samples for the present study were collected from tectonically raised surfaces or terraces, incised channels and dug up trenches (Fig. 4.2). Since the primary focus of the study was the purported delta of the mythical river, we planned to examine in detail the bet zone north of the Allah Bund Fault scarp (Fig. 4.2). Samples from this zone came from five sequences in five locations, in the western GRK, which were topographically higher than the present-day high tide strands. Figure 4.2 presents stratigraphy of these horizons and the already known depositional ages from the work of Tyagi et al., (2012). Three of the sampling locations were on or near the channel of the river Nara (Fig. 4.2).
- *Eastern Great Rann of Kachchh*: Samples representing the central and eastern GRK were collected from the western periphery of Khadir Island and from Nada Bet (Fig. 4.2 and 4.3). These sediments are exposed on fault controlled terraces, which occur as sandy deposits in the centre of silt dominated GRK basin. Figure 4.3 presents the stratigraphy of the alluvium exposed along the Khadir and Bhanjada islands (Fig. 4.4) and their depositional

ages from Ngangom et al., (2016). The alluvium of the eastern GRK varies significantly in grain size compared to that of the western GRK. The eastern GRK sediments are sand dominated, whereas, the western GRK sediments are silt and clay dominated with occasional occurrences of sandy horizons. Sub-recent sediment samples were also collected from the channels inside the Khadir island.

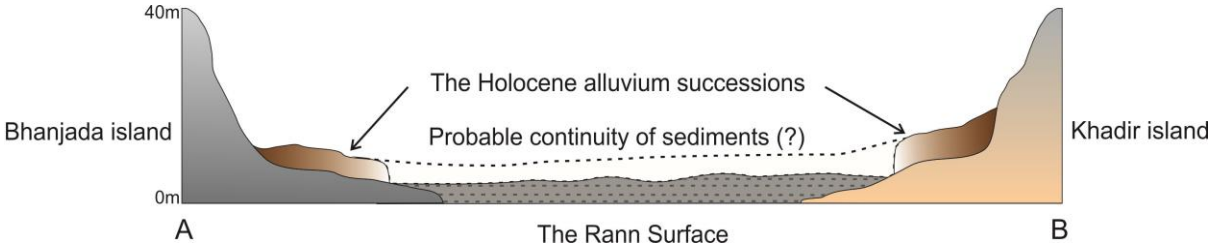

Figure 4.4: A schematic cross-section of the sedimentary successions along the AB line marked in the figure 4.3.

4.3.2 Sampling of Sediment Sources

Apart from the river Nara, other potential sources of sediments to the western GRK during the mid-Holocene include the Thar Desert, the Luni river, the Indus and the Mesozoic rocks of the rocky islands along the GRK.

- *The Thar Desert*: The Thar Desert occurs as the most dominant landscape along the northern margin of the basin. In absence of any major fluvial system from the desert into the Great Rann of Kachchh basin, the only mode of sediment transportation from the north could have been through wind. There was a need to characterize this source as only limited geochemical data existed that too from the far north-eastern margin of the desert, located ~800 km inland (Tripathi et al., 2013). In any case, the dune field at this margin cannot be considered as a potential aeolian sediment source for the GRK since the southwest monsoonal winds are believed to be the primary carrier of the desert sand (Singhvi and Kar, 2004). However, aeolian contribution from the sand dunes present in the vicinity of the GRK is more likely through local sand storms and disturbances as they lack directionality. Therefore, to accurately predict sediment contribution from the Thar, we planned to sample sand dunes that are located very close to the northern margin of the GRK. However, because of inaccessibility of the north-western and northern margin of the basin (located in Pakistan),

we could sample only the dunes located along the north-eastern margin (Fig. 4.2). These samples were sub-recent sediments from stabilized parabolic dune field.

- *The Luni River*: The river Luni is the only river system in India that drains from the Aravalli mountain ranges into the GRK (Fig. 4.1). The river currently is ephemeral and has been so since ~8ka (Kar et al., 2001). Therefore, the sediment supply through it takes place only during heavy rainfall events linked to the southwest Indian monsoon. Because of its very nature, sediments transported by the Luni are mostly reworked alluvial and aeolian deposits. To constrain its contribution to the GRK we sampled sub-surface sediments along the river mouth (Fig. 4.2). These samples would likely to provide average compositions of the Holocene sediments transported by the river.
- *The Nara River*: Although the river Nara today brings in sediments from the river Indus into the GRK, there exists no evidence to suggest if the same were true in the past. However, it has been recognized that recycled Indus sediments have been getting into the basin through creeks via tidal currents as suspended load (mostly clay, Tyagi et al., 2012). In this work we make use of the geochemical data of Clift et al., (2010) and Limmer et al., (2012) for such sediments.

- *The Mesozoic rocks of Kachchh*: The Mesozoic rocks exposed along the margin and islands of the GRK can deliver sediments into the basin via numerous seasonal streams draining through these lithologies. For constraining the sediment contributions from the Mesozoic rocks of Kachchh, we have analysed samples from the Khadir, Bela, Patcham islands and the Kachchh Mainland bordering the GRK basin.

4.4 Results and Discussion

4.4.1 Alluvial deposits of Eastern GRK

To understand the paleo-environmental condition of the eastern Great Rann of Kachchh during the Holocene we have studied the sediments deposited along the outer margins of Khadir and the Bhanjada islands. The nature, source and depositional environment of the alluvial deposits exposed along the rocky islands of the eastern GRK are highly debated. Whereas Khonde et al., (2011) argued for a shallow marine deposition of materials transported from a distant source (Indus shelf sediments), Ngangom et al., (2016) argued for

local sources and a fluvial depositional environment for these sediments. However, in the absence of detailed geochemical data it is difficult to arrive to an unequivocal answer. Besides, there are major differences in the depositional ages of these sequences as reported by these studies. In the course of the present work we aimed to constrain the geochemical composition of the local sources and correlate them with that of the sediments deposited along the island margins. The alluvial deposits are sand dominated with intercalated clay horizons and deposited over the Holocene period (Fig. 4.3). The elevated northern parts of the Khadir island are mainly composed of Mesozoic sandstones and the southern fringes are occupied with Tertiary rocks. It can be also observed that there are both south and north flowing channels draining the island.

A cross-section from the north-western fringe of the Khadir island to the Bhanjada island (AB in fig 4.3) is presented in figure 4.4. Based on the field studies we make the following observations. The alluvial sequences were deposited directly over the Mesozoic rocks in both the islands. The silty-clay deposits of the GRK lie in the space between the two islands. The Rann sediments are neither a part of the island alluvial sequences nor do they overlie.

As discussed earlier, understanding the sedimentation history of the deposits along the Khadir island has archaeological importance too. It is of great importance to understand the depositional environment of alluvium deposited on the perimeter of the Khadir island (marine vs. fluvial) during the Harappan period (mid-Holocene) because, this has a direct implication on the maritime activity of the Harappans.

4.4.1.1 Provenance of alluvial deposits of Khadir and Bhanjada islands

Figure 4.5 presents ε_{Nd} vs $^{87}Sr/^{86}Sr$ plot of the Quaternary alluvial sediments and Mesozoic rocks of the Khadir and Bhanjada islands. The Sr-Nd isotopic composition of the sediments from Khadir region, potteries from Dholavira and Mesozoic rocks are presented in the table 4.1. The plot also shows our data for several other Mesozoic rocks of nearby rocky islands of GRK and in the Kachchh Mainland bordering the GRK. From the figure the following observations and inferences can be made.

- The ~80 ma old volcanic rocks (personal communication from K. Pande) of the Bhanjada island and their weathered horizons have positive ε_{Nd} (0.8 - 2.6) and low radiogenic Sr ($^{87}Sr/^{86}Sr$ = 0.71-0.73).
- The Mesozoic sandstones of Khadir island and other places bordering the eastern GRK have low ε_{Nd} (-15 to -25). These rocks show large spread in their $^{87}Sr/^{86}Sr$ composition (0.71- 0.76).
- The alluvium exposed along the periphery of both Khadir and Bhanjada islands (Fig. 4.4) show overlapping Sr-Nd isotopic compositions indicating their common parentage. The sticky clay deposits of the Rann surface exposed between the two islands have similar isotopic composition as well. The sediments deposited within the island and at the eastern margin of Khadir also possess similar isotopic compositions.
- The observed variation in $^{87}Sr/^{86}Sr$ and ε_{Nd} of these sediments (Fig. 4.5) can be explained by a binary mixing of sediments from the two major island sources present in the vicinity viz. the volcanic rocks of Bhanjada and the Mesozoic sandstones. However, the dominance of the Mesozoic rocks as sediment source is apparent (70 – 80%, Fig. 4.5).

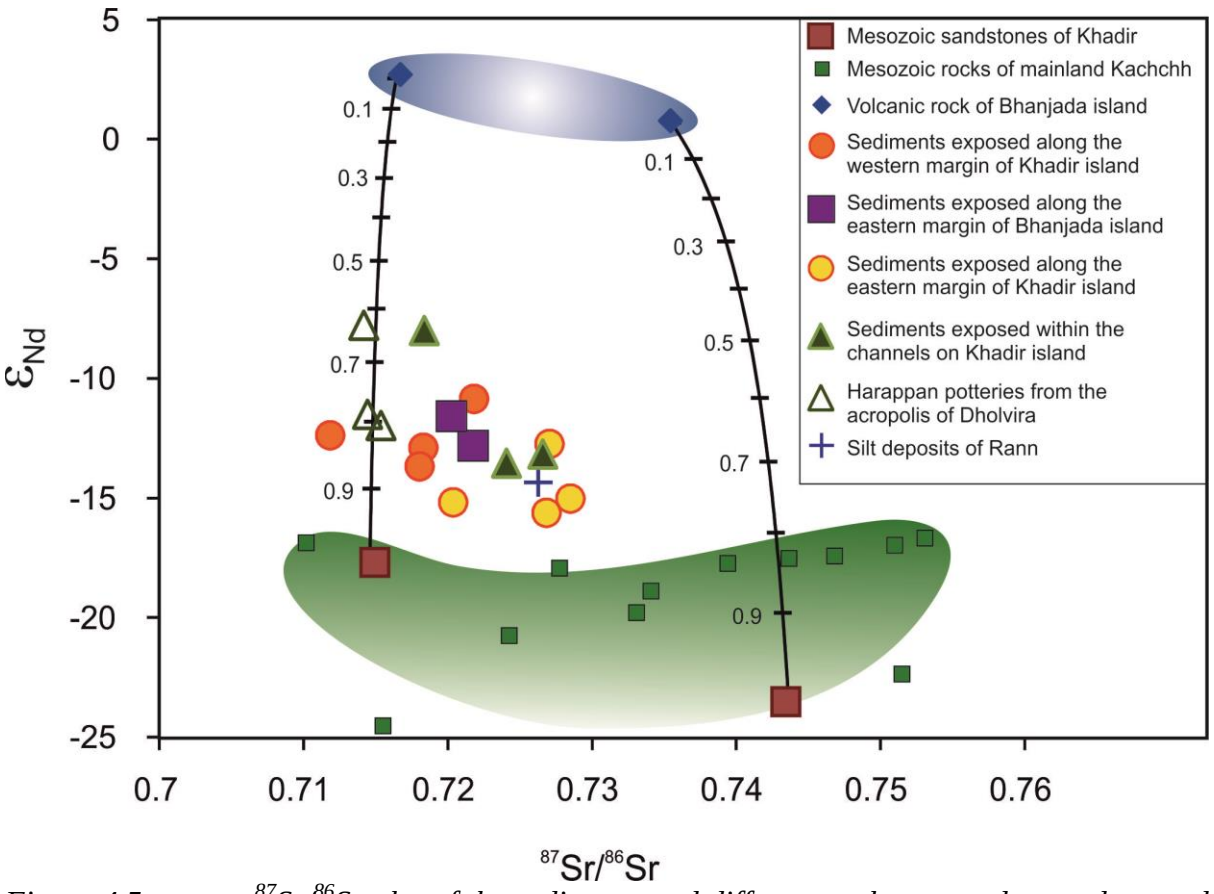

Figure 4.5: ε_{Nd} vs. $^{87}Sr/^{86}Sr$ plot of the sediments and different rocks exposed on and around the Khadir island of the eastern Great Rann of Kachchh.

- Therefore, the sediments deposited around the Khadir island of eastern GRK are clearly locally derived. There is no need to invoke any far-away source to explain the chemical composition of these alluvial deposits.
- Indirect inferences on the sediment provenance for the alluvial deposits can be derived from the isotopic compositions of the Harappan potteries found in the acropolis of Dholavira on Khadir. As discussed in the earlier chapter, the ancient potters generally used local materials to prepare their potteries. Hence, the isotopic composition of the potteries can provide information on the composition of the raw material used and hence the composition of local sediments available during the mid-Holocene period. From the figure 4.5, it can be seen that the potteries have overlapping isotopic composition with the sediments exposed on and around the Khadir island. Even the modern clay horizons found in the seasonal streams around the acropolis of Dholavira have similar compositions. This further confirms that the sediments getting deposited around Khadir island were of local origin, at least since mid-Holocene.

Our inference on the local origin of Khadir sediments is in contradiction with the findings of Khonde et al., (2011), that these alluvial deposits were of marine origin. Their conclusion was based on the presence of abundant foraminifera shells in these sediments. However, the foraminifera shells are abundant only in the topmost part of the sections and the lower parts have very less or no foraminifera shells. In addition Nangom et al., (2016) had argued that these forams do not represent deposition in a marine environment, instead they are reworked from earlier deposits. To resolve this issue, we determined C-14 ages of inorganic (carbonate) carbon from bulk sediment samples from the two horizons exposed along the Khadir and Bhanjada islands. This exercise was done with the assumption that the influx of dead carbon into the system, in form of detrital carbonates from surrounding Mesozoic rocks, had remained constant throughout. Our study revealed that the sediment horizons with very little foraminifera tests have C-14 ages of 3000±100 yrs BP and 5000±90 yrs BP in the Khadir and Bhanjada islands respectively (Fig. 4.3). The zone of maximum abundance of foraminifera at Khadir island yielded an age of 4280±80 yrs BP.

The topmost horizon with abundant foraminifera shells gives an older age than the stratigraphically older sediment layer located 3m below (Fig. 4.3). Therefore, it can be suggested that the forams found in the topmost sediment horizon are mostly reworked fossils

from older deposits. This is not in accordance with the conclusion of Khonde et al., (2011) that the forams grew in situ and the depositional environment around the Khadir island was marine. Earlier Rao et al., (1989) demonstrated how fossil forams originating from the coastal regions of Arabian Sea and the Great Rann of Kachchh as well as from the fossil bearing Tertiary rocks, can be transported in suspension by wind, into the interiors of the Thar desert without getting abraded. Probably, following the same transport mechanism reworked fossil forams were deposited along with the locally derived sediments of the Khadir island. This further indicates that the sediment depositional environment around the Khadir island was probably not marine. Estuarine condition prevailed in that region where sediments transported by local streams got deposited along with the reworked foraminifera shells.

In figure 4.6 a model for the sedimentary environment that prevailed since the mid-Holocene, around the Khadir island is presented. The key inferences on the evolution of the basin are presented below:

- During the mid-Holocene when the sea level was higher in the GRK, the streams flowing through the rocky island of Khadir were depositing their sediments all around the island before meeting the sea further to the west. The depositional environment was most probably estuarine. Overlapping chemical compositions of sediments all around the island as well as those away from the island are the evidence of this wide-spread deposition of locally derived sediments in the eastern GRK.
- Due to the gradual uplift of the Rann surface, the sea started receding since 2000 yrs BP. The local streams then incised the older deposits to reach the sea located further to the west. This caused a lot of older sediments to get eroded away exposing the Rann surface below. The remnant of these deposits remained as the alluvial sequences along the island peripheries (Fig. 4.4).

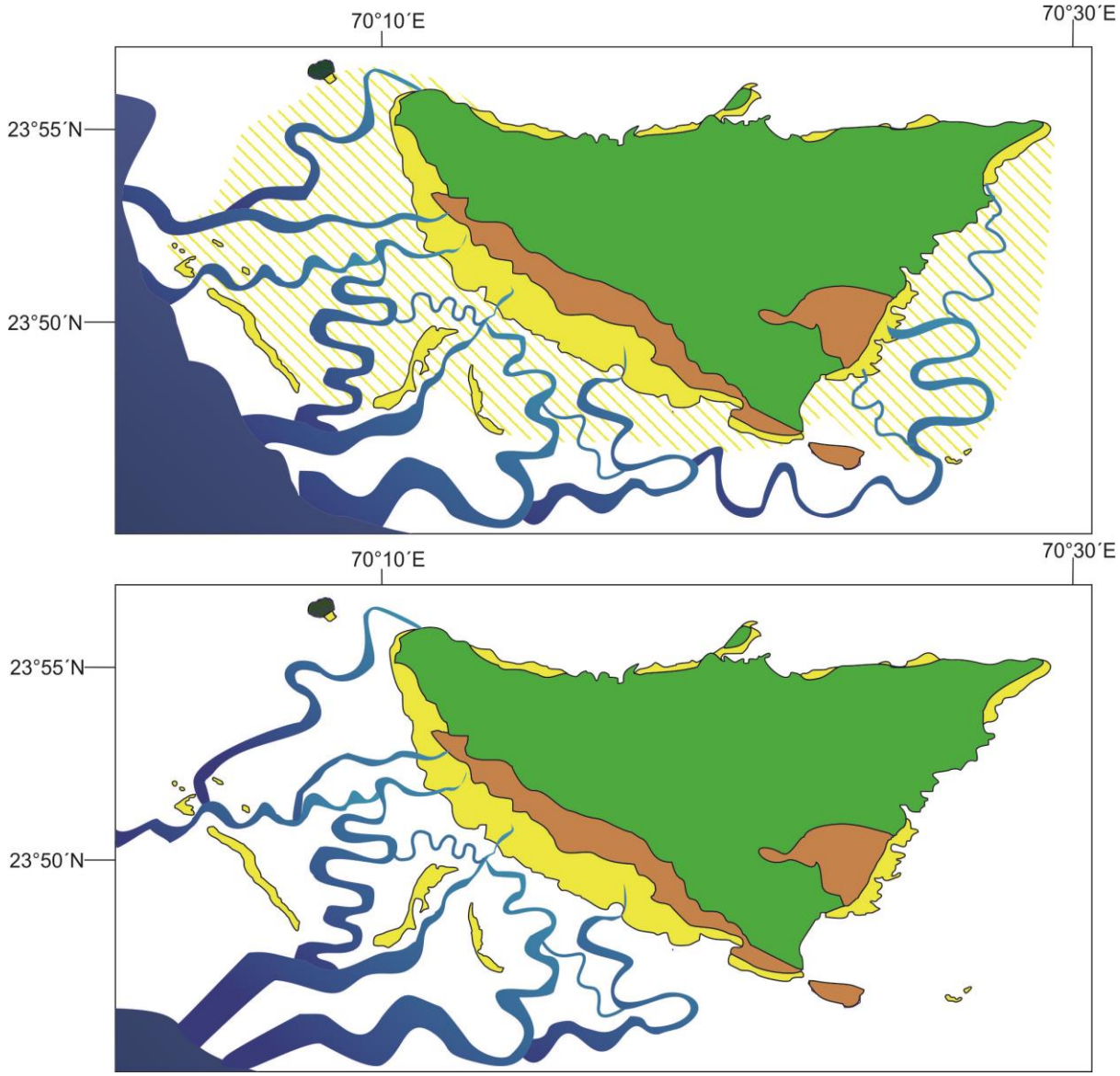

Figure 4.6: (A) A schematic representation of the sedimentation at the eastern GRK during 5-1 Ka. The sea was probably near the western part of the Khadir island and the streams which used to drain the island deposited their sediments in the vicinity of the island, probably in an estuarine condition.
(B) When the sea retreated further west, the streams incised the older sediments to reach the sea and in that process eroded most of the older alluvium, only leaving behind a few remnant cliffs around the Khadir.

4.4.2 Alluvial deposits of the Western Great Rann of Kachchh

4.4.2.1 Geochemistry of siliciclastic sediments

Our geochemical and isotopic data for bulk sediment samples and different grain size fractions from them are presented in Table 4.2 and Table 4.3, respectively. Figure 4.7 presents various trace element and isotopic plots for the sediments deposited in the western GRK. Following observations can be made from these figures.

- The chondrite normalized REE patterns (Fig. 4.7A) for the GRK sediments show pronounced light REE (LREE) enrichment and a negative Eu anomaly - characteristics of continental crust derived detritus.
- The upper continental crust normalized patterns of the sediments (Fig. 4.7B) show a flat LREE and depleted heavy REE (HREE) patterns. The latter possibly hints at removal of heavy minerals such as zircon from sediments prior to their deposition in the basin.
- Negative anomalies of Zr and Hf and depleted patterns of HREE seen in the Post Archean Australian Shale (PAAS) normalized trace element data for these samples (Fig. 4.7C) are consistent with the above observation.
- Interestingly, these patterns are, to a large extent, comparable to that observed in the sediments in the five major rivers of Punjab (Alizai et al., 2011b) and sand dunes of the Thar. These, however, are different from that reported for the sediments from the Indus Delta (Clift et al., 2002, Fig. 4.7C). This is at variance with the earlier belief that the western GRK is predominantly filled with the Indus derived sediments (Maurya et al., 2003; Tyagi et al., 2012). To further understand the nature of probable sediment sources we have made use of various cross plots of elemental and isotopic ratios wherein the fields of these sources (end-members) could be easily distinguished (Fig. 4.7D-F).
- Sediments from the Indus is known to enter the western GRK through the Kori Creek during storm tides with the help of long-shore currents, and having significant contributions from the juvenile (mantle derived) rocks of the Indus-Tsangpo Suture Zone (ITSZ). These have higher Nb/Ba, Cr/Th, ε_{Nd} and Sr content, and lower $^{87}Sr/^{86}Sr$ and Th/Y compared to the Higher-Himalaya-derived sediments in the five rivers of Punjab. Absence of adequate geochemical data does not allow us to create a field/envelope for the Thar Desert; however, we make use of our data from the dune field at the north-eastern margin of the GRK for

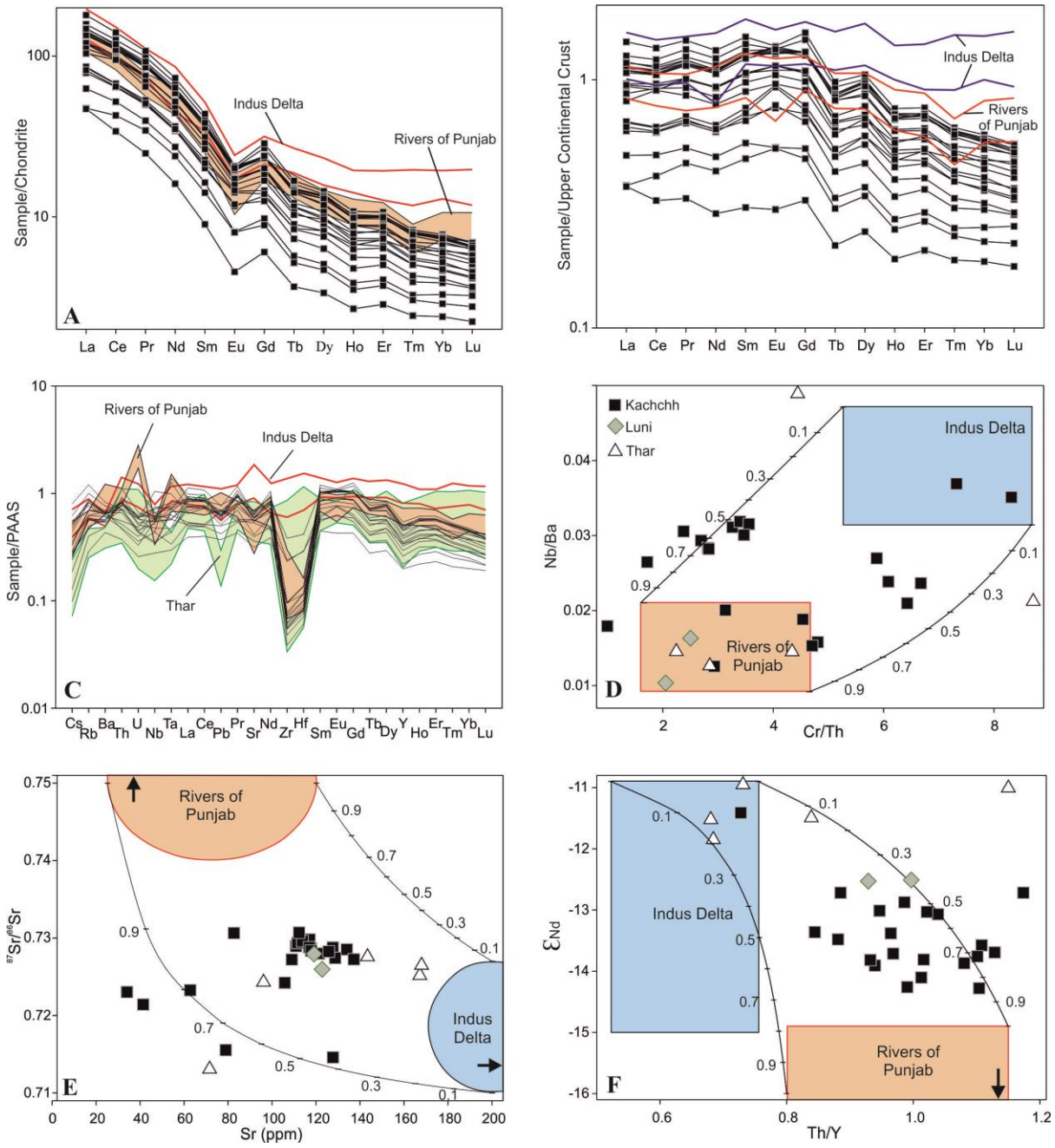

Figuer 4.7: (A) Chondrite normalised, (B) Upper Continental Crust normalised and (C) PAAS normalised multi-element trace element patterns of sediment samples from the Great Rann of Kachchh (this work) compared with that of sediments from rivers of Punjab (Orange field; Alizai et al., 2011a), Indus delta sediments (red envelop; Clift et al., 2002), and Thar desert sand (green field; this work).
(D) Nb/Ta vs. Cr/Th (E) $^{87}Sr/^{86}Sr$ vs. Sr, and (F) ε_{Nd} vs. Th/Y plots for the Kachchh, Luni and Thar samples compared with binary mixing model curves drawn considering sediments in Indus delta and rivers of Punjab as two end-members. Tick marks on mixing curves are fraction of Punjabi rivers' contributions to the mixture.
All the diagrams are modified from Chatterjee and Ray, (2017b).

comparisons. In these plots most of our samples fall in the space in-between the two major end-members (Fig. 4.7D-F) suggesting contributions from all of these sources, not just the Indus, to the sediment budget of the GRK.

Being rare-earth elements, the Sm-Nd isotopic system does not easily get disturbed by the surficial processes like erosion, transportation and sedimentation (Goldstein and Jacobsen, 1988; Najman, 2006). Therefore, this systematics is ideal for provenance study using bulk sediments. The measured ε_{Nd} of samples (with a precision of ±0.2 at 2σ) from the western GRK, the southern Thar Desert and the Luni river mouth varies in ranges of -14.3 to -11.4, -11.8 to -11.0, and -12.5 to -11.5, respectively. In figure 4.8, we compare these data with that from the Holocene sediments in the Ghaggar-Hakra channels, Indus delta and Indus shelf (Alizai et al., 2011a; Clift et al., 2008; East et al., 2015; Limmer et al., 2012; Singh et al., 2016a). From the figure the following inferences can be made.

- It can be inferred that since mid-Holocene there has been little influence of Sutlej or Yamuna in the western GRK sedimentation thus excluding the possibility of the sediments being transported by the Higher Himalayan, glacier-fed rivers.
- On the contrary, ε_{Nd} of the GRK sediments overlap with that observed in the north-eastern Thar Desert, deposited during 9.1 to 1.8 ka (Fig. 4.8A). However, as discussed in the previous section, the only possible mode by which this distal source could have contributed is through reworking by a fluvial system. The present-day ephemeral Ghaggar-Hakra river system, which is believed to have been connected to the Nara during the mid-Holocene (Valdiya, 2013), is the most suitable candidate for the above pathway. The overlapping ε_{Nd} values of pre-modern sediments in the Ghaggar-Hakra system with that of the western GRK sediments (Fig. 4.8B) may be considered as an evidence for the above.
- It is also observed that ε_{Nd} data of the GRK sediments overlap with that of the sediments in the Indus delta (Fig. 4.8B), however, they do not follow the regional trend (with age) shown by the latter thus making it an unlikely source.
- The trend seen in the GRK data (Fig. 4.8B) appears to suggest mixing between sediments from the Ghaggar-Hakra fluvial system (containing reworked aeolian sand from northern desert margin) and Indus borne detritus, in addition to possible contributions from the Luni and the southern Thar (Fig. 4.8A and 4.8B).

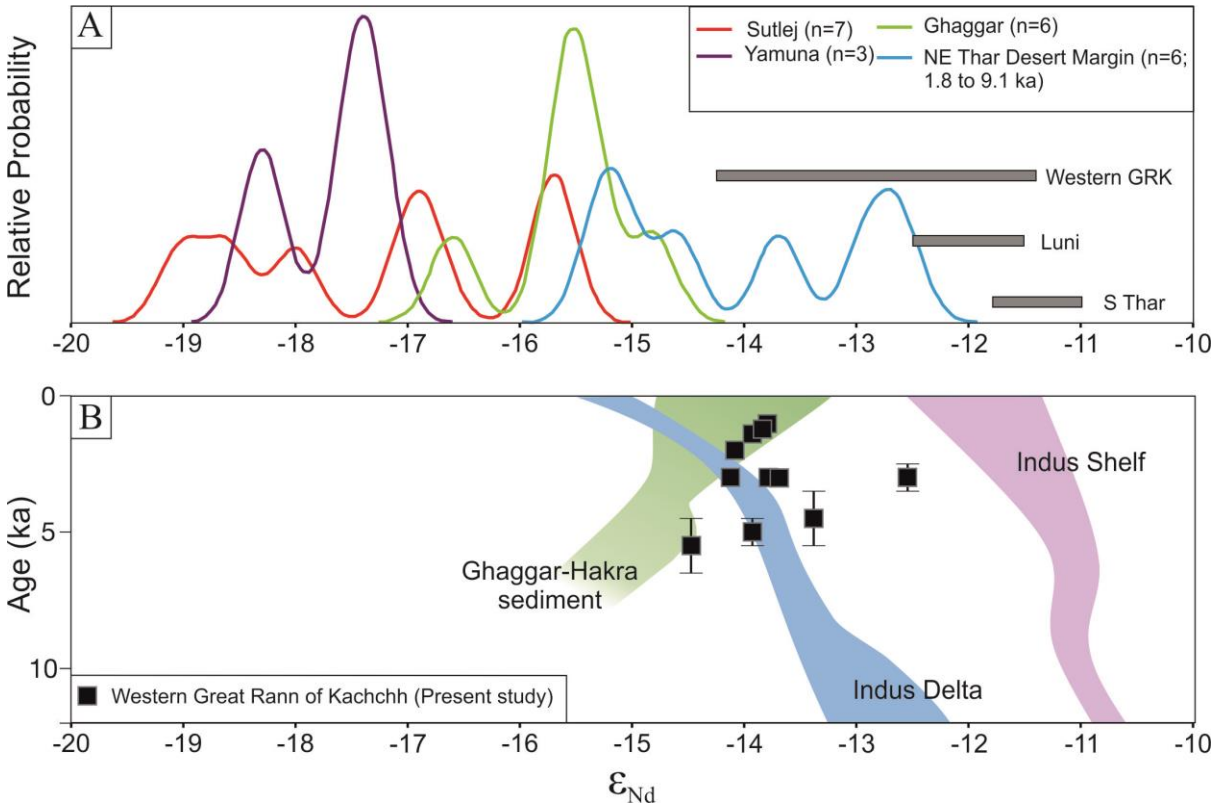

Figure 4. 8: (A) Kernel density estimation (KDE) plot of ε_{Nd} re-drawn from (Singh et al., 2016b) displaying the Nd-isotopic variability in Sutlej, Yamuna, Ghaggar and Thar desert (present work and Singh et al., 2016a; Tripathi et al., 2013).
(B) The Western Great Rann of Kachchh sediments deposited since 5.5 ka are compared with the sediments of Ghaggar-Hakra River (East et al., 2015; Singh et al., 2016a), Indus delta (Clift et al., 2010) and shelf (Limmer et al., 2012) deposited during the Holocene.
All the diagrams are modified from Chatterjee and Ray, (2017b).

4.4.2.2 Grain size dependency of isotopic compositions

For a better characterization of the provenances, we utilize Sr isotopic ratios of these sediments along with their Nd isotopic ratios, keeping in mind the limitations of the former (Najman, 2006). It is generally believed that unlike the ^{147}Sm-^{143}Nd isotopic system, the ^{87}Rb-^{87}Sr system is susceptible to chemical weathering, because of selective fractionation of parent element from the daughter which leads to dissimilar Sr isotopic ratio between the source rocks and the product sediments (Meyer et al., 2011). Higher chemical weathering leads to more radiogenic detritus which is largely controlled by higher $^{87}Sr/^{86}Sr$ bearing fine-grained (clay) fraction, primarily derived from high-Rb bearing micas in the source rocks

(Garçon et al., 2014; Meyer et al., 2011). Below we discuss the effect of grain size on Sr isotopic composition of the GRK sediments and evaluate its bearing on determination of provenances.

Six western GRK samples were selected for studying the effect of grain size on the $^{87}Sr/^{86}Sr$ variation. Different grain size fractions were separated namely: clay (<4μ), silt (4-15.6μ), fine sand (45-75μ) and coarse sand (75-90 μ). By weight coarse sand was found to be the dominant fraction (> 70%) in these samples. All the fractions were decarbonated using dilute HCl before being analyzed for Sr isotopic compositions. These data are plotted in Figure 4.9. As can be seen from the plot, although there is a large variation of $^{87}Sr/^{86}Sr$, our data show an overall increasing $^{87}Sr/^{86}Sr$ value with increasing grain size (Fig. 4.9A). This is entirely opposite of what is generally observed in most fluvial systems wherein the finest fractions (suspended load/clay) contain more radiogenic Sr than the coarser fractions (Garçon et al., 2014).

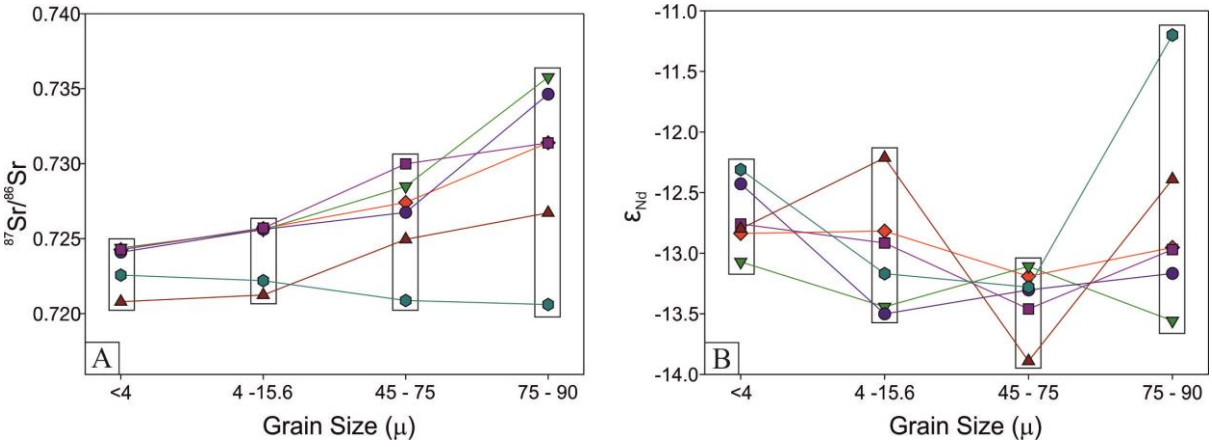

Figure 4.9: (A) Variation of $^{87}Sr/^{86}Sr$ ratio in different grain size fractions (clay, silt, fine and coarse sand) of sediments from Nara river mouth and bet zones are shown. Also plotted are Sr-isotopic ranges of various probable sources. The different symbols represent six separate samples.
(B) Variation of ε_{Nd} values in different grain size fractions of the same sediments mentioned above. The different symbols represent six separate samples.
All the diagrams are modified from Chatterjee and Ray, (2017b).

One plausible explanation for the GRK data could be that different sources with distinct isotopic signatures contributed to different grain size fractions. However, such a phenomenon should have been reflected more prominently is Nd isotopic compositions,

because ε_{Nd} is a more robust provenance indicator compared to $^{87}Sr/^{86}Sr$. However, we do not observe any such dependency in Fig. 4.9B. In fact, a closer look reveals that different grain size fractions of four samples show overlapping ε_{Nd} (within ±0.5, where experimental reproducibility is ±0.2 at 2σ). We therefore believe that the observed variation of $^{87}Sr/^{86}Sr$ ratios with grain-size (Fig. 4.9A) is a product of lesser chemical weathering compared to physical weathering in the source, similar to that observed in many parts of the Himalaya (Singh et al., 2008). Since during chemical weathering, high-Rb bearing minerals (containing high radiogenic Sr) in the source (e.g., muscovite; K-feldspar) break down to clays, finer fractions of sediments produced exhibit higher $^{87}Sr/^{86}Sr$ compared to that in coarser fractions (Garçon et al., 2014). Interestingly, however, we encountered significant amount of muscovite in coarser fractions of our samples, which prompted us to make the above inference. In such a scenario, the $^{87}Sr/^{86}Sr$ of the clay fractions in our samples might not represent the composition of the sources, and therefore, the use of bulk sediment composition for provenance study.

4.4.2.3 Provenance of sediments and implications

- The sediment load of the Indus in its upper reaches, north of its confluence with the rivers of Punjab (Fig. 4.1), is dominated by material derived from sources in the Trans-Himalayas and its Sr-Nd isotopic compositions (IS: Indus at Skardu; Fig. 4.10A) are largely controlled by sediments derived from the ITSZ, Karakoram Batholith, and Ladakh Batholith (Clift et al., 2002).
- Sediments in the Indus delta and shelf (Fig. 4.10A) possess less radiogenic Nd (more radiogenic Sr) compared to that in sediments in the upper Indus. This is due to mixing with sediments from much older crustal rocks in the Higher Himalayan Crystalline (HHC) and Lesser Himalayas (LH), contributed through the rivers of Punjab (Clift et al., 2010).
- The sediments of the GRK having $^{87}Sr/^{86}Sr$ in the range of 0.7146 to 0.7307 and ε_{Nd} in the range of -14.3 to -11.4 although overlap with the field for the Indus Delta (Fig. 4.10A), mostly possess more radiogenic Sr - a characteristic feature of the Lesser and Higher Himalayan sediments.
- The Luni and southern Thar (bordering the GRK basin) sediments have comparable ε_{Nd} and marginally higher $^{87}Sr/^{86}Sr$ values than those of the Indus sediments; however, possess more radiogenic Nd than the GRK sediments (Fig. 4.10A).

- These data clearly suggest that the GRK sediments neither represent any of the pure end-members such as the IS, the Luni, the Thar, the HHC, and the LH nor they are exclusively derived from the river Indus in its lower reaches or the Indus shelf. Since most of our samples are from the western GRK and that there was very limited (if any) sediment transport from the eastern GRK into the western GRK in the past (Glennie and Evans, 1976), the river Luni could not have been a major sediment source or pathway for the latter. Persistent ephemerality and aeolian activity from 8 ka onwards in the Luni basin (Kar et al., 2001), and dissimilar isotopic compositions of the Luni sediments with those of the western GRK sediments (Fig. 4.10A) also support this inference.
- A three component mixing model involving compositions of the IS, HHC and LH (Fig. 4.10A) reveals that although the GRK sediments deposited between 5.5 and 1.0 ka contain a large Trans-Himalayan component (up to 70%), there exists a significant component of the combined Higher and Lesser Himalayan sources. The Trans-Himalayan component can easily be explained by the deposition of the Indus sediments (in lower reaches), directly or reworked, via the Thar desert, and/or through storm tides entering into the western GRK through the Kori Creek that brings in silt and clay from the Indus delta with the help of long-shore currents. It should be noted that although the river Indus transports HHC-LH sediments contributed to it through its eastern tributaries, $^{87}Sr/^{86}Sr$ of the bulk sediments is lowered by a significant non-radiogenic Trans Himalayan component in the main channel - which is reflected in the isotopic composition of the Indus Delta (Clift et al., 2010).
- We, however, observe higher $^{87}Sr/^{86}Sr$ values (> 1.3%) in the sediments of western GRK (Fig. 4.10A), which suggest that there could have been other sources than the river Indus. Since in the present geomorphic set up, direct deposition of the HHC-LH derived sediments into the basin is not possible, contribution from a third source is envisaged.

As mentioned earlier, the Ghaggar-Hakra channel originating from the Siwaliks, made of rocks derived from the HHC-LH (Tripathi et al., 2013), could have been a pathway for the Himalayan contribution to the GRK basin were through the river Nara in the past. Interestingly, the modern sediments of the Ghaggar, which should have had $^{87}Sr/^{86}Sr$ and ε_{Nd} in the range of that of the HHC/LH (Fig. 4.10A), possess lower $^{87}Sr/^{86}Sr$ and higher ε_{Nd} (Tripathi et al., 2013). This has been attributed to contributions from the Paleogene, sub-Himalayan foreland deposits of the Subathu Group (Tripathi et al., 2013). Assuming that the

nature of various sediment sources has not changed since the mid-Holocene, we evaluated their contributions in the samples studied in this work (Fig. 4.10B).

- It is clear from the figure that the pre-modern sediments of the central and eastern GRK, from the Khadir Island (K) and Nada bet (N), although have Sr-Nd isotopic compositions similar to that of the Indus Delta (or Indus in lower reaches), are most likely derived from the river Luni, the Thar Desert and Mesozoic rocks exposed on the islands. In any case, the local sources do not produce significant amount of sediment and their compositions are very different from that of the western GRK sediments.
- Comparison of our isotopic data with model grids of a three component mixing, where sediments from the Ghaggar, southern Thar and the Indus delta/shelf are the end-members (Fig. 4.10B), suggests that 20 to 30% of the sediments deposited in the western GRK during 5.5 to 1.0 ka could have been delivered through the now-defunct pathway connecting the Ghaggar, Hakra and Nara channels.
- The samples that possess high radiogenic Sr (> 0.728) are both sand and clay rich sediments and these are not confined to any age bracket in the studied period. A large number of them come from fluvially deposited horizons.

If the finding of (Giosan et al., 2012) that there was fluvial activity in the Nara valley ~2.9 kyr ago were to be believed then our younger samples most likely represent monsoonal flooding events. Although the geochemical data for the GRK sediments clearly point towards a significant presence of sub-Himalayan (Siwalik) sediments that are not part of the Indus detritus.The overwhelming presence of the latter and southern Thar sand (up to 70%) makes it apparent that no perennial fluvial system was active in the Ghaggar-Hakra-Nara system during the Mature Harappan period. Our data nonetheless suggest that the Ghaggar-Hakra-Nara channels had remained active, possibly as a monsoon-fed system, until ~1.0 kyr ago. It was a sub-parallel system to the Indus, which transported sediments from the southern flanks of the Himalayas along with reworked aeolian sands into the GRK. Such an inference is not inconsistent with the inferences of (Giosan et al., 2012) and that these channels were active through intermittent flooding during the mid-Holocene, even after a substantial weakening of the monsoon post 4.2 ka (Enzel et al., 1999; Staubwasser et al., 2003; Wünnemann et al., 2010), before being covered by aeolian deposits. Although it is difficult to directly infer about the prevailing climatic conditions from our geochemical study, the sedimentological

observations that substantial fluvial sand was deposited during 5.0-3.0 ka and 1.4-1.0 ka (Fig. 4.2) suggest enhanced rainfall, possibly caused by stronger Indian monsoon. Such an inference is supported by studies that propose short phases of monsoonal strengthening in peninsular India during 5100-4700 ka, 4105-2640 ka, and medieval warm period (Band et al., 2016; Banerji et al., 2016; Ngangom et al., 2012; Sarkar et al., 2000; Yadava and Ramesh, 2005) in the background of a regional decreasing trend since ~7 ka (Dixit et al., 2014; Sarkar et al., 2016).

4.5. Conclusions

Field studies, geochemistry and Sr-Nd isotopic data for mid-Holocene terrigenous detritus from the GRK reveal that the river Luni, Mesozoic rocks on the islands, and parabolic dune field of the south-eastern Thar are the primary contributors of sediments to the central and eastern GRK. The sediments deposited around the rocky islands of eastern GRK are primarily derived from local sources and deposited by seasonal local streams.

On the other hand, sediments deposited in the western GRK during 5.5 to 1.0 kyr ago, although are primarily derived from the river Indus and transported into the basin by storm tides from the Indus delta and/or shelf; contain a significant amount of an independent sub-Himalayan component (30 - 40%). This sub-Himalayan component most likely was transported through the now defunct Ghaggar-Hakra-Nara river system. Since this river system, which ran parallel to the Indus, had dwindling water supply during the Harappan period, sediments carried by it must have reached the GRK only during heavy flooding events. Overwhelming presence of Indus detritus in the GRK makes it difficult to test the hypothesis of existence of a mega, glacial-fed river through the Ghaggar-Hakra-Nara channels during this period. These channels, however, were active until as late as 1.0 ka and therefore, their drying up may not have any causal relationship with the decline of the Harappan civilization.

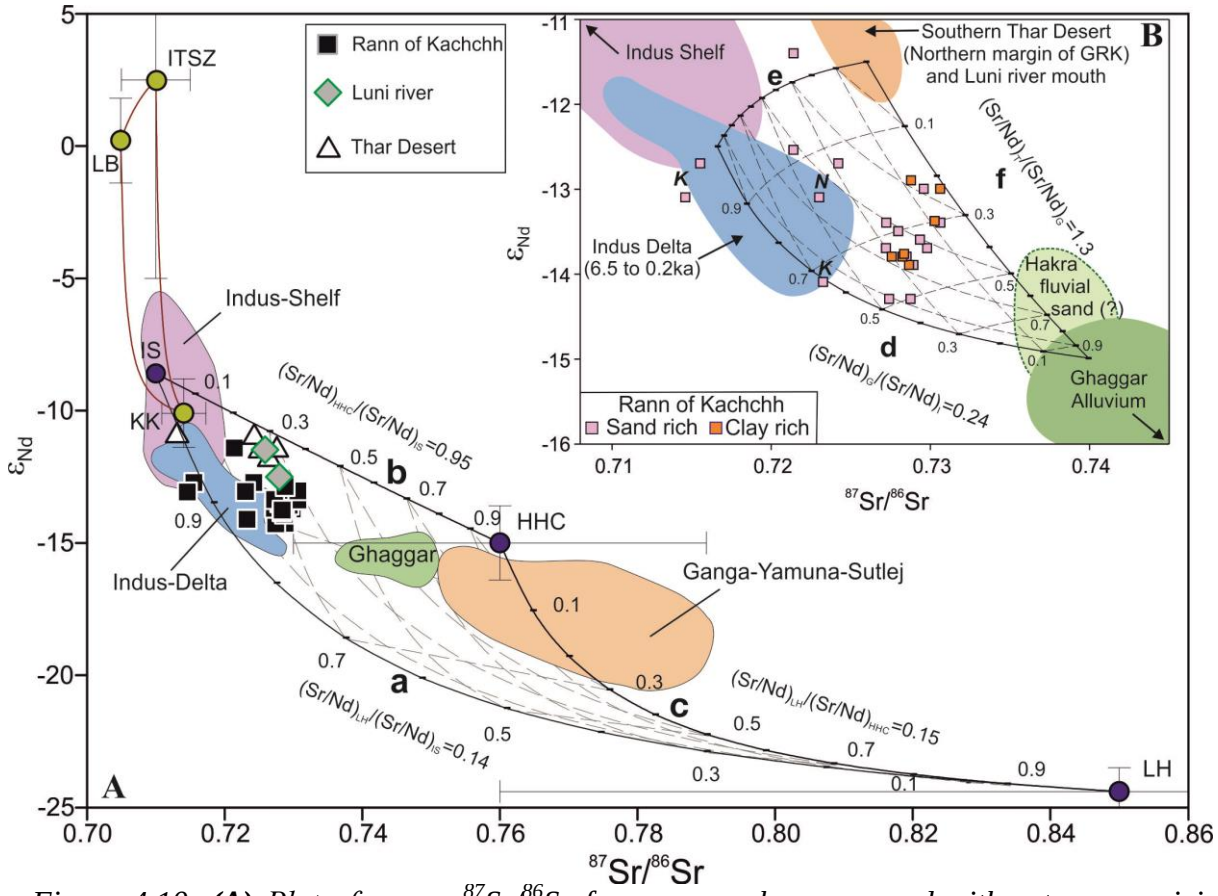

Figure 4.10: ***(A)*** *Plot of* ε_{Nd} *vs.* $^{87}Sr/^{86}Sr$ *for our samples compared with a ternary mixing grid. The three end-members are: (1) Indus sediments at Skardu (IS), (2) sediments derived from the Higher Himalayan Crystallines (HHC), and (3) sediments derived from the Lesser Himalayas (LH). IS component itself plots within another three component mixing grid involving the Indo-Tsangpo Suture Zone (ITSZ), Karakoram (KK) and Ladakh Batholith (LB) as end-members. Error bars cover the entire range of values for various components. Also shown are fields for sediments in the Indus Delta, present-day Ghaggar, and Ganga-Yamuna-Sutlej river systems. Curves a, b, and c represent binary mixing between typical compositions of two each of the end-members, whose compositions are: IS: Nd = 25 ppm; Sr = 210 ppm;* ε_{Nd}*= -8.6;* $^{87}Sr/^{86}Sr$*= 0.71, HHC: Nd = 30 ppm; Sr = 240 ppm;* ε_{Nd}*= -15.0;* $^{87}Sr/^{86}Sr$*= 0.76, and LH: Nd = 100 ppm; Sr = 120 ppm;* ε_{Nd}*= -24.4;* $^{87}Sr/^{86}Sr$*= 0.85. Error bars of end-member compositions are at* 3σ*. The diagram is modified from Chatterjee and Ray, (2017b).* ***(B)*** *Plot of* ε_{Nd} *vs.* $^{87}Sr/^{86}Sr$ *for only the Great Rann of Kachchh samples, compared with a ternary mixing grid involving Indus river sediments, Thar Desert, and Ghaggar. Only* ε_{Nd} *values are available for fluvial sands of Hakra stream*(East et al., 2015). *However considering the fact that, Hakra is the downstream extension of Ghaggar, we have considered the range of* $^{87}Sr/^{86}Sr$ *values for Hakra sediments to be similar to Ghaggar. Hence, the zone defined for Hakra sediments in the figure are question marked. K and N represent samples from the Khadir Island and Nada Bet, respectively, in the eastern Rann of Kachchh (Fig. 1B). Curves d, e, and f represent binary mixing between typical compositions of two each of the end-members and these are: Indus Shelf/Delta: Nd = 30 ppm; Sr = 350 ppm;* ε_{Nd}*= -12.5;* $^{87}Sr/^{86}Sr$*= 0.7166, southern Thar Desert: Nd = 40 ppm; Sr = 150 ppm;* ε_{Nd}*= -11.5;* $^{87}Sr/^{86}Sr$*= 0.726, and Ghaggar: Nd = 100 ppm; Sr = 280 ppm;* ε_{Nd}*= -15;* $^{87}Sr/^{86}Sr$*= 0.740. Data sources: present work and refs (Allègre and Othman, 1980; Clift et al., 2002; Najman, 2006; Scharer et al., 1990; Singh et al., 2016a; Tripathi et al., 2013). The diagram is modified from Chatterjee and Ray, (2017b).*

Table 4.1 Sr-Nd isotopic compositions of sediments from the Khadir island, Bhanjada island, potteries from Dholavira and various Mesozoic rocks.

Samples	Description	$^{87}Sr/^{86}Sr$	e_{Nd}
KH-15-6	White Weathered sandstone (Khadir)	**0.714940**	**-17.7**
KH-15-11	Alkaline Rock (Bhanjada island)	**0.716780**	**2.6**
KH-15-14	weathered Alkaline Rock (Bhanjada island)	**0.735500**	**0.8**
KH-15-27	Yellow sandstone (Khadir)	**0.743415**	**-23.5**
KH-15-27R		**0.743439**	
KH-15-22	Sand near western gully	**0.721850**	**-10.9**
KH-15-28	Silty-sand on Khadir island	**0.726640**	**-13.2**
KH-15-33	sediments from the eastern margin of Khadir	**0.727085**	**-12.9**
KH-15-34		**0.728468**	**-15.1**
KH-15-35		**0.720501**	**-15.3**
KH-15-37	Top fine sand	**0.724140**	**-13.6**
KH-15-23	Rann sediment from the western margin of Khadir	**0.726327**	**-14.4**
KH-15-23R		**0.726325**	
KH-15-40	Rann sediment from the eastern margin of Khadir	**0.726999**	**-15.7**
KH-15-15	Sediments along the western margin of Khadir	**0.718329**	**-12.9**
KH-15-17		**0.718072**	**-13.7**
KH-15-20		**0.711865**	**-12.4**
BJ-15-3	Sediments along the eastern margin of Bhanjada	**0.720350**	**-11.6**
BJ-15-5		**0.721822**	**-12.9**
KH-15-30	Clay from sream around Dholavira	**0.718440**	**-8.0**
DV-1	Dholavira Pottery Samples	**0.713944**	**-11.8**
DV-2		**0.713626**	**-7.9**
DV-3		**0.714845**	**-12.2**
KS-1	Mesozoic rocks of Kachchh mainland bordering the GRK and Paccham island	**0.715403**	**-24.6**
M-61		**0.710273**	**-16.9**
G-1		**0.753146**	**-16.7**
G-2		**0.714821**	**-12.3**
WD-2		**0.733121**	**-19.8**
FS-7		**0.743703**	**-17.6**
DB-1		**0.751619**	**-22.4**
FS-0		**0.739414**	**-17.7**
BHU-1		**0.734185**	**-18.9**
GS-09		**0.724305**	**-20.7**
JUM-1		**0.746849**	**-17.4**
JHN-7		**0.727765**	**-17.9**
JHN-12		**0.751035**	**-17**

Table 4.2: Geochemical data for sediment samples from the Great Rann of Kachchh

Sample	SBTL-1[K]	NRMOSL-1[K]	ABP-1a[K]	KHTL-1[D]	KSTL-1[K]
Cs	1.92	3.84	3.99	8.33	3.97
Rb	64.2	94.4	91.8	123.1	90.4
Ba	313	363	354	402	348
Th	13.5	12.3	16.1	8.1	10.4
U	1.83	1.64	2.07	1.50	1.42
Nb	8	11	11	14	10
Ta	1.77	0.85	0.91	0.93	1.62
La	37	35	43	19	28
Ce	77	72	86	39	58
Pb	12.2	13.1	15.3	8.4	12.8
Pr	9.4	8.5	10.2	4.7	7.1
Sr	128	134	129	79	117
Nd	31	27	33	16	23
Zr	12	13	15	49	11
Hf	0.4	0.4	0.5	1.5	0.4
Sm	6.3	5.7	6.7	3.2	4.8
Eu	1.2	1.1	1.2	0.7	1.0
Gd	5.5	4.9	5.9	2.8	4.1
Tb	0.60	0.53	0.63	0.32	0.46
Dy	3.5	3.1	3.7	2.1	2.7
Y	13.6	12.1	14.6	9.1	10.7
Ho	0.58	0.50	0.61	0.38	0.46
Er	1.6	1.5	1.8	1.2	1.3
Tm	0.2	0.2	0.2	0.2	0.2
Yb	1.2	1.1	1.3	1.0	1.0
Lu	0.16	0.15	0.18	0.15	0.13
Sc	6.7	7.3	8.4	11.0	6.7
V	39	49	56	86	43
Cr	23	33	38	67	29
Co	3	4	5	7	4
$^{87}Sr/^{86}Sr$	0.72878	0.72853	0.72743	0.71553	0.72982
$^{143}Nd/^{144}Nd$	0.511907	0.511930	0.511906	0.511982	0.511935
$\varepsilon_{Nd}(0)$	-14.3	-13.8	-14.3	-12.7	-13.7

Sample	KHTL-3[D]	BBMF[K]	KH/DV/TL1[D]	ABP-2[K]	KSTL-2[K]
Cs	1.48	9.28	3.88	7.57	7.75
Rb	46.2	160.1	73.6	131.9	137.3
Ba	281	497	17	427	426
Th	5.4	10.4	4.8	10.3	9.7
U	0.80	1.36	0.79	1.37	1.33
Nb	5	12	6	7	7
Ta	0.38	0.75	0.38	0.56	0.61
La	15	29	11	29	26
Ce	32	62	26	60	59
Pb	7.4	12.7	3.0	12.2	12.7
Pr	3.8	7.2	3.3	7.2	6.6
Sr	63	109	128	111	112
Nd	12	23	11	23	21
Zr	20	14	18	12	8
Hf	0.6	0.5	0.6	0.4	0.3
Sm	2.5	4.7	2.2	4.8	4.4
Eu	0.5	1.0	0.5	1.0	0.9
Gd	2.0	4.0	1.8	4.1	3.7
Tb	0.21	0.43	0.19	0.43	0.40

Dy	1.3	2.5	1.2	2.5	2.3
Y	5.4	9.2	4.6	9.5	8.7
Ho	0.22	0.40	0.20	0.42	0.38
Er	0.7	1.2	0.6	1.2	1.1
Tm	0.1	0.1	0.1	0.1	0.1
Yb	0.6	0.9	0.5	0.9	0.8
Lu	0.08	0.12	0.07	0.12	0.11
Sc	3.3	12.2	5.6	9.9	9.6
V	33	97	45	77	68
Cr	25	63	32	49	45
Co	2	8	4	7	8
$^{87}Sr/^{86}Sr$	0.72327	0.72723	0.71459	0.72896	0.72937
$^{143}Nd/^{144}Nd$	0.511915	0.511936	0.511968	0.511927	0.511942
$\varepsilon_{Nd}(0)$	-14.1	-13.7	-13.1	-13.9	-13.6

Sample	KRNOSL-3[K]	ABTL-2[K]	SBTL-4[K]	KH/DV/TL2[D]	BdB(b)-1[K]
Cs	0.77	3.79	4.34	5.82	6.60
Rb	39.3	90.4	99.9	99.6	130.6
Ba	201	375	438	394	420
Th	1.3	11.4	11.8	7.0	7.5
U	0.30	1.89	1.84	1.11	1.23
Nb	3	12	14	8	11
Ta	0.13	1.00	1.05	0.43	0.80
La	3	33	34	20	20
Ce	6	68	70	41	41
Pb	8.4	15.6	11.5	10.0	13.8
Pr	0.7	8.3	8.5	4.9	5.1
Sr	41	121	118	106	114
Nd	2	26	27	15	16
Zr	8	16	20	20	13
Hf	0.3	0.6	0.7	0.7	0.5
Sm	0.5	5.7	5.7	3.1	3.5
Eu	0.2	1.2	1.1	0.7	0.8
Gd	0.5	4.9	4.9	2.6	3.0
Tb	0.06	0.56	0.54	0.27	0.34
Dy	0.4	3.4	3.3	1.6	2.1
Y	1.7	13.0	12.6	5.9	7.9
Ho	0.08	0.58	0.55	0.27	0.36
Er	0.2	1.7	1.6	0.8	1.1
Tm	0.0	0.2	0.2	0.1	0.1
Yb	0.2	1.3	1.2	0.7	0.8
Lu	0.03	0.18	0.16	0.09	0.11
Sc	1.2	8.5	8.9	8.1	8.8
V	14	53	60	64	65
Cr	4	37	40	45	44
Co	1	4	3	5	7
$^{87}Sr/^{86}Sr$	0.72141	0.72800	0.72869	0.72423	0.72961
$^{143}Nd/^{144}Nd$	0.512053	0.511947	0.511925	0.511986	0.511971
$\varepsilon_{Nd}(0)$	-11.4	-13.5	-13.9	-12.7	-13.0

Sample	NRMOSL-3[K]	GdB-2[K]	C-16/13[K]	C-16/17[K]	C-16/21[K]
Cs	2.81	7.09	4.97	11.98	5.27
Rb	79.3	136.7	111.2	192.3	111.4
Ba	365	445	429	538	419
Th	11.2	6.8	12.1	10.4	12.0
U	1.79	1.02	1.95	1.79	1.87
Nb	10	11	14	20	13

Ta	0.73	0.73	0.96	1.27	0.92
La	33	19	33	25	32
Ce	67	40	70	58	67
Pb	13.7	13.6	12.7	10.2	12.5
Pr	8.2	4.8	8.3	6.1	8.1
Sr	137	112	126	83	117
Nd	26	15	27	20	25
Zr	12	10	20	50	16
Hf	0.4	0.4	0.7	1.4	0.6
Sm	5.7	3.3	5.7	4.0	5.5
Eu	1.2	0.8	1.2	0.8	1.1
Gd	4.9	2.9	4.9	3.5	4.8
Tb	0.56	0.31	0.55	0.39	0.54
Dy	3.5	1.9	3.4	2.4	3.3
Y	13.3	7.0	13.0	10.2	12.2
Ho	0.58	0.32	0.56	0.45	0.56
Er	1.7	0.9	1.7	1.4	1.6
Tm	0.2	0.1	0.2	0.2	0.2
Yb	1.3	0.7	1.3	1.2	1.2
Lu	0.17	0.09	0.17	0.16	0.16
Sc	7.9	8.6	9.5	13.6	9.8
V	49	61	65	119	69
Cr	32	45	43	76	42
Co	3	6	4	7	4
$^{87}Sr/^{86}Sr$	0.72725	0.73066	0.72832	0.73064	0.72881
$^{143}Nd/^{144}Nd$	0.511953	0.511952	0.511930	0.511970	0.511978
$\varepsilon_{Nd}(0)$	-13.4	-13.4	-13.8	-13.0	-12.9

Sample	C-16/26[K]	NB-1[N]	MS-1[L]	BKS-4[L]	BKS-1[T]
Cs	4.97	0.47	1.46	1.25	1.53
Rb	110.7	23.9	64.6	57.8	55.9
Ba	451	128	340	315	281
Th	12.2	6.0	5.5	8.1	6.7
U	1.58	1.43	0.79	1.12	0.94
Nb	9	2	4	5	6
Ta	0.61	0.06	0.32	0.91	0.55
La	35	11	15	24	23
Ce	73	21	29	50	45
Pb	11.8	4.0	13.0	12.3	4.7
Pr	8.8	2.4	3.5	6.0	4.9
Sr	118	34	119	123	167
Nd	28	7	11	19	18
Zr	80	14	7	10	13
Hf	2.1	0.5	0.3	0.4	0.4
Sm	5.9	1.4	2.2	3.9	3.1
Eu	1.2	0.3	0.6	0.8	0.7
Gd	4.9	1.2	1.9	3.3	2.9
Tb	0.53	0.14	0.22	0.36	0.34
Dy	3.0	0.9	1.4	2.2	2.0
Y	11.1	3.6	5.6	8.7	9.8
Ho	0.50	0.15	0.23	0.37	0.36
Er	1.4	0.5	0.7	1.1	1.1
Tm	0.2	0.1	0.1	0.1	0.1
Yb	1.0	0.4	0.5	0.9	1.0
Lu	0.14	0.06	0.07	0.12	0.13
Sc	9.6	1.6			5.8
V	65	10			41

Cr	38	6	11	20	58
Co	4	1	2	2	3
$^{87}Sr/^{86}Sr$	0.72837	0.72303	0.72794	0.72610	0.72516
$^{143}Nd/^{144}Nd$	0.511933	0.511969	0.511997	0.512050	0.512047
$\varepsilon_{Nd}(0)$	-13.8	-13.1	-12.5	-11.5	-11.5
Sample	BKS-1-CLAY^{T}	BKS-2^{T}	BKS-3^{T}	BKS-5^{T}	BHVO-2
Cs	3.60	1.73	1.65	1.08	0.12
Rb	75.0	64.0	57.0	40.3	10.3
Ba	260	313	280	201	130
Th	16.1	6.3	5.0	6.4	1.1
U	3.37	0.72	0.62	0.63	0.42
Nb	13	5	4	3	17
Ta	0.46	0.47	0.30	0.28	0.95
La	32	21	18	21	15
Ce	78	40	36	41	39
Pb	2.7	5.2	5.9	4.1	1.2
Pr	7.3	4.3	4.0	4.4	5.2
Sr	72	168	143	96	388
Nd	23	15	11	11	24
Zr	181	16	7	13	163
Hf	5.8	0.5	0.3	0.5	3.9
Sm	5.0	2.7	2.6	2.5	5.9
Eu	0.9	0.7	0.8	0.6	2.0
Gd	5.1	2.5	2.4	2.4	6.1
Tb	0.67	0.30	0.28	0.27	0.84
Dy	4.6	1.9	1.6	1.5	5.2
Y	22.0	9.2	6.0	5.5	23.4
Ho	0.92	0.34	0.30	0.29	0.89
Er	3.0	1.1	0.9	0.9	2.5
Tm	0.4	0.1	0.1	0.1	0.3
Yb	3.0	1.0	0.8	0.9	1.9
Lu	0.44	0.14	0.11	0.13	0.26
Sc	9.5	6.1	3.9	3.1	31.6
V	78	32	27	22	337
Cr	71	27	14	14	291
Co	3	3	2	2	48
$^{87}Sr/^{86}Sr$	0.71307	0.72648	0.72758	0.72429	0.70346
$^{143}Nd/^{144}Nd$	0.512077	0.512031	0.512049	0.512074	0.512967
$\varepsilon_{Nd}(0)$	-11.0	-11.8	-11.5	-11.0	6.4

Superscripts: ^{K} = Western Great Rann of Kachchh; ^{D} = Khadir Island, Eastern Great Rann of Kachchh; ^{N} = Nada Bet, Eastern Great Rann of Kachchh; ^{L} = Luni River mouth; ^{T} = Thar dune sand. Trace element concentrations are in ppm.Data for BHVO-2 is averages of 10 analyses. . $\varepsilon_{Nd} = [(^{143}Nd/^{144}Nd)_{sample}/(^{143}Nd/^{144}Nd)_{Chondrite}-1]*10^{4}$. Reproducibility (2$\sigma$): $^{87}Sr/^{86}Sr = \pm 0.000005$; $\varepsilon_{Nd} = \pm 0.1$For $\varepsilon_{Nd}(0)$ calculation a value of 0.512638 was taken for present-day $^{143}Nd/^{144}Nd$ for chrondrite meteorite.

Table 4.3: Isotopic data for different grain sizes separated from sediments of the Nara river mouth and Western Great Rann of Kachchh

<4μm	NRM-OSL-1C	NRM-OSL-2C	NRM-OSL-3C	KRM-OSL-1C	KRM-OSL-2C	KRM-OSL-3C
$^{87}Sr/^{86}Sr$	0.72427	0.72438	0.72409	0.72427	0.72079	0.72257
$^{143}Nd/^{144}Nd$	0.51198	0.511968	0.512001	0.511984	0.511982	0.512007
$\varepsilon_{Nd}(0)$	-12.8	-13.1	-12.4	-12.8	-12.8	-12.3

4-15.6 μm	NRM-OSL-1S	NRM-OSL-2S	NRM-OSL-3S	KRM-OSL-1S	KRM-OSL-2S	KRM-OSL-3S
$^{87}Sr/^{86}Sr$	0.72568	0.72559	0.72562	0.72570	0.72124	0.7222
$^{143}Nd/^{144}Nd$	0.511981	0.511949	0.511946	0.511976	0.512012	0.511963
$\varepsilon_{Nd}(0)$	-12.8	-13.4	-13.5	-12.9	-12.2	-13.2

45-75 μm	NRM-OSL-1A	NRM-OSL-2A	NRM-OSL-3A	KRM-OSL-1A	KRM-OSL-2A	KRM-OSL-3A
$^{87}Sr/^{86}Sr$	0.72741	0.72849	0.72674	0.72999	0.72495	0.72087
$^{143}Nd/^{144}Nd$	0.511962	0.511966	0.511956	0.511948	0.511926	0.511957
$\varepsilon_{Nd}(0)$	-13.2	-13.1	-13.3	-13.5	-13.9	-13.3

75-90 μm	NRM-OSL-1B	NRM-OSL-2B	NRM-OSL-3B	KRM-OSL-1B	KRM-OSL-2B	KRM-OSL-3B
$^{87}Sr/^{86}Sr$	0.73140	0.73576	0.73463	0.73138	0.72672	0.72060
$^{143}Nd/^{144}Nd$	0.511974	0.511943	0.511963	0.511973	0.512003	0.512064
$\varepsilon_{Nd}(0)$	-12.3	-13.6	-13.2	-13.0	-12.4	-11.2

Chapter - 5

Geochemistry of Quaternary Alluvium in the Luni River Basin

5.1 Introduction

Weathering and subsequent sedimentary processes play a major role in sculpting Earth's surface and redistributing the eroded material from source rocks to depositional sinks. Globally, rivers are the main transporting agents of these eroded sediments (Martin and Whitfield, 1983). Thus, the geochemistry of river borne clastic sediments provides important insights into the source rock characteristics. However, the geochemical behaviour of sediments also depends on the extent of chemical weathering, physical sorting during transportation and diagenetic alterations. Therefore, the geochemical provenance study of sediments can also be utilized to understand weathering in the source region (Singh and Rajamani, 2001). Trace elements, especially the Rare Earth Elements (REE), are considered useful for understanding these processes (Taylor and McLennan, 1985). In many instances, however, the REE can also be redistributed within a weathering profile without a net loss or gain (Condie, 1991; Duddy, 1980; Nesbitt, 1979; Sharma and Rajamani, 2000) and as a consequence, different sediment loads (suspended and bed loads) may show different REE abundances/patterns in comparison to their source rocks. It has been observed that REE fractionations are more prominent when physical weathering dominates over chemical weathering (Viers et al., 2009),whereas intense chemical weathering obliterates any such discrepancy between the source and the product. Predominance of chemical weathering over physical weathering, however, requires appropriate climatic conditions in the catchment. Therefore, provenance studies need to evaluate the weathering conditions in the source regions carefully before interpreting the geochemical data of clastic sediments.

Present study deals with the fluvial deposits of the Luni River originating from a Pre-Cambrian terrain and flows along the southern margin of the Thar desert (Fig. 5.1). Generally, arid zone rivers respond quickly to minor perturbations in climate and the Luni River is not an exception (Kar et al., 2001). The river originates from the Proterozoic Delhi-Aravalli fold belt in the east and flows through a granitic-rhyolitic catchment. However, the contributions of these lithologies to the sediment budget is not well constrained. The dominance of physical weathering over chemical weathering in this region makes the problem more interesting. In the present work we have studied trace element geochemistry and Sr -Nd isotopic ratios of sediments deposited in the Luni basin during the Quaternary period. The elemental geochemistry of different fluvial deposits has been studied to

understand the changing effect of weathering on different source rocks and sediment produced by it. Using the Sr-Nd isotopic ratio of the sediments the contributions from different source rocks have been quantified.

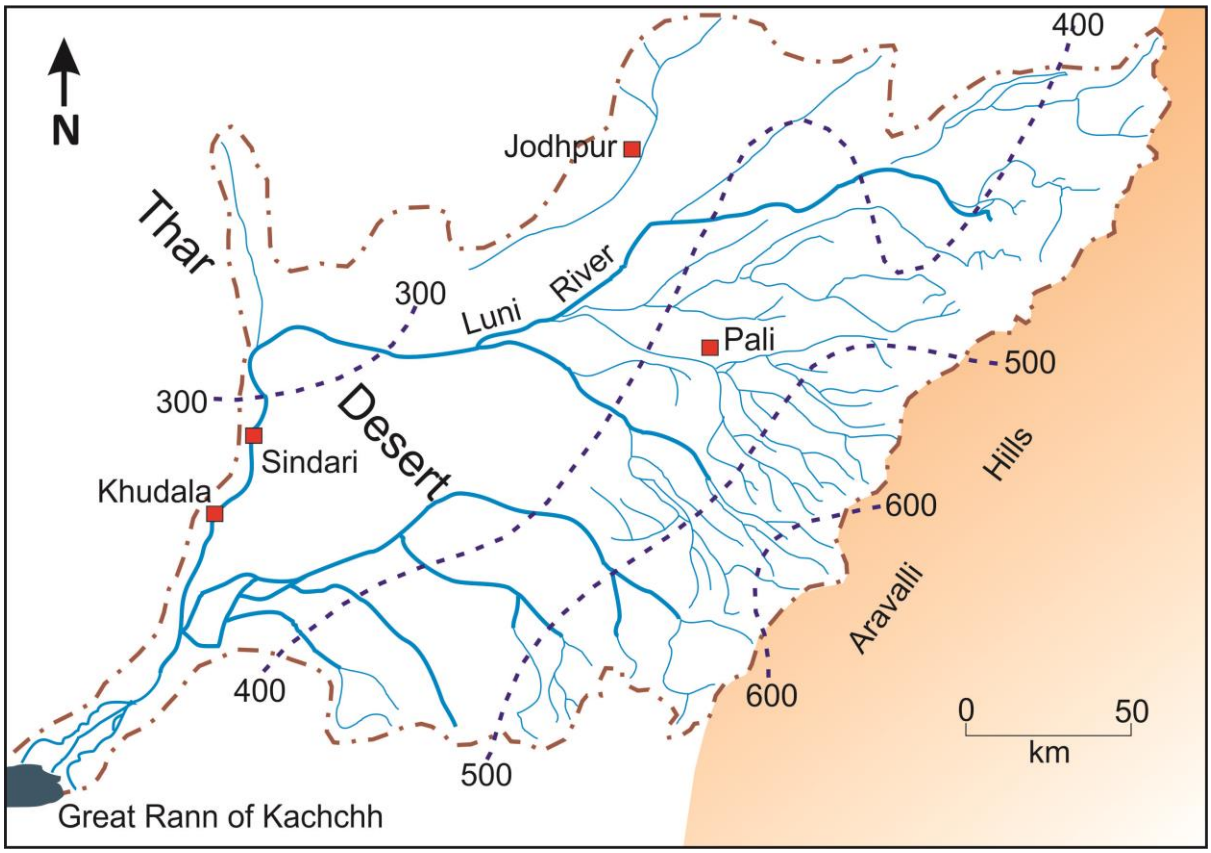

Figure 5.1: The drainage system of the Luni river basin and the isohyets are representing the average rainfall of the basin.

5.2 Alluvial stratigraphy, the catchment and the study area of the Luni basin

The Luni river system is the major drainage of the Thar Desert and flows in the south-east corner of the desert. The river originates in the Aravalli range and flows westward draining into the Great Rann of Kachchh (Fig.5.1). The upper catchment of the river generally receives 500-600 mm/yr of rainfall (Fig. 5.1). However, most of its drainage lies within the semi-arid region with annual rainfall of 300-400 mm, a large amount of which is received during the SW Indian Monsoon. Rest of the year, the discharge is almost absent and

aeolian sands accumulate in the river channel. In monsoonal floodings the aeolian sands get washed out and re-deposited downstream. The Luni possesses all the traits of an ephemeral river.

5.2.1 Stratigraphy of the Luni Alluvium

The general stratigraphy and facies architecture of the Luni alluvium have been worked out by many earlier workers (Jain et al., 2005; Kale et al., 2000; Kar et al., 2001; Sharma et al., 1984). Figure 5.2 presents a general stratigraphy of the Luni alluvium (Jain et al., 2005). The facies architecture of the Luni alluvium is described below.

- There are two distinct types of sedimentary sequences in the Luni basin.
- The older Type-1 sequence was deposited probably during the Pliocene (ages beyond luminescence dating, thus the minimum age is considered 200 ka).
- Type -1 sequences consist of fining upward sequences of alternate gravelly beds and mud-dominated horizons. These facies mainly represent deposition in a braided river system. Absence of aeolian sand horizons indicate a much wetter depositional condition, probably before the formation of the dune fields in this region.
- There exist a long hiatus after the deposition of Type- 1 sequence.
- Type – 2 sequences were deposited during the Pleistocene to Holocene periods over the last 100 ka.
- The facies architecture of Type-2 sequence is quite different from the older deposits. The successions in it suggest a change in the depositional environment. They represent deposition in fluctuating fluvio-aeolian environment. Three incision events with ages of 14ka, 9-11 ka and 3-1 ka have been identified with periods of increased rainfall.
- Unlike, the older deposits these horizons are dominated with sand.
- The deposition started with a gravelly bed followed by aeolian sand sheet and sheet wash deposits.
- The following period witnessed an increase in monsoonal precipitation during the beginning of the Holocene. As a consequence, several fining upward fluvial sand-silt units were deposited during the higher fluvial activities.
- Finally, the alluvial deposits were covered by aeolian sands reworked from older fluvial deposits. In the recent times slack water deposits get generated due to seasonal floods.

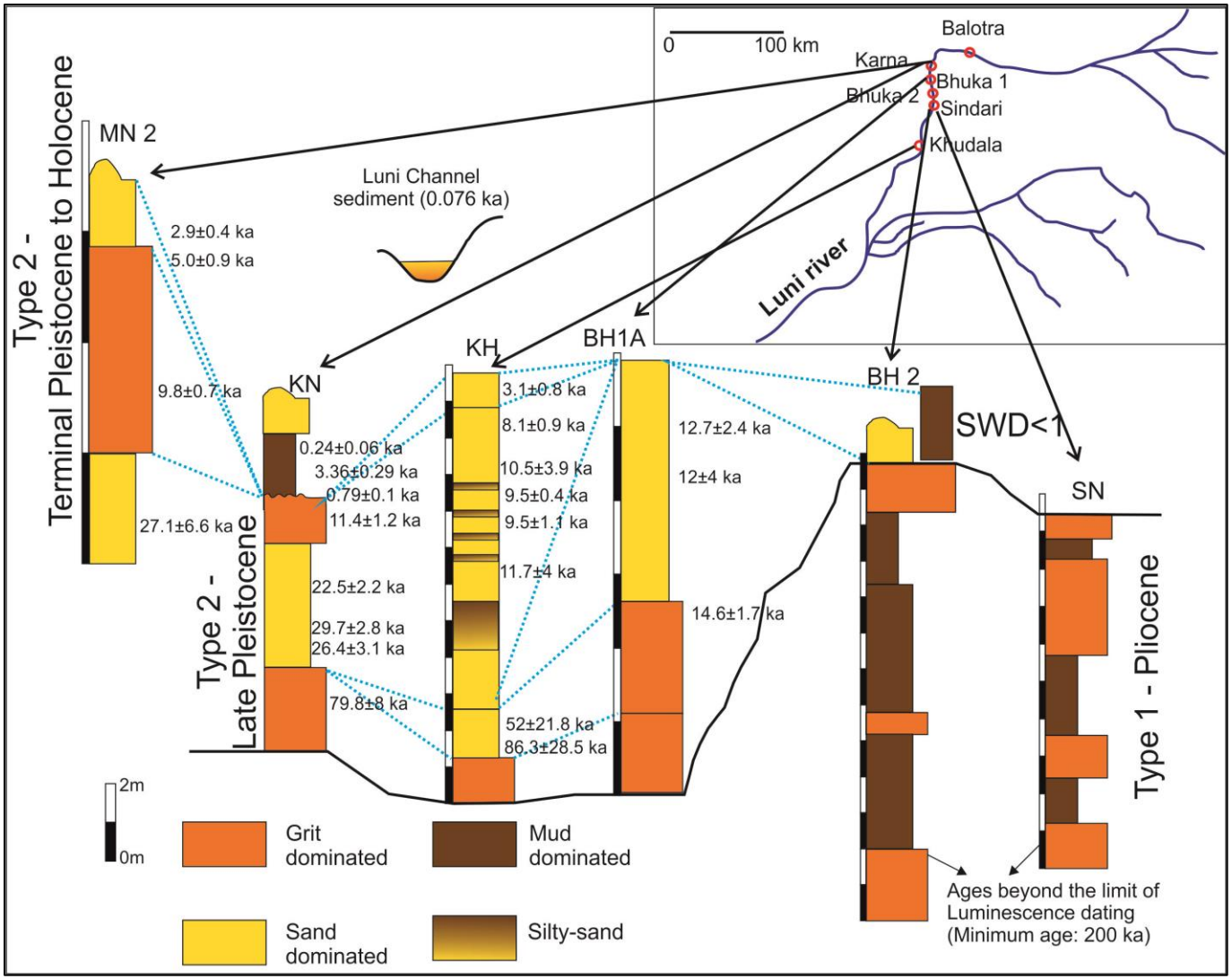

Figure 5.2: The stratigraphic framework of the Luni alluvium (modified after Jain et al., 2005).

- In the piedmont regions of the river and on the river bed, locally derived modern gritty-sand deposits can be observed.

5.2.2 Catchment of the Luni river

Figure 5.3 represents the catchment lithology of the Luni river basin. Based on the existing information the following observations can be made about this river system and its catchment.

- The river originates from the piedmont region of the major axial section of the Aravalli range where its elevation is highest (~1200m, between Ajmer and Mt. Abu).
- The rocks exposed along the upper catchment (the Aravalli ridges flanking the piedmont) of the river are mainly composed of schists, slates, gneisses and calc-silicates of Delhi Supergroup.
- Along with the metasedimentary rocks of the Delhi Supergroup, a suit of metamorphosed mafic-ultramafic rocks are exposed along the western margin of the Aravalli ranges (Volpe and Macdougall, 1990). They are representative of the suture zone between the Aravalli and the Delhi Supergroups (the type section is the Phulad Ophiolite). These rocks are exposed all along the catchment of the Luni (from Ajmer to Desuri) and its tributaries. They are mainly composed of massive amphibolites, hornblendites, meta-gabbros, serpentinites and dioritic dykes.
- Pockets of pre-Aravalli Banded Gneissic Complex (BGC) rocks are also exposed at the western margin of the mountain ranges.
- Syn to Post orogenic granites (e.g., Erinpura Granite) are exposed in the western part of the Aravalli ranges. At places exposures of the Malani rhyolites can also be found.
- Minor exposures of sedimentary rocks belonging to the Marwar Supergroup can be observed at the lower catchment of the Luni.
- In the downstream, most of the catchment is covered with old alluvium deposits and sand dunes.

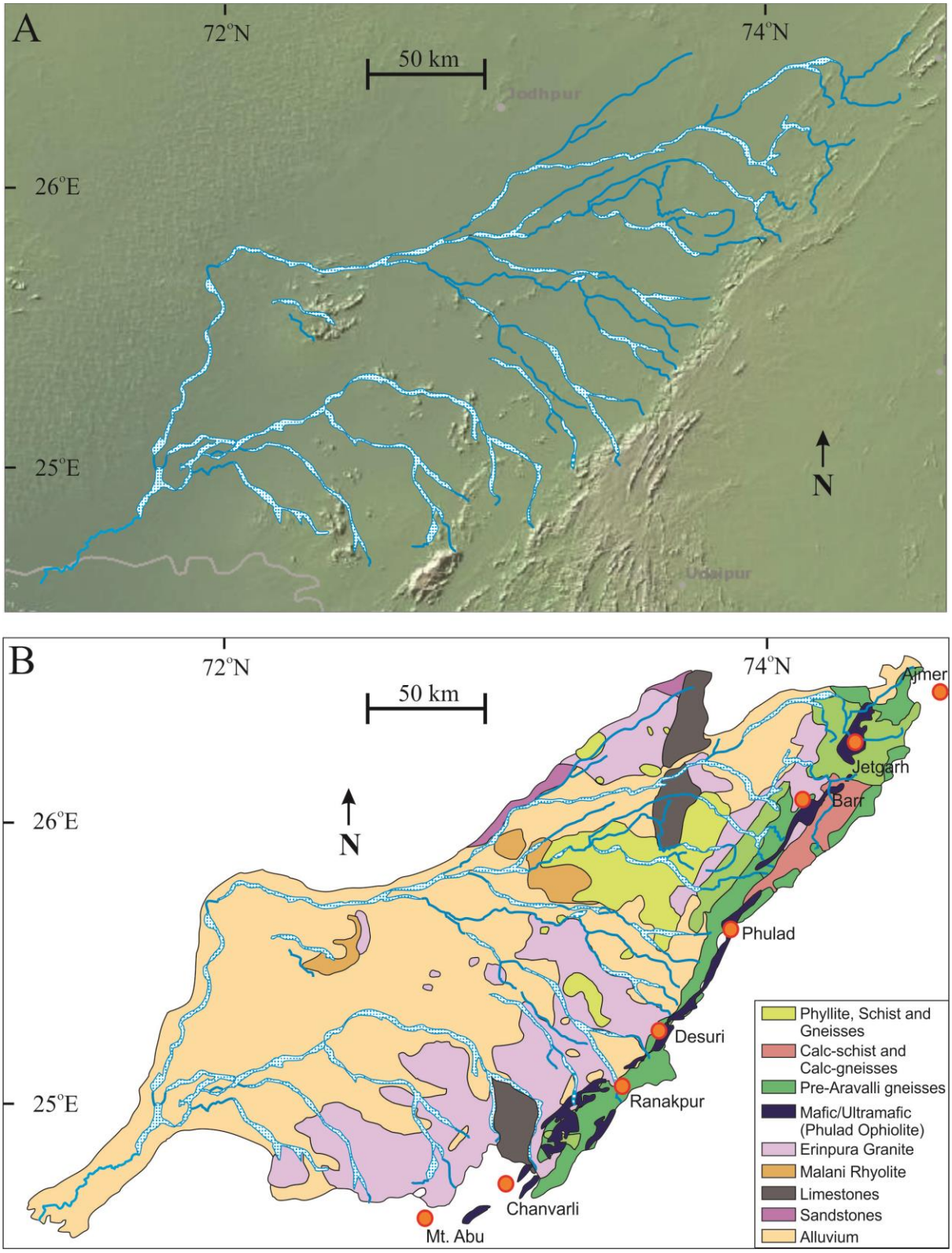

Figure 5.3: (A) Topographic map of the Luni river basin (National Centers For Environmental Information) showing the major elevated regions in the catchment. It can be observed that the river emerges from the piedmont region of the major axial heights of the Aravalli ranges.

(B) The lithological map of the catchment of the Luni river (modified from Sharma et al., 1984; Volpe and Macdougall, 1990).

5.2.3 The Study Area

Description of sample locations and samples used in the present study are presented below.

- Sampling for the Type-1 successions was done in the Sindari – Karna sector. The grity-sand sediment horizons are heavily altered to clay and show compaction. A few unaltered grity-sand deposits were found and sampled. We also sampled the silt-clay dominated horizons.
- The Type-2 successions were sampled at the Khudala section. At Khudala, samples were collected in regular intervals in a vertical profile. Sampling was done mainly from the fining upward sequences, from which alternate sand and silty-clay bands were sampled.
- Modern bed-load sediment comprising of gritty-sand were collected from the Dhal river bed (a tributary of the Luni) near the piedmont region where the river comes out of the Aravalli ranges. In adition, modern bedload sediment comprising mainly of grity-sand was collected from the Karna region, further downstream of the river where it passes through very different lithologies.
- Modern deposits of suspended sediment were collected from the river banks.

5.3 Results and discussion

5.3.1 Trace element geochemistry

The trace element concentration and Sr-Nd isotopic compositions of the Luni river sediments are presented in table 5.1. The chondrite normalised and PAAS normalised REE patterns of different facies from the Luni alluvium are presented in figure 5.4A and 5.4B. From the figures following observations can be made:

- The overall REE patterns are similar for all the facies, however, contents vary and so does the Eu anomalies.
- The Luni sediments show enriched LREE and flat HREE patterns, akin to upper continental rocks. This is expected as the catchment of the river is dominated with Precambrian crustal rocks.

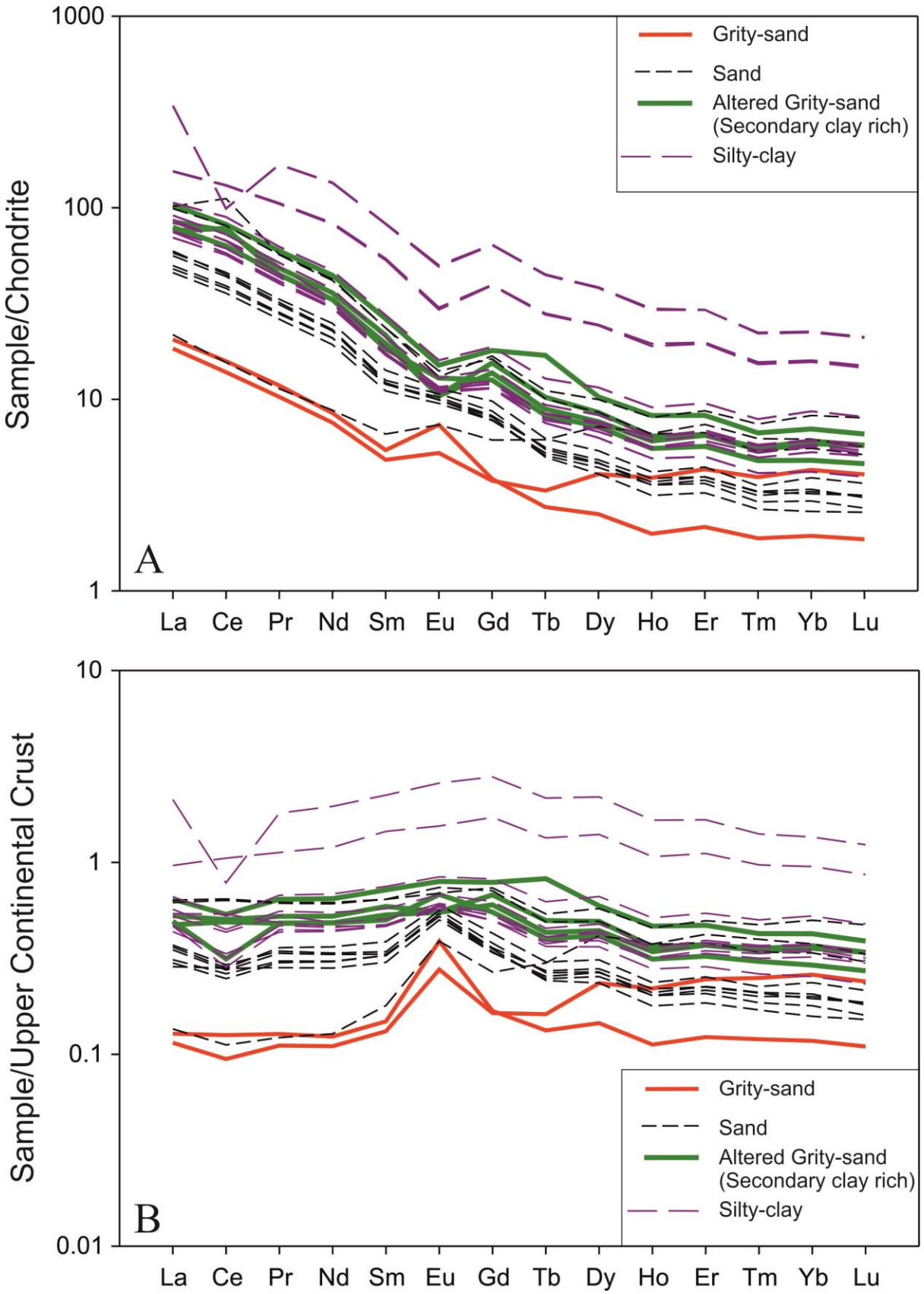

Figure 5.4: (A) Chondrite normalised and (B) Upper continental crust normalised REE patterns of different sedimentary facieses observed in the Luni alluvium.

- Both the modern gritty-sand bedload sediments and the older gritty horizon (Pliocene) have lowest REE abundance and show positive Eu anomaly.
- The altered gritty horizons with clay matrix, however, shows negative Eu anomaly.
- The sand dominated facies has higher REE abundance than the gritty layers. They show no Eu anomaly or relatively small negative Eu anomaly.
- Silt and clay dominated finer sediments have highest abundance of REE and possess negative Eu anomaly.
- In the PAAS normalised REE patterns, the positive Eu anomalies become more pronounced. The gritty-sand layers have the most pronounced anomaly followed by the sandy horizons. The silt-clay rich layers show a more flattened REE pattern with no Eu anomaly.

It is generally assumed that the REE patterns of the sediments reflect that of their sources. However, REE patterns observed in sediments are dependent on many factors of which the most important being the degree of weathering. In case when the weathering is incipient and degree of chemical weathering is less, then the REE patterns of sediments may not truly represent the source (Singh and Rajamani, 2001). In such scenarios care must be taken before interpreting the data.

In case of the Luni alluvium, there are distinct differences in REE patterns among different sediment facies in spite of the fact that, the sediment source remained same (the Aravalli range). The sediment source region in the Aravalli receives limited rainfall and that too only for a limited period during the SW monsoon. Therefore, the source region of the river undergoes lower chemical weathering compared to the physical processes. In such an environment the more weathering prone mafic-ultramafic (and their metamorphic counterparts) rocks would weather faster than the gneissic and granitoid rocks. This would likely produce a chemical bias in the sediments, produced by the weathering in the Aravallis and carried by the Luni, towards that of the constituent minerals of the mafic/ultramafic rocks.

Furthermore, sediment transport in the ephemeral rivers like the Luni is highly seasonal and depends on the stream intensity. This causes a strong grain size sorting along the course of the river. Also, heavy transmission loss occurs downstream of the Luni river (Sharma et al., 1984). These factors would affect the ultimate chemistry of the sediments and make them

chemically dissimilar with the source. Considering these, our interpretation for the observed REE patterns in various sedimentary facies of Luni are as follows.

- The positive Eu anomalies observed in the gritty sediments (Fig. 5.4A and 5.4B) are most likely due to the presence of un-weathered plagioclase feldspars. The easily weathering prone source rocks in the catchment (the mafic-ultramafic rocks, meta-pellites etc.) have plenty of plagioclase feldspar in them. However, due to low degree of chemical weathering other constituent minerals (mafic ones) move out of the system much quickly leaving behind the quartz-plagioclase grains in the gritty horizons.
- The low abundance of REE in the sediments (Fig. 5.4A and 5.4B) can be explained by the quartz dilution effect. Also fewer amounts of the coatings of REE rich secondary phases over coarser fraction of sediments can be the reason for less abundant REE (Singh and Rajamani, 2001).
- In the sand dominated sediments the positive Eu anomaly becomes less pronounced and in some cases even negative (Fig. 5.4B). Due to accumulation of more REE bearing secondary phases the feldspar effect decreases in the sandy layers.
- The inference is further confirmed by the negative Eu anomaly observed in the fine grained clastics (silty-clay deposits) and altered gritty horizons. Singh and Rajamani, (2001) has observed similar signatures in the Kaveri alluvium and suggested that, in case of fine grained clastics, REE rich secondary phases create coatings over the grains occur which mask the feldspar effect and increase the elemental abundance of REE.

From these observations we infer that the trace element compositions of the Luni sediments are not true representatives of their sources. The REE abundance and the patterns are mainly controlled by the weathering intensity and sorting in the Luni basin. To constrain the sediment provenance we made use of the Sr-Nd isotopic fingerprinting.

5.3.2 Sr-Nd isotopic fingerprinting

The Sr-Nd isotopic composition of various sedimentary facies observed at the Luni alluvium are compared with that of various probable source rocks in the ε_{Nd} vs. $^{87}Sr/^{86}Sr$ bivariate plot (Fig. 5.5). A three component mixing grid is also presented in the figure for

quantifying the differential sediment contributions. From the figure the following inferences can be drawn.

- The mafic-ultramafic suit of rocks exposed along the western flank of the Aravalli ranges which stand high just above the piedmont region of the Luni, show low $^{87}Sr/^{86}Sr$ and high ε_{Nd}.
- The pelitic schists and calc-silicate rocks of the Delhi Supergroup show low ε_{Nd} and low $^{87}Sr/^{86}Sr$.
- On the other hand the quartzite and other rocks of the Delhi Supergroup exposed along the western flank of the Aravalli Range show high $^{87}Sr/^{86}Sr$ and low ε_{Nd}. The Erinpura granites have comparable Sr-Nd isotopic ratios.
- The pockets of the BGC rocks exposed along the western margin of the Aravalli as well as the Malani rhyolites have different Sr-Nd isotopic ratios and do not seem to contribute much to the Luni alluvium.

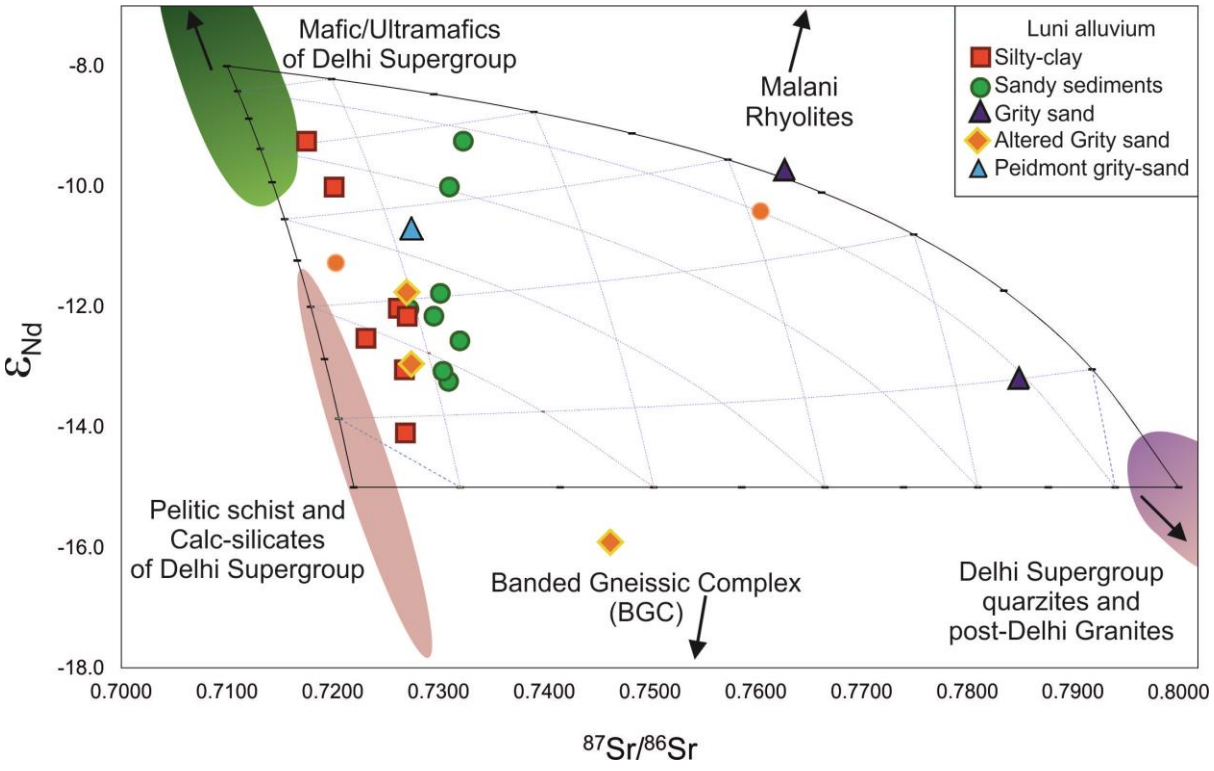

Figure 5.5: ε_{Nd} vs. $^{87}Sr/^{86}Sr$ plot of the Luni river sediments compared with a ternary mixing grid involving the probable sources. Data source for end-members: (George and Ray, 2017; Volpe and Macdougall, 1990).

- The contribution of the mafic-ultramafic suit of rocks and the schistose rocks of the Delhi Supergroup to the Luni river sediments can be easily discerned.
- Other important sediment contributors to the Luni alluvium are the metamorphosed rocks (pelitic schists and calc-silicates) of the Delhi Supergroup exposed along the western Aravalli Ranges.
- Other varieties of the Delhi Supergroup rocks such as the quartzite and the post-Delhi Erinpura Granite contribute very little to the Luni alluvium (~10%).

5.4 Conclusions

From our limited geochemical study of the Luni alluvium we concluded following about the sources of sediments deposited in this sink.

- The REE geochemistry of the Luni river sediments are mainly controlled by the weathering and sediment transport processes.
- Due to incipient weathering different sediment loads represent different REE patterns and abundances.
- The gritty-sand horizons show positive Eu anomalies due to the presence of unweathered plagioclase grains. However, the finer sediments have no such anomalies.
- Our study indicates that the REE patterns of the sediments generated in physical weathering dominated regions are influenced by the weathering and transportation processes rather than REE character of the source regions.
- The provenances have been identified by the Sr-Nd isotopic fingerprinting of the sediments. Major sediment sources of the Luni river alluvium are the mafic/ultramafic rocks, pelitic schists and calc-silicate rocks of the Delhi Supergroup. The post-Delhi granites and granitoids have contributed a little to the sediment budget of the basin.

Table 5.1 Trace element concentration and Sr-Nd isotopic composition of the Luni river sediments.

Samples	LUNI-2013-1 (Grit)	LUNI-2013-2	LUNI-2013-3(Silty clay)	LUNI-2013-4	LUNI-2013-5(Silty clay)	LUNI-2013-6(Silty clay)
Sc	0.53	3.57	7.7	4.35	11.53	6.53
V	5.67	29.2	55.34	30.1	138.2	122.4
Cr	100.9	205.3	78.67	82.44	85.19	91.94
Co	0.92	4.15	8.5	2.68	4.46	32.23
Cs	2.31	3.86	5.75	1.3	5.79	3.53
Rb	102.9	81.7	92.1	56	71	47.5
Ba	381	303	299	289	293	1328
Th	2.6	8.6	10.1	7	13.3	7.7
U	0.32	1.2	1.77	1.03	1.37	1.94
Nb	1	7	10	5	12	7
Ta	0.1	0.58	0.78	0.48	0.79	0.45
La	5	18	25	24	37	81
Ce	10	48	55	50	80	60
Pb	7.8	6.3	5.9	4.9	4.6	13.5
Pr	1.1	4.2	5.9	5.6	9.9	15.9
Sr	46	59	136	135	65	108
Nd	4	13	17	18	40	64
Zr	18	40	36	14	73	40
Hf	0.5	1.2	1.3	0.5	1.9	1.1
Sm	0.8	3	4.2	3.7	8.1	12.5
Eu	0.4	0.6	0.9	0.8	1.7	2.8
Gd	0.8	2.8	3.9	3.3	8.1	13.1
Tb	0.1	0.33	0.48	0.4	1.03	1.66
Dy	0.6	1.9	2.9	2.4	6.1	9.7
Y	3.1	7.3	10.1	10	31.6	47.8
Ho	0.11	0.34	0.51	0.43	1.07	1.66
Er	0.4	1.1	1.6	1.3	3.2	4.8
Tm	0	0.1	0.2	0.2	0.4	0.6
Yb	0.3	1	1.5	1.2	2.7	3.8
Lu	0.05	0.15	0.21	0.17	0.37	0.53
$^{87}Sr/^{86}Sr$	0.784908		0.723135		0.720122	0.717509
ε_{Nd}	-13.2		-12.5		-10	-9.3
Samples	LUNI-2013-7 (Altered Grit)	LUNI-2013-8 (Sand)	LUNI-2013-9 (Altered Grit)	LUNI-2013-10 (Altered Grit)	LUNI-2013-11 (Grit)	KU-AEOLIAN
Sc	3.76	5.16	2.84	5.5	1.66	4.97
V	26.47	36.01	20.97	34.06	4.6	25
Cr	153.3	192.8	114.9	47.22	37.09	18.48
Co	2.85	4.05	2.04	3.36	0.7	1.86
Cs	3.76	2.37	1.41	1.67	1.49	1.78

Rb	76.6	71.6	45.5	56.6	63.8	64.6
Ba	281	343	219	271	246	336
Th	10.6	7.5	5.8	7.8	1.9	4.2
U	1.35	0.98	0.8	1.52	0.3	0.58
Nb	6	7	4	5	1	4
Ta	0.48	0.51	0.32	0.49	0.16	0.46
La	20	23	19	24	4	19
Ce	46	49	39	50	8	35
Pb	5.2	5.5	5.2	4.9	4.3	5.5
Pr	4.6	5.4	4.2	5.6	1	3.7
Sr	61	166	112	143	42	158
Nd	15	20	10	18	3	13
Zr	32	17	10	20	6	12
Hf	1.1	0.5	0.4	0.6	0.2	0.3
Sm	3.3	3.6	2.8	4	0.7	2.1
Eu	0.6	0.8	0.7	0.9	0.3	0.6
Gd	3.2	3.3	2.6	3.7	0.8	2
Tb	0.38	0.38	0.31	0.63	0.12	0.23
Dy	2.2	2.2	1.8	2.6	1	1.4
Y	8.2	10	5.4	10.3	5.3	6.4
Ho	0.36	0.37	0.31	0.47	0.22	0.25
Er	1.1	1.1	0.9	1.4	0.7	0.8
Tm	0.1	0.1	0.1	0.2	0.1	0.1
Yb	1	0.9	0.8	1.2	0.7	0.7
Lu	0.15	0.13	0.12	0.17	0.1	0.09
$^{87}Sr/^{86}Sr$	0.746266	0.727213	0.727464	0.727026	0.762735	
ε_{Nd}	-15.9	-12	-13	-11.8	-9.7	
Samples	KU-1-CS (Silty clay)	KU-1-S (Sand)	KU-2-CS(Silty clay)	KU-2-S (Sand)	KU-3-CS(Silty clay)	KU-3-S (Sand)
Sc	3.72	2.96	7.98	3.47	6.47	3.48
V	29.82	20.57	60.95	21.82	56.15	24.03
Cr	20.73	13.94	43.86	15.65	37.85	16.36
Co	2.24	1.59	4.68	1.69	4.35	1.86
Cs	3.24	1.85	6.57	1.63	5.01	2.4
Rb	61.5	62.1	94.5	58.2	76.5	69.5
Ba	229	298	306	288	278	325
Th	6	4.4	7.1	3.7	5.9	4
U	0.95	0.54	1.34	0.56	1.16	0.75
Nb	5	3	9	3	8	4
Ta	0.39	0.26	0.68	0.35	0.72	0.38
La	18	13	20	11	17	12
Ce	35	27	41	23	35	24
Pb	4.7	5.5	4.2	5.2	4.2	5.3
Pr	3.9	3	4.7	2.6	3.8	2.7
Sr	106	141	122	141	102	137

Nd	9	9	13	8	11	9
Zr	12	7	38	10	31	16
Hf	0.6	0.3	1.3	0.3	1	0.5
Sm	2.6	1.9	2.8	1.8	2.6	1.8
Eu	0.6	0.6	0.7	0.6	0.6	0.6
Gd	2.3	1.7	2.6	1.7	2.3	1.6
Tb	0.28	0.19	0.31	0.21	0.3	0.19
Dy	1.6	1	1.9	1.2	1.7	1.1
Y	4.7	3.8	7.9	4.9	6.7	4.8
Ho	0.28	0.18	0.34	0.22	0.31	0.2
Er	0.8	0.5	1.1	0.6	1	0.6
Tm	0.1	0.1	0.1	0.1	0.1	0.1
Yb	0.7	0.4	1	0.5	0.9	0.6
Lu	0.1	0.07	0.14	0.08	0.13	0.08
$^{87}Sr/^{86}Sr$	0.726857	0.729562	0.726209	0.730178	0.726779	0.730967
ε_{Nd}	-14.1	-12.2	-12	-11.8	-13	-13.2
Samples	KU-4-CS(Silty clay)	KU-4-S (Sand)	KU-5-CS(Silty clay)	KU-5-S (Sand)	KU-6-CS(Silty clay)	KU-6-S (Sand)
Sc	6.97	3.54	5.71	3.04	9.31	4.08
V	52.57	25.76	44.83	21.38	59.56	21.46
Cr	35.04	16.45	31.61	14.35	44.95	13.49
Co	3.88	1.94	3.35	1.6	4.44	1.56
Cs	5.17	2.54	4.27	1.98	6.26	2.24
Rb	84.6	65	69.1	62.7	105.5	76.6
Ba	291	294	237	302	368	340
Th	6.7	4.8	6.7	4.3	6.9	3.2
U	1.28	0.75	1.28	0.63	1.3	0.59
Nb	8	4	7	3	10	3
Ta	0.63	0.37	0.5	0.35	0.8	0.25
La	22	14	18	14	21	11
Ce	44	28	37	27	41	22
Pb	4.4	5.3	4.5	5.3	4.8	5.7
Pr	4.9	3.2	4.1	3	4.3	2.5
Sr	122	128	88	137	139	165
Nd	14	9	10	9	16	9
Zr	30	16	29	11	44	12
Hf	1	0.5	1.2	0.3	1.2	0.3
Sm	3.2	2.2	2.7	1.9	2.6	1.7
Eu	0.7	0.7	0.6	0.6	0.7	0.6
Gd	2.9	2	2.5	1.8	2.5	1.6
Tb	0.35	0.23	0.29	0.2	0.31	0.2
Dy	2.1	1.4	1.8	1.2	1.9	1.2
Y	7.7	5	6.3	4.7	10.4	6
Ho	0.36	0.24	0.32	0.2	0.36	0.21
Er	1.1	0.7	1	0.6	1.1	0.7

Tm	0.1	0.1	0.1	0.1	0.1	0.1
Yb	1	0.7	1	0.5	1	0.6
Lu	0.14	0.09	0.13	0.07	0.15	0.08
$^{87}Sr/^{86}Sr$	0.727042	0.730431		0.731032		0.732354
ε_{Nd}	-12.2	-13.1		-10		-9.3
Samples	KU-7 (Sand)	KU-8 (Sand)	PH-15-13 (Peidmont sediment)			
Sc	1.1	9.3				
V	6.96	71.09				
Cr	3.86	50.34				
Co	0.78	7.31				
Cs	1.99	9.52				
Rb	96.4	124.6				
Ba	350	311				
Th	1.7	11.4				
U	0.42	1.67				
Nb	3	11				
Ta	0.3	0.83				
La	5	24				
Ce	10	68				
Pb	6.4	5.2				
Pr	1.1	5.4				
Sr	66	90				
Nd	4	15				
Zr	67	46				
Hf	1.7	1.7				
Sm	1	3.6				
Eu	0.4	0.8				
Gd	1.3	3.5				
Tb	0.23	0.41				
Dy	1.8	2.5				
Y	10.1	9.2				
Ho	0.37	0.45				
Er	1.2	1.4				
Tm	0.2	0.2				
Yb	1.1	1.4				
Lu	0.14	0.2				
$^{87}Sr/^{86}Sr$		0.732031	0.727464			
ε_{Nd}		-12.6	-10.7			

Chapter - 6

Geochemical Provenance of the Thar Desert Sand

6.1 Introduction

One of the major sand seas occurs within the Thar Desert of western India and eastern Pakistan (Lancaster, 2009). It is located along the eastern most stretch of the great Sahara-Arabian desert system of the horse latitudes and hosts a variety of aeolian sand dunes, including stabilised fossil dunes. The Desert extends from the foothills of the Aravalli mountain ranges in the east up to the Indus floodplain in the west covering an area over 4000 sq. km (Fig.6.1). Aeolian activity of the Thar Desert began around 150 ka and is majorly controlled by the South-west monsoonal winds (Singhvi and Kar, 2004). One of the major steps towards understanding the development of this vast tract of sandy desert is to determine the source of the accumulated aeolian sediments. Although, many efforts have been made in understanding the dune dynamics and antiquity of the desert, the provenance of the sand deposits of the Thar remains largely speculative. Considering the vastness of the desert, it is natural to assume that there would be variation in sediment sources in different parts of the desert. Earlier workers however, had proposed very different provenance scenarios. Wadia (1960) had hypothesized the Arabian sea coast and the Great Rann of Kachchh to be the primary sediment sources, whereas Singhvi and Kar, (2004) had suggested a local origin due to absence of grain size variation in the down wind direction. On the contrary, Tripathi et al., (2013) had suggested a sub-Himalayan source for the sand based on isotopic fingerprinting. However, their sampling locations were limited to the far north-east corner of the desert, which consisted of stabilised (ancient) dune fields. A contrasting idea has been suggested in a recent detrital zircon based provenance study (East et al., 2015) from the Cholistan Desert that forms a part of the Thar Desert in Pakistan. According to this the desert sand was derived mainly from the trunk Indus, especially the delta region of the river.

In this study, we have strategically collected aeolian sand samples deposited in different parts of the Thar Desert and determined their provenance. Using trace element geochemistry and Sr-Nd isotopic ratios as tracers, we have quantified sediment contributions from plausible sources into the desert.

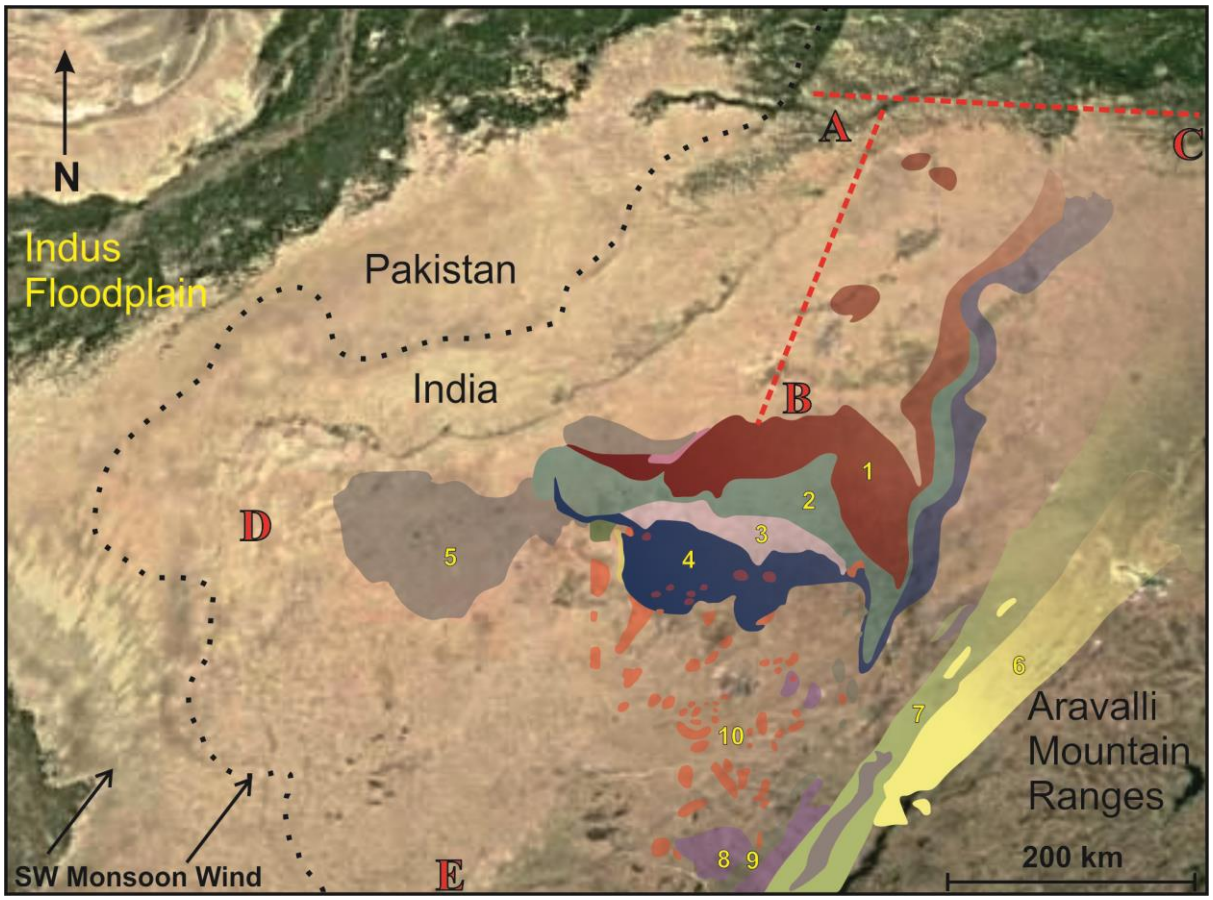

Figure 6.1: Google earth image of the Thar Desert with superimposed lithological map showing the major possible sediment contributors to the basin. Samples had been collected along the AB and AC transects D and E regions on the map. Lithology legends: 1. Nagaur Group, 2. Bilara Group, 3. Girbhankar Formation, 4. Sonia Formation, 5. Mesozoic and Tertiary rocks of Jaisalmer basin, 6. Banded Gneissic Complex-II, 7. Delhi Supergroup, 8. Erinpura Granite, 9. Sirohi Group, 10. Malani Rhyolite. The lithological map is modified from George and Ray, (2017).

6.2 Geology and Geomorphology of the Thar Desert

In last two decades, a significant progress has been made in our understanding of the geological history and antiquity of the Thar Desert. The most important findings of the earlier research are listed below.

- The Quaternary deposits of the Thar Desert are not unequivocally aeolian in character. They are a complex deposit of fluvial, fluvio-lacustrine and aeolian sediments (Dhir et al., 1992; Singhvi and Kar, 2004).
- Neogene tectonic movements had generated a series of NE-SW trending horst-graben structures which acted as the sinks where the Quaternary sediments of the desert got deposited (Dhir et al., 1992). The basement of these basins range from the Proterozoic Delhi ranges in the east, Pre-Cambrian Marwar Supergroup of rocks in the central part and Mesozoic-Tertiary rocks of Jaisalmer basin in the west (Fig.6.1).
- The antiquity of aeolian activities in the desert can be traced back to 200 ka (Dhir and Singhvi, 2012).
- The Desert at present is in a shrinking stage with its most active part limited to the western margin. The paleo desert, however, had a larger active region (Singhvi and Kar, 2004).
- The Thar Desert houses different kinds of dunes such as - transverse, longitudinal, star, parabolic etc. (Wasson et al., 1983). Amongst these, the parabolic dune field is the most dominant geomorphic feature of this desert.
- The orientations of the parabolic dunes (both active and stabilised) suggests that the aeolian activities of the desert is primarily controlled by the SW monsoonal winds (Kar, 1996).

6.3 Results and Discussion

6.3.1 Trace element geochemistry

The trace element composition of the aeolian sediments of the Thar Desert are presented in table 6.1 and are plotted in different tectonic discrimination diagrams and binary plots of elemental ratios in the figure 6.2. Based on these I have made the following observations and discussed their implications:

- From the tectonic discrimination diagrams (Fig. 6.2A and 6.2B) it appears that both passive continental margin and continental island arc types of sources could have contributed to the sediment budget of the desert. Contribution from the passive margin sources are very much expected as the basin is in the vicinity of Archean cratons of western India.

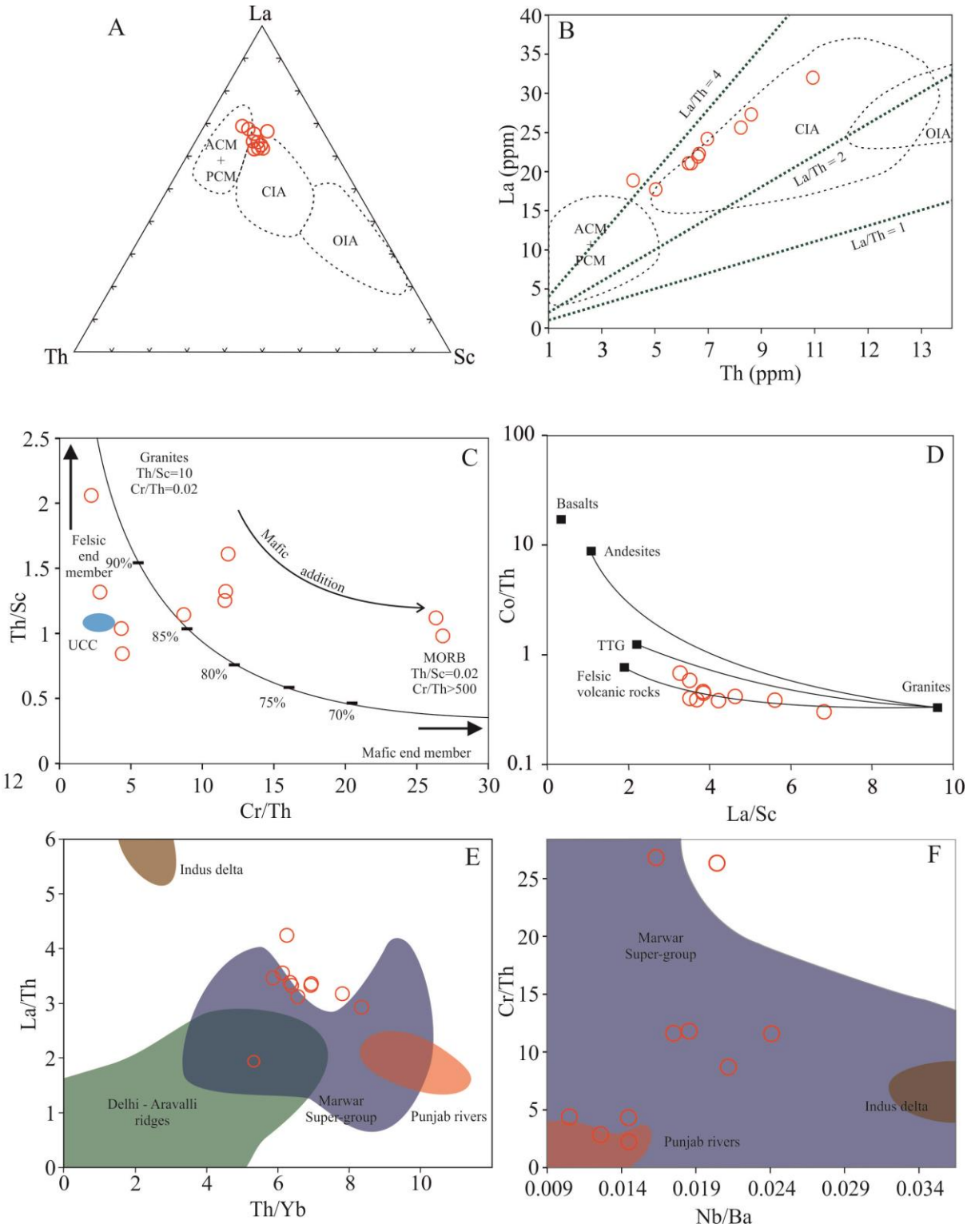

Figure 6.2: (A) & (B) Tectonic discrimination diagrams (After Bhatia and Crook, 1986) for the Thar Desert. ACM: Active Continental Margin; PCM: Passive Continental Margin; CIA: Continental Island Arc; OIA: Ocean Island Arc (C) Th/Sc vs. Cr/Th diagram after Totten et al., (2000), (D) Co/Th vs. La/Sc diagram after Gu et al., (2002), (E) & (F) bivariate plots of different elemental ratios for discriminating the sediment provenance of the Thar Desert sand.

However, considering that the arc related sources are limited to the trans-Himalayan suture zone, contribution from these would most likely have been from the floodplains of the Indus river which is draining through those rocks. Another likely arc provenance could be the Luni river alluvium which derives its sediment from the mafic/ultramafic rocks exposed along the Proterozoic Delhi-Aravalli suture zone.

- As can be inferred from figures 6.2C and 6.2D, the Thar sands have, apart from a strong basement component, a significant component of juvenile mafic and felsic rocks.
- To further discriminate the differential provenances, we made use of various bivariate plots of trace element ratios (Fig. 6.2E and 6.2F). However, it was observed that discrimination of sources/provenances is difficult solely on the basis of trace element contents. This could simply because contribution from multiple sediment sources having widely varying compositions.

6.3.2 Sr-Nd isotopic compositions

In the previous chapters it has already been demonstrated that the Sr and Nd istopic ratios are robust proxies for determining the sediment provenance of the Quaternary deposits of western India. Given the fact that the possible source regions are isotopically well constrained, in the present study attempts have been made to quantify different sources which might have contributed into the sedimentary deposits of the Thar Desert. The Sr-Nd isotopic compositions of the Thar Desert sands are presented in the table 6.2. It is expected that there will be differential sediment contribution from various provenances in various parts of the desert. This is further confirmed by the observed variation in Sr-Nd isotopic compositions of the dune sands along two transects: NNW-SSE (AB transect in Fig. 6.1) and W-E (AC transect in Fig.6.1). The variation in Sr-Nd isotopic compositions have been plotted in the figure 6.3. I have made the following observations from the data and discussed their implications:

- Along the AB transect $^{87}Sr/^{86}Sr$ gradually becomes more radiogenic (increasing) towards south. Complimentary variation is seen (i.e. decreasing) in ε_{Nd} (Fig. 6.3A).
- Similar observation can be made along the AC transect too. $^{87}Sr/^{86}Sr$ shows an increasing trend and ε_{Nd} shows a decreasing trend eastward. However, a reversal is observed towards the furthest end of the desert (Fig 6.3B).

These trends simply indicate that there are gradual but consistent mixing of two different source derived sediments along the AB and AC transects on the map.

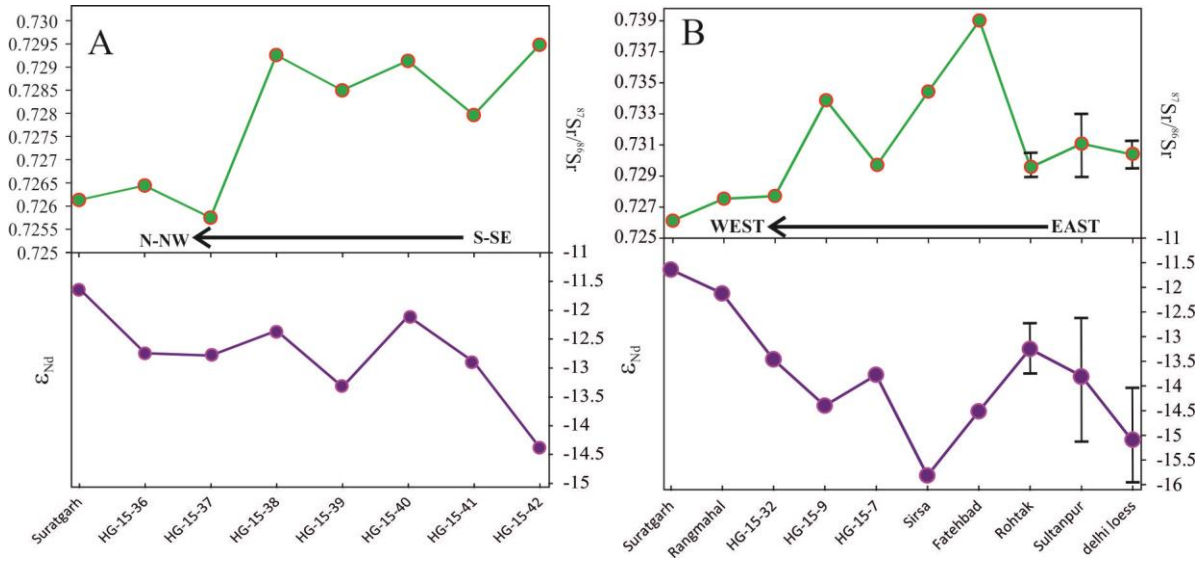

Figure 6.3: (A) Variation of $^{87}Sr/^{86}Sr$ and ε_{Nd} of dune sands along the AB transect of Fig. 6.1. (B) Variation of $^{87}Sr/^{86}Sr$ and ε_{Nd} of dune sands along the AC transect of Fig. 6.1.

The Sr-Nd isotopic composition of the desert sands collected from different locations are compared with that of various probable source rocks in the ε_{Nd} vs. $^{87}Sr/^{86}Sr$ bivariate plot (Fig. 6.4). A three component mixing grid is also presented in the figure for quantifying the differential sediment contributions. A map of the Thar Desert and its various sediment sources along with their differential contribution have been presented in the figure 6.5. From the figures following inferences can be drawn.

- Maximum contribution of the Indus river sediments is observed along the western margin of the desert near Jaisalmer (the region D in Fig 6.4A and Fig. 6.5). The contribution from the Indus floodplain is ~50% of the total (Fig. 6.4A). Given the fact that the SW monsoon winds control the aeolian activity of the Thar and that the Indus floodplain lies at the upwind direction, it is expected that the Indus borne detritus will be a major sediment source. The rest of the sediment contributions are from the rocks of the Marwar Supegroup (Nagaur and Jodhpur Groups) which are located at the heart of the desert (Fig. 6.5).

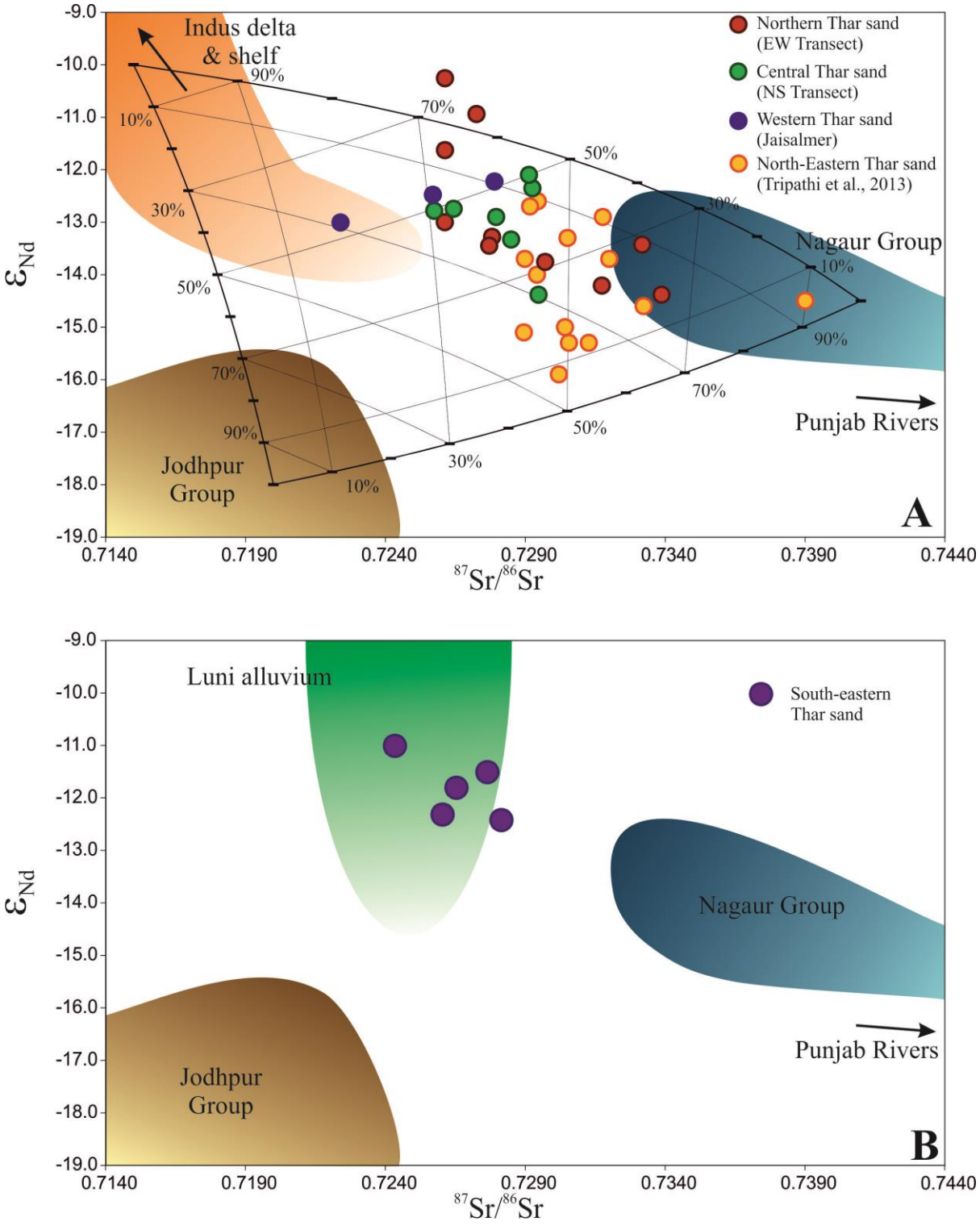

Figure 6.4: (A) and (B) ε_{Nd} vs. $^{87}Sr/^{86}Sr$ diagram showing the composition of the Thar Desert sand compared to the probable sediment sources. End members: Indus delta & shelf: (Clift et al., 2010; Limmer et al., 2012); Nagaur and Jodhpur Group: (George and Ray, 2017); Luni alluvium: Present study.

- The influence of the Indus sediments, however, decreases gradually towards the east and central part of the desert (Fig. 6.5).
- The sands at the northern and north-eastern region of the desert have variable contributions from multiple sources. Towards east, contribution of the Nagaur Group increases (up to ~60%). The contribution from the Jodhpur Group is nearly constant (~20%). Remaining sediments were derived from the Indus river alluvium.
- Similar observation can be made for sediments along the NNW-SSE oriented AC transect. The influence of the Nagaur group increases in the desert sediments towards the central part of the basin.
- The sands in the southern parts (the region E in Fig. 6.5) of the desert have a clearly different provenance. The Luni alluvium becomes the major source for the sediments at this margin. The influence of Indus river is not indiscernible in this part of the desert.

These observations clearly suggest that the Thar Desert is not homogeneous in term of sediment composition. In contrast to the previous observations by East et al., (2013), our data indicate that the composition of the desert sand is highly controlled by the local sources. Maximum contribution of distant source (Indus delta) has been observed to be ~50% and that too restricted to the western margin of the desert.

6.4 Conclusions

The main conclusions inferred from the present work are listed below:

- The Thar Desert sand is derived from multiple sources and not from the Indus alluvium only as suggested by East et al., (2013).
- The maximum influence of the Indus sediments has been observed only at the western margin of the desert (~50%).
- The contribution from the Indus alluvium decreases significantly towards east.
- Towards the central and eastern part of the basin, contributions of sediment derived from the Marwar Supergroup dominate.
- The south eastern part of the desert is heavily influenced by the Luni river alluvium, which masks any contribution from the Indus delta.

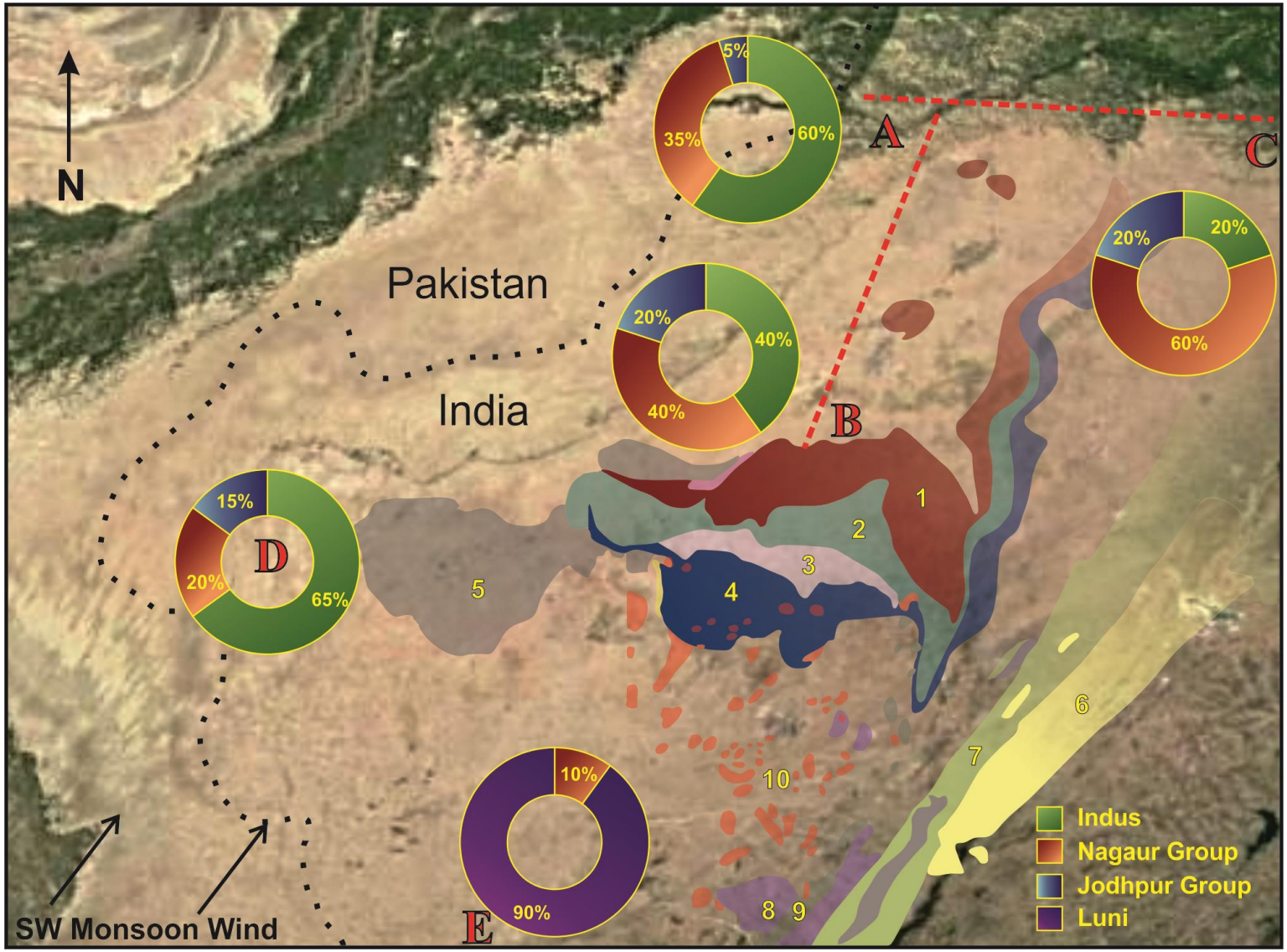

Figure 6.5: Pie diagrams of variation in sediment contribution from different provenances shown over the map of the Thar Desert. Lithology legends: 1. Nagaur Group, 2. Bilara Group, 3. Girbhankar Formation, 4. Sonia Formation, 5. Mesozoic and Tertiary rocks of Jaisalmer basin, 6. Banded Gneissic Complex-II, 7. Delhi Supergroup, 8. Erinpura Granite, 9. Sirohi Group, 10. Malani Rhyolite.

Table 6.1 Trace element concentrations of the sands from different sectors of the Thar Desert. All concentrations are in ppm.

	Southern Thar Desert						Northern Thar Desert			
Samples	LUNI-2013-4	BKS-1	BKS-2	BKS-3	BKS-5	KU-Aeolian	HG-14-23	HG-14-24	R-14-1	R-14-3
Sc	4.35	5.84	6.06	3.88	3.12	4.97	8.75	6.53	7.37	6.77
V	30.10	41.28	31.97	26.59	21.82	25.00	49.14	39.68	46.33	42.45
Cr	82.44	58.09	27.24	14.36	14.32	18.48	126.80	100.40	217.10	177.90
Co	2.68	2.99	2.50	2.09	1.92	1.86	4.23	3.28	4.79	4.49
Cs	1.30	1.53	1.73	1.65	1.08	1.78	2.18	1.76	2.14	1.99
Rb	56.0	55.9	64.0	57.0	40.3	64.6	63.2	62.3	66.8	65.6
Ba	289	281	313	280	201	336	331	345	352	366
Th	7.0	6.7	6.3	5.0	6.4	4.2	10.9	8.6	8.2	6.6
U	1.03	0.94	0.72	0.62	0.63	0.58	1.11	0.77	0.90	0.73
Nb	5	6	5	4	3	4	8	6	7	6
Ta	0.48	0.55	0.47	0.30	0.28	0.46	0.66	0.58	0.57	0.47
La	24	23	21	18	21	19	32	28	26	22
Ce	50	45	40	36	41	35	63	53	51	44
Pb	4.9	4.7	5.2	5.9	4.1	5.5	16.7	17.4	18.3	18.2
Pr	5.6	4.9	4.3	4.0	4.4	3.7	7.0	5.9	5.8	5.1
Sr	135	167	168	143	96	158	181	184	172	180
Nd	20	18	15	15	15	13	25	21	21	18
Zr	14	13	16	7	13	12	11	8	0	8
Hf	0.5	0.4	0.5	0.3	0.5	0.3	0.4	0.3	0.4	0.3
Sm	3.7	3.1	2.7	2.6	2.5	2.1	4.5	3.7	3.8	3.4
Eu	0.8	0.7	0.7	0.8	0.6	0.6	0.9	0.8	0.9	0.8
Gd	3.3	2.9	2.5	2.4	2.4	2.0	3.9	3.1	3.3	3.0
Tb	0.40	0.34	0.30	0.28	0.27	0.23	0.49	0.38	0.41	0.37
Dy	2.4	2.0	1.9	1.6	1.5	1.4	2.7	2.1	2.3	2.1
Y	10.0	9.8	9.2	6.0	5.5	6.4	14.6	11.6	11.0	11.3
Ho	0.43	0.36	0.34	0.30	0.29	0.25	0.51	0.41	0.45	0.40
Er	1.3	1.1	1.1	0.9	0.9	0.8	1.5	1.2	1.3	1.1
Tm	0.2	0.1	0.1	0.1	0.1	0.1	0.2	0.2	0.2	0.2
Yb	1.2	1.0	1.0	0.8	0.9	0.7	1.3	1.1	1.2	1.0
Lu	0.17	0.13	0.14	0.11	0.13	0.09	0.18	0.15	0.18	0.15

Table 6.2 Sr-Nd isotopic composition of the Thar Desert sands

	Suratgarh			N. Thar	
Samples	HG-14-23	HG-14-24	Avg.	HG-15-22	HG-15-27
$^{87}Sr/^{86}Sr$	0.726126	0.726132	0.726129	0.731738	0.733181
ε_{Nd}	-13.0	-10.3	-11.6	-14.2	-13.4
	West to East transect (N. Thar Desert)				
Samples	R-14-1	R-14-3	HG-15-32	HG-15-9	HG-15-7
$^{87}Sr/^{86}Sr$	0.727257	0.727815	0.727714	0.733874	0.729716
ε_{Nd}	-10.9	-13.3	-13.4	-14.4	-13.8
	NNW to SSE transect				
Samples	HG-15-36	HG-15-37	HG-15-38	HG-15-39	HG-15-40
$^{87}Sr/^{86}Sr$	0.726441	0.72575	0.729257	0.728496	0.729133
ε_{Nd}	-12.7	-12.8	-12.4	-13.3	-12.1
	NNw to SSE Transect		W. Thar (Jaisalmer)		
Samples	HG-15-41	HG-15-42	JA-16-2	JA-16-3	JA-16-4
$^{87}Sr/^{86}Sr$	0.727963	0.729478	0.727900	0.725700	0.722400
ε_{Nd}	-12.9	-14.4	-12.2	-12.5	-13.0
	SE Thar				
Samples	KU-Aeolian	LUNI-2013-4	BKS2	BKS3	BKS5
$^{87}Sr/^{86}Sr$	0.728100	0.726000	0.726500	0.727600	0.724300
ε_{Nd}	-12.4	-12.3	-11.8	-11.5	-11.0

Chapter – 7

Summary and Conclusions

In my Ph.D. work I have studied the late Quaternary sedimentary deposits of the western India using field, geochronological, geochemical and isotopic methods to understand the origin and evolution of the major landscapes of this region by understanding the sources and depositional pathways of the siliciclastic sediments. Apart from stratigraphic principles, the geochronological methods included radiocarbon and OSL datings. Geochemical methods included trace element studies, whereas the Sr-Nd isotopic compositions were utilized for source fingerprinting. Ar-Ar dating of detrital mica was also used as a technique to study the sediment provenance. The results and findings from each studied geomorphic feature are discussed in the concluding section of respective chapters. Here I summarize the major conclusions of my work and discuss the scope for future works.

7.1 Region specific conclusions

7.1.1 The Ghaggar river alluvium

The present work draws a conclusion to the long standing debate regarding the palaeo condition of the Ghaggar river of NW India and its influence on the evolution of the Bronze age Harappan civilization. Following findings are the major contributions of my thesis work to this issue:

- The presently ephemeral Ghaggar-Hakra river system had a strong fluvial past. During 70 – 20 ka the river was receiving water from glacier sources through its tributaries, probably the Sutlej and the Yamuna. The Yamuna probably left the Ghaggar channel and moved eastward sometime around 45ka. However, the Ghaggar river still used to flow in its vigour due to contributions from its other tributaries.
- The hydrological conditions of the river first got severely affected during the onset of the last glacial maxima (LGM). Discharges from the glacier sources got drastically reduced.
- In the aftermath of the LGM with the Indian Monsoon returning to its original intensity and with increase in the glacial water input most of the Himalayan rivers got rejuvinated. These changes in the hydrological conditions rejuvenated the Ghaggar channel once again and the distributaries from the Sutlej river flooded the main Ghaggar channel.

- With this reactivated phase of the Ghaggar another interesting development occurred in the Ghaggar valley. The first agro-pastoral community of pre-Harappan people started settling down at the Ghaggar floodplains.
- The settlements gradually flourished further to wide geographical localities which would eventually give rise to the Harappan Civilization.
- The human settlements along the Ghaggar valley enjoyed the vigour of the river until the mid-Holocene when the last of the glacial tributary of the river shifted away. However, it appears that the absence of glacial melt water did not affect the Harappan settlement possibly because the rain water was sufficient for their survival.
- The terminal blow to this system was delivered by the reduction of ISM around 4.2 ka (Enzel et al., 1999; Staubwasser et al., 2003). During this period the discharge in the Ghaggar got severely affected. The situation became detrimental for the Harappan settlements.
- Whereas the demise of the glacial phase of the river might not be the main reason for the decline of the Harappans, its rejuvenated phase appears to have triggered the beginning of the pre-Harappan settlements.

7.1.2 The Great Rann of Kachchh

In the present study, I have quantified the sediment provenance of the Great Rann of Kachchh for the first time. This on the other hand helped in the understanding of the palaeo-drainages active in and around the GRK. The major findings of the present work are as follows:

- There was probably no independent glacier-fed river flowing into the GRK during mid-Holocene. However, a continuous Ghaggar-Hakra-Nara channel was active during 5.5 to 1ka.
- Apart from the local sediment sources the western part of the GRK was receiving recycled detritus of the Ghaggar alluvium through the Ghaggar-Hakra-Nara channel mainly during the monsoonal floods.
- Considering that the Ghaggar-Hakra-Nara system was mainly ephemeral during the mature Harappan period and sedimentation persisted long after the decline of the Harappan civilization, changes in the fluvial conditions might not be the main reason for the demise of the Harappans.

- The sedimentation in the eastern part of the GRK was dominated by local sources during the Holocene. The Mesozoic rocks exposed surrounding this part of the basin was the main source of sediments.
- The eastern GRK, especially the area around the Khadir island was probably estuarine in condition during the period when the Harappan acropolis of Dholavira was occupied. The sea had already started receding by mid-Holocene exposing the eastern GRK.

7.1.3 The Luni river alluvium

The Luni river system, being the only major drainage of the Thar Desert is an important window to the weathering and sediment transport processes in a desert environment. The major outcomes from the present work are as follows:

- The REE geochemistry of the Luni river sediments are controlled mainly by weathering intensity and sediment sorting. Due to incipient weathering, the source rock compositions are not reflected in the sediment characteristics.
- Although the major lithology exposed in the Luni river catchment is the post-Delhi orogenic granites and rhyolites, their contributions to the sedimentary budget are meagre.
- The major sediment contribution to the Luni alluvium was from the pockets of mafic/ultrmafic rocks exposed along the suture zone in the western flank of the Aravalli mountain ranges.

7.1.4 The Thar Desert

The provenance of the Thar Desert sands is one of the most complex and highly debated issues amongst the Quaternary deposits of the western India. The present geochemical work has helped us quantify the complex provenance of the aeolian sands deposited over the Thar Desert. Followings are the major outcomes of our effort:

- The sands in the Thar Desert are derived from multiple provenances. Contrary to the earlier proposal of distant sources (Indus delta and shelf), we find that the sands are dominantly derived from local sources.

- Only in the western and north-western margins of the desert the influence of the Indus derived detritus is maximum (up to ~60%).
- Towards the eastern side and the central parts of the Thar, influence of the Indus derived sediment gradually decreases. The sedimentary rocks of the Marwar Supergroup which sits at the heart of the desert contributes the most to the sediment budget of these parts of the desert.
- The south-eastern part of the desert, however, has sands derived from a completely different provenance. This part of the desert sands are mainly sourced from the Luni river alluvium.

7.2 Quaternary sediments and landscape evolution of NW India

The Quaternary sedimentary deposits of the north-western Indian sub-continent are distributed across a wide range of geomorphic landscapes and exchanged sediments with each other through different geological processes (Fig. 7.1). Landscape evolution of this part of the sub-continent is a direct outcome of the interactions between these geomorphic environments. The oldest sedimentary deposits (>200 ka) were encountered in the Luni alluvium. The pre-dominant sources for the sediments were the mafic-ultramafic units exposed along the western flank of the Aravalli Mountains and the meta-sedimentary rocks of the Delhi Super-group (Fig. 7.1). The granitoid rocks exposed in this area have minimum contribution to the sedimentary budget. The sediment provenance in the Luni alluvium remained unchanged during the Quaternary period and the major alluvium deposition ceased when progressing desert dunes covered the alluviuim at ~8ka. At present, Aravalli derived sediments are restricted mainly at the piedmont zone. In the lower reaches, the river reworks local sediments and older alluvium deposits mainly during the monsoonal rains. A part of Luni river sediments get reworked into the eastern Great Rann of Kachchh. The Kachchh basin on the other hand has several other sediment contributors. The eastern part of the basin received sediments from the Luni River as well as Mesozoic rocks exposed around the basin (Fig 7.1). On the other hand, the western part of the basin received a significant amount of sediments from the Indus River. However, the western GRK also received recycled sediments derived from older alluvium deposits, episodically through a continuous Ghaggar-Hakra-Nara in the past (up to ~1 ka). The Ghaggar-Hakra alluvium however, had a very strong fluvial past. From ~70 ka onwards up to ~15 ka it was a strong glacier fed river system which

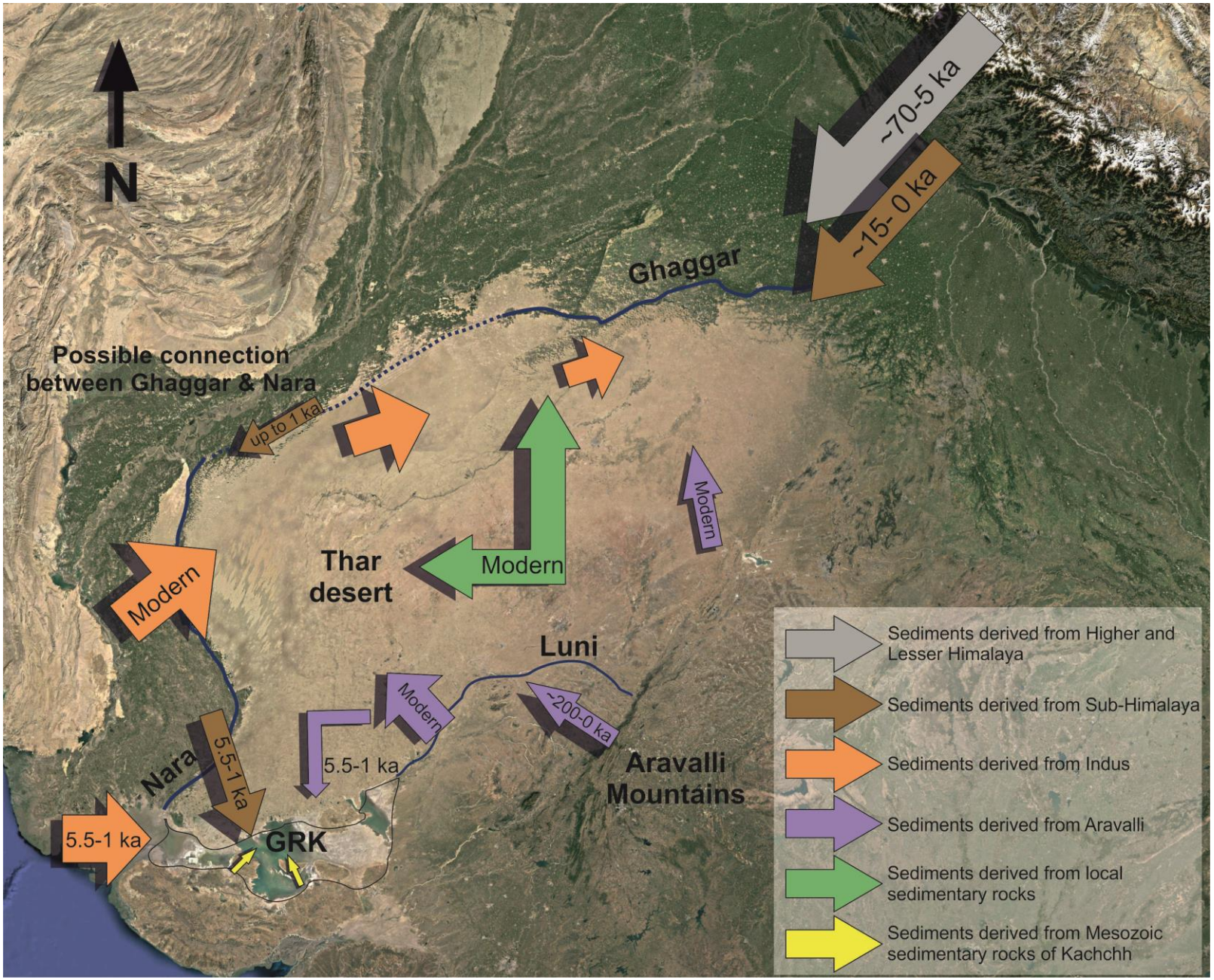

Figure 7.Graphical representation of sediment provenance and transportation pathways in various geomorphic terrains of NW Indian Sub-continent. The sizes of the arrows represent their relative contribution to different sedimentary sinks. The period of deposition are mentioned along the arrows. As the provenance study for the desert was done on recent sub-surface sand, the period is presented as modern.

derived its sediments from the higher and lesser Himalayas after which it received sediments maily from the Sub-Himalayas and local reworking (Fig 7.1). All these landforms surrounding the Thar Desert delivered sediment into it (Fig. 7.1). Unlike the recent conclusions derived from detrital zircon provenance studies, we have shown that the Thar Desert sand composition is controlled by local sources mainly. The sediment contribution from the Indus delta region reduces significantly towards inland. The sand in the central and northern part of the desert are derived mainly from the sedimentary rocks (from Marwar Supergroup) exposed along the heart of the desert. On the other hand the south-eastern part of the desert received its sediments mainly from the older alluvium deposits of the Luni river.

7.3 Summary of the thesis work

The western part of the Indian sub-continent is a natural laboratory of various Quaternary geomorphological terrains. Also the development of one of the earliest human civilization was closely linked to the evolution of these terrains. The present study sheds some light on the long standing debates on the evolution of these terrains. This work establishes that mega glacier fed river system did exist along the palaeo channels of the presently ephemeral Ghaggar-Hakra river of the NW India, however, it was in its full force much before the Mature Harappan period. The river used to be a glacier-fed until at least ~ 5 ka, albeit its flow was much reduced during the Holocene than its pre-LGM condition. Even after the river became ephemeral during the mid-Holocene, the channel was present and used to deliver sediments into the Great Rann of Kachchh, as late as ~1 ka. Therefore, the demise of the river was never the main reason for the decline of the Harappan Civilization around 3.9 ka. Rather the present work opens up a new understanding regarding the River-Culture interrelationship in this region. The rejuvenated phase of the Ghaggar river during the early Holocene helped the earliest agro-pastoral communities to build their settlements along the river bank. They flourished for a few millennia and developed into an urban civilization. It is the gradual decrease in the river discharge associated with severe decrease in monsoonal rain and its associated effects which became detrimental for the mature Harappans.

Our study offers new insights into the evolution of the Thar Desert also. Contradicting the recent propositions that the desert sand was mainly derived from the Indus river detritus, our study confirms that the Thar Desert sands are dominantly originated from local sources from sedimentary rocks of the Marwar Supergroup. The SE part of the desert

receives its sediments mainly from the Luni river alluvium which itself derives its sediments from the Proterozoic rocks of Delhi-Aravalli suture zone.

7.4 Recommendations for Future Studies

Although the present work reveals many interesting aspects regarding the evolution of the Late Quaternary continental deposits of western India and its connection with the development of the Harappan Civilization, there still exist several gaps in our knowledge. The present work is more like a reconnaissance study which gives us a platform to further explore these landscapes. I recommend the following important aspects which should be taken up for study to further advance the hypotheses proposed in this thesis and resolve all the outstanding issues in Quaternary evolution of the western India.

- Even though the palaeo-Ghaggar river has been traced between Sirsa and Anupgarh, its downstream extension is yet to be worked out. The fact that researchers working downstream of the river in the Pakistan region could not trace the river activity during the Holocene, suggests that the river was probably flowing along a different track further downstream than its present day course or that proposed earlier. This aspect needs to be investigated.
- The fluvial deposits studied in the Great Rann of Kachchh date back to the mid-Holocene only. Therefore, the older deposits of the GRK only can reveal what was the discharge condition of the rivers draining into the GRK during the early Holocene and whether any higher-Himalayan river was discharging into the GRK during that period.
- More sections of Thar Desert need to be sampled covering the entire extent of the desert for a rigorous geochemical provenance study. In addition, the temporal evolution of the desert needs to be constrained well.

References

Aitken, M.J., 1998. An Introduction to Optical Dating. Oxford University Press: Oxford.

Alizai, A., Carter, A., Clift, P.D., VanLaningham, S., Williams, J.C., Kumar, R., 2011a. Sediment provenance, reworking and transport processes in the Indus River by U–Pb dating of detrital zircon grains. Glob. Planet. Change 76, 33–55.

Alizai, A., Clift, P.D., Giosan, L., VanLaningham, S., Hinton, R., Tabrez, A.R., Danish, M., 2011b. Pb isotopic variability in the modern-Pleistocene Indus River system measured by ion microprobe in detrital K-feldspar grains. Geochim. Cosmochim. Acta 75, 4771–4795. doi:10.1016/j.gca.2011.05.039

Alizai, A., Clift, P.D., Still, J., 2016. Indus Basin Sediment Provenance Constrained Using Garnet Geochemistry. J. Asian Earth Sci. 126, 29–57.

Alizai, A., Hillier, S., Clift, P.D., Giosan, L., Hurst, A., VanLaningham, S., Macklin, M., 2012. Clay mineral variations in Holocene terrestrial sediments from the Indus Basin. Quat. Res. 77, 368–381. doi:10.1016/j.yqres.2012.01.008

Allègre, C.J., Othman, D. Ben, 1980. Nd–Sr isotopic relationship in granitoid rocks and continental crust development: a chemical approach to orogenesis. Nature 286, 335–342.

Awasthi, N., Ray, J.S., Pande, K., 2015. Origin of the Mile Tilek Tuff , South Andaman : evidence from 40 Ar – 39 Ar chronology and geochemistry. Curr. Sci. 108, 1–6.

Awasthi, N., Ray, J.S., Singh, A.K., Band, S.T., Rai, V.K., 2014. Provenance o the Late Quaternary sediments in the Andaman Sea: Implications for monsoon variabilty and ocean circulation. Geochemistry, Geophys. Geosystems 15, 3890–3906. doi:10.1002/2014GC005462

Band, S., Yadava, M.G., Ramesh, R., Gupta, S., Polyak, V.J., Asmerom, Y., 2016. Holocene Monsoon variability using stalagmite record from Dandak cave , India, in: Goldschmidt Conference Abstracts, 2016. p. 152.

Banerji, U.S., Bhushan, R., Jull, A.J.T., 2016. Mid−late Holocene monsoonal records from the partially active mudflat of Diu Island, southern Saurashtra, Gujarat, western India. Quat. Int. doi:http://dx.doi.org/10.1016/j.quaint.2016.09.060

Basu, A.R., Sharma, M., DeCelles, P.G., 1990. Nd, Sr-isotopic provenance and trace element geochemistry of Amazonian Foreland Basin Fluvial Sands, Bolivia and Peru: implications for Ensialic Andean Orogeny. Earth Planet. Sci. Lett. 105, 149–169.

Bhatia, M.R., 1983. Plate Tectonics and geochemical composition of sandstone. J. Geol. 91, 611–627.

Bhatia, M.R., Crook, K.A.W., 1986. Trace element characteristics of greywackes and tectonic discrimination of sedimentary basins. Contrib. to Mineral. Petrol. 92, 181–193.

Biswas, S.K., 1987. Regional tectonics framework, structue and evolution of the western marginal basins of India. Tectonophysics 135, 307–327.

Bollinger, L., Avouac, J.P., Beyssac, O., Catlos, E.J., Harrison, T.M., Grove, M., Goffe, B.,

Sapkota, S., 2004. Thermal structure and exhumation history of the Lesser Himalaya in central Nepal. Tectonics 23.

Bookhagen, B., Rasmus, C.T., Strecker, M.R., 2005. Late Quaternary intensified monsoon phases control landscape evolution in the northwest Himalaya. Geology 33, 149–152. doi:10.1130/G20982.1

Catlos, E.J., Harrison, T.M., Kohn, M.J., Grove, M., Ryerson, F.J., Manning, C.E., Upreti, B.N., 2001. Geochronologic and thermobarometric constraints on the evolution of the Main Central Thrust, central Nepal Himalaya. J. Geophys. Res. 106, 16 177–16 204.

Chandel, H.N., Patel, A.D., Vaghela, H.R., Ubale, G.P., 2006. An effective and reusable sampling pipe for luminescence dating. Anc. TL 26, 21–23.

Chatterjee, A., Ray, J.S., 2017a. Geochemistry of Harappan potteries from Kalibangan and sediments in the Ghaggar River: Clues for a dying river. Geosci. Front. doi:https://doi.org/10.1016/j.gsf.2017.07.006

Chatterjee, A., Ray, J.S., 2017b. Sources and depositional pathways of mid-Holocene sediments in the Great Rann of Kachchh, India: Implications for fluvial scenario during the Harappan Culture. Quat. Int. 443, 177–187. doi:10.1016/j.quaint.2017.06.008

Clark, P.U., Dyke, A.S., Shakun, J.D., Karlson, A.E., Clark, J., Wohlfarth, B., Mitrovica, J.X., Hostetler, S.W., McCabe, A.M., 2009. The Last Glacial Maximum. Science (80-.). 325, 710–714. doi:10.1126/science.1172873

Clift, P.D., Carter, a., Giosan, L., Durcan, J., Duller, G. a. T., Macklin, M.G., Alizai, a., Tabrez, a. R., Danish, M., VanLaningham, S., Fuller, D.Q., 2012. U-Pb zircon dating evidence for a Pleistocene Sarasvati River and capture of the Yamuna River. Geology 40, 211–214. doi:10.1130/G32840.1

Clift, P.D., Giosan, L., Blusztajn, J., Campbell, I.H., Allen, C., Pringle, M., Tabrez, A.R., Danish, M., Rabbani, M.M., Alizai, A., Carter, A., Lückge, A., 2008. Holocene erosion of the Lesser Himalaya triggered by intensified summer monsoon. Geology 36, 79–82. doi:10.1130/G24315A.1

Clift, P.D., Giosan, L., Carter, A., Garzanti, E., Galy, V., Tabrez, A.R., Pringle, M., Campbell, I.H., France-Lanord, C., Blusztajn, J., Allen, C., Alizai, A., Luckge, A., Danish, M., Rabbani, M.M., 2010. Monsoon control over erosion patterns in the Western Himalaya: possible feed-back into the tectonic evolution, in: Clift, P.D., Tada, R., Zheng, H. (Eds.), Monsoon Evolution and Tectonics - Climate Linkage in Asia. The Geological Society of London, pp. 185–218. doi:10.1144/SP342.12

Clift, P.D., Lee, J.I., Hildebrand, P., Shimizu, N., Layne, G.D., Blusztajn, J., Blum, J.D., Garzanti, E., Ali, A., 2002. Nd and Pb isotope variability in the Indus River System : implications for sediment provenance and crustal heterogeneity in the Western Himalaya. Earth Planet. Sci. Lett. 200, 91–106.

Condie, K.C., 1991. Another look at the rare earth elements in shales. Geochim. Cosmochim. Acta 35, 2527–2531.

Danino, M., 2010. The Lost River - On the trail of the SARASVATI. Penguin Books.

DePaolo, D.J., 1988. Age dependence of the composition of continental crust as determined

from Nd isotopic variations in igneous rocks. Earth Planet. Sci. Lett. 59, 263–271.

Dhir, R.P., Kar, A., Wadhawan, S.K., Rajaguru, S.N., Misra, V.N., Singhvi, A.K., Sharma, S.B., 1992. Thar Desert in Rajasthan: Land, Man and Environment. Geological Society of India, Bangalore.

Dhir, R.P., Singhvi, A.K., 2012. The Thar Desert and its antiquity. Curr. Sci. 102, 1001–1008.

Dickin, A.P., 2000. Radiogenic Isotope Geology. Cambridge University Press, United Kingdom.

Dikshit, K.N., 2013. Origin of Early Harappan cultures in the Sarasvati Valley: Recent Archaeological Evidence and Radiometric dates. J. Indian Ocean Archeol. 9, 87–141.

Dixit, Y., Hodell, D.A., Sinha, R., Petrie, C.A., 2014. Abrupt weakening of the Indian summer monsoon at 8.2 kyrB.P. Earth Planet. Sci. Lett. 391, 16–23. doi:10.1016/j.epsl.2014.01.026

Duddy, I.R., 1980. Redistribution and fractionation of REE and other elements in a weathering profile. Chem. Geol. 30, 363–380.

East, A.E., Clift, P.D., Carter, A., Alizai, A., VanLaningham, S., 2015. Fluvial – Eolian interactions in Sediment routing and sedimentary signal buffering : An example from the Indus basin and Thar Desert. J. Sediment. Res. 85, 715–728. doi:http://dx.doi.org/10.2110/jsr.2015.42

Enzel, Y., Ely, L.L., Mishra, S., Ramesh, R., Amit, R., Lazar, B., Rajaguru, S.N., Baker, V.R., Sandler, A., 1999. High-Resolution Holocene Environmental Changes in the Thar Desert , Northwestern India. Science (80-.). 284, 125–128.

Gangal, K., Vahia, M.N., Adhikari, R., 2010. Spatio-temporal analysis of the Indus urbanisation. Curr. Sci. 98, 846–852.

Garçon, M., Chauvel, C., France-lanord, C., Limonta, M., Garzanti, E., 2014. Which minerals control the Nd – Hf – Sr – Pb isotopic compositions of river sediments ? Chem. Geol. 364, 42–55. doi:http://dx.doi.org/10.1016/j.chemgeo.2013.11.018

Garzanti, E., Vezzoli, G., Andò, S., Paparella, P., Clift, P.D., 2005. Petrology of Indus River sands: a key to interpret erosion history of the Western Himalayan Syntaxis. Earth Planet. Sci. Lett. 229, 287–302. doi:10.1016/j.epsl.2004.11.008

Gaur, A.S., Vora, K.H., Murali, R.M., Jayakumar, S., 2013. Was the Rann of Kachchh navigable during the Harappan times (Mid-Holocene)? An archaeological perspective. Curr. Sci. 105, 1485–1491.

George, B.G., Ray, J.S., 2017. Provenance of sediments in the Marwar Supergroup, Rajasthan, India: Implications for basin evolution and Neoproterozoic global events. J. Asian Earth Sci. 147, 254–270.

Ghose, B., Kar, A., Husain, Z., 1979. The lost courses of the Saraswati River in the Great Indian Desert: new evidence from Landsat imagery. Geogr. J. 145, 446–451.

Giosan, L., Clift, P.D., Macklin, M.G., Fuller, D.Q., Constantinescu, S., Durcan, J. a,

Stevens, T., Duller, G. a T., Tabrez, A.R., Gangal, K., Adhikari, R., Alizai, A., Filip, F., VanLaningham, S., Syvitski, J.P.M., 2012. Fluvial landscapes of the Harappan civilization. Proc. Natl. Acad. Sci. U. S. A. 109, E1688-94. doi:10.1073/pnas.1112743109

Gleason, J.D., Patchett, P.J., Ruiz, W.R.D., 1994. Nd isotopes link Ouachita turbidites to Appalachian sources. Geology 22, 347–350.

Glennie, K.W., Evans, G., 1976. A reconnaissance of the Recent sediments of the Ranns of Kutch , India. Sedimentology 23, 625–647.

Goldstein, S.J., Jacobsen, S.B., 1988. Nd and Sr isotopic systematics of river water suspended material: implications for crustal evolution. Earth Planet. Sci. Lett. 87, 249–265.

Gu, X.X., Liu, J.M., Zheng, M.H., Tang, J.X., Qi, L., 2002. Provenance and Tectonic Setting of the Proterozoic Turbidites in Hunan , South China : Geochemical Evidence. J. Sediment. Res. 72, 393–407.

Gupta, A.K., Sharma, J.R., Sreenivasan, G., 2011. Using satellite imagery to reveal the course of an extinct river below the Thar Desert in the Indo-Pak region. Int. J. Remote Sens. 32, 5197–5216.

Hodges, K. V., 2003. Geochronology and Thermochronology in Orogenic Systems, in: The Crust, 3. Elsevier Science, Amsterdam, pp. 263–292.

Inger, S., 1998. Timing of an extensional detachment during convergent orogeny; new Rb-Sr geochronological data from the Zanskar shear zone, northwestern Himalaya. Geology 26.

Jain, M., Tandon, S.K., Singhvi, A.K., Mishra, S., Bhatt, S.C., 2005. Quaternary Alluvial Stratigraphical Development in a Desert Setting : A Case Study from the Luni River Basin , Thar Desert of western India. IMemoires - Geol. Soc. India 35, 349–371. doi:10.1002/9781444304350.ch19

Jochum, K.P., Nohl, U., Herwig, K., Lammel, E., Stoll, B., Hofmann, A.W., 2005. GeoReM: a new geochemical database for reference materials and isotopic standards. Geostand. Geoanalytical Res. 29, 333–338. doi:10.1111/j.1751-908X.2005.tb00904.x

Judd, J.W., 1886. Report on a series of specimens of the deposits of the Nile delta. Proc. R. Soc. 39, 213–227.

Juyal, N., Chamyal, L.S., Bhandari, S., Bhushan, R., Singhvi, A.K., 2006. Continental record of the southwest monsoon during the last 130 ka: evidence from the southern margin of the Thar desert, India. Quat. Sci. Rev. 25, 2632–2650.

Kale, V.S., Singhvi, A.K., Mishra, P.K., Banerjee, D., 2000. Sedimentary records and luminescence chronology of Late Holocene palaeofloods in the Luni River , Thar Desert , northwest India. Catena 40, 337–358.

Kar, A., 1996. Morphology And Evolution Of Sand Dunes In The Thar Desert As Ket To Sand Control Measures. Indian J. Geomorphol. 1, 177–206.

Kar, A., Singhvi, A.K., Rajaguru, S.N., Juyal, N., Thomas, J. V., Banerjee, D., Dhir, R.P., 2001. Reconstruction of the late Quaternary environment of the lower Luni plains , Thar

Desert , India. J. Quat. Sci. 16, 61–68.

Karim, A., Veizer, J., 2000. Weathering processes in the Indus River Basin : Implications from riverine carbon , sulfur , oxygen , and strontium isotopes. Chem. Geol. 170, 153–177. doi:10.1016/S0009-2541(99)00246-6

Kenoyer, J.M., 2008. Indus Civilization, in: Encyclopedia of Archaeology. Elsevier, New York, pp. 715–733.

Kenoyer, J.M., 1998. Ancient Cities of the Indus Valley Civilization. Oxford University Press: Oxford.

Khonde, N., Maurya, D.M., Singh, A.D., Chowksey, V., Chamyal, L.S., 2011. Environmental significance of raised ran sediments along the margins of Khadir , Bhanjada and Kaur wet islands in Great Rann of Kachchh , Western India. Curr. Sci. 101, 1429–1434.

Kochar, R., 2000. Vedic People: Their History and Geography. Orient Longman, Hyderabad.

Krishnan, K., 2002. Survey of Ceramic Analysis with Specific Reference to Pottery, Indian Archaeology in Retrospect, Prehistory-Archaeology of South Asia. Manohar, New Delhi.

Krishnan, K., Rao, L.S., Vinod, V., Kumar, S.S., Sukumaran, P., Kushwaha, D.K., 2012. Petrography of Ceramics from Bhirrana : A Preliminary Study. Man Environ. 37, 18–27.

Krishnan, K., Rao, V., 1994. A Study of Clay Paste Preperation by Potters Through Grain Size Analysis. South Asian Stud. 10, 113–117.

Lancaster, N., 2009. Dune Morphology and Dynamics, in: Parsons, A.J., Abrahams, A.D. (Eds.), Geomorphology of Desert Environments. Springer, pp. 557–596.

Limmer, D.R., Böning, P., Giosan, L., Ponton, C., Köhler, C.M., Cooper, M.J., Tabrez, A.R., Clift, P.D., 2012. Geochemical record of Holocene to Recent sedimentation on the Western Indus continental shelf, Arabian Sea. Geochemistry, Geophys. Geosystems 13. doi:10.1029/2011GC003845

Lindstrom, K.E., 2013. Pottery Preferences and Community Dynamics in the Indus Civilization. University of Wisconsin- Madison.

Ludwig, K.R., 2000. User's Manual for Isoplot/Ex version 2.2 A Geochronological Toolkit for Microsoft Excel. Berkeley Geochronology Center Special Publication No. 1a.

Mackie, W., 1899a. The sands and sandstones of eastern Moray. Trans. Edinburgh Geol. Soc. 7, 148–172.

Mackie, W., 1899b. The feldspars present in sedimentary rocks as indicators of the conditions of contemporaneous climates. Trans. Edinburgh Geol. Soc. 7, 443–468.

Malik, J.N., Merh, S.S., Sridhar, V., 1999. Palaeo-delta complex of Vedic Saraswati and other ancient rivers of north-western India. Mem. Geol. Soc. India 42, 163–174.

Mani, B.R., 2008. Kashmir Neolithic and Early Harappan: A Linkage. Pragdhara 18, 229–247.

Martin, J.-M., Whitfield, M., 1983. The Significance of the River Input of Chemical

Elements to the Ocean, in: Wong, C.S. (Ed.), Trace Metals in Sea Water. Springer, New York, pp. 265–296.

Mathew, G., Singhvi, A.K., Karanth, V., 2006. Luminescence chronometry and geomorphic evidence of active fold growth along the Kachchh Mainland Fault (KMF), Kachchh, India: Seismotectonic implications. Tectonophysics 422, 71–87.

Maurya, D.M., Khonde, N., Das, A., Chowksey, V., Chamyal, L.S., 2013. Subsurface sediment characteristics of the Great Rann of Kachchh , western India based on preliminary evaluation of textural analysis of two continuous sediment cores. Curr. Sci. 104, 859–862.

Maurya, D.M., Thakkar, M.G., Chamyal, L.S., 2003. Quaternary Geology of the Arid Zone of Kachchh: Terra Incognita. Proc. Indian Natl. Sci. Acad. 69A, 123–135.

Maurya, D.M., Thakkar, M.G., Patidar, A.K., Bhandari, S., Goyal, B., Chamyal, L.S., 2008. Late Quaternary geomorphic evolution of the coastal zone of Kachchh, Western India. J. Coast. Res. 24, 746–758.

Mehdi, M., Pant, N.C., Saini, H.S., Mujtaba, S.A.I., 2016. Identification of palaeochannel configuration in the Saraswati River basin in parts of Haryana and Rajasthan , India , through digital remote sensing and GIS. Episodes 39, 1–10. doi:10.18814/epiiugs/2016/v39i1/89234

Merh, S.S., 2005. The Great Rann of Kachchh: Perceptions of a Field Geologist. J. Geol. Soc. India 65, 9–25.

Metcalfe, R.P., 1993. Pressure, temperature and time constraints on metamorphism across the Main Central Thrust zone and high Himalayan slab in the Garhwal Himalaya. Himal. Tectonics. Geol. Soc. London, Spec. Publ. 74.

Meyer, I., Davies, G.R., Stuut, J.-B.W., 2011. Grain size control on Sr-Nd isotope provenance studies and impact on paleoclimate reconstructions: An example from deep-sea sediments offshore NW Africa. Geochemistry, Geophys. Geosystems 12. doi:10.1029/2010GC003355

Miller, R.J., O'Nions, R.K., 1984. The provenance and crustal residence ages of British sediments in relation to palaeogeographic reconstructions. Earth Planet. Sci. Lett. 68, 459–470.

Misra, V.N., 2001. Prehistoric human colonization of India. J. Biosci. 26, 491–531.

Misra, V.N., 1984. Climate: A factor in the rise and fall of Indus Civilization, in: Frontiers of the Indus Civilzation. Books and Books, New Delhi, pp. 469–489.

Mughal, M.R., 1997. Ancient Cholistan: Archaeology and architecture. Ferozsons, Lahore, Pakistan.

Murray, A.S., Wintle, A.G., 2000. Luminescence dating of quartz using an improved single-aliquot regenerative-dose protocol. Radiat. Meas. 32, 57–73.

Najman, Y., 2006. The detrital record of orogenesis: A review of approaches and techniques used in the Himalayan sedimentary basins. Earth-Science Rev. 74, 1–72. doi:10.1016/j.earscirev.2005.04.004

Najman, Bickle, Chapman, Yang, H., 2000. Early Himalayan exhumation: Isotopic constraints from the Indian foreland basin. Terra Nov. 12, 28–34. doi:10.1046/j.1365-3121.2000.00268.x

Nelson, B.K., DePaolo, D.J., 1988. Application of Sm-Nd and Rb-Sr isotope systematics to studies of provenance and basin analysis. J. Sediment. Petrol. 58, 348–357.

Nesbitt, H.W., 1979. Mobility and Fractionation of REE during weathering of granodiorite. Nature 279, 206–210.

Ngangom, M., Bhandari, S., Thakkar, M.G., Shukla, A.D., Juyal, N., 2016. Mid-Holocene extreme hydrological events in the eastern Great Rann of Kachchh, western India. Quat. Int. doi:10.1016/j.quaint.2016.10.017

Ngangom, M., Thakkar, M.G., Bhushan, R., Juyal, N., 2012. Continental – marine interaction in the vicinity of the Nara River during the last 1400 years , Great Rann of. Curr. Sci. 103, 1339–1342.

Oldham, C.F., 1893. The Saraswati and the lost river of the Indian desert. J. R. Asiat. Soc. 34, 49–76.

Oldham, R.D., 1926. The Cutch (Kachh) earthquake of 16th June 1819 with a riviusion of the great earthquake of 12th June 1897. Mem. Geol. Surv. India 46, 71–147.

Pal, Y., Sahai, B., Sood, R.K., Agarwal, D.P., 1980. Remote sensing of the “Lost” Saraswati river. Proceeding Indian Natl. Sci. Acad. (Earth Planetry Sci. 89, 317–331.

Pande, K., Sarin, M.M., Trivedi, J.R., Krishnaswami, S., Sharma, K.K., 1994. The Indus river system (India- Pakistan): Major-ion chemistry , uranium and strontium isotopes. Chem. Geol. 116, 245–259. doi:10.1016/0009-2541(94)90017-5

Pande, K., Yatheesh, V., Sheth, H., 2017. 40Ar/39Ar dating of theMumbai tholeiites and Panvel flexure: intense 62.5Ma onshore–offshore Deccan magmatism during India-Laxmi Ridge–Seychelles breakup. Geophys. J. Int. 210, 1160–1170. doi:10.1093/gji/ggx205

Petit, J.R., Jouzel, J., Raynaud, D., Barkov, N.I., Barnola, J.M., Basile, I., Bender, M., Chappellaz, J., Davis, M., Delaugue, G., Delmotte, M., Kotlyakov, V.M., Legrand, M., Lipenkov, V.Y., Lorius, C., Pepin, L., Ritz, C., Saltzman, E., Steivenard, M., 1999. Climate and atmospheric history of the past 420,000 years from the Vostok ice core, Antarctica. Nature 399, 429–436.

Pettijohn, F.J., Potter, P.. E., Siever, R., 1972. Sand and Sandstone. Springer.

Possehl, G.L., 2002. The Indus Civilization: A contemporary perspective. AltaMira Press, Lanham, Maryland.

Raczek, I., Jochum, K.P., Hofmann, A.W., 2001. Neodymium and Strontium Isotope Data for USGS Reference GSP-1 , GSP-2 and Eight MPI-DING Reference Glasses. Geostand. Newsl. 27, 173–179.

Radhakrishan, B.P., Merh, S.S., 1999. Vedic Sarasvati: Evolutionary History of a Lost River of Northwestern india. Mem. Geol. Soc. India 42, 5–13.

Raikes, R., 1968. Kalibangan: Death from Natural Causes. Antiquity XLII, 286–291.

Rajendran, C.P., Rajendran, K., 2003. The surface deformation and earthquake history associated with the 1819 Kachchh earthquake. Mem. Geol. Soc. India 54, 87–142.

Rajendran, C.P., Rajendran, K., Thakkar, M.G., Goyal, B., 2008. Assessing the previous activity at the source zone of the 2001 Bhuj earthquake based on the nearsource and distant paleoseismological indicators. J. Geophys. Res. Res. 113, B05311.

Rajendran, C.P., Ranjendran, K., 2001. Characteristics of Deformation and Past Seismicity Associated with the 1819 Kutch Earthquake, Northwestern India. Bull. Seismol. Soc. Am. 91, 407–426.

Rajesh, S. V., 2011. A Comprehensive Study of the Regional Chalcolithic Cultures of Gujarat [Unpublished Ph.D. thesis]. The Maharaja Sayajirao University of Baroda, Vadodara, India.

Rao, K.K., Wasson, R.J., Kutty, M.K., 1989. Foraminifera from Late Quaternary Dune Sands of the Thar Desert, India. Palaios 4, 168–180.

Rao, L.S., Sahu, N.B., Sahu, P., Shastry, U.A., Diwan, S., 2005. New light on the excavation of Harappan settlement at Bhirrana. Puratattva 35, 67–75.

Ray, J.S., Pande, K., Bhutani, R., 2015. 40Ar / 39Ar geochronology of subaerial lava flows of Barren Island volcano and the deep crust beneath the Andaman Island Arc, Burma Microplate. Bull. Volcanol. 77: 57. doi:10.1007/s00445-015-0944-9

Ray, J.S., Pattanayak, S.K., Pande, K., 2005. Rapid emplacement of the Kerguelen plume–related Sylhet Traps, eastern India: Evidence from 40Ar-39Ar geochronology. Geophys. Res. Lett. 32, L10303.

Ray, R., Shukla, A.D., Sheth, H.C., Ray, J.S., Duraiswami, R.A., Vanderkluysen, L., Rautela, C.S., Mallik, J., 2008. Highly heterogeneous Precambrian basement under the central Deccan Traps, India: Direct evidence from xenoliths in dykes. Gondwana Res. 13, 375–385.

Reimer, P.J., Bard, E., Bayliss, A., Beck, J.W., Blackwell, P.G., Bronk Ramsey, C., Buck, C.E., Cheng, H., Edwards, R.L., Friedrich, M., Grootes, P.M., Guilderson, T.P., Haflidason, H., Hajdas, I., Hatté, C., Heaton, T.J., Hoffmann, D.L., Hogg, A.G., Hughen, K.A., Kaiser, K.F., Kromer, B., Manning, S.W., Niu, M., Reimer, R.W., Richards, D.A., Scott, E.M., Southon, J.R., Staff, R.A., Turney, C.S.M., van der Plicht, J., 2013. IntCal13 and Marine13 Radiocarbon Age Calibration Curves 0–50,000 Years cal BP. Radiocarbon 55, 1869–1887. doi:10.2458/azu_js_rc.55.16947

Renne, P.R., Swisher, C.C., Deino, A.L., Karner, D.B., Owens, T.L., Depaolo, D.J., 1998. Intercalibration of standards , absolute ages and uncertainties in 40Ar / 39Ar dating. Chem. Geol. 145, 117–152.

Richards, D.A., Andersen, M.B., 2013. Time Constraints and Tie-Points in the Quaternary Period. Elements 9, 45–51. doi:10.2113/gselements.9.1.45

Roser, B.P., Korsch, R.J., 1986. Determination of tectonic settings of sandstone-mudstone suits using SiO2 content and K2O/Na2O ratio. J. Geol. 94, 635–650.

Sachan, H.K., Kohn, M.J., Saxena, A., Corrie, S.L., 2010. The Malari leucogranite , Garhwal Himalaya , northern India : Chemistry , age , and tectonic implications. GSA Bull. 122, 1865–1876. doi:10.1130/B30153.1

Saini, H.S., Mujtaba, S.A.I., 2012. Depositional history and palaeoclimatic variations at the northeastern fringe of Thar Desert, Haryana plains, India. Quat. Int. 250, 37–48. doi:10.1016/j.quaint.2011.06.002

Saini, H.S., Mujtaba, S. a. I., 2010. Luminescence Dating of the Sediments from a Buried Channel Loop in Fatehabad Area, Haryana: Insight into Vedic Saraswati River and its Environment. Geochronometria 37, 29–35. doi:10.2478/v10003-010-0021-5

Saini, H.S., Tandon, S.K., Mujtaba, S.A.I., Pant, N.C., Khorana, R.K., 2009. Reconstruction of buried channel-floodplain system of the northwestern Haryana Plains and their relation to the " Vedic " Saraswati. Curr. Sci. 97, 1634–1643.

Sarkar, A., Mukherjee, A.D., Bera, M.K., Das, B., Juyal, N., Morthekai, P., Deshpande, R.D., Shinde, V.S., Rao, L.S., 2016. Oxygen isotope in archaeological bioapatites from India: Implications to climate change and decline of Bronze Age Harappan civilization. Sci. Rep. 6, 26555. doi:10.1038/srep26555

Sarkar, A., Ramesh, R., Somayajulu, B.L.K., Agnihotri, R., Jull, A.J.T., Burr, O.S., 2000. High resolution Holocene monsoon record from the eastern Arabian Sea. Earth Planet. Sci. Lett. 177, 209–218. doi:10.1016/S0012-821X(00)00053-4

Scharer, U., Copeland, P., Harrison, T.M., Searle, M.P., 1990. Age, cooling history and origin of post-collisional leucogranite in the Karakoram batholith: a multi-system isotope study. J. Geol. 98, 233–251.

Searle, M.P., Waters, D.J., Rex, D.C., Wilson, R.N., 1992. Pressure, temperature, and time constraints on Himalayan metamorphism from eastern Kashmir and western Zanskar. J. Geol. Soc. London 149, 753–773.

Sharma, A., Rajamani, V., 2000. Weathering of gneissic rocks in the upper reaches of the Cauvery River, south India: implications to neotectonic of the region. Chem. Geol. 166, 203–233.

Sharma, K.D., Vangani, N.S., Choudhary, J.S., 1984. Sediment transport characteristics of the desert streams in India. J. Hydrol. 67, 261–272.

Singh, A., Paul, D., Sinha, R., Thomsen, K.J., Gupta, S., 2016a. Geochemistry of buried river sediments from Ghaggar Plains , NW India : Multi-proxy records of variations in provenance , paleoclimate , and paleovegetation patterns in the Late Quaternary. Paleogeography, Paleoclimatology, Paleoecol. 449, 85–100. doi:http://dx.doi.org/10.1016/j.palaeo.2016.02.012

Singh, A., Paul, D., Sinha, R., Thomsen, K.J., Gupta, S., 2016b. Reply to the comment on “Geochemistry of buried river sediments from Ghaggar Plains, NW India: Multi-proxy records of variations in provenance, paleoclimate, and paleovegetation patterns in the late quaternary” by Singh et al. (2016), Palaeogeography, Pal. Palaeogeogr. Palaeoclimatol. Palaeoecol. 455, 68–70. doi:10.1016/j.palaeo.2016.05.001

Singh, M., Sharma, M., Tobschall, H.J., 2005. Weathering of the Ganga alluvial plain,

northern India: Implications from fluvial geochemistry of the Gomati River. Appl. Geochemistry 20, 1–21. doi:10.1016/j.apgeochem.2004.07.005

Singh, P., Rajamani, V., 2001. REE geochemistry of recent clastic sediments from the Kaveri floodplains , Southern India : Implication to source area weathering and sedimentary processes. Geochim. Cosmochim. Acta 65, 3093–3108. doi:10.1016/S0016-7037(01)00636-6

Singh, S.K., Rai, S.K., Krishnaswami, S., 2008. Sr and Nd isotopes in river sediments from the Ganga Basin: Sediment provenance and spatial variability in physical erosion. J. Geophys. Res. 113. doi:10.1029/2007JF000909

Singhvi, A.K., Bluszcz, A., Bateman, M.D., Someshwar Rao, M., 2001. Luminescence dating of loess-palaeosol sequences and coversands: methodological aspects and palaeoclimatic implications. Earth-Science Rev. 54, 193–211.

Singhvi, A.K., Kar, A., 2004. The aeolian sedimentation record of the Thar desert. Proc. Indian Acad. Sci. (Earth Planetry Sci. 113, 371–401.

Sinha, R., Friend, P.F., 1994. River systems and their sediment flux, Indo Gangetic plains, Northern Bihar, India. Sedimentology 41, 825–845.

Sinha, R., Yadav, G.S., Gupta, S., Singh, A., Lahiri, S.K., 2013. Geo-electric resistivity evidence for subsurface palaeochannel systems adjacent to Harappan sites in northwest India. Quat. Int. 308–309, 66–75. doi:10.1016/j.quaint.2012.08.002

Staubwasser, M., Sirocko, F., Grootes, P.M., Segl, M., 2003. Climate change at the 4.2 ka BP termination of the Indus valley civilization and Holocene south Asian monsoon variability. Geophys. Res. Lett. 30, 1425. doi:10.1029/2002GL016822

Stein, A., 1942. A survey of ancient sites along the lost Saraswati river. Geogr. J. 99, 173–182.

Stephenson, B.J., Searle, M.P., Waters, D.J., Rex, D.C., 2001. Structure of the Main Central Thrust zone and extrusion of the High Himalayan deep crustal wedge, Kishtwar-Zanskar Himalaya. J. Geol. Soc. London 158, 637–652.

Syvitski, J.P.M., Kettner, A.J., Overeem, I., Giosan, L., Brakenridge, G.R., Hannon, M., Bilham, R., 2013. Anthropocene metamorphosis of the Indus Delta and lower floodplain. Anthropocene 3, 24–35. doi:10.1016/j.ancene.2014.02.003

Szulc, A.G., Najman, Y., Sinclair, H.D., Pringle, M., Bickle, M., Chapman, H., Garzanti, E., Ando, S., Huyghe, P., Mugnier, J.-L., Ojha, T., DeCelles, P., 2006. Tectonic evolution of the Himalaya constrained by detrital 40Ar/39Ar, Sm/Nd and petrographic data from the Siwalik foreland basin succession, SW Nepal. Basin Res. 18, 375–391.

Tanaka, T., Togashi, S., Kamioka, H., Amakawa, H., 2000. JNdi-1 : a neodymium isotopic reference in consistency with LaJolla neodymium. Chem. Geol. 168, 279–281.

Taylor, S.R., McLennan, S.M., 1985. The continental crust: Its Composition and evolution. Blackwell, London.

Thapar, B.K., 1975. Kalibangan: A Harappan Metropolis Beyond The Indus Valley, in: Expedition. pp. 19–32.

Thurach, H., 1884. U ber das Vorkommen mikroskopischer Zirkoneund Titanmineralien in den. Gesteinen. Verh. Phys. Med. Ges. Wurzbrg. 18, 203–284.

Totten, M.W., Hanan, M.A., Weaver, B.L., 2000. Beyond whole-rock geochemistry of shales. The importance of assessing mineralogic controls for revealing tectonic discriminants of multiple sediment sources for the Ouachita Mountain flysch deposits. Geol. Soc. Am. Bull. 112, 1012–1022.

Tripathi, J.K., Bock, B., Rajamani, V., 2013. Nd and Sr isotope characteristics of Quaternary Indo-Gangetic plain sediments: Source distinctiveness in different geographic regions and its geological significance. Chem. Geol. 344, 12–22. doi:10.1016/j.chemgeo.2013.02.016

Tripathi, J.K., Bock, B., Rajamani, V., 2013. Nd and Sr isotope characteristics of Quaternary Indo-Gangetic plain sediments : Source distinctiveness in different geographic regions and its geological signi fi cance 344, 12–22.

Tripathi, J.K., Bock, B., Rajamani, V., Eisenhauer, A., 2004. Is River Ghaggar, Saraswati? Geochemical constraints. Curr. Sci. 87, 1141–1145.

Tyagi, A.K., Shukla, A.D., Bhushan, R., Thakker, P.S., Thakkar, M.G., Juyal, N., 2012. Mid-Holocene sedimentation and landscape evolution in the western Great Rann of Kachchh,India. Geomorphology 151, 89–98. doi:10.1016/j.geomorph.2012.01.018

Valášková, M., 2015. Clays, clay minerals and cordierite ceramics - A review. Ceram. - Silikaty 59, 331–340.

Valdiya, K.S., 2017. Prehistoric River Saraswati , Western India Geological Appraisal and Social Aspects, Society of. ed. Springer.

Valdiya, K.S., 2013. The River Saraswati was a Himalayan-born river. Curr. Sci. 104, 42–54.

Valdiya, K.S., 2010. The Making of India Geodynamic Evolution, First. ed. Macmillan Publishers India LTD, New Delhi.

Vannay, J.-C., Grasemann, B., Rahn, M., Frank, W., Carter, A., Baudraz, V., Cosca, M., 2004. Miocene to Holocene exhumation of metamorphic crustal wedges in the NW Himalaya; evidence for tectonic extrusion coupled to fluvial erosion. Tectonics 23, 24.

Viers, J., Dupré, B., Gaillardet, J., 2009. Chemical composition of suspended sediments in World Rivers : New insights from a new database. Sci. Total Environ. 407, 853–868. doi:10.1016/j.scitotenv.2008.09.053

Volpe, A.M., Macdougall, J.D., 1990. Geochemistry and isotopic characteristics of mafic (Phulad Ophiolite) and related rocks in the Delhi Supergroup, Rajasthan, India: implications for rifting in the Proterozoic. Precambrian Res. 40, 167–191.

Wadia, D.N., 1960. The post-glacial desiccation of Central India, in: Monograph of National Institute of Sciences of India. p. 1.

Walker, J., Martin, M.W., Bowring, S.A., Searle, M., Waters, D.J., Hodges, K., 1999. Metamorphism, melting, and extension: age constraints from the High Himalayan Slab of southeast Zanskar and northwest Lahaul. J. Geol. 107, 473–495.

Walker, J.D., Geissman, J.W., Bowring, S.A., Babcock, L.E., 2013. The Geological Society of America Geologic Time Scale. GSA Bull. 125, 259–272. doi:10.1130/B30712.1

Wasson, R.J., Rajaguru, S.N., Misra, V.N., Agrawal, D.P., Dhir, R.P., Singhvi, A.K., Rao, K.K., 1983. Geomorphology , late Quaternary stratigraphy and palaeoclimatology of the Thar dunefield. Zeitschrift für Geomorphol. Suppl.-Bd., 117–151.

White, N.M., Pringle, M., Garzanti, E., Bickle, M., Najman, Y., Chapman, H., Friend, P., 2002. Constraints on the exhumation and erosion of the High Himalayan Slab, NW India, from foreland basin deposits. Earth Planet. Sci. Lett. 195, 29–44.

Wright, R.P., Bryson, R.A., Schuldenrein, J., 2008. Water supply and history : Harappa and the Beas regional survey. Antiquity 82, 37–48.

Wünnemann, B., Demske, D., Tarasov, P., Kotlia, B.S., Reinhardt, C., Bloemendal, J., Diekmann, B., Hartmann, K., Krois, J., Riedel, F., Arya, N., 2010. Hydrological evolution during the last 15 kyr in the Tso Kar lake basin (Ladakh, India), derived from geomorphological, sedimentological and palynological records. Quat. Sci. Rev. 29, 1138–1155. doi:10.1016/j.quascirev.2010.02.017

Yadava, M.G., Ramesh, R., 2005. Monsoon reconstruction from radiocarbon dated tropical Indian speleothems. Holocene 15, 48–59. doi:10.1191/0959683605h1783rp

Yadava, M.G., Ramesh, R., 1999. Speleothems - Usefull Proxies for Past Monsoon Rainfall. J. Sci. Ind. Res. 58, 339–348.

Yang, Y.-H., Chu, Z.-Y., Wu, F.-Y., Xie, L.-W., Yang, J.-H., 2011. Precise and accurate determination of Sm, Nd concentrations and Nd isotopic compositions in geological samples by MC-ICP-MS. J. Anal. At. Spectrom. 26, 1237. doi:10.1039/c1ja00001b

List of Publications

- **Anirban Chatterjee** and Jyotiranjan S. Ray, 2017. Sources and depositional pathways of mid-Holocene sediments in the Great Rann of Kachchh, India: Implications for fluvial scenario during the Harappan Culture. Quaternary International, 443, p 177-187. http://dx.doi.org/10.1016/j.quaint.2017.06.008

- **Anirban Chatterjee** and Jyotiranjan S. Ray, 2017. Geochemistry of Harappan Potteries from Kalibangan and sediments in the Ghaggar River: Clues for a Dying River. Geoscience Frontiers, https://doi.org/10.1016/j.gsf.2017.07.006

- **Anirban Chatterjee**, 2017. The Lost River of the Harappan Civilization: A Review of Recent Provenance Studies from the Ghaggar-Hakra-Nara Alluvium. Proceedings of the Indian National Science Academy (Under review)

Abstracts in International Conferences

- **Anirban Chatterjee** and Jyotiranjan S. Ray, 2017. Provenance of Mid-Holocene Sediments in the Great Rann of Kachchh, India: Implications for Fluvial Scenario of Harappan Civilisation (Oral presentation). International Meeting of Sedimentology 2017, Toulouse, France.

- **Anirban Chatterjee** and Jyotiranjan S. Ray, 2017. Geochemical evidence for a Holocene Saraswati river and its role in the evolution of the Harappan Civilisation (Poster presentation). International Meeting of Sedimentology 2017, Toulouse, France.

- **Anirban Chatterjee**, 2017. The Lost River of Harappan Civilization: Recent Geochemical Perspectives (Poster presentation). International Conference: Geology: Emerging Methods and Applications (GEM-2017) abstract volume, Page 5, Kerala, India.

- **Anirban Chatterjee** and Jyotiranjan S. Ray, 2016. Evidence for a Mid-Holocene Buried Himalayan River beneath the Ghaggar Plains, NW India: A Geochemical Provenance Study (Oral presentation). Goldschmidt Conference Abstracts (2016), P-414. Presented at Yokohama, Japan.

Quaternary International 443 (2017) 177–187

Contents lists available at ScienceDirect

Quaternary International

journal homepage: www.elsevier.com/locate/quaint

Sources and depositional pathways of mid-Holocene sediments in the Great Rann of Kachchh, India: Implications for fluvial scenario during the Harappan Culture

Anirban Chatterjee [a, b, *], Jyotiranjan S. Ray [a]

[a] Physical Research Laboratory, Navrangpura, Ahmedabad, 380009, India
[b] Department of Geology, The Maharaja Sayajirao University of Baroda, Vadodara, 390002, India

ARTICLE INFO

Article history:
Received 20 February 2017
Received in revised form
29 May 2017
Accepted 3 June 2017
Available online 17 June 2017

Keywords:
Great Rann of Kachchh
Ghaggar-Hakra-Nara river channel
Harappan civilization
Sediments
Geochemistry

ABSTRACT

The decline of the Harappan Culture (5300-3300 yrs BP), one of the earliest urban settlements, has often been linked to the demise of a perennial river (vedic Saraswati?) that originated in the Himalayan Mountain Belt and flowed through the Thar Desert into the Arabian Sea. To test this hypothesis we have studied the mid-Holocene (5.5–1.0 ka) sedimentation history of the Great Rann of Kachchh, an uplifted former gulf of the Arabian Sea, which is believed to have housed the delta of the river. Using trace element geochemistry and Sr-Nd isotopic ratios of sediments as tracers we have determined their provenances. Results of our study suggest that the basin received significant sediment contributions (20–30%) from a distinct sub-Himalayan source, apart from the other proximal sources such as the river Indus, Thar Desert and the ephemeral river Luni. It, however, did not receive any sediment from an independent glacier-fed river. Based on geological and geochemical arguments we infer that these sub-Himalayan sediments could have only been transported through a continuous Ghaggar-Hakra-Nara river channel, possibly seasonal, that flowed through the Harappan heartland. The fact that there was no major change in fluvial sedimentation in the Great Rann of Kachchh and it persisted at least until ~1.0 ka, suggests that drying up of this river system may not have been the primary cause for the decline of the civilization.

1. Introduction

The Bronze Age Harappan culture is one of the earliest known urban civilizations. Yet, its mysterious decline, within a few centuries of its zenith (4600-3900 yrs BP; Kenoyer, 2008; Possehl, 2002), remains one of the most enigmatic topics in the history of ancient India. The Harappan sites are mostly concentrated along the river systems of Indus and present-day ephemeral Ghaggar-Hakra (which disappears in the Cholistan Desert of Pakistan) and Nara river channel (Fig. 1A). This led to the suggestion that the Ghaggar-Hakra and Nara perhaps was a continuous and perennial fluvial system during the mature Harappan period and that the decline of the civilization was triggered by drying up of the river (Misra, 1984; Mughal, 1997; Wright et al., 2008). Indeed some workers, with the help of satellite based studies, historical documents and geophysical studies, have identified paleo-river channels that flowed through the present-day arid western margin of Thar Desert into the Arabian Sea (Ghose et al., 1979; Gupta et al., 2011; Sinha et al., 2013; Syvitski et al., 2013) and created a delta system in the western Great Rann of Kachchh (Malik et al., 1999). Moreover, a continuous Ghaggar-Hakra-Nara river system has often been equated with the mythical glacier-fed perennial river Saraswati (Ghose et al., 1979; Kochar, 2000; Oldham, 1893; Pal et al., 1980; Radhakrishan and Merh, 1999; Valdiya, 2013). Although the presence of buried paleo-channels and a delta complex may hint at the past existence of a fluvial system, in the absence of robust sedimentological and chronological constrains, its existence during the Harappan civilization remains, at the best, a conjecture. Interestingly, sediment provenance studies based on U-Pb dating of detrital zircons along the relict course of Ghaggar-Hakra channel, in its middle segment, seem to suggest that there possibly was a large, glacier-fed Himalayan river along these channels but it was active much before the Harappan civilization in the region, more than 10

* Corresponding author. Physical Research Laboratory, Navrangpura, Ahmedabad, 380009, India.
E-mail address: anirban@prl.res.in (A. Chatterjee).

http://dx.doi.org/10.1016/j.quaint.2017.06.008
1040-6182/

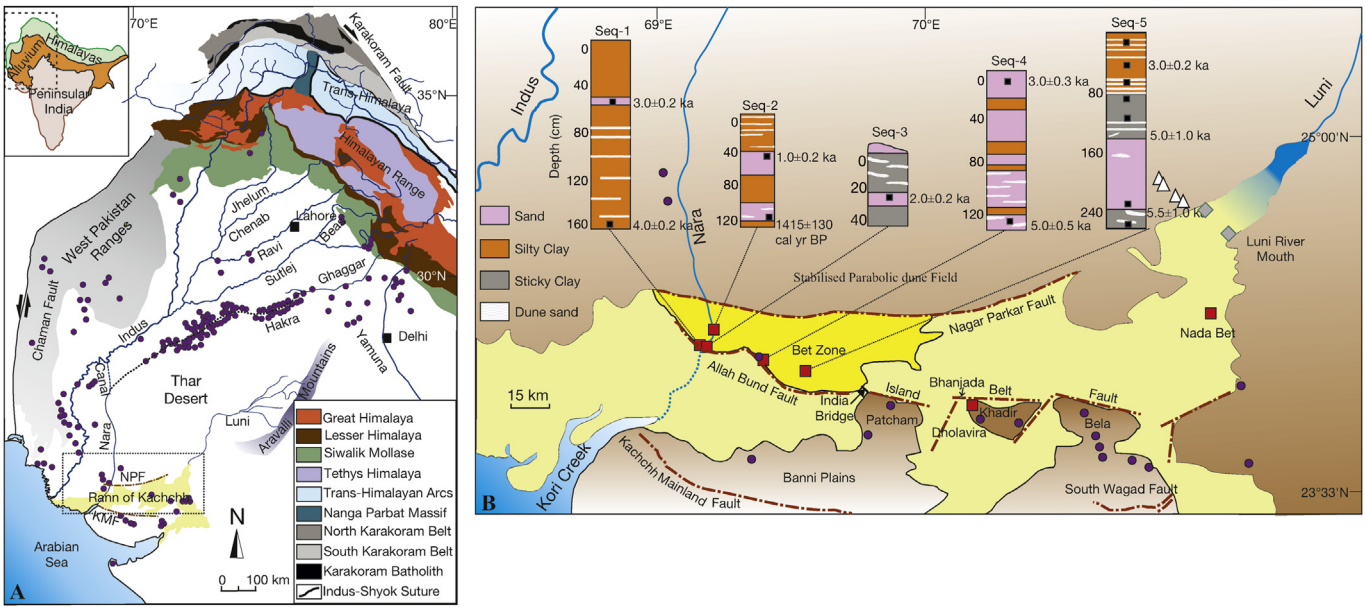

Fig. 1. **(A)** Schematic geological sketch map (modified from Garzanti et al., 2005) showing the major river systems of north-western India and eastern Pakistan (highlighted portion of the map shown in the inset) and lithology of their catchments. Also shown are different geomorphic features/divisions of the region. The dotted line is the speculated major paleochannel (Vedic Saraswati) that connected the Ghaggar with Hakra and Nara during the Harappan period. NPF = Nagar Parker Fault; KMF = Kachchh Mainland Fault. Harappan sites are marked as purple circles. **(B)** Schematic sketch map (modified from Tyagi et al., 2012) of the blow up of the area marked in (A) showing the major geological/morphological features of the Great Rann of Kachchh (light/dark yellow) and adjoining region. Sampling locations are marked: red squares for Rann (low lands) and bet (uplifted surfaces), grey diamonds for the Luni river mouth, and white triangles for the Thar dune field. Also shown is the stratigraphy of the sedimentary sequences of the sampled horizons (Seq-1 through Seq-5) in the western Great Rann of Kachchh with OSL/radiocarbon ages marked (in ka/cal yr BP). Positions of the samples on the stratigraphic columns are marked as black squares. (For interpretation of the references to colour in this figure legend, the reader is referred to the web version of this article.)

kyr ago (Clift et al., 2012). These studies also propose that the channels were seasonal (monsoon-fed) during the Holocene (Giosan et al., 2012) and got abandoned during 4–5 ka, eventually getting buried under the parabolic dunes of the Thar Desert by ~1.4 ka (Clift et al., 2012). However, younger fluvial activities (2.9–0.7 ka) have also been reported both from the upper and lower Ghaggar-Hakra floodplains (Giosan et al., 2012). A meandering river system frequently changes its course and creates numerous abandoned channels and therefore, depositional ages of sand from only a few sections may not reveal the true temporal extent of the river (Valdiya, 2013). Furthermore, geochemical studies of Alizai et al. (2011b, 2016) on K-feldspars and garnets in sediments of the river Nara suggest that either Nara was a former distributary of the river Indus or it was an ephemeral stream receiving reworked sediments. However, the former idea seems less likely as Tyagi et al. (2012) have clearly demonstrated that no major river system had flowed into the Nara channel since mid-Holocene.

In the above scenario, the Great Rann of Kachchh (GRK) of western India (Fig. 1A), which is located in the confluence zone between the lost river (vedic Saraswati?) and the Arabian Sea (Valdiya, 2013), becomes an important piece of the puzzle. Located marginally above the mean sea level (~4 m), the GRK is a desolate landscape of salty wasteland. It is believed to have supported maritime activities of the Harappans (Gaur et al., 2013) as evident from the ruins of Dholavira, one of the major Harappan towns - located in the very heart of the GRK, and many such sites in the region (Fig. 1B). While the eastern GRK primarily receives fluvial contribution from the river Luni, the western GRK is inundated by storm tides during the southwest Indian monsoon (Glennie and Evans, 1976), and receives some contribution from the ephemeral Nara during flooding in the Indus (Fig. 1A), channelized through man-made canals (Syvitski et al., 2013). Sediments exposed in structurally raised sandy mounds ('bet' in local language) and layered sand-silt sediments in the terraces around the margins of the islands (Patcham, Khadir and Bhanjada; Fig. 1B) bear testimony to a fluvial past of the GRK. Therefore, unravelling of the sedimentation history of the GRK since the mid-Holocene, besides being geologically important, has profound geo-archaeological implications towards deciphering the existence of any notable fluvial system (other than Indus) during the proliferation of Harappan civilization. To investigate this aspect of the GRK, we have studied trace element and Sr -Nd isotope geochemistry of sediments deposited in the basin during the last 5.5 kyr (Fig. 1), and quantified, for the first time, sediment contributions from various terrigenous sources. We have also made an attempt to decipher sediment transport pathways in order to throw light on the fluvial scenario of the Harappan period and in the process explored possible existence of a glacial fed river, originating from the higher Himalaya, draining into the Kachchh basin. Our samples came from the relict delta of the river Nara – the purported delta of the Saraswati, central and eastern GRK, mouth of the river Luni, and dunes of the southern-eastern Thar Desert (Fig. 1B).

2. Study area and sampling

2.1. The Great Rann of Kachchh

The GRK is an enigmatic geomorphic terrain that encompasses a vast stretch of low-lying salty desert (~16,000 sq. km) at the western margin of India, and is devoid of any major drainage; except for the ephemeral river Luni and river Nara (Fig. 1). It is flanked by parabolic dunes in the north and northwest, Banni Plain and the Wagad Upland in the south (Fig. 1B). Structurally, the GRK is part of an east-west trending paleo-rift graben believed to have formed in the Early Mesozoic (Biswas, 1987) and is bounded in the north by the Nagar Parkar Fault and in the south by the Kachchh Mainland and the South Wagad faults (Fig. 1B). In between, there exist two other east-west trending faults; namely the Allah Bund

and Island Belt (Fig. 1B), which are known to have influenced the Quaternary morphology of the GRK (Mathew et al., 2006; Maurya et al., 2008; Rajendran and Ranjendran, 2001). It has been suggested that the present day Rann surface is an uplifted floor of a former shallow marine gulf of the Arabian Sea that had formed during sea level rise at the immediate aftermath of the last glacial period (Maurya et al., 2008; Merh, 2005; Oldham, 1926). The latest uplift is believed to have occurred at ~2 kyr ago (Tyagi et al., 2012). At present, the central and eastern GRK remains detached from the western GRK, along a median high that passes through north-west of the Patcham Island along the India Bridge (Fig. 1B).

Monotonously flat topography, except for small bets, makes it difficult to determine the history of sedimentation in the GRK. It is believed that much of the Holocene sediments in the western part of the basin were derived from the Indus and Nara rivers that once flowed into the basin (Glennie and Evans, 1976; Khonde et al., 2016). Modern silty-clay deposits are attributed to storm tides, which bring in material from the Indus Delta aided by long-shore current, during the southwest monsoon (Glennie and Evans, 1976; Tyagi et al., 2012). The Banni Plain, which receives sediments from the Mesozoic sedimentary rocks of the northern Kachchh Mainland (Glennie and Evans, 1976; Maurya et al., 2013; Fig. 1B), acts as a buffer between the Mainland and the western GRK. Considering that the dry highlands and deserts surround the entire GRK, it is reasonable to expect aeolian contribution in the Rann sedimentation during periods of intense wind activity.

2.2. Sampling strategy and samples

Sediment samples for the present study were collected from tectonically raised surfaces or terraces, incised channels and dug up trenches (Fig. 1B). Since the primary focus of the study was the purported delta of the mythical river, we planned to examine in detail the bet zone north of the Allah Bund Fault scarp (Fig. 1B). Samples from this zone came from five sequences in five locations, in the western GRK, which were topographically higher than the present-day high tide strands. Fig. 1B presents stratigraphy of these horizons and the already known depositional ages from the work of Tyagi et al. (2012). Three of the sampling locations were on or near the channel of the river Nara (Fig. 1B). Samples representing the central and eastern GRK were collected from the western periphery of Khadir Island and from Nada Bet (Fig. 1B). These samples are sub-recent sediments exposed on fault controlled terraces, which occur as sandy deposits in the centre of silt dominated GRK basin. The geomorphology of these sites suggests that these sediments were derived from the surrounding rocky islands containing Mesozoic sediments and transported by local drainage. Apart from the river Nara, other potential sources of sediments to the western GRK during the mid-Holocene include the Thar Desert, the river Luni, and the river Indus.

The Thar Desert occurs as the most dominant landscape along the northern margin of the GRK basin. In absence of any fluvial system from the desert into the Great Rann of Kachchh basin, the only mode of sediment transportation from the northern margin could have been through wind. There was a need to characterize this source as only limited geochemical data existed that to from the far north-eastern margin of the desert, located ~800 km inland (Tripathi et al., 2013). In any case, the dune field at this margin cannot be considered as a potential aeolian sediment source for the GRK since the southwest monsoonal winds are believed to be the primary carrier of the desert sand (Singhvi and Kar, 2004). However, aeolian contribution from the sand dunes present in the near vicinity of the GRK is more likely through local sand storms and disturbances as they lack directionality. Therefore, to accurately predict sediment contribution from the Thar, we planned to sample sand dunes that are located very close to the northern margin of the GRK. However, because of inaccessibility of the north-western and northern margin of the basin (located in Pakistan), we could sample only the dunes located along the north-eastern margin (Fig. 1B). These samples were sub-recent sediments from stabilized parabolic dune field.

Luni is the only river system in India that drains from the Aravalli mountain ranges into the GRK (Fig. 1). The river remains ephemeral since ~8 ka (Kar et al., 2001), therefore, the sediment supply through it takes place only during heavy rainfall events linked to the southwest Indian monsoon. Because of its very nature, sediments transported by the Luni are mostly consisting of reworked alluvial and aeolian deposits. To constrain its contribution to the GRK we sampled sub-surface sediments along the river mouth (Fig. 1B). These samples would likely to provide average compositions of the Holocene sediments transported by the river.

Although the river Nara today brings in sediments from the river Indus into the GRK, there exists no evidence to suggest if the same was true in the past. However, it has been recognized that recycled Indus sediments have been getting into the basin through creeks via tidal currents as suspended load (mostly clay, Tyagi et al., 2012). In this work we make use of the geochemical data of Clift et al. (2010) and Limmer et al. (2012) for such sediments.

3. Methods

Nine sediment samples were dated by OSL method using single aliquot regeneration (SAR) protocol of (Murray and Wintle, 2000), whereas one sample of gastropod shells was dated by radiocarbon method using conventional β-counting (Yadava and Ramesh, 1999). Texturally, the samples are dominated by fine-grained sand and silty-clay which were believed to have been deposited in a tidal flat environment (Tyagi et al., 2012). As per the age information, the sediment samples from the western GRK, studied for geochemistry, represent a depositional history between 5.5 and ~1.0 kyr BP.

All the geochemical and isotopic measurements were done on silicate fractions of bulk sediments. Samples were washed with MILLI-Q water multiple times to remove salt, dried at 110 °C, powdered and homogenised. Prior to dissolution, powdered samples were heated at 650 °C for 2 h to remove organic matter and leached in dilute HCl to remove carbonates. Decarbonated samples were then dissolved using standard HF-HNO_3-HCl dissolution procedure for silicates. Concentrations of trace elements including rare earth elements (REEs) were measured using a Q-ICPMS at Physical Research Laboratory (PRL). USGS rock standard BHVO-2 was used as unknown for accuracy check. Reproducibility of trace element contents, based on repeated analyses of the standard, was $\leq$3% for REEs and $\leq$6% for all other trace elements at 2σ level. Sr separation was done by conventional cation exchange column chemistry and Nd was separated from other REEs using Ln-specific resin from Eichrom with dilute HCl as elutant. $^{87}Sr/^{86}Sr$ and $^{143}Nd/^{144}Nd$ were measured in static multicollection mode on an Isoprobe-T TIMS (Awasthi et al., 2014). The measured isotopic ratios were corrected for fractionation using $^{86}Sr/^{88}Sr = 0.1194$ and $^{146}Nd/^{144}Nd = 0.7219$, respectively. The average values for NBS987 and JNdi measured over a period of 5 years are $^{87}Sr/^{86}Sr = 0.71023 \pm 0.00001$ (n = 70) and $^{143}Nd/^{144}Nd = 0.512104 \pm 0.000004$ (n = 60; ±0.1 in ε_{Nd} units) at 2σ level of uncertainty. The value of $^{143}Nd/^{144}Nd = 0.512104$ for JNdi corresponds to a value of 0.511847 for the widely used La Jolla Nd standard (Tanaka et al., 2000). $^{87}Sr/^{86}Sr$ and $^{143}Nd/^{144}Nd$ for BHVO-2 measured gave values of 0.70346 ± 0.00004 and 0.512967 ± 0.000008 (n = 10; ±0.2 in ε_{Nd} units at 2σ) respectively, which are same as the reported values of 0.70344 ± 0.00003 and

0.51296 ± 0.00004 within 2σ (Raczek et al., 2001). To compare our data with that from literature, all the $^{87}Sr/^{86}Sr$ and $^{143}Nd/^{144}Nd$ ratios were normalized to 0.71025 for NBS987 and 0.511858 for La Jolla, respectively. All plots and discussion below are based on the normalized ratios.

4. Results and discussion

4.1. Geochemistry of siliciclastic sediments

Our geochemical and isotopic data for bulk sediment samples and different grain size fractions from them are presented in Tables 1 and 2, respectively. The chondrite normalized REE patterns for the GRK sediments show pronounced light REE (LREE) enrichment and a negative Eu anomaly (not presented here) - characteristics of continental crust derived detritus. The upper continental crust normalized patterns show a flat LREE and depleted heavy REE (HREE) pattern (not presented here), with the latter possibly hinting at removal of heavy minerals such as zircon from sediments prior to their deposition in the basin. Negative anomalies of Zr and Hf and depleted patterns of HREE seen in the Post Archean Australian Shale (PAAS) normalized trace element data for these samples (Fig. 2A) are consistent with the above observation. Interestingly, these patterns are, to a large extent, comparable to that observed in the sediments in the five major rivers of Punjab (Alizai et al., 2011a) and sand dunes of the Thar, however, are different from that reported for the sediments from the Indus Delta (Clift et al., 2002, Fig. 2A). This is at variance with the earlier belief that the western GRK is predominantly filled with the Indus derived sediments (Maurya et al., 2003; Tyagi et al., 2012). To further understand the nature of probable sediment sources we have made use of various cross plots of elemental and isotopic ratios wherein the fields of these sources (end-members) could be easily distinguished (Fig. 2B–D). Sediments from the Indus is known to enter the western GRK through the Kori Creek with the help of long-shore currents, and having significant contributions from the juvenile (mantle derived) rocks of the Indus-Tsangpo Suture Zone (ITSZ). These have higher Nb/Ba, Cr/Th, ε_{Nd} and Sr content, and lower $^{87}Sr/^{86}Sr$ and Th/Y compared to the Higher-Himalaya-derived sediments in the five rivers of Punjab. Absence of adequate geochemical data does not allow us to create a field/envelope for the Thar Desert; however, we make use of our data from the dune field at the north-eastern margin of the GRK for comparisons. In these plots most of our samples fall in the space in-between the two major end-members (Fig. 2B–D) suggesting contributions from all of these sources, not just the Indus, to the sediment budget of the GRK.

Being rare-earth elements, the Sm-Nd system is not easily disturbed by the surficial processes like erosion, transportation and sedimentation (Goldstein and Jacobsen, 1988; Najman, 2006). Hence, this systematics is ideal for bulk sediment provenance study. The measured ε_{Nd} of samples (with a precision of ±0.2 at 2σ) from the western GRK, the southern Thar Desert and the Luni river mouth varies in ranges of −14.3 to −11.4, −11.8 to −11.0, and −12.5 to −11.5, respectively. In Fig. 3, we compare these data with that from the Holocene sediments in the Ghaggar-Hakra channels, Indus delta and Indus shelf (Alizai et al., 2011a; Clift et al., 2008; East et al., 2015; Limmer et al., 2012; Singh et al., 2016a). From Fig. 3 it can be inferred that since mid-Holocene there has been little influence of Sutlej or Yamuna in western GRK sedimentation excluding the possibilities of the sediments being transported by Greater Himalayan glacier-fed rivers. On the contrary, ε_{Nd} of the GRK sediments overlap with that observed in the north-eastern Thar Desert, deposited during 9.1 to 1.8 ka (Fig. 3A). However, as discussed in the previous section, the only possible mode by which this distal source

Table 1
Geochemical data for sediment samples from the Great Rann of Kachchh.

Sample	SBTL-1^{K}	NRMOSL-1^{K}	ABP-1a^{K}	KHTL-1^{D}	KSTL-1^{K}
Cs	1.92	3.84	3.99	8.33	3.97
Rb	64.2	94.4	91.8	123.1	90.4
Ba	313	363	354	402	348
Th	13.5	12.3	16.1	8.1	10.4
U	1.83	1.64	2.07	1.50	1.42
Nb	8	11	11	14	10
Ta	1.77	0.85	0.91	0.93	1.62
La	37	35	43	19	28
Ce	77	72	86	39	58
Pb	12.2	13.1	15.3	8.4	12.8
Pr	9.4	8.5	10.2	4.7	7.1
Sr	128	134	129	79	117
Nd	31	27	33	16	23
Zr	12	13	15	49	11
Hf	0.4	0.4	0.5	1.5	0.4
Sm	6.3	5.7	6.7	3.2	4.8
Eu	1.2	1.1	1.2	0.7	1.0
Gd	5.5	4.9	5.9	2.8	4.1
Tb	0.60	0.53	0.63	0.32	0.46
Dy	3.5	3.1	3.7	2.1	2.7
Y	13.6	12.1	14.6	9.1	10.7
Ho	0.58	0.50	0.61	0.38	0.46
Er	1.6	1.5	1.8	1.2	1.3
Tm	0.2	0.2	0.2	0.2	0.2
Yb	1.2	1.1	1.3	1.0	1.0
Lu	0.16	0.15	0.18	0.15	0.13
Sc	6.7	7.3	8.4	11.0	6.7
V	39	49	56	86	43
Cr	23	33	38	67	29
Co	3	4	5	7	4
$^{87}Sr/^{86}Sr$	0.72878	0.72853	0.72743	0.71553	0.72982
$^{143}Nd/^{144}Nd$	0.511907	0.511930	0.511906	0.511982	0.511935
$\varepsilon_{Nd}(0)$	−14.3	−13.8	−14.3	−12.7	−13.7

Sample	KHTL-3^{D}	BBMF^{K}	KH/DV/TL1^{D}	ABP-2^{K}	KSTL-2^{K}
Cs	1.48	9.28	3.88	7.57	7.75
Rb	46.2	160.1	73.6	131.9	137.3
Ba	281	497	17	427	426
Th	5.4	10.4	4.8	10.3	9.7
U	0.80	1.36	0.79	1.37	1.33
Nb	5	12	6	7	7
Ta	0.38	0.75	0.38	0.56	0.61
La	15	29	11	29	26
Ce	32	62	26	60	59
Pb	7.4	12.7	3.0	12.2	12.7
Pr	3.8	7.2	3.3	7.2	6.6
Sr	63	109	128	111	112
Nd	12	23	11	23	21
Zr	20	14	18	12	8
Hf	0.6	0.5	0.6	0.4	0.3
Sm	2.5	4.7	2.2	4.8	4.4
Eu	0.5	1.0	0.5	1.0	0.9
Gd	2.0	4.0	1.8	4.1	3.7
Tb	0.21	0.43	0.19	0.43	0.40
Dy	1.3	2.5	1.2	2.5	2.3
Y	5.4	9.2	4.6	9.5	8.7
Ho	0.22	0.40	0.20	0.42	0.38
Er	0.7	1.2	0.6	1.2	1.1
Tm	0.1	0.1	0.1	0.1	0.1
Yb	0.6	0.9	0.5	0.9	0.8
Lu	0.08	0.12	0.07	0.12	0.11
Sc	3.3	12.2	5.6	9.9	9.6
V	33	97	45	77	68
Cr	25	63	32	49	45
Co	2	8	4	7	8
$^{87}Sr/^{86}Sr$	0.72327	0.72723	0.71459	0.72896	0.72937
$^{143}Nd/^{144}Nd$	0.511915	0.511936	0.511968	0.511927	0.511942
$\varepsilon_{Nd}(0)$	−14.1	−13.7	−13.1	−13.9	−13.6

Sample	KRNOSL-3^{K}	ABTL-2^{K}	SBTL-4^{K}	KH/DV/TL2^{D}	BdB(b)-1^{K}
Cs	0.77	3.79	4.34	5.82	6.60
Rb	39.3	90.4	99.9	99.6	130.6

Table 1 (*continued*)

Sample	SBTL-1[K]	NRMOSL-1[K]	ABP-1a[K]	KHTL-1[D]	KSTL-1[K]
Ba	201	375	438	394	420
Th	1.3	11.4	11.8	7.0	7.5
U	0.30	1.89	1.84	1.11	1.23
Nb	3	12	14	8	11
Ta	0.13	1.00	1.05	0.43	0.80
La	3	33	34	20	20
Ce	6	68	70	41	41
Pb	8.4	15.6	11.5	10.0	13.8
Pr	0.7	8.3	8.5	4.9	5.1
Sr	41	121	118	106	114
Nd	2	26	27	15	16
Zr	8	16	20	20	13
Hf	0.3	0.6	0.7	0.7	0.5
Sm	0.5	5.7	5.7	3.1	3.5
Eu	0.2	1.2	1.1	0.7	0.8
Gd	0.5	4.9	4.9	2.6	3.0
Tb	0.06	0.56	0.54	0.27	0.34
Dy	0.4	3.4	3.3	1.6	2.1
Y	1.7	13.0	12.6	5.9	7.9
Ho	0.08	0.58	0.55	0.27	0.36
Er	0.2	1.7	1.6	0.8	1.1
Tm	0.0	0.2	0.2	0.1	0.1
Yb	0.2	1.3	1.2	0.7	0.8
Lu	0.03	0.18	0.16	0.09	0.11
Sc	1.2	8.5	8.9	8.1	8.8
V	14	53	60	64	65
Cr	4	37	40	45	44
Co	1	4	3	5	7
$^{87}Sr/^{86}Sr$	0.72141	0.72800	0.72869	0.72423	0.72961
$^{143}Nd/^{144}Nd$	0.512053	0.511947	0.511925	0.511986	0.511971
$\varepsilon_{Nd}(0)$	−11.4	−13.5	−13.9	−12.7	−13.0

Sample	NRMOSL-3[K]	GdB-2[K]	C-16/13[K]	C-16/17[K]	C-16/21[K]
Cs	2.81	7.09	4.97	11.98	5.27
Rb	79.3	136.7	111.2	192.3	111.4
Ba	365	445	429	538	419
Th	11.2	6.8	12.1	10.4	12.0
U	1.79	1.02	1.95	1.79	1.87
Nb	10	11	14	20	13
Ta	0.73	0.73	0.96	1.27	0.92
La	33	19	33	25	32
Ce	67	40	70	58	67
Pb	13.7	13.6	12.7	10.2	12.5
Pr	8.2	4.8	8.3	6.1	8.1
Sr	137	112	126	83	117
Nd	26	15	27	20	25
Zr	12	10	20	50	16
Hf	0.4	0.4	0.7	1.4	0.6
Sm	5.7	3.3	5.7	4.0	5.5
Eu	1.2	0.8	1.2	0.8	1.1
Gd	4.9	2.9	4.9	3.5	4.8
Tb	0.56	0.31	0.55	0.39	0.54
Dy	3.5	1.9	3.4	2.4	3.3
Y	13.3	7.0	13.0	10.2	12.2
Ho	0.58	0.32	0.56	0.45	0.56
Er	1.7	0.9	1.7	1.4	1.6
Tm	0.2	0.1	0.2	0.2	0.2
Yb	1.3	0.7	1.3	1.2	1.2
Lu	0.17	0.09	0.17	0.16	0.16
Sc	7.9	8.6	9.5	13.6	9.8
V	49	61	65	119	69
Cr	32	45	43	76	42
Co	3	6	4	7	4
$^{87}Sr/^{86}Sr$	0.72725	0.73066	0.72832	0.73064	0.72881
$^{143}Nd/^{144}Nd$	0.511953	0.511952	0.511930	0.511970	0.511978
$\varepsilon_{Nd}(0)$	−13.4	−13.4	−13.8	−13.0	−12.9

Sample	C-16/26[K]	NB-1[N]	MS-1[L]	BKS-4[L]	BKS-1[T]
Cs	4.97	0.47	1.46	1.25	1.53
Rb	110.7	23.9	64.6	57.8	55.9
Ba	451	128	340	315	281
Th	12.2	6.0	5.5	8.1	6.7

Table 1 (*continued*)

Sample	SBTL-1[K]	NRMOSL-1[K]	ABP-1a[K]	KHTL-1[D]	KSTL-1[K]
U	1.58	1.43	0.79	1.12	0.94
Nb	9	2	4	5	6
Ta	0.61	0.06	0.32	0.91	0.55
La	35	11	15	24	23
Ce	73	21	29	50	45
Pb	11.8	4.0	13.0	12.3	4.7
Pr	8.8	2.4	3.5	6.0	4.9
Sr	118	34	119	123	167
Nd	28	7	11	19	18
Zr	80	14	7	10	13
Hf	2.1	0.5	0.3	0.4	0.4
Sm	5.9	1.4	2.2	3.9	3.1
Eu	1.2	0.3	0.6	0.8	0.7
Gd	4.9	1.2	1.9	3.3	2.9
Tb	0.53	0.14	0.22	0.36	0.34
Dy	3.0	0.9	1.4	2.2	2.0
Y	11.1	3.6	5.6	8.7	9.8
Ho	0.50	0.15	0.23	0.37	0.36
Er	1.4	0.5	0.7	1.1	1.1
Tm	0.2	0.1	0.1	0.1	0.1
Yb	1.0	0.4	0.5	0.9	1.0
Lu	0.14	0.06	0.07	0.12	0.13
Sc	9.6	1.6			5.8
V	65	10			41
Cr	38	6	11	20	58
Co	4	1	2	2	3
$^{87}Sr/^{86}Sr$	0.72837	0.72303	0.72794	0.72610	0.72516
$^{143}Nd/^{144}Nd$	0.511933	0.511969	0.511997	0.512050	0.512047
$\varepsilon_{Nd}(0)$	−13.8	−13.1	−12.5	−11.5	−11.5

Sample	BKS-1-CLAY[T]	BKS-2[T]	BKS-3[T]	BKS-5[T]	BHVO-2
Cs	3.60	1.73	1.65	1.08	0.12
Rb	75.0	64.0	57.0	40.3	10.3
Ba	260	313	280	201	130
Th	16.1	6.3	5.0	6.4	1.1
U	3.37	0.72	0.62	0.63	0.42
Nb	13	5	4	3	17
Ta	0.46	0.47	0.30	0.28	0.95
La	32	21	18	21	15
Ce	78	40	36	41	39
Pb	2.7	5.2	5.9	4.1	1.2
Pr	7.3	4.3	4.0	4.4	5.2
Sr	72	168	143	96	388
Nd	23	15	11	11	24
Zr	181	16	7	13	163
Hf	5.8	0.5	0.3	0.5	3.9
Sm	5.0	2.7	2.6	2.5	5.9
Eu	0.9	0.7	0.8	0.6	2.0
Gd	5.1	2.5	2.4	2.4	6.1
Tb	0.67	0.30	0.28	0.27	0.84
Dy	4.6	1.9	1.6	1.5	5.2
Y	22.0	9.2	6.0	5.5	23.4
Ho	0.92	0.34	0.30	0.29	0.89
Er	3.0	1.1	0.9	0.9	2.5
Tm	0.4	0.1	0.1	0.1	0.3
Yb	3.0	1.0	0.8	0.9	1.9
Lu	0.44	0.14	0.11	0.13	0.26
Sc	9.5	6.1	3.9	3.1	31.6
V	78	32	27	22	337
Cr	71	27	14	14	291
Co	3	3	2	2	48
$^{87}Sr/^{86}Sr$	0.71307	0.72648	0.72758	0.72429	0.70346
$^{143}Nd/^{144}Nd$	0.512077	0.512031	0.512049	0.512074	0.512967
$\varepsilon_{Nd}(0)$	−11.0	−11.8	−11.5	−11.0	6.4

Superscripts: [K] = Western Great Rann of Kachchh; [D] = Khadir Island, Eastern Great Rann of Kachchh; [N] = Nada Bet, Eastern Great Rann of Kachchh; [L] = Luni River mouth; [T] = Thar dune sand. Trace element concentrations are in ppm. Data for BHVO-2 is averages of 10 analyses. . $\varepsilon_{Nd} = [(^{143}Nd/^{144}Nd)_{sample}/(^{143}Nd/^{144}Nd)_{Chondrite}-1] \times 10^4$. $(^{143}Nd/^{144}Nd)_{Chondrite}$ is taken as 0.512638. External reproducibility (2σ) of $^{87}Sr/^{86}Sr$ and ε_{Nd} determined by multiple analyses of NBS987 and JNdi-1 are ±0.000001 and ± 0.1, respectively.

Table 2
Isotopic data for different grain sizes separated from sediments of the Nara river mouth and Western Great Rann of Kachchh.

<4 μm	NRM-OSL-1C	NRM-OSL-2C	NRM-OSL-3C	KRM-OSL-1C	KRM-OSL-2C	KRM-OSL-3C
$^{87}Sr/^{86}Sr$	0.72427	0.72438	0.72409	0.72427	0.72079	0.72257
$^{143}Nd/^{144}Nd$	0.51198	0.511968	0.512001	0.511984	0.511982	0.512007
$\varepsilon_{Nd}(0)$	−12.8	−13.1	−12.4	−12.8	−12.8	−12.3
4–15.6 μm	NRM-OSL-1S	NRM-OSL-2S	NRM-OSL-3S	KRM-OSL-1S	KRM-OSL-2S	KRM-OSL-3S
$^{87}Sr/^{86}Sr$	0.72568	0.72559	0.72562	0.72570	0.72124	0.7222
$^{143}Nd/^{144}Nd$	0.511981	0.511949	0.511946	0.511976	0.512012	0.511963
$\varepsilon_{Nd}(0)$	−12.8	−13.4	−13.5	−12.9	−12.2	−13.2
45-75 μm	NRM-OSL-1A	NRM-OSL-2A	NRM-OSL-3A	KRM-OSL-1A	KRM-OSL-2A	KRM-OSL-3A
$^{87}Sr/^{86}Sr$	0.72741	0.72849	0.72674	0.72999	0.72495	0.72087
$^{143}Nd/^{144}Nd$	0.511962	0.511966	0.511956	0.511948	0.511926	0.511957
$\varepsilon_{Nd}(0)$	−13.2	−13.1	−13.3	−13.5	−13.9	−13.3
75-90 μm	NRM-OSL-1B	NRM-OSL-2B	NRM-OSL-3B	KRM-OSL-1B	KRM-OSL-2B	KRM-OSL-3B
$^{87}Sr/^{86}Sr$	0.73140	0.73576	0.73463	0.73138	0.72672	0.72060
$^{143}Nd/^{144}Nd$	0.511974	0.511943	0.511963	0.511973	0.512003	0.512064
$\varepsilon_{Nd}(0)$	−12.3	−13.6	−13.2	−13.0	−12.4	−11.2

could have contributed is through reworking by a fluvial system. The present-day ephemeral Ghaggar-Hakra river system, which is believed to have been connected to the Nara during the mid-Holocene (Valdiya, 2013), is the most suitable candidate for the above pathway. The overlapping ε_{Nd} values of pre-modern sediments in the Ghaggar-Hakra system with that of the western GRK sediments (Fig. 3B) may be considered as an evidence for the above. It is also observed that ε_{Nd} data from GRK sediments overlap with that of the sediments in the Indus delta (Fig. 3B), however, they do not follow the regional trend (with age) shown by the latter thus making it an unlikely source. The trend seen in the GRK data (Fig. 3B) appears to suggest mixing between sediments from the Ghaggar-Hakra fluvial system (containing reworked aeolian sand from northern desert margin) and Indus borne detritus, in addition to possible contributions from the Luni and the southern Thar (Fig. 3A and B).

4.2. Grain size and isotopic compositions

For a better characterization of the provenances, we utilize Sr isotopic ratios of these sediments along with their Nd isotopic ratios, keeping in mind the limitations of the former (Najman, 2006). It is generally believed that unlike the ^{147}Sm-^{143}Nd isotopic system,

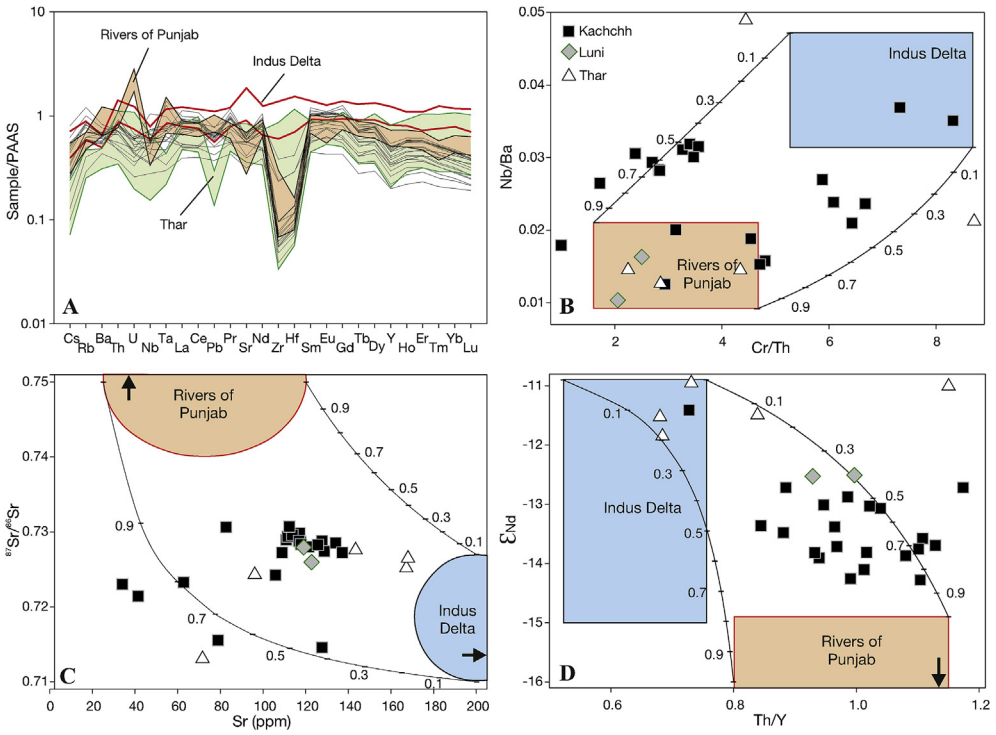

Fig. 2. **(A)** PAAS normalized multi-element trace element patterns of sediment samples from the Great Rann of Kachchh (this work) compared with that of sediments from rivers of Punjab (Orange field; Alizai et al., 2011a), Indus delta sediments (red envelop; Clift et al., 2002), and Thar desert sand (green field; this work). **(B)** Nb/Ta vs. Cr/Th **(C)** $^{87}Sr/^{86}Sr$ vs. Sr, and **(D)** ε_{Nd} vs. Th/Y plots for the Kachchh, Luni and Thar samples compared with binary mixing model curves drawn considering sediments in Indus delta and rivers of Punjab as two end-members. Tick marks on mixing curves are fraction of Punjabi rivers' contributions to the mixture. (For interpretation of the references to colour in this figure legend, the reader is referred to the web version of this article.)

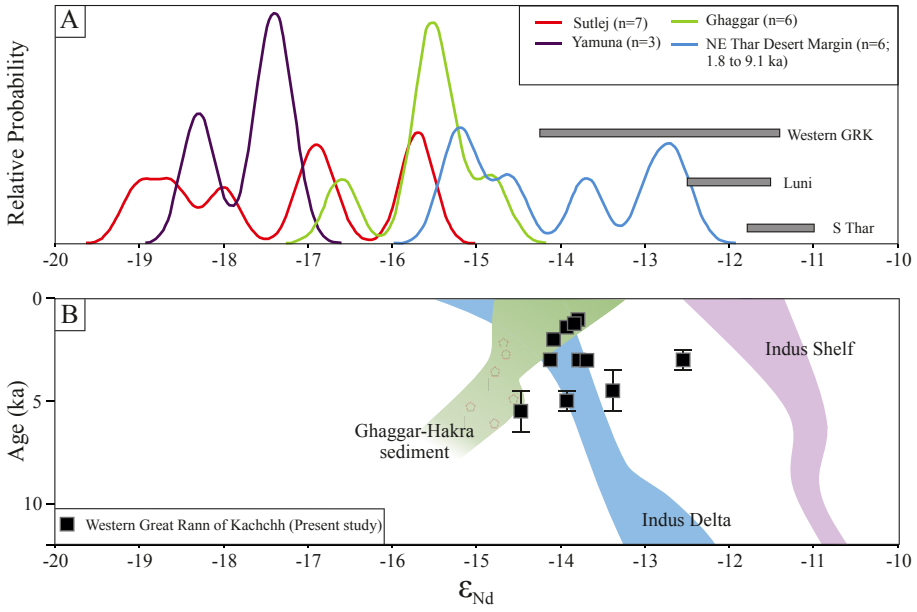

Fig. 3. **(A)** Kernel density estimation (KDE) plot of ε_{Nd} re-drawn from (Singh et al., 2016b) displaying the Nd-isotopic variability in Sutlej, Yamuna, Ghaggar and Thar desert (present work and Singh et al., 2016a; Tripathi et al., 2013). (**B**) The Western Great Rann of Kachchh sediments deposited since 5.5 ka are compared with the sediments of Ghaggar-Hakra River (East et al., 2015; Singh et al., 2016a), Indus delta (Clift et al., 2010) and shelf (Limmer et al., 2012) deposited during the Holocene.

the ^{87}Rb-^{87}Sr system is susceptible to chemical weathering which leads to dissimilar Sr isotopic ratio between the source rocks and the product sediments (Meyer et al., 2011). Higher chemical weathering leads to more radiogenic detritus which is largely controlled by higher $^{87}Sr/^{86}Sr$ bearing fine-grained (clay) fraction, primarily derived from high-Rb bearing micas in the source rocks (Garçon et al., 2014; Meyer et al., 2011). Below we discuss the effect of grain size on Sr isotopic composition of the GRK sediments and evaluate its bearing on determination of provenances.

Six western GRK samples were selected for studying the effect of grain size on the $^{87}Sr/^{86}Sr$ variation. Different grain size fractions were separated namely: clay (<4μ), silt (4-15.6μ), fine sand (45-75μ) and coarse sand (75–90 μ). By weight coarse sand was found to be the dominant fraction (>70%) in these samples. All the fractions were decarbonated using dilute HCl before being analyzed for Sr and Nd isotopic compositions. These data are presented in Fig. 4. As can be seen from the data, although there is a large variation of $^{87}Sr/^{86}Sr$, it shows an overall increasing trend with increasing grain size (Fig. 4A). This is entirely opposite of what is generally observed in most fluvial systems where in the finest fractions (suspended load/clay) contain more radiogenic Sr than the coarser fractions (Garçon et al., 2014).

One plausible explanation for the observation could be that different sources with distinct isotopic signature contributed to different grain size fractions. However, such a phenomenon should have been reflected more prominently in Nd isotopic compositions, because ε_{Nd} is a more robust provenance indicator compared to $^{87}Sr/^{86}Sr$. However, we do not observe any such dependency in Fig. 4B. In fact a closer look reveals that different grain size fractions of four samples possess overlapping ε_{Nd} (within ±0.5, where experimental reproducibility is ±0.2 at 2σ). We therefore believe that the observed variation of $^{87}Sr/^{86}Sr$ ratios with grain-size (Fig. 4A) is a product of lesser chemical weathering compared to physical weathering in the source, similar to that observed in many parts of the Himalaya (Singh et al., 2008). Since during chemical weathering, high-Rb bearing minerals (containing high radiogenic

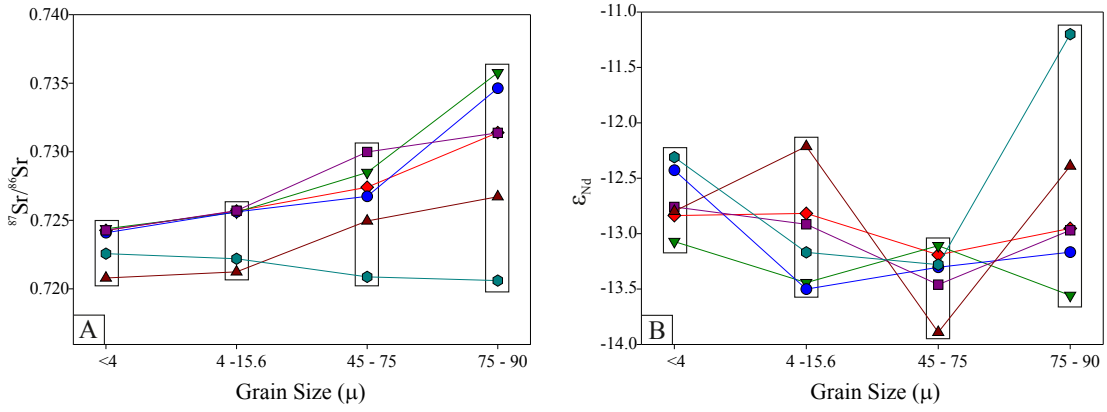

Fig. 4. **(A)** Variation of $^{87}Sr/^{86}Sr$ ratio in different grain size fractions (clay, silt, fine and coarse sand) of sediments from Nara river mouth and bet zones are shown. Also plotted are Sr-isotopic ranges of various probable sources. The different symbols represent six separate samples. (**B**) Variation of ε_{Nd} values in different grain size fractions of the same sediments mentioned above. The different symbols represent six separate samples .

Sr) in the source (e.g., muscovite; K-feldspar) break down to clays, finer fractions of sediments produced exhibit higher $^{87}Sr/^{86}Sr$ compared to that in coarser fractions (Garçon et al., 2014). Interestingly, however, we encountered significant amount of muscovite in coarser fractions of our samples, which prompted us for the above inference. In such a scenario, the $^{87}Sr/^{86}Sr$ of the clay fractions in our samples might not represent the composition of the sources, and therefore, the use of bulk sediment composition for provenance study would be the best bet.

4.3. Provenance of sediments and implications

The sediment load of the Indus in its upper reaches, north of its confluence with the rivers of Punjab (Fig. 1A), is dominated by material derived from sources in the Trans-Himalayas and its Sr-Nd isotopic compositions (IS: Indus at Skardu; Fig. 5A) are largely controlled by sediments derived from the ITSZ, Karakoram Batholith, and Ladakh Batholith (Clift et al., 2002). Predictably, sediments in the Indus delta and shelf (Fig. 5A) possess less radiogenic Nd (more radiogenic Sr) compared to that in sediments in the upper Indus, due to mixing with sediments from much older crustal rocks in the Higher Himalayan Crystalline (HHC) and Lesser Himalayas (LH), contributed through the rivers of Punjab (Clift et al., 2010). The sediments of the GRK having $^{87}Sr/^{86}Sr$ in the range of 0.7146–0.7307 and ε_{Nd} in the range of −14.3 to −11.4 although overlap with the field for the Indus Delta (Fig. 5A), mostly possess more radiogenic Sr - a characteristic feature of the Lesser and Higher Himalayan sediments. The Luni and southern Thar (bordering the GRK basin) sediments have comparable ε_{Nd} and marginally higher $^{87}Sr/^{86}Sr$ values than those of the Indus sediments; however, possess more radiogenic Nd than the GRK sediments (Fig. 5A). These data clearly suggest that the GRK sediments neither represent any of the pure end-members such as the IS, the Luni, the Thar, the HHC, and the LH nor they are exclusively derived from the river Indus in its lower reaches or the Indus shelf. Since most of our samples are from the western GRK and that there was very limited (if any) sediment transport from the eastern GRK into the western GRK in the past (Glennie and Evans, 1976), the river Luni could not have been a major sediment source or pathway for the latter. Persistent ephemerality and aeolian activity from 8 ka onwards in the Luni basin (Kar et al., 2001), and dissimilar isotopic compositions of the Luni sediments with those of the western GRK sediments (Fig. 5A) also support this inference. A three component mixing model involving compositions of the IS, HHC and LH (Fig. 5A) reveals that although the GRK sediments deposited between 5.5 and 1.0 ka contain a large Trans-Himalayan component (up to 70%), there exists a significant component of the combined Higher and Lesser Himalayan rocks. The Trans-Himalayan component can easily be explained by the deposition of the Indus sediments (in lower reaches), directly or reworked, via the Thar desert,

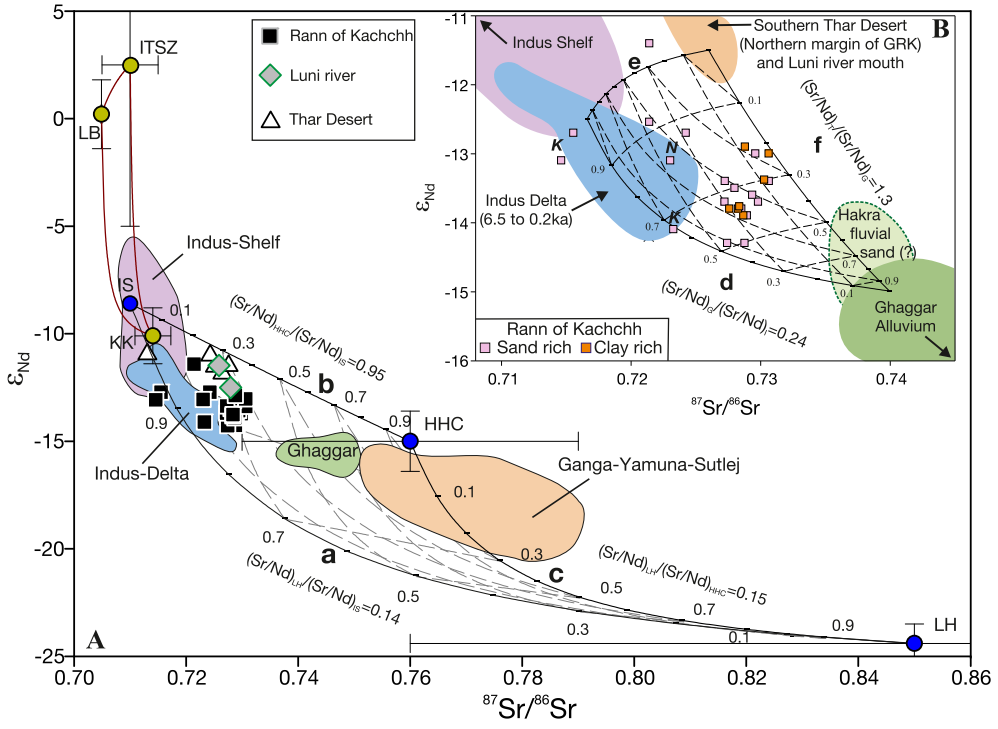

Fig. 5. **(A)** Plot of ε_{Nd} vs. $^{87}Sr/^{86}Sr$ for our samples compared with a ternary mixing grid. The three end-members are: (1) Indus sediments at Skardu (IS), (2) The Higher Himalayan Crystallines (HHC), and (3) The Lesser Himalayas (LH). IS component itself plots within another three component mixing grid involving the Indo-Tsangpo Suture Zone (ITSZ), Karakoram (KK) and Ladakh Batholith (LB) as end-members. Error bars cover the entire range of values for various components. Also shown are fields for sediments in the Indus Delta, present-day Ghaggar, and Ganga-Yamuna-Sutlej river systems. Curves *a*, *b*, and *c* represent binary mixing between typical compositions of two each of the end-members, whose compositions are: IS: Nd = 25 ppm; Sr = 210 ppm; ε_{Nd} = −8.6; $^{87}Sr/^{86}Sr$ = 0.71, HHC: Nd = 30 ppm; Sr = 240 ppm; ε_{Nd} = −15.0; $^{87}Sr/^{86}Sr$ = 0.76, and LH: Nd = 100 ppm; Sr = 120 ppm; ε_{Nd} = −24.4; $^{87}Sr/^{86}Sr$ = 0.85. Error bars of end-member compositions are at 3σ. **(B)** Plot of ε_{Nd} vs. $^{87}Sr/^{86}Sr$ for only the Great Rann of Kachchh samples, compared with a ternary mixing grid involving Indus river sediments, Thar Desert, and Ghaggar. Only ε_{Nd} values are available for fluvial sands of Hakra stream (East et al., 2015). However considering the fact that, Hakra is the downstream extension of Ghaggar, we have considered the range of $^{87}Sr/^{86}Sr$ values for Hakra sediments to be similar to Ghaggar. Hence, the zone defined for Hakra sediments in the figure are question marked. *K* and *N* represent samples from the Khadir Island and Nada Bet, respectively, in the eastern Great Rann of Kachchh (Fig. 1B). Curves *d*, *e*, and *f* represent binary mixing between typical compositions of two each of the end-members and these are: Indus Shelf/Delta: Nd = 30 ppm; Sr = 350 ppm; ε_{Nd} = −12.5; $^{87}Sr/^{86}Sr$ = 0.7166, southern Thar Desert: Nd = 40 ppm; Sr = 150 ppm; ε_{Nd} = −11.5; $^{87}Sr/^{86}Sr$ = 0.726, and Ghaggar: Nd = 100 ppm; Sr = 280 ppm; ε_{Nd} = −15; $^{87}Sr/^{86}Sr$ = 0.740. Data sources: present work and following references (Allègre and Othman, 1980; Clift et al., 2002; Najman, 2006; Scharer et al., 1990; Singh et al., 2016a; Tripathi et al., 2013).

and/or through storm tides entering into the western GRK through the Kori Creek that brings in silt and clay from the Indus delta with the help of long-shore currents. It should be noted that although the river Indus transports HHC-LH sediments contributed to it through its eastern tributaries, $^{87}Sr/^{86}Sr$ of the bulk sediments is lowered by a significant non-radiogenic Trans Himalayan component in the main channel - which is reflected in the isotopic composition of the Indus Delta (Clift et al., 2010). We, however, observe higher $^{87}Sr/^{86}Sr$ values (>1.3%) in the sediments of western GRK (Fig. 5A), which suggest that there could have been other sources than the river Indus. Since in the present geomorphic set up direct deposition of the HHC-LH derived sediments into the basin is not possible, contribution from a third source is envisaged.

As mentioned earlier, the Ghaggar-Hakra channel originating from Siwaliks, made of rocks derived from the HHC-LH (Tripathi et al., 2013), could have been a pathway for the Himalayan contribution to the GRK basin, if it was connected to the river Nara in the past. Interestingly, the modern sediments of the Ghaggar, which should have had $^{87}Sr/^{86}Sr$ and ε_{Nd} in the range of that of the HHC/LH (Fig. 5A), possess lower $^{87}Sr/^{86}Sr$ and higher ε_{Nd} (Tripathi et al., 2013). This has been attributed to contributions from the Paleogene, sub-Himalayan foreland deposits of the Subathu Group (Tripathi et al., 2013). Assuming that the nature of various sediment sources has not changed since the mid-Holocene, we evaluated their contributions in the samples studied in this work (Fig. 5B). It is clear from the figure that the pre-modern sediments of the central and eastern GRK, from the Khadir Island (K) and Nada bet (N), although have Sr-Nd isotopic compositions similar to that of the Indus Delta (or Indus in lower reaches) are most likely derived from the river Luni, the Thar Desert and Mesozoic rocks exposed on the islands. In any case, the local sources do not produce significant amount of sediment and their compositions are very different from that of the western GRK sediments. Comparison of our isotopic data with model grids of a three component mixing, where sediments from the Ghaggar, southern Thar and the Indus delta/shelf are the end-members (Fig. 5B), suggests that 20–30% of the sediments deposited in the western GRK during 5.5 to 1.0 ka could have come through a now-defunct pathway connecting the Ghaggar, Hakra and Nara channels.

The samples that possess high radiogenic Sr (>0.728) are both sand and clay rich sediments, are not confined to any age bracket in the studied period, and a large number of them come from fluvially deposited horizons. If the finding of (Giosan et al., 2012) that there was fluvial activity in the Nara valley ~2.9 kyr ago were to be believed then our younger samples most likely represent monsoonal flooding events. Although the geochemical data for the GRK sediments clearly point towards a significant presence of sub-Himalayan (Siwalik) sediments that are not part of the Indus detritus, the overwhelming presence of the latter and southern Thar sand (up to 70%) makes it apparent that no perennial fluvial system was active in the Ghaggar-Hakra-Nara system during the Mature Harappan period. Our data nonetheless suggest that the Ghaggar-Hakra-Nara channels had remained active, possibly as a monsoon-fed system, until ~1.0 kyr ago. It was a sub-parallel system to the Indus, which transported sediments from the southern flanks of the Himalayas along with reworked aeolian sands into the GRK. Such an inference is not inconsistent with the inferences of (Giosan et al., 2012) and that these channels were active through intermittent flooding during the mid-Holocene, even after a substantial weakening of the monsoon post 4.2 ka (Enzel et al., 1999; Staubwasser et al., 2003; Wünnemann et al., 2010), before being covered by aeolian deposits. Although it is difficult to directly infer about the prevailing climatic conditions from our geochemical study, the sedimentological observations that substantial fluvial sand was deposited during 5.0–3.0 ka and 1.4–1.0 ka (Fig. 1B) suggest enhanced rainfall, possibly caused by stronger Indian monsoon. Such an inference is supported by studies that propose short phases of monsoonal strengthening in peninsular India during 5100-4700 ka, 4105-2640 ka, and medieval warm period (Band et al., 2016; Banerji et al., 2016; Kotlia et al., 2015; Ngangom et al., 2016, 2012; Sarkar et al., 2000; Yadava and Ramesh, 2005) in the background of a regional decreasing trend since ~7 ka (Dixit et al., 2014; Sarkar et al., 2016).

5. Conclusions

Geochemistry and Sr-Nd isotopic data for mid-Holocene terrigenous detritus from the GRK reveal that the river Luni, Mesozoic rocks on the islands, and parabolic dune field of the south-eastern Thar are the primary contributors of sediments to the central and eastern GRK. On the other hand, sediments deposited in the western GRK during 5.5 to 1.0 kyr ago, although are primarily derived from the river Indus and transported into the basin by storm tides from the Indus delta and/or shelf; contain a significant amount of an independent sub-Himalayan component (20–30%). This sub-Himalayan component most likely was transported through the now defunct Ghaggar-Hakra-Nara river system. Since this river system, which ran parallel to the Indus, had dwindling water supply during the Harappan period, sediments carried by it must have reached the GRK only during heavy flooding events. Overwhelming presence of Indus detritus in the GRK makes it difficult to test the hypothesis of existence of a mega, glacial-fed river through the Ghaggar-Hakra-Nara channels during this period. These channels, however, were active until as late as 1.0 ka and therefore, their drying up may not have any causal relationship with the decline of the Harappan civilization.

Acknowledgments

We thank Navin Juyal for his encouragement, valuable suggestions and sharing of samples. Navin Juyal, P.S. Thakkar and A.D. Shukla participated in one of the field trips to the Great Rann of Kachchh. We also thank the two anonymous reviewers for their comments and suggestions. This work was supported by funding from the Department of Space, Government of India.

References

Alizai, A., Carter, A., Clift, P.D., VanLaningham, S., Williams, J.C., Kumar, R., 2011a. Sediment provenance, reworking and transport processes in the Indus River by U–Pb dating of detrital zircon grains. Glob. Planet. Change 76, 33–55.

Alizai, A., Clift, P.D., Giosan, L., VanLaningham, S., Hinton, R., Tabrez, A.R., Danish, M., 2011b. Pb isotopic variability in the modern-Pleistocene Indus River system measured by ion microprobe in detrital K-feldspar grains. Geochim. Cosmochim. Acta 75, 4771–4795. http://dx.doi.org/10.1016/j.gca.2011.05.039.

Alizai, A., Clift, P.D., Still, J., 2016. Indus basin sediment provenance constrained using garnet geochemistry. J. Asian Earth Sci. 126, 29–57.

Allègre, C.J., Othman, D. Ben, 1980. Nd–Sr isotopic relationship in granitoid rocks and continental crust development: a chemical approach to orogenesis. Nature 286, 335–342.

Awasthi, N., Ray, J.S., Singh, A.K., Band, S.T., Rai, V.K., 2014. Provenance o the Late Quaternary sediments in the Andaman Sea: implications for monsoon variabilty and ocean circulation. Geochem. Geophys. Geosyst. 15, 3890–3906. http://dx.doi.org/10.1002/2014GC005462.

Band, S., Yadava, M.G., Ramesh, R., Gupta, S., Polyak, V.J., Asmerom, Y., 2016. Holocene Monsoon variability using stalagmite record from Dandak cave, India. In: Goldschmidt Conference Abstracts, vol. 2016, p. 152.

Banerji, U.S., Bhushan, R., Jull, A.J.T., 2016. Mid–late Holocene monsoonal records from the partially active mudflat of Diu Island, southern Saurashtra, Gujarat, western India. Quat. Int. http://dx.doi.org/10.1016/j.quaint.2016.09.060.

Biswas, S.K., 1987. Regional tectonics framework, structue and evolution of the western marginal basins of India. Tectonophysics 135, 307–327.

Clift, P.D., Carter, A., Giosan, L., Durcan, J., Duller, G. a. T., Macklin, M.G., Alizai, A., Tabrez, a. R., Danish, M., VanLaningham, S., Fuller, D.Q., 2012. U-Pb zircon dating evidence for a pleistocene sarasvati river and capture of the Yamuna river. Geology 40, 211–214. http://dx.doi.org/10.1130/G32840.1.

Clift, P.D., Giosan, L., Blusztajn, J., Campbell, I.H., Allen, C., Pringle, M., Tabrez, A.R., Danish, M., Rabbani, M.M., Alizai, A., Carter, A., Lückge, A., 2008. Holocene erosion of the Lesser Himalaya triggered by intensified summer monsoon. Geology 36, 79–82. http://dx.doi.org/10.1130/G24315A.1.

Clift, P.D., Giosan, L., Carter, A., Garzanti, E., Galy, V., Tabrez, A.R., Pringle, M., Campbell, I.H., France-Lanord, C., Blusztajn, J., Allen, C., Alizai, A., Luckge, A., Danish, M., Rabbani, M.M., 2010. Monsoon control over erosion patterns in the Western Himalaya: possible feed-back into the tectonic evolution. In: Clift, P.D., Tada, R., Zheng, H. (Eds.), Monsoon Evolution and Tectonics - Climate Linkage in Asia. The Geological Society of London, pp. 185–218. http://dx.doi.org/10.1144/SP342.12.

Clift, P.D., Lee, J.I., Hildebrand, P., Shimizu, N., Layne, G.D., Blusztajn, J., Blum, J.D., Garzanti, E., Ali, A., 2002. Nd and Pb isotope variability in the Indus River System: implications for sediment provenance and crustal heterogeneity in the Western Himalaya. Earth Planet. Sci. Lett. 200, 91–106.

Dixit, Y., Hodell, D.A., Sinha, R., Petrie, C.A., 2014. Abrupt weakening of the Indian summer monsoon at 8.2 kyrB.P. Earth Planet. Sci. Lett. 391, 16–23. http://dx.doi.org/10.1016/j.epsl.2014.01.026.

East, A.E., Clift, P.D., Carter, A., Alizai, A., VanLaningham, S., 2015. Fluvial – eolian interactions in Sediment routing and sedimentary signal buffering: an example from the Indus basin and Thar Desert. J. Sediment. Res. 85, 715–728. http://dx.doi.org/10.2110/jsr.2015.42.

Enzel, Y., Ely, L.L., Mishra, S., Ramesh, R., Amit, R., Lazar, B., Rajaguru, S.N., Baker, V.R., Sandler, A., 1999. High-Resolution Holocene environmental changes in the thar desert, northwestern India. Sci. (80-.) 284, 125–128.

Garçon, M., Chauvel, C., France-lanord, C., Limonta, M., Garzanti, E., 2014. Which minerals control the Nd – Hf – Sr – Pb isotopic compositions of river sediments. Chem. Geol. 364, 42–55. http://dx.doi.org/10.1016/j.chemgeo.2013.11.018.

Garzanti, E., Vezzoli, G., Andò, S., Paparella, P., Clift, P.D., 2005. Petrology of Indus river sands: a key to interpret erosion history of the western himalayan syntaxis. Earth Planet. Sci. Lett. 229, 287–302. http://dx.doi.org/10.1016/j.epsl.2004.11.008.

Gaur, A.S., Vora, K.H., Murali, R.M., Jayakumar, S., 2013. Was the Rann of Kachchh navigable during the harappan times (mid-holocene)? An archaeological perspective. Curr. Sci. 105, 1485–1491.

Ghose, B., Kar, A., Husain, Z., 1979. The lost courses of the Saraswati river In the great indian desert: new evidence from landsat imagery. Geogr. J. 145, 446–451.

Giosan, L., Clift, P.D., Macklin, M.G., Fuller, D.Q., Constantinescu, S., Durcan, J. a, Stevens, T., Duller, G. a T., Tabrez, A.R., Gangal, K., Adhikari, R., Alizai, A., Filip, F., VanLaningham, S., Syvitski, J.P.M., 2012. Fluvial landscapes of the Harappan civilization. Proc. Natl. Acad. Sci. U. S. A 109, E1688–E1694. http://dx.doi.org/10.1073/pnas.1112743109.

Glennie, K.W., Evans, G., 1976. A reconnaissance of the recent sediments of the ranns of Kutch, India. Sedimentology 23, 625–647.

Goldstein, S.J., Jacobsen, S.B., 1988. Nd and Sr isotopic systematics of river water suspended material: implications for crustal evolution. Earth Planet. Sci. Lett. 87, 249–265.

Gupta, A.K., Sharma, J.R., Sreenivasan, G., 2011. Using satellite imagery to reveal the course of an extinct river below the Thar Desert in the Indo-Pak region. Int. J. Remote Sens. 32, 5197–5216.

Kar, A., Singhvi, A.K., Rajaguru, S.N., Juyal, N., Thomas, J.V., Banerjee, D., Dhir, R.P., 2001. Reconstruction of the late quaternary environment of the lower Luni plains, thar desert, India. J. Quat. Sci. 16, 61–68.

Kenoyer, J.M., 2008. Indus civilization. In: Encyclopedia of Archaeology. Elsevier, New York, pp. 715–733.

Khonde, N.N., Maurya, D.M., Chamyal, L.S., 2016. Late Pleistocene-Holocene clay mineral record from the Great Rann of Kachchh basin, Western India: implications for palaeoenvironments and sediment sources. Quat. Int. 1–13. http://dx.doi.org/10.1016/j.quaint.2016.07.024.

Kochar, R., 2000. Vedic People: Their History and Geography. Orient Longman, Hyderabad.

Kotlia, B.S., Singh, A.K., Joshi, L.M., Dhaila, B.S., 2015. Precipitation variability in the indian central Himalaya during last ca. 4,000 years inferred from a speleothem record: impact of indian summer monsoon (ISM) and Westerlies. Quat. Int. 371, 244–253. http://dx.doi.org/10.1016/j.quaint.2014.10.066.

Limmer, D.R., Böning, P., Giosan, L., Ponton, C., Köhler, C.M., Cooper, M.J., Tabrez, A.R., Clift, P.D., 2012. Geochemical record of Holocene to recent sedimentation on the western Indus continental shelf, Arabian sea. Geochem. Geophys. Geosyst. 13 http://dx.doi.org/10.1029/2011GC003845.

Malik, J.N., Merh, S.S., Sridhar, V., 1999. Palaeo-delta complex of Vedic Saraswati and other ancient rivers of north-western India. Mem. Geol. Soc. India 42, 163–174.

Mathew, G., Singhvi, A.K., Karanth, V., 2006. Luminescence chronometry and geomorphic evidence of active fold growth along the Kachchh Mainland Fault (KMF), Kachchh, India: seismotectonic implications. Tectonophysics 422, 71–87.

Maurya, D.M., Khonde, N., Das, A., Chowksey, V., Chamyal, L.S., 2013. Subsurface sediment characteristics of the Great Rann of Kachchh, western India based on preliminary evaluation of textural analysis of two continuous sediment cores. Curr. Sci. 104, 859–862.

Maurya, D.M., Thakkar, M.G., Chamyal, L.S., 2003. Quaternary geology of the arid zone of Kachchh: terra Incognita. Proc. Indian Natl. Sci. Acad. 69A, 123–135.

Maurya, D.M., Thakkar, M.G., Patidar, A.K., Bhandari, S., Goyal, B., Chamyal, L.S., 2008. Late Quaternary geomorphic evolution of the coastal zone of Kachchh, Western India. J. Coast. Res. 24, 746–758.

Merh, S.S., 2005. The great Rann of Kachchh: perceptions of a field geologist. J. Geol. Soc. India 65, 9–25.

Meyer, I., Davies, G.R., Stuut, J.-B.W., 2011. Grain size control on Sr-Nd isotope provenance studies and impact on paleoclimate reconstructions: an example from deep-sea sediments offshore NW Africa. Geochem. Geophys. Geosyst. 12 http://dx.doi.org/10.1029/2010GC003355.

Misra, V.N., 1984. Climate: a factor in the rise and fall of Indus Civilization. In: Frontiers of the Indus Civilzation. Books and Books, New Delhi, pp. 469–489.

Mughal, M.R., 1997. Ancient Cholistan: Archaeology and Architecture. Ferozsons, Lahore, Pakistan.

Murray, A.S., Wintle, A.G., 2000. Luminescence dating of quartz using an improved single- aliquot regenerative-dose protocol. Radiat. Meas. 32, 57–73.

Najman, Y., 2006. The detrital record of orogenesis: a review of approaches and techniques used in the Himalayan sedimentary basins. Earth-Sci. Rev. 74, 1–72. http://dx.doi.org/10.1016/j.earscirev.2005.04.004.

Ngangom, M., Bhandari, S., Thakkar, M.G., Shukla, A.D., Juyal, N., 2016. Mid-Holocene extreme hydrological events in the eastern Great Rann of Kachchh, western India. Quat. Int. http://dx.doi.org/10.1016/j.quaint.2016.10.017.

Ngangom, M., Thakkar, M.G., Bhushan, R., Juyal, N., 2012. Continental – marine interaction in the vicinity of the Nara river during the last 1400 years, great Rann of. Curr. Sci. 103, 1339–1342.

Oldham, C.F., 1893. The Saraswati and the lost river of the Indian desert. J. R. Asiat. Soc. 34, 49–76.

Oldham, R.D., 1926. The Cutch (Kachh) earthquake of 16th June 1819 with a riviusion of the great earthquake of 12th June 1897. Mem. Geol. Surv. India 46, 71–147.

Pal, Y., Sahai, B., Sood, R.K., Agarwal, D.P., 1980. Remote sensing of the "lost" Saraswati river. Proc. Indian Natl. Sci. Acad. (Earth Planetry Sci. 89, 317–331.

Possehl, G.L., 2002. The Indus Civilization: a Contemporary Perspective. AltaMira Press, Lanham, Maryland.

Raczek, I., Jochum, K.P., Hofmann, A.W., 2001. Neodymium and strontium isotope data for USGS reference GSP-1, GSP-2 and eight MPI-DING reference glasses. Geostand. Newsl. 27, 173–179.

Radhakrishan, B.P., Merh, S.S., 1999. Vedic sarasvati: evolutionary history of a lost river of northwestern India. Mem. Geol. Soc. India 42, 5–13.

Rajendran, C.P., Ranjendran, K., 2001. Characteristics of deformation and past seismicity Associated with the 1819 Kutch earthquake, northwestern India. Bull. Seismol. Soc. Am. 91, 407–426.

Sarkar, A., Mukherjee, A.D., Bera, M.K., Das, B., Juyal, N., Morthekai, P., Deshpande, R.D., Shinde, V.S., Rao, L.S., 2016. Oxygen isotope in archaeological bioapatites from India: implications to climate change and decline of Bronze Age Harappan civilization. Sci. Rep. 6, 26555. http://dx.doi.org/10.1038/srep26555.

Sarkar, A., Ramesh, R., Somayajulu, B.L.K., Agnihotri, R., Jull, A.J.T., Burr, O.S., 2000. High resolution Holocene monsoon record from the eastern Arabian Sea. Earth Planet. Sci. Lett. 177, 209–218. http://dx.doi.org/10.1016/S0012-821X(00)00053-4.

Scharer, U., Copeland, P., Harrison, T.M., Searle, M.P., 1990. Age, cooling history and origin of post-collisional leucogranite in the Karakoram batholith: a multi-system isotope study. J. Geol. 98, 233–251.

Singh, A., Paul, D., Sinha, R., Thomsen, K.J., Gupta, S., 2016a. Geochemistry of buried river sediments from Ghaggar Plains, NW India: multi-proxy records of variations in provenance, paleoclimate, and paleovegetation patterns in the Late Quaternary. Paleogeogr. Paleoclimatol., Paleoecol. 449, 85–100. http://dx.doi.org/10.1016/j.palaeo.2016.02.012.

Singh, A., Paul, D., Sinha, R., Thomsen, K.J., Gupta, S., 2016b. Reply to the comment on "Geochemistry of buried river sediments from Ghaggar Plains, NW India: multi-proxy records of variations in provenance, paleoclimate, and paleovegetation patterns in the late quaternary" by Singh et al. (2016). Palaeogeogr. Pal. Palaeogeogr. Palaeoclimatol. Palaeoecol. 455, 68–70. http://dx.doi.org/10.1016/j.palaeo.2016.05.001.

Singh, S.K., Rai, S.K., Krishnaswami, S., 2008. Sr and Nd isotopes in river sediments from the Ganga Basin: sediment provenance and spatial variability in physical erosion. J. Geophys. Res. 113 http://dx.doi.org/10.1029/2007JF000909.

Singhvi, A.K., Kar, A., 2004. The aeolian sedimentation record of the Thar desert. Proc. Indian Acad. Sci. (Earth Planetry Sci. 113, 371–401.

Sinha, R., Yadav, G.S., Gupta, S., Singh, A., Lahiri, S.K., 2013. Geo-electric resistivity evidence for subsurface palaeochannel systems adjacent to Harappan sites in northwest India. Quat. Int. 308–309, 66–75. http://dx.doi.org/10.1016/j.quaint.2012.08.002.

Staubwasser, M., Sirocko, F., Grootes, P.M., Segl, M., 2003. Climate change at the 4.2 ka BP termination of the Indus valley civilization and Holocene south Asian monsoon variability. Geophys. Res. Lett. 30, 1425. http://dx.doi.org/10.1029/2002GL016822.

Syvitski, J.P.M., Kettner, A.J., Overeem, I., Giosan, L., Brakenridge, G.R., Hannon, M., Bilham, R., 2013. Anthropocene metamorphosis of the Indus Delta and lower floodplain. Anthropocene 3, 24–35. http://dx.doi.org/10.1016/j.ancene.2014.02.003.

Tanaka, T., Togashi, S., Kamioka, H., Amakawa, H., 2000. JNdi-1: a neodymium isotopic reference in consistency with LaJolla neodymium. Chem. Geol. 168, 279–281.

Tripathi, J.K., Bock, B., Rajamani, V., 2013. Nd and Sr isotope characteristics of Quaternary Indo-Gangetic plain sediments: source distinctiveness in different geographic regions and its geological significance. Chem. Geol. 344, 12–22. http://dx.doi.org/10.1016/j.chemgeo.2013.02.016.

Tyagi, A.K., Shukla, A.D., Bhushan, R., Thakker, P.S., Thakkar, M.G., Juyal, N., 2012.

Mid-Holocene sedimentation and landscape evolution in the western Great Rann of Kachchh,India. Geomorphology 151, 89–98. http://dx.doi.org/10.1016/j.geomorph.2012.01.018.
Valdiya, K.S., 2013. the river Saraswati was a himalayan-born river. Curr. Sci. 104, 42–54.
Wright, R.P., Bryson, R.A., Schuldenrein, J., 2008. Water supply and history: harappa and the Beas regional survey. Antiquity 82, 37–48.
Wünnemann, B., Demske, D., Tarasov, P., Kotlia, B.S., Reinhardt, C., Bloemendal, J., Diekmann, B., Hartmann, K., Krois, J., Riedel, F., Arya, N., 2010. Hydrological evolution during the last 15 kyr in the Tso Kar lake basin (Ladakh, India), derived from geomorphological, sedimentological and palynological records. Quat. Sci. Rev. 29, 1138–1155. http://dx.doi.org/10.1016/j.quascirev.2010.02.017.
Yadava, M.G., Ramesh, R., 2005. Monsoon reconstruction from radiocarbon dated tropical Indian speleothems. Holocene 15, 48–59. http://dx.doi.org/10.1191/0959683605h1783rp.
Yadava, M.G., Ramesh, R., 1999. Speleothems - usefull proxies for past monsoon rainfall. J. Sci. Ind. Res. 58, 339–348.

Contents lists available at ScienceDirect

Geoscience Frontiers

journal homepage: www.elsevier.com

Research paper

Geochemistry of Harappan potteries from Kalibangan and sediments in the Ghaggar River: Clues for a dying river

Anirban Chatterjee*, Jyotiranjan S. Ray

Physical Research Laboratory, Ahmedabad, India

ARTICLE INFO

Article history:
Received 18 January 2017
Received in revised form 5 July 2017
Accepted 30 July 2017
Available online xxx

Handling Editor: Sohini Ganguly

Keywords:
Ghaggar alluvium
Holocene
Sediment provenance
Kalibangan
Mature Harappan pottery
Geochemistry; Vedic Saraswati

ABSTRACT

The ephemeral Ghaggar-Hakra River of north-western India has always been considered to be the remnant of an ancient perennial glacier-fed river (Vedic Saraswati). The exact reason and timing of major hydrological change of this river remains speculative. The river's purported association with the zenith of the Harappan civilisation remains a conjecture because the timings of its fluvial past are still being debated. In this study we have made an attempt to resolve this issue using geochemical provenance of sediments from some dated horizons in the Ghaggar flood plain and that of the material used in the potteries from the Mature Harappan period (4600 to 3900 yr BP) at Kalibangan. Sampled sedimentary horizons were dated by radiocarbon and optically stimulated luminescence (OSL) methods. Results of our study from the Ghaggar alluvium indicate that the river did have glacial sources during the early Holocene. However, the data from the potteries suggest that during the Mature Harappan period, the sediments in the Ghaggar as used by the potters did not have a higher Himalayan provenance and hence, were not derived from glaciated Himalayas. These findings imply that during the time of the Mature Harappans the Ghaggar had already become a foothill-fed river.

1. Introduction

Rivers have always played major roles in shaping the history of mankind. They are the silent witnesses of rise and fall of civilisations across the globe, and have remained part of the cultural identity of these civilisations. One such fascinating example has been the story of a supposedly mighty river in the heart of the Bronze Age Harappan settlements and its purported link to the evolution of the civilisation. More than a century of research have confirmed existence of several paleo-channels along the present day, mostly defunct Ghaggar-Hakra streams in the semi-arid northern margin of the Thar Desert (Fig. 1A and B; Valdiya, 2013). However, no conclusive evidence has yet been provided establishing a link between the paleo channels and a pre-historic, glacial fed river system. Many hypothesise that these paleo-channels are the remnants of the mythical river Saraswati, which was first described in the three millennia old scriptures of Rig-Veda (Oldham, 1893; Ghose et al., 1979; Pal et al., 1980; Radhakrishan and Merh, 1999; Kochar, 2000; Valdiya, 2013). It is well known that a great majority of Harappan settlements are concentrated along the present-day dry beds of the Ghaggar-Hakra channels (Mughal, 1997; Possehl, 2002; Fig. 1A). Since availability of water is one of the key requirements for development of civilisations, it is quite natural to believe that the Ghaggar-Hakra streams had a strong fluvial past during the peak of the Indus Valley civilisation. Hypotheses based on this idea suggest that the drying up of the Ghaggar-Hakra River, owing to river reorganisation, triggered the abrupt decline of the Indus Valley tradition in the north-western India, four millennia ago (Misra, 1984; Mughal, 1997; Possehl, 2002; Kenoyer, 2008; Wright et al., 2008). However, lack of geochronological data makes it difficult to constrain the exact timing of these events. Competing hypotheses, based on geochemical studies, propose that the Ghaggar-Hakra system had already become rain-fed (by ~10 ka) by the time the early Harappans had started settling down in its flood plain (Clift et al., 2012; Giosan et al., 2012; Tripathi et al., 2013), and that subsequent climate change leading to extreme aridity sealed the fate of the civilisation (e.g. Sarkar et al., 2016). Therefore, the issue of a possible glacial past of the Ghaggar-Hakra river system remains unresolved. Even if the river did have a glacial history, the timings and reasons of the hydrological changes remain to be unravelled.

Apart from indecipherable information about their lifestyle, the Indus valley people had left behind a plethora of artefacts including sophisticated potteries and ceramics. These have the potential to reveal a lot about their living environments. It has been observed that ancient potters generally used materials available in their near geographical vicinity to create potteries (Krishnan, 2002). In the case of the Indus valley potteries, source material would have been the abundant flood-plain sediments deposited by the rivers, on which the cities were built. Thus, geochemical composition of potteries is likely to give us an insight into the sediment composition of the river during that period. This in turn can reveal about the catchment of the river,

Peer-review under responsibility of China University of Geosciences (Beijing).

* Corresponding author.
Email address: anirban@prl.res.in (A. Chatterjee)

https://doi.org/10.1016/j.gsf.2017.07.006
1674-9871/

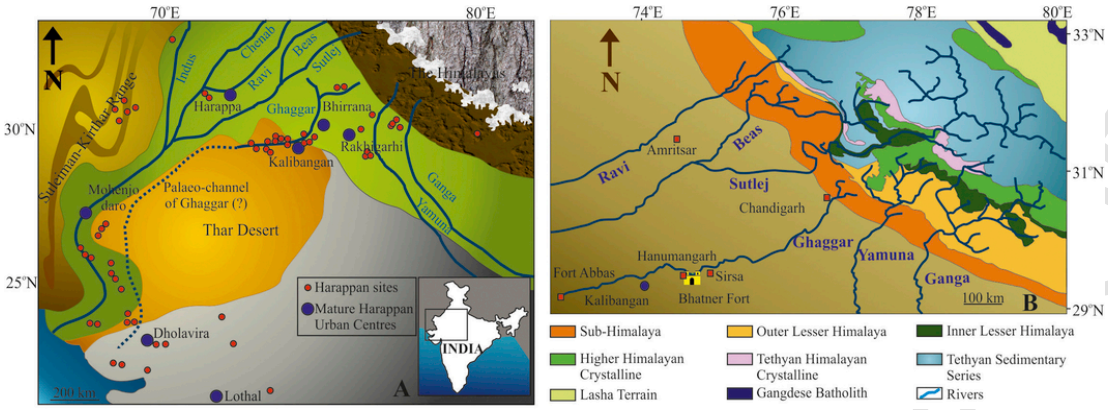

Figure 1. (A) Regional geomorphological map of north-western India showing the major landscapes. The putative course of paleo-Ghaggar is shown as dotted line and the pre-historic Harappan settlements are shown. Map is modified after Sarkar et al. (2016). (B) Different litho-tectonic units of the Himalayas from where different western Indian rivers have originated. Also shown are the positions of Kalibangan and Bhatner Fort on the bank of the Ghaggar. Map is modified after Singh et al. (2016).

glaciated higher Himalayas versus piedmont origin, because the sediment in the Indo-Gangetic plains are geochemically well co-related with their sources in the Himalayas (Najman, 2006). However, this method of source fingerprinting has its own limitations because of overlapping chemical compositions of the sources, differential chemical weathering at the source and in the alluvial plain, and alteration of original signals due to recycling. In spite of these, isotopic fingerprinting has remained the most promising tool for provenance study in the sediments derived from the Himalaya (Najman, 2006). In the present study, for the first time, we have made an attempt to address the issue of the lost river Saraswati from an entirely new angle, using geochemistry of well-dated Ghaggar alluvial deposits and comparing them with that of the potteries of the Mature Harappan period (4600–3900 yr BP), recovered from the Harappan acropolis of Kalibangan.

2. Harappan settlements along Ghaggar

The Indus Valley/Harappan cultural tradition developed along the river valleys of the Indus and Ghaggar-Hakra during mid-Holocene (Fig. 1). People of this culture settled over an area larger than the contemporaneous Mesopotamian and Egyptian civilisations (~8,00,000 km^2; Danino, 2010). The duration of existence of this culture, based on dates from Harappa and nearby localities, have been divided into four phases/periods (Kenoyer, 1998; Wright et al., 2008; Dikshit, 2013). Around 5.7 kyr BP agro-pastoral Ravi culture flourished, followed by the transitional Kot Diji Phase (~4.8 kyr BP). The sophisticated urban civilization of the Mature Harappan phase started around 4.6 kyr BP and disintegrated at ~3.9 kyr BP, followed by a de-urbanisation era of Late Harappan phase that lasted until ~3.3 kyr BP. However, Possehl (2002) had proposed a much older age for the Harappan culture based on spatio-temporal distribution of archaeological remains that spread across the Indian sub-continent. Earlier, Mughal (1997) had reported such older pre-Harappan settlements along the Hakra river of Cholistan desert and named it as the Hakra Phase. Later, numerous sites of the Hakra phase were discovered along the dry beds of the Ghaggar-Hakra including Kalibangan (the present study site), Farmana, Bhirrana, Rakhigarhi etc. Based on available chronological information the antiquity of the Hakra Phase can be pushed back to ~9.5 kyr BP (Sarkar et al., 2016 and references therein).

Kalibangan is one of the important Harappan cities situated on the southern bank of the river Ghaggar (Fig. 3) and has a continuous history since the Hakra Phase, up to the Late Harappan (Thapar, 1975). The oldest dated sequence of Kalibangan is 7.6 kyr BP (Sarkar et al., 2016). The settlement has two fortified sections, the Citadel (KLB-I) and the lower city (KLB-II) located to the east of the citadel (Fig. 2A). The KLB-I mound contains ruins of the settlements since the Hakra Phase until the late Harappan phase, whereas the KLB-II mound is characterised by only the mature Harappan settlements. Fig. 2B shows the mound of KLB-II as photographed during our field work in 2014. The remains of brick walls and terracotta pipelines can be seen in Fig. 2C. To understand the source of the clay used in making the potteries and bricks by the Mature Harappans we restricted our sampling to the KLB-II mound. Photographs of some of these samples are shown in Fig. 2D.

Giosan et al. (2012) had suggested that subsequent to de-urbanisation, Harappan settlements gradually shifted north-eastward to the upper Haryana plains. The Ghaggar-Hakra valley was later re-occupied by Painted Grey Ware sites during 3000–2600 kyr BP. Also during the medieval period fortifications were made along these floodplains (Mughal, 1997). The Bhatner Fort (12th century AD) of Hanumangarh is one of them (Fig. 1B). For the present study we also sampled bricks from this fort.

3. Methodology

Optically Simulated Luminescence (OSL) dating of the sand horizons was done in Physical research Laboratory using single aliquot regeneration (SAR) protocol of Murray and Wintle (2000). One sample of gastropod shells collected from a silty-clay horizon was dated by AMS C-14 at Centro Nacional de Aceleradores (CNA), Spain. The C-14 date have been calibrated using INTCAL 13 curve of Reimer et al. (2013).

All the geochemical and isotopic measurements were done on carbonate free siliciclastic/silicate fractions of samples. Samples were washed with 18.2 MΩ cm water multiple times, dried at 110 °C, powdered and homogenised. Prior to dissolution, powdered samples were heated at 650 °C for 2 h to remove organic matter and leached in 2 N HCl to remove carbonates. ~50 mg each of de-carbonated powdered samples was dissolved using standard HF-HNO_3 (2:1) acid digestion technique. 15 mL Savillex Teflon vials were used for the purpose. Complete dissolution was achieved through repeated ultrasonication, heating, aqua regia and 8 N HNO_3 treatments. It was made sure that no residue was left. Final (stock) solutions were prepared in 0.2 N HNO_3. Ultra pure (low blank) acids were used for the purpose.

Concentrations of trace elements including rare earth elements (REEs) were measured using a Thermo X-Series 2 Q-ICPMS at

Figure 2. (A) The settlement map of the Harappan acropolis of Kalibangan. Map is modified after Thapar (1975). (B) The KLB-II mound of Kalibangan as photographed during field work in 2014. (C) The remains of brick walls can be seen through the gaps in the mound. In the inset image terracotta drainage pipes can be seen. (D) Samples of Mature Harappan potteries collected from the KLB-II mound.

Physical Research Laboratory (PRL). USGS rock standard BHVO-2 was used as unknown for accuracy check. Reproducibility of trace element contents, based on repeated analyses of the standard, was ≤3% for REEs and ≤6% for all other trace elements at 2σ level. Sr separation was done by conventional cation exchange column chemistry using AG®50W-X8 resin and Nd was separated from other REEs using Ln-specific resin from Eichrom® with dilute HCl as elutant (Dickin, 2000; Awasthi et al., 2014). $^{87}Sr/^{86}Sr$ and $^{143}Nd/^{144}Nd$ were measured in static multicollection mode on an IsoProbe-T TIMS (Ray et al., 2013). The measured isotopic ratios were corrected for fractionation using $^{86}Sr/^{88}Sr = 0.1194$ and $^{146}Nd/^{144}Nd = 0.7219$, respectively. The average values for NBS987 and JNdi measured over a period of 5 years are $^{87}Sr/^{86}Sr = 0.71023 \pm 0.00001$ (n = 70) and $^{143}Nd/^{144}Nd = 0.512104 \pm 0.000004$ (n = 60; ±0.1 in ε_{Nd} units) at 2σ level of uncertainty. The value of $^{143}Nd/^{144}Nd = 0.512104$ for JNdi corresponds to a value of 0.511847 for the widely used La Jolla Nd standard (Tanaka et al., 2000). $^{87}Sr/^{86}Sr$ and $^{143}Nd/^{144}Nd$ for BHVO-2 were 0.70346 ± 0.00004 and 0.512967 ± 0.000008 (n = 10; ±0.2 in ε_{Nd} units at 2σ), respectively, which are same as the reported values of 0.70344 ± 0.00003 and 0.51296 ± 0.00004 within 2σ (Raczek et al., 2001). To compare our data with that from literature, all $^{87}Sr/^{86}Sr$ and $^{143}Nd/^{144}Nd$ ratios were normalized to 0.71025 for NBS987 and 0.511858 for La Jolla, respectively. All plots and discussion below are based on the normalized ratios.

4. Results and discussion

4.1. Sedimentary facies and depositional ages

The present course of the Ghaggar River is almost non-existent beyond Sirsa in Haryana due to damming and heavy farming on and along its shallow channel. The flood plain topography is monotonously flat and is bordered by sand dunes. Interestingly, the subsurface sedimentary facies is very different from that of the dry river bed. Fig. 3 presents a comparison of the subsurface stratigraphy from different localities along the flood plain as determined by us (Fig. 3A and B) and Saini et al. (2009) (Fig. 3C and D). The modern surface mud covers the Ghaggar alluvium near the present course of the Ghaggar channel. The older floodplain deposit of brown coloured silty-clay directly underlies the surface mud. The brown silty-clay directly overlies either a yellowish-brown fine fluvial sand layer or a grey micaceous sand layer.

The thickness of the overlying brown silty-clay varies from 1 to 10 m. AMS C-14 dating of gastropod shells from this horizon near Hanumangarh yielded an age of 3109 ± 35 cal yr BP, which can be considered as the age of deposition of the layer (Fig. 3A). Earlier Saini et al. (2009) had reported OSL depositional ages of 2.9 ± 0.2 kyr BP and 3.4 ± 0.2 kyr BP for the similar stratigraphic horizons around Sirsa (Fig. 3C and D). The silty-clay layers can be traced further downstream until the river bed vanishes in the desert. In deeper sections the silty-clay facies can be observed as intermittent thin layers stacked within the thick sand horizons deposited around 7–5 kyr BP (Clift et al., 2012; Singh et al., 2016). Based on the available chronological information it can be suggested that even though the deposition of the silty-clay sediments started around mid-Holocene, it had become a dominant facies by 3 kyr BP.

A detailed clay mineralogical study has been conducted by Alizai et al. (2012) which characterises the clay depositions of the Ghaggar alluvium, further downstream at Fort Abbas, Marot and Tilwala in Pakistan (Fig. 4). Considering that no tributaries join the Ghaggar downstream beyond Shatrana, it can be inferred that the clay mineralogical composition should have remained similar all along the floodplain. As suggested by Alizai et al. (2012) the most abundant clay mineral in the Ghaggar alluvium is smectite (51–59%), followed by illite (30–37%). The minor constituents are chlorite (5–7%) and kaolinite (2–5%). It can be observed in Fig. 4 that the abundances of these four clay minerals had remained spatially and temporally invariant during the Holocene. The presence of illite as a major clay indicates that the sediments were sourced from the Himalaya where physical weathering dominates. On the other hand dominance of smectite, which is primarily a product of chemical weathering, is not in accordance with a Himalayan source where chemical weathering is very less. Such a scenario can be explained by two-cycle weathering (Singh et al., 2005), one at the source and the other within the floodplains with smectite being generated in the latter as a result of chemical weathering.

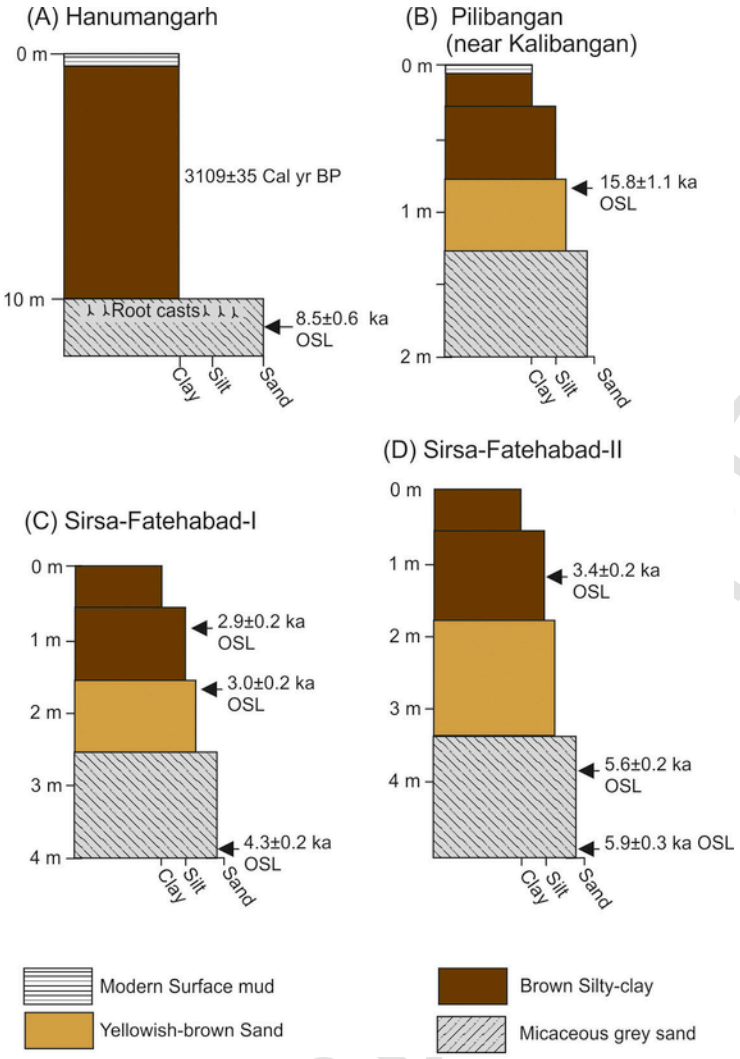

Figure 3. The subsurface facies architecture of the Ghaggar alluvium at (A) Hanumangarh, (B) Pilibangan and (C) Sirsa-Fatehbad-I and (D) Sirsa-Fatehbad-II regions. The stratigraphies of Sirsa-Fatehbad region are from Saini et al. (2009).

Raikes (1968) first reported coarse grained micaceous grey sand facies, resembling the sediment carried by modern higher Himalayan glacier-fed rivers like Ganga and Yamuna, buried ~10 m below the silty-clay floodplain deposits of the Ghaggar near Kalibangan. During the field survey for the present study similar grey sand was encountered at several places along the Ghaggar floodplain. Several other workers have also reported such sub-surface sand horizons from many locations in the floodplain (Saini et al., 2009; Saini and Mujtaba, 2012; Singh et al., 2016). The immature character of these coarse grained sand layers bears the testimony of a once active major fluvial system and they probably represent bedload sediments. Presence of a sharp contact between the micaceous sand and silty-clay layers points to a depositional hiatus/erosional surface between the two. Quartz is the most dominant mineral in the grey sandy facies, followed by feldspar and muscovite. Accessory phases include biotite, amphibole, kyanite, sillimanite, garnet and pyroxene (Saini et al., 2009). The clay content of the grey micaceous sand is almost negligible implying that these were high energy depositions. OSL dating of this sand layer at Hanumangarh yielded a depositional age of 8.5 ± 0.6 ka (Fig. 3A). The youngest age for similar grey sand from the upstream part of the river is reported to be 4.3 ± 0.2 ka (Saini et al., 2009; Fig. 3C). Singh et al. (2016) had reported depositional timing of these grey micaceous sands from Kalibangan region to be from ~70 to ~20 kyr BP.

At other locations, the grey sand is overlain by yellowish-brown fluvial sands which gradually grades upward into the brown silty-clay. This fine fluvial sand appears to have been deposited by a weaker phase of fluvial activity and local sediment reworking from dunes (Saini et al., 2009; Saini and Mujtaba, 2012). The OSL age of this yellowish-brown fluvial sand from the Pilibangan region (near Kalibangan), determined by us, is 15.8 ± 1.1 ka (Fig. 3B), whereas, Saini et al. (2009) had reported much younger depositional age of 3 ± 0.2 ka for similar deposits near Sirsa (Fig. 3C). These young sand layers (younger than the grey sand) were likely deposited during a weaker phase of the river when suspended load dominated the system. Mineralogically, these sand deposits are predominantly composed of quartz and feldspar. Unlike the grey sandy facies, mica is less abundant and occurs as fine round-edged grains (recycled).

A graphical representation of temporal dominance, during the last 70 kyrs, of different sedimentary facies within the Ghaggar flood plain is given in Fig. 5. The age data from earlier studies and those presented here suggest that during early Holocene both types of sands

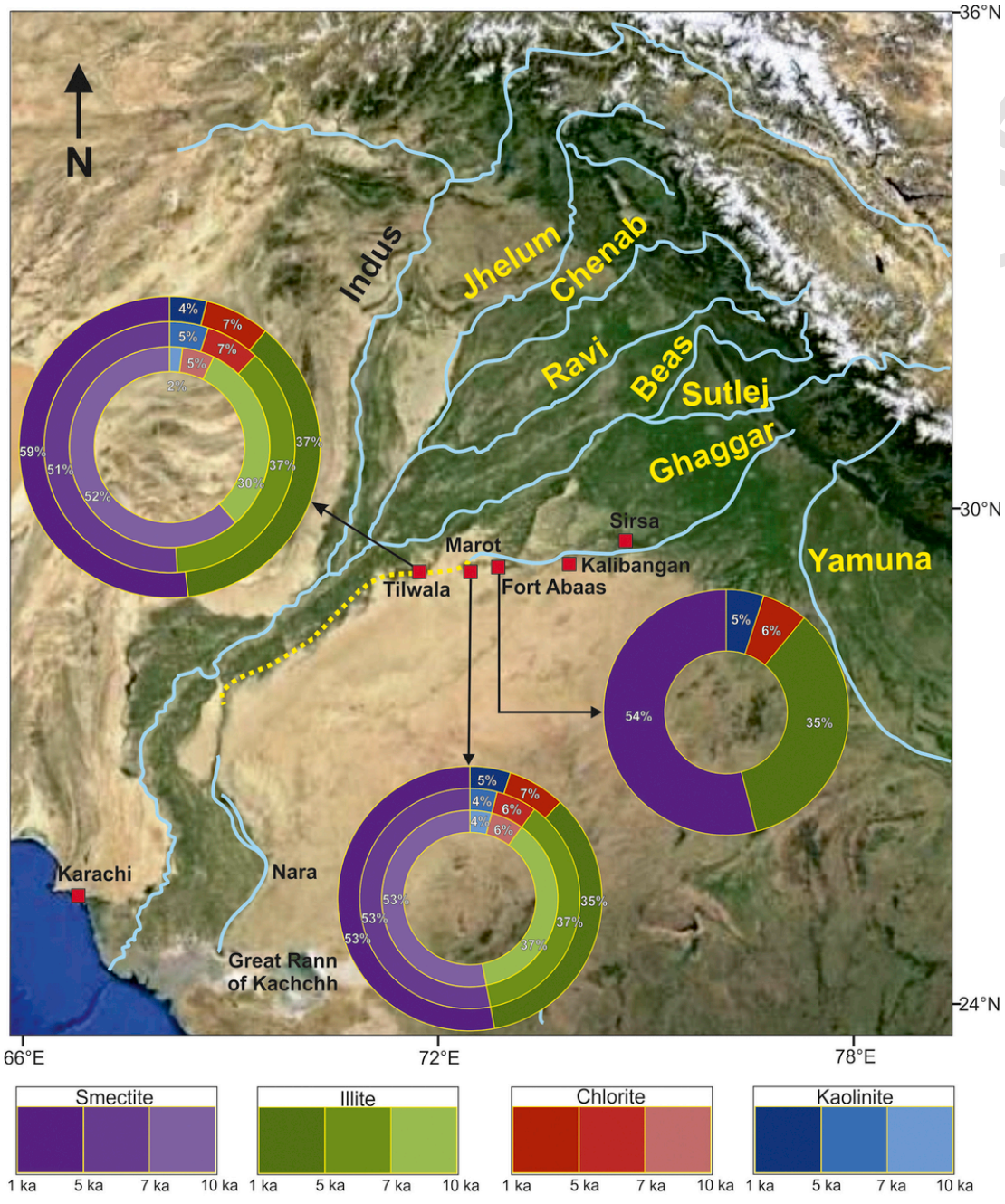

Figure 4. Pie chart showing the compositional variations of clay minerals across the Ghaggar alluvium during the Holocene.

(coarse grey and fine yellowish-brown) were getting deposited in the Ghaggar valley, whereas the sedimentation was dominated by only the grey sand during earlier times (Singh et al., 2016). This implies that the Ghaggar River was a much stronger fluvial system in the past and gradually, over a period of ~10 kyrs, reduced into a dwindling meandering system dominated with reworked and suspended sediments. For proper characterization of the sources of the sediments and to understand the depositional pathways, we studied the geochemical properties of these sediments along the Ghaggar flood plain near Hanumangarh and Pilibangan.

4.2. Geochemistry of Ghaggar alluvium

The trace element data of sediment samples are presented in Table 1 and plotted in Post Archean Australian Shale (PAAS) normalized diagram in Fig. 6. As can be seen, all different types of sediments show similar trace element patterns. Even the modern surface mud deposited during the latest flooding event shows a similar pattern. The only difference between these is the elemental concentrations. The modern mud in the river has the highest trace element contents, whereas the oldest alluvium, the coarse grey sand, has the lowest. This can be attributed to effect of dilution because of presence of

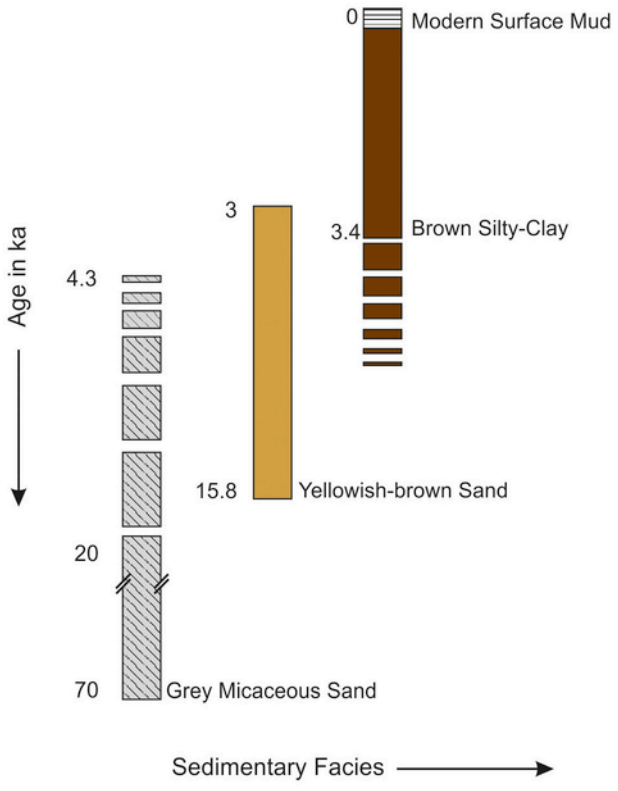

Figure 5. A graphical representation of composite stratigraphy of different sedimentary facies deposited within the Ghaggar floodplain over the past 70 kyr.

abundant quartz in the latter. Notwithstanding the differences in the contents, comparable patterns of trace elements in different sediments point to their derivation from analogous sources. The strong negative PAAS-normalized anomalies observed for Zr and Hf in the Ghaggar alluvium (Fig. 6) has also been reported from the sediments in the five rivers of Punjab (Alizai et al., 2011). Such a resemblance points to a similarity of provenances of sediments in Ghaggar and the rivers of Punjab, i.e., the Himalayas. The above depletions in the Zr and Hf could also be attributed to the removal of heavy mineral such as zircon from the sediments during long distance transport (Carpentier et al., 2009; Chatterjee and Ray, 2017), however, we do not envisage such a scenario considering that the sampled locations in all the rivers were not very far from the catchment. Therefore, the only likely possibility remains is that the sources of these sediments already had these depletions. Considering that the sources were located in the Himalayas, it needs to be determined if they were located either in the Higher Himalaya, or the Lesser Himalaya, or the Siwaliks.

To resolve the above issue we took the help of Sr—Nd isotopic composition of bulk sediments. The isotopic data of the Ghaggar alluvium are presented in Table 2. Different litho-tectonic units of the Himalayas are well characterised with respect to Sr and Nd isotopic compositions and can be used for tracing the provenance of the sediments in frontal alluvial plain. The Sr—Nd isotopic ratios of different Himalayan litho-tectonic units, based on the available data from literature, are shown in Fig. 7A. The glaciated regions of the Himalayas comprise rocks of the Higher Himalayan Crystalline Series (HHCS) and Lesser Himalayan Series (LHS). Rivers originating from the glaciers carry sediments derived from these two sources and hence they possess a mixed signal. In Fig. 7B we compare the Sr—Nd isotopic data for the Ghaggar alluvium, ours as well as that from literature (Tripathi et al., 2013; Singh et al., 2016), with that of the sub-Himalayan lithologies (Subathu, Kasauli, Dagsahi and Siwaliks) and for sediments in the rivers originating from the higher Himalaya

Table 1
Trace element data (in ppm) for samples from the Ghaggar flood-plain.

Sample	HG-14-4 (Brown silty-clay)	HG-14-8 (Brown silty-clay)	HG-14-16 (Brown silty-clay)	HG-14-18 (Modern surface mud)	HG-14-20 (Brown silty-clay)	HG-14-21 (Brown silty-clay)	HG-14-22 (Yellowish-brown sand)	HG-14-39 (Brown silty-clay)	HG-14-17 (Grey sand)	BHVO-2 (Measured)	BHVO-2 (Reported)
Cs	7.49	8.98	6.67	9.14	9.67	6.48	3.38	7.78	3.40	0.12	0.1 ± 0.01
Rb	124.1	145.2	113.7	151.9	148.7	109.7	76.0	115.6	74.2	10.3	9.11 ± 0.04
Ba	501	565	414	546	589	493	396	396	292	130	131 ± 1
Th	20.0	15.0	13.7	20.7	15.9	14.0	10.4	13.6	15.1	1.1	1.22 ± 0.06
U	2.27	1.34	1.54	2.50	2.91	2.02	1.37	1.69	1.57	0.42	0.403 ± 0.001
Nb	14	13	12	14	13	11	9	14	8	17	18.1 ± 1
Ta	1.11	1.04	0.93	1.14	1.16	0.86	0.71	1.03	0.75	0.95	1.14 ± 0.06
La	51	42	36	49	38	36	33	40	37	15	15.2 ± 0.1
Ce	99	86	73	98	76	72	67	79	73	39	37.5 ± 0.2
Pb	22.1	25.0	21.2	25.7	21.3	18.7	18.5	13.8	15.4	1.2	1.6 ± 0.3
Pr	11.9	9.8	8.3	11.2	8.6	8.3	7.6	9.0	8.2	5.2	5.35 ± 0.17
Sr	72	72	69	98	147	159	179	109	69	388	396 ± 1
Nd	43	36	31	41	31	30	28	32	29	24	24.5 ± 0.1
Zr	17	19	9	21	17	14	11	20	10	163	172 ± 11
Hf	0.6	0.7	0.6	0.8	0.8	0.5	0.4	0.7	0.3	3.9	4.36 ± 0.14
Sm	8.1	6.7	5.7	7.6	5.5	5.5	5.0	5.7	5.3	5.9	6.07 ± 0.01
Eu	1.4	1.3	1.1	1.4	1.0	1.0	1.0	1.0	0.8	2.0	2.07 ± 0.02
Gd	7.0	5.7	4.9	6.7	4.7	4.6	4.3	4.8	4.5	6.1	6.24 ± 0.03
Tb	0.81	0.69	0.60	0.82	0.56	0.55	0.52	0.57	0.53	0.84	0.92 ± 0.03
Dy	4.1	3.6	3.2	4.1	2.9	2.9	2.7	2.9	2.7	5.2	5.31 ± 0.02
Y	19.4	16.9	13.7	18.8	10.7	14.5	13.9	14.1	13.4	23.4	26 ± 2
Ho	0.70	0.64	0.55	0.72	0.51	0.51	0.50	0.50	0.46	0.89	0.98 ± 0.04
Er	1.9	1.8	1.6	2.0	1.5	1.4	1.4	1.4	1.3	2.5	2.54 ± 0.01
Tm	0.2	0.2	0.2	0.3	0.2	0.2	0.2	0.2	0.2	0.3	0.33 ± 0.01
Yb	1.6	1.5	1.3	1.6	1.3	1.2	1.2	1.2	1.1	1.9	2 ± 0.01
Lu	0.20	0.20	0.17	0.22	0.18	0.17	0.17	0.16	0.14	0.26	0.274 ± 0.005

Reproducibility (2σ): REE ≤ 3%; others ≤ 6%. Reported values for BHVO-2 are from Jochum et al. (2005).

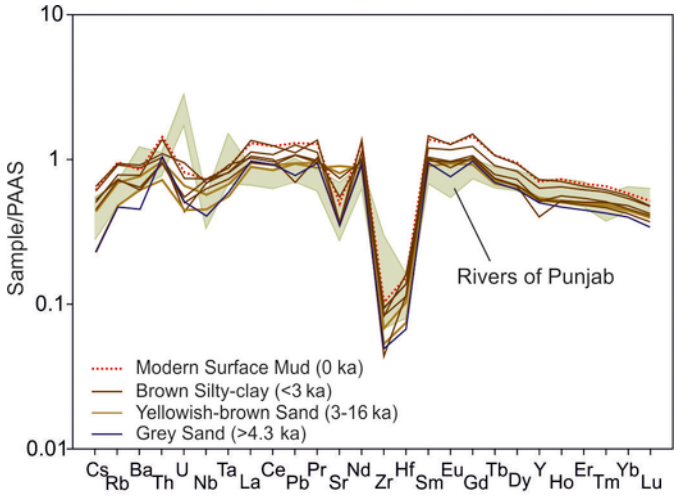

Figure 6. PAAS normalised trace element distribution of various sedimentary facies from the Ghaggar alluvium. The green coloured field in the background shows the range of composition observed in the rivers of Punjab. Data source: Alizai et al. (2011).

(Ganga, Yamuna and Sutlej; Singh et al., 2008; Tripathi et al., 2013). The micaceous grey sand layers near Kalibangan (>20 kyr BP; Singh et al., 2016) have overlapping isotopic compositions with that of the sediments in most glacier fed rivers, thus suggesting a provenance in the glaciated Himalayas (Fig. 7B).

The brown coloured silty-clay and the yellowish-brown fluvial sand possess distinctly different isotopic ratios than that of the grey sand (Fig. 7B); implying that the provenance of the brown silty-clay and yellowish brown sand is different from that of the Higher-Himalaya originated grey sands. The brown silty-clay and the yellowish-brown sand are less radiogenic in Sr and more radiogenic in Nd isotopic composition. They are also different in composition from the surrounding sand dunes, indicating very little, if any, input from the dunes via reworking. Fig. 1B shows that the modern river Ghaggar has its catchment in the sub-Himalayas which includes the Siwalik Group, Kasauli, Dagsahi and Subathu Formations. Consequently, the river is expected to carry sediments derived from these lithologies. Sr—Nd isotopic compositions of these lithologies are shown in Fig. 7B. Tripathi et al. (2013) have argued for a significant contribution of the Subathu Formation in the Ghaggar Alluvium. However, our observations suggest that the Subathu Formation having very different isotopic compositions might have had very little influence on the Ghaggar sediments (Fig. 7B). It appears that the rocks of the Siwalik Group, Kasauli and Dagsahi Formations are the major sources for the brown mud and yellowish-brown sand of the Ghaggar flood-plain (Fig. 7B). The more radiogenic Nd of the marginal desert dunes can very well be the results of sediment mixing from the river Indus. Given the fact that the sedimentation in the Ghaggar was dominated

Table 2
Isotopic data for sediment samples and archaeological artefacts from the Ghaggar flood-plain.

Samples	Brown Silty-clay (<3 ka)				Yellowish brown sand		Modern surface mud	
	HG-14-4	HG-14-8	HG-14-16	HG-14-20	HG-14-21	HG-14-22	HG-14-18	HG-14-18R
$^{87}Sr/^{86}Sr$	0.743022	0.745287	0.747306	0.733185	0.731733	0.730670	0.738182	0.738182
ε_{Nd}	−14.7	−14.6	−14.8	−14.3	−14.3	−13.4	−14.1	−13.8

Samples	Thar Dune sand (sub-surface, no age control)					
	HG-14-23	HG-14-24	RM-14-1	RM-14-3	HG-15-7	HG-15-32
$^{87}Sr/^{86}Sr$	0.726126	0.726132	0.727257	0.727815	0.729716	0.727714
ε_{Nd}	−13.0	−10.3	−10.9	−13.3	−13.8	−13.4

Samples	Kalibangan Pottery and brick (4.6–3.9 ka)				Bhatner Fort Brick (~0.9 ka)
	KBP-1	KBP-2	KBP-3	KBP-4	HGP-1
$^{87}Sr/^{86}Sr$	0.739043	0.731819	0.737543	0.726857	0.730976
ε_{Nd}	−12.4	−14.2	−13.1	−13.5	−12.9

$\varepsilon_{Nd} = [(^{143}Nd/^{144}Nd)_{sample}/(^{143}Nd/^{144}Nd)_{Chondrite}-1] \times 10^4$. Reproducibility ($2\sigma$): $^{87}Sr/^{86}Sr = \pm 0.000005$; $\varepsilon_{Nd} = \pm 0.1$.

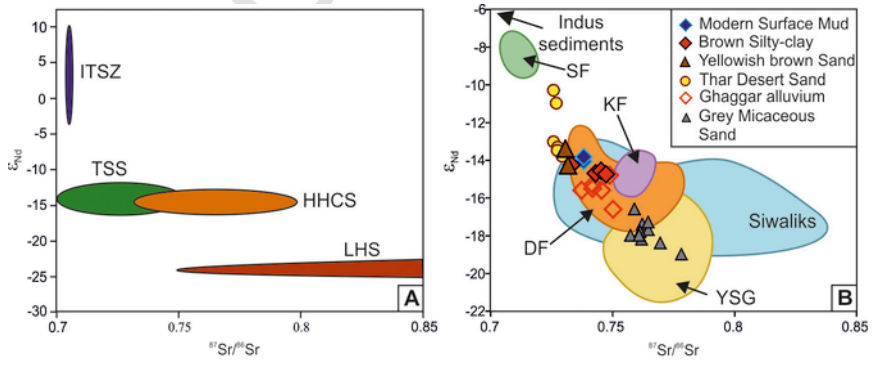

Figure 7. (A) ε_{Nd} vs. $^{87}Sr/^{86}Sr$ plot of major Himalayan litho-tectonic units showing their range of values. Data: Najman et al. (2000). ITSZ: Indo Tsangpo Suture Zone; TSS: Tibetian Sedimentary Series; HHCS: Higher Himalayan Crystalline Series; LHS: Lesser Himalayan Series. (B) ε_{Nd} vs. $^{87}Sr/^{86}Sr$ plot of various types of sediments from the Ghaggar alluvium compared with the sub-Himalayan provenances. Data for Ghaggar alluvium (red open diamonds) and grey micaceous sand (grey triangles) are from Tripathi et al. (2013) and Singh et al. (2016) respectively. SF: Subathu Formation; KF: Kasauli Formation; DF: Dagsahi Formation; YSG: Yamuna-Sutlej-Ganga sediment.

with suspended material by ~3 kyr BP, it can be suggested that the river likely had become a foothill fed river similar to its present condition by then.

From our geochemical provenance study it is clear that the Ghaggar had changed from a glacier fed strong fluvial system to a rain fed alluvial river during the Holocene. Interestingly, there is no geomorphic evidence of a glacial origin of the river. Therefore, the only plausible pathway for the higher Himalayan sediments to reach the Ghaggar channel would have been through the neighbouring rivers; the Sutlej and Yamuna, which used to flow into the Ghaggar during the pre-historic times (Valdiya, 2017 and references therein). This might explain the strong fluvial past of the river. The reason for the gradual hydrological changes in the Ghaggar could have been due to the progressive migration of these glacial-fed tributaries (Sutlej or Yamuna) away from it.

4.3. Isotopic fingerprinting of Kalibangan potteries

Potters of Bhirrana, a Harappan acropolis on the bank of the Ghaggar, used to make earthenware using clay from nearby localities (Krishnan et al., 2012). Extending this finding to Kalibangan it could be argued that potters here too had utilized the silty-clay which was available aplenty in the nearby Ghaggar floodplain. The very fact that common clay (illite/smectite, kaolinite and micas) can be utilized for general ceramics (Valášková, 2015) it is highly likely that the Harappans at Kalibangan made use of locally available clays, the mineralogical details of which are shown in Fig. 4 and discussed in Section 4.1. The usability of these silty-clay horizons is very much evident even today in the numerous active brick kilns all along the Ghaggar floodplain.

Another important understanding of ancient pottery making is that pure clay was never used for the purpose (Krishnan and Rao, 1994; Krishnan, 2002). For strengthening and creating different textures, various amounts of coarser material, generally sand, were mixed with pure clay to prepare the raw material. Therefore, one expects to find mixed geochemical signatures of sand and clay of the Ghaggar flood plain in the Kalibangan potteries. Fig. 8 presents ε_{Nd} versus $^{87}Sr/^{86}Sr$ plot comparing the compositions of Harappan potteries with that of the different types of Ghaggar flood plain sediments. It can be observed that the isotopic compositions of pottery samples lie within the range of brown silty-clay/surface mud and yellowish-brown sand. Possible contribution from surrounding aeolian sand cannot be ruled out. However, there appears to be a clear absence of any grey micaceous sand component within the pottery, which suggests non-availability of such sediment during pottery making. This on the other hand implies that by the time the Mature Harappans settled in Kalibangan, the glacial connection to the Ghaggar was significantly reduced and little sediment originating from glaciated terrains was depositing in the channels. Validation of this hypothesis comes from isotopic compositions of the brick sampled from the Bhatner Fort. It is a well-known historical fact that the Fort was established on the banks of an ephemeral Ghaggar during 12th century AD. The bricks of the fort, made using Ghaggar sediments, show similar compositions as that of the pre-historic potteries. This clearly suggests use of identical raw materials even after two millennia which in turn supports the theory that the river was already ephemeral (not glacier fed) during the Mature Harappan period.

5. Conclusion

The Ghaggar alluvium is a repository of sediments originated from two distinct provenances. The oldest grey micaceous sand (~70–4.3 ka) originated from the glaciated Higher Himalayas, thus, indicating a strong fluvial past of the river. The younger yellowish-brown sand and brown silty-clay (16–0 ka) were sourced from the Sub-Himalayan rocks, in particular from the Siwalik Group, Kasauli and Dagsahi Formations. Temporally overlapping depositions of sediments derived from both the Higher Himalayas and the Sub-Himalayas during the late Pleistocene and early Holocene point to the dwindling state of the river and gradual disappearance of its perennial water sources. The depositional ages of the topmost brown coloured silty-clay horizon confirm that the river had already lost its glacial sources and became an ephemeral foothill-fed river by 3 ka. The exact period of the hydrological changes has been narrowed down by the Nd—Sr isotopic fingerprinting of the Kalibangan potteries. This study suggests that the local sediments, which were most likely used for manufacturing the pottery, were not derived from the glacier covered parts of the Himalayas but were derived from the foothills of the

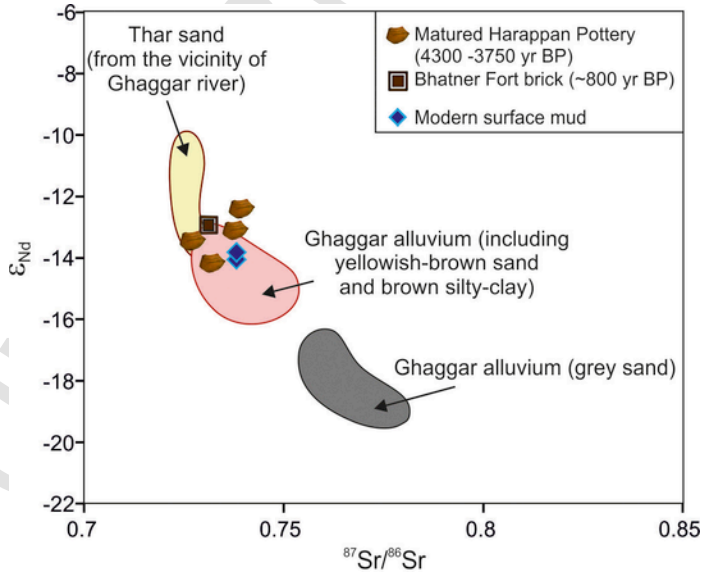

Figure 8. ε_{Nd} vs. $^{87}Sr/^{86}Sr$ plot of different archaeological artefacts compared with the probable raw material sources in the Ghaggar flood plain.

Himalayas. This in turn suggests that the Ghaggar had already transitioned from being a glacier-fed river to a rain-fed river during the Mature Harappan period.

Acknowledgements

We thank Ms. Ikshu Gautam and Mr. Bivin Geo George for participating and helping during the field work. We also thank Dr. Anil D. Shukla for helping in determining the OSL ages. Constructive reviews by two anonymous referees are highly appreciated. This project was funded by the Department of Space, Government of India.

References

Alizai, A., Carter, A., Clift, P.D., VanLaningham, S., Williams, J.C., Kumar, R., 2011. Sediment provenance, reworking and transport processes in the Indus River by U–Pb dating of detrital zircon grains. Global and Planetary Change 76, 33–55.

Alizai, A., Hillier, S., Clift, P.D., Giosan, L., Hurst, A., VanLaningham, S., Macklin, M., 2012. Clay mineral variations in Holocene terrestrial sediments from the Indus Basin. Quaternary Research 77, 368–381. https://doi.org/10.1016/j.yqres.2012.01.008.

Awasthi, N., Ray, J.S., Singh, A.K., Band, S.T., Rai, V.K., 2014. Provenance of the Late Quaternary sediments in the Andaman Sea: implications for monsoon variability and ocean circulation. Geochemistry, Geophysics, Geosystems 15, 3890–3906. https://doi.org/10.1002/2014GC005462.

Carpentier, M., Chauvel, C., Maury, R.C., Mattielli, N., 2009. The "zircon effect" as recorded by the chemical and Hf isotopic compositions of Lesser Antilles forearc sediments. Earth and Planetary Science Letters 287, 86–99. https://doi.org/10.1016/j.epsl.2009.07.043.

Chatterjee, A., Ray, J.S., 2017. Sources and depositional pathways of mid-Holocene sediments in the Great Rann of Kachchh, India: implications for fluvial scenario during the Harappan culture. Quaternary International 443, 177–187. https://doi.org/10.1016/j.quaint.2017.06.008.

Clift, P.D., Carter, A., Giosan, L., Durcan, J., Duller, G.A.T., Macklin, M.G., Alizai, A., Tabrez, A.R., Danish, M., VanLaningham, S., Fuller, D.Q., 2012. U-Pb zircon dating evidence for a Pleistocene Sarasvati River and capture of the Yamuna River. Geology 40, 211–214. https://doi.org/10.1130/G32840.1.

Danino, M., 2010. The Lost River: on the Trail of the Sarasvati. Penguin Books, India.

Dickin, A.P., 2000. Radiogenic Isotope Geology. Cambridge University Press, United Kingdom.

Dikshit, K.N., 2013. Origin of Early Harappan cultures in the Sarasvati Valley: recent archaeological evidence and radiometric dates. Journal of Indian Ocean Archaeology 9, 87–141.

Ghose, B., Kar, A., Husain, Z., 1979. The lost courses of the Saraswati River in the Great Indian Desert: new evidence from Landsat imagery. Geographical Journal 145, 446–451.

Giosan, L., Clift, P.D., Macklin, M.G., Fuller, D.Q., Constantinescu, S., Durcan, J.A., Stevens, T., Duller, G.A.T., Tabrez, A.R., Gangal, K., Adhikari, R., Alizai, A., Filip, F., VanLaningham, S., Syvitski, J.P.M., 2012. Fluvial landscapes of the Harappan civilization. Proceedings of the National Academy of Sciences 109, E1688–E1694. https://doi.org/10.1073/pnas.1112743109.

Jochum, K.P., Nohl, U., Herwig, K., Lammel, E., Stoll, B., Hofmann, A.W., 2005. GeoReM: a new geochemical database for reference materials and isotopic standards. Geostandards and Geoanalytical Research 29, 333–338. https://doi.org/10.1111/j.1751-908X.2005.tb00904.x.

Kenoyer, J.M., 2008. Indus civilization. In: Encyclopedia of Archaeology. Elsevier, New York, pp. 715–733.

Kenoyer, J.M., 1998. Ancient Cities of the Indus Valley Civilization. Oxford University Press, Oxford.

Kochar, R., 2000. Vedic People: Their History and Geography. Orient Longman, Hyderabad.

Krishnan, K., 2002. Survey of ceramic analysis with specific reference to pottery. Indian Archaeology in Retrospect, Prehistory-archaeology of South Asia. Manohar, New Delhi.

Krishnan, K., Rao, V., 1994. A study of clay paste preparation by potters through grain size analysis. South Asian Studies 10, 113–117.

Misra, V.N., 1984. Climate: a factor in the rise and fall of Indus Civilization. In: Frontiers of the Indus Civilization. Books and Books, New Delhi, pp. 469–489.

Mughal, M.R., 1997. Ancient Cholistan: Archaeology and Architecture. Ferozsons, Lahore, Pakistan.

Murray, A.S., Wintle, A.G., 2000. Luminescence dating of quartz using an improved single- aliquot regenerative-dose protocol. Radiation Measurements 32, 57–73.

Najman, Y., 2006. The detrital record of orogenesis: a review of approaches and techniques used in the Himalayan sedimentary basins. Earth-Science Reviews 74, 1–72. https://doi.org/10.1016/j.earscirev.2005.04.004.

Najman, Bickle, Chapman, Yang, H., 2000. Early Himalayan exhumation: isotopic constraints from the Indian foreland basin. Terra Nova 12, 28–34. https://doi.org/10.1046/j.1365-3121.2000.00268.x.

Oldham, C.F., 1893. The Saraswati and the lost river of the Indian desert. Journal of the Royal Asiatic Society 34, 49–76.

Pal, Y., Sahai, B., Sood, R.K., Agarwal, D.P., 1980. Remote sensing of the "Lost" Saraswati river. Proceedings of the Indian National Science Academy (Earth Planetary Sciences) 89, 317–331.

Possehl, G.L., 2002. The Indus Civilization: a Contemporary Perspective. AltaMira Press, Lanham, Maryland.

Raczek, I., Jochum, K.P., Hofmann, A.W., 2001. Neodymium and strontium isotope data for USGS reference GSP-1, GSP-2 and eight MPI-DING reference glasses. Geostandards and Geoanalytical Research 27, 173–179.

Radhakrishan, B.P., Merh, S.S., 1999. Vedic Sarasvati: evolutionary history of a lost river of northwestern India. Geological Society of India 42, 5–13.

Raikes, R., 1968. Kalibangan: death from natural causes. Antiquity XLII, 286–291.

Ray, J.S., Pande, K., Bhutani, R., Shukla, A.D., Rai, V.K., Kumar, A., Awasthi, N., Smitha, R.S., Panda, D.K., 2013. Age and geochemistry of the Newania dolomite carbonatites, India: implications for the source of primary carbonatite magma. Contributions to Mineralogy and Petrology 166, 1613–1632. https://doi.org/10.1007/s00410-013-0945-7.

Reimer, P.J., Bard, E., Bayliss, A., Beck, J.W., Blackwell, P.G., Bronk Ramsey, C., Buck, C.E., Cheng, H., Edwards, R.L., Friedrich, M., Grootes, P.M., Guilderson, T.P., Haflidason, H., Hajdas, I., Hatté, C., Heaton, T.J., Hoffmann, D.L., Hogg, A.G., Hughen, K.A., Kaiser, K.F., Kromer, B., Manning, S.W., Niu, M., Reimer, R.W., Richards, D.A., Scott, E.M., Southon, J.R., Staff, R.A., Turney, C.S.M., van der Plicht, J., 2013. IntCal13 and Marine13 radiocarbon age calibration curves 0–50,000 years cal BP. Radiocarbon 55, 1869–1887. https://doi.org/10.2458/azu_js_rc.55.16947.

Saini, H.S., Mujtaba, S.A.I., 2012. Depositional history and palaeoclimatic variations at the northeastern fringe of Thar Desert, Haryana plains, India. Quaternary International 250, 37–48. https://doi.org/10.1016/j.quaint.2011.06.002.

Saini, H.S., Tandon, S.K., Mujtaba, S.A.I., Pant, N.C., Khorana, R.K., 2009. Reconstruction of buried channel-floodplain system of the northwestern Haryana Plains and their relation to the 'Vedic' Saraswati. Current Science 97, 1634–1643.

Sarkar, A., Mukherjee, A.D., Bera, M.K., Das, B., Juyal, N., Morthekai, P., Deshpande, R.D., Shinde, V.S., Rao, L.S., 2016. Oxygen isotope in archaeological bioapatites from India: implications to climate change and decline of Bronze Age Harappan civilization. Scientific Reports 6, 26555. https://doi.org/10.1038/srep26555.

Singh, A., Paul, D., Sinha, R., Thomsen, K.J., Gupta, S., 2016. Geochemistry of buried river sediments from Ghaggar Plains, NW India: multi-proxy records of variations in provenance, paleoclimate, and paleovegetation patterns in the Late Quaternary. Paleogeography, Paleoclimatology, Paleoecology 449, 85–100 http://dx.doi.org/10.1016/j.palaeo.2016.02.012.

Singh, S.K., Rai, S.K., Krishnaswami, S., 2008. Sr and Nd isotopes in river sediments from the Ganga Basin: sediment provenance and spatial variability in physical erosion. Journal of Geophysical Research 113, https://doi.org/10.1029/2007JF000909.

Tanaka, T., Togashi, S., Kamioka, H., Amakawa, H., 2000. JNdi-1 : a neodymium isotopic reference in consistency with LaJolla neodymium. Chemical Geology 168, 279–281.

Thapar, B.K., 1975. Kalibangan: a Harappan metropolis beyond the Indus Valley. Expedition 17 (2), 19–32.

Tripathi, J.K., Bock, B., Rajamani, V., 2013. Nd and Sr isotope characteristics of Quaternary Indo-Gangetic plain sediments: source distinctiveness in different geographic regions and its geological significance. Chemical Geology 344, 12–22. https://doi.org/10.1016/j.chemgeo.2013.02.016.

Valášková, M., 2015. Clays, clay minerals and cordierite ceramics – a review. Ceramics-Silikáty 59, 331–340.

Valdiya, K.S., 2017. Prehistoric River Saraswati, Western India: Geological Appraisal and Social Aspects. Springer.

Valdiya, K.S., 2013. The River Saraswati was a Himalayan-born river. Current Science 104, 42–54.

Wright, R.P., Bryson, R.A., Schuldenrein, J., 2008. Water supply and history: Harappa and the Beas regional survey. Antiquity 82, 37–48.